GL01461

AREA
NEWZEA
Gthm
Biblio

New Zealand

FC-253	Browne, P.R.L.; Sulfide Mineralization in a Broadlands Geothermal Drill Hole, Taupo Volcanic Zone, New Zealand 1969.
FC-199	Mahon, W.A.J. and Finlayson, J.B.; The Chemistry of the Broadlands Geothermal area New Zealand; 1972
FC-179	MacDonald, W.J.P.; 1972; Recent Exploration of the Kawerau Geothermal Field, North Island New Zealand
FC-200	Bowen, F.E. and Skinner, D.N.B.; 1970?; Geological Interpretation of Ngawha ~~Deep Drill hole~~, Kaikohe, Northland (N10), New Zealand
G. Therm IB	Grindley, G.W.; 1965; The Geology, Structure, and Exploitation of the Wairakei Geothermal Field, Taupo New Zealand, NZGS.
P Geot 4 V.3 No.1	Brander, J.L.; 1974; Evidence for Two Possible Relationships between Observable Surface Deformation and Geothermal Activity; Geothermics; Vol 3, No. I; Mar, 1974, p.17-20
	Hochstein, M.P. and Hunt, T.M.; 1970; Seismic Gravity and Magnetic Studies; Broadlands Geothermal Field New Zealand. U.N. Symposium (Pisa)

FC-287 Gordon, E.W.; New Zealand's volcanoes create power

FC-290. Marshall, D.C.; 1975; Theory of the Wairakei geothermal Field; 1. Single phase, drawdown Model

FC-277 Marshall D.C.; 1966; Preliminary theory of the Wairakei Geothermal Field,

FC-270. Clacy, G.R.T; 1968; Geothermal Ground Noise Amplitude and Frequency Spectra in the New Zealand Volcanic Region

Area N.Z. Broad l | Hunt, T.M. and Hicks, S.R; 1975; Repeat Gravity Measurement at Broadlands Geothermal Field, 1967-7? Geophysics Div., Dept of Sci and Industr Research Wellington, N.Z.; Rpt NO. 113.

Area NZ Wairakei | Hunt, T.M.; 1975; Repeat Gravity Measurements at Wairakei, 1961-1974. Geoph. Div; Dept. of Sci. and Indu Research, N.Z.; Rpt no. 111

Area N.Z. Wairakei | Mercer, J.W; Pinder, G.F. and Donaldson, I.G.; 1975; A Galerkin-Finite Element Analysis of the Hydrotherm System at Wairakei, New Zealand; Jour. Geoph. Research Vol. 80, NO. 17

FC 269	James, R.; 1968; Wairakei and Larderello: Geothermal Power systems Compared.
Area N.Z. Wairakei	Hunt, T.M.; 1970; Gravity Changes at Wairakei Geotherm Field, New Zealand.
Area NZ EM	Keller G.V.; 1969; Electro-magnetic Survey in the central Volcanic Region; Preliminary Report
Ser SSS 77-2998	Pritchett, J.W and Others; 1976; Geohydrological Environmental Effects of Geothermal Power Production Phase IIA
Sibbett LBL-8669	Pritchet, J.W, Rice, L.F. & Garg, S.K.; 1979, Summary of Reservoir Engineering Data: Wairakei Geothermal Field, New Zealand.
Ser SSS 78-3597 V-1 / Ser SSS 78-3597 V-2	2 Pritchet, J.W.; Rice, L.F. and Garg, S.K; 1978. Reservoir Engineering Data: Wairakei Geothermal Field, New Zealand, Vol. 1 + Vol. 2
SER COO 4051-23	Dipippo, Ronald; Geothermal Power Plants of New Zealand, Philippines and Idonesia. A Technical survey of Existing and Planned Installations.

From: First International Symposium on
Water / Rock Interaction, 1974
Prague, Czechoslovakia.

N.Z.

1. Browne, P.R.L.; ROEDDER, E. and WODZICKI, A.;
"Comparison of Past and Present Geothermal
Waters, From A STUDY OF FLUID INCLUSIONS,
BROADLANDS FIELD, NEW ZEALAND."; p. 140

2. STEINER, A.; Interaction Between Hot Water
and Silicic Rocks IN The Active Geothermal
Area AT WAIRAKEI New Zealand.

The following Articles are from: Proceeding Second UN Symposium of the Development and Use of Geothermal Resources

N.Z

(1) Macdonald, W.J.P; "The Useful Heat Contained in the Broadlands Geothermal Field"; p. 1113

(2) Risk, G.F.; Monitoring the Boundary of the Broadlands Geothermal Field, New Zealand" p. 1185

(3) Stilwell, W.B.; Hall, W.K. and Tawhai, J.; "Ground movement in New Zealand Geothermal Fields"; p. 1427.

(4) Hitchcock, G.W.; Bixley, P.F.; "Observations of the Effect of a Three-Year Shutdown at Broadlands Geothermal Field, New Zealand"; p. 1657

(5) Mahon, W.A.; "Review of Hydrogeochemistry of Geothermal Systems — Prospecting, Development and Use" p. 775

AREA
NZ
Wairakei

REPEAT GRAVITY MEASUREMENTS AT WAIRAKEI 1961-1974

by

T. M. HUNT

1975

REPORT No111

GEOPHYSICS DIVISION

Department of Scientific and Industrial Research
New Zealand

REPEAT GRAVITY MEASUREMENTS AT WAIRAKEI,

1961 - 1974

by

T. M. HUNT

GEOPHYSICS DIVISION

REPORT NO. 111

Geophysics Division,
Department of Scientific and Industrial Research,
Wellington, New Zealand

1975 AUGUST

CONTENTS

REPEAT GRAVITY MEASUREMENTS AT WAIRAKEI, 1961-1974

T. M. Hunt

ABSTRACT

Repeat gravity measurements made to examine the effects of mass changes associated with exploitation of the Wairakei Geothermal Field are described. The standard errors of the gravity values are generally about 0.1 μN/kg, but observations over several days suggest the accuracy is about 0.3 μN/kg. The effect of ground noise in the geothermal area is negligible. Differences between surveys caused by topographic and groundwater level changes are less than 0.2 μN/kg, and less than 0.3 μN/kg for uncertainties in instrument calibration. Differences due to regional gravity variations are thought to be negligible.

= .01 mgal

INTRODUCTION

Gravity measurements have been made on benchmarks in the Wairakei geothermal area in order to examine the effects of mass changes resulting from water being drawn out of the ground for generating electricity. The results of measurements in 1961, 1967 and 1968 were discussed by Hunt (1970) but no information about gravity values, dates, or instrument stability were presented, nor were details of the measurements and their errors given. Since this publication further surveys, in April 1971 and December 1974, have been made. The purpose of this report is to catalogue the basic information available and to discuss the errors in measurement and in comparing surveys. The results of the measurements will be discussed in a separate publication.

GRAVITY MEASUREMENTS

Gravity observations were made in August 1961 by W. I. Reilly, November 1962 by C. J. Banwell, J. Coggon, G. Dawson and P. Wellman, April 1967 and May 1968 by T. M. Hunt, April 1971 by T. M. Hunt and P. C. Whiteford, and in December 1974 by T. M. Hunt. The values of gravity determined from these observations are given in the Appendix. The approximate locations of the benchmarks used in the surveys are shown in Figures 1 and 2; detailed finder diagrams can be obtained from Ministry of Works and Development, Wairakei.

Gravity meters and their calibration

The 1961 and 1962 surveys were made using North American gravity meter AG1-96. Subsequent surveys were made using LaCoste and Romberg gravity meter G106. In the 1967 and later surveys a looping technique was used to minimise instrument reading errors and to determine instrument drift. The looping sequence used was generally A B A B C B C D C D E .... . In the 1961 and 1962 surveys this technique was not used but the gravity base (WAIRAKEI A) was occupied at least three times each day, so that an instrument drift correction could be obtained. The gravity meters were calibrated over the Wellington Calibration Interval of 638.1 μN/kg (Cowan and Robertson 1964). Because the greatest difference in gravity values between the survey points in the Wairakei area is less than 500 μN/kg, errors associated with determination of the calibration factor will be less than those associated with the measurement of the calibration interval (about 0.3 μN/kg). A linear calibration factor was used for the North American gravity meter. The manufacturers scale curve adjusted on the basis of the calibration over the Wellington Calibration Interval was used for the LaCoste and Romberg instrument.

Gravity base stations

Gravity observations in the 1961 and 1962 surveys were made relative to WAIRAKEI A gravity base which can no longer be occupied. These values have been put in terms of a base on Taupo Fundamental benchmark (TAUPO FUNDAMENTAL), using the relationship:

$$g_{\text{TAUPO FUNDAMENTAL}} = g_{\text{WAIRAKEI A}} - 117.4\ (\pm 0.2)\ \mu N/kg$$

determined from twelve occupations of TAUPO FUNDAMENTAL made by W. I. Reilly during the 1961 survey. TAUPO FUNDAMENTAL has been used as a gravity base for the 1967 and later surveys, and has the advantage of being outside the area likely to be affected by mass changes associated with the Wairakei Geothermal Field.

Tripod heights

The North American gravity meter (AG1-96) was mounted on a tripod such that the base of the meter was normally 0.58 m (23 inches) above ground level. The survey pins in some benchmarks however were not at ground level and since the tripod base rested on the ground and not directly on the benchmark there were differences in the height of the meter above some survey points. Field notes indicate that the base of the North American gravity meter varied between 0.41 m (16 inches) and 0.76 m (30 inches) above the pin in the benchmark. The LaCoste and Romberg gravity meter was set up on its standard baseplate on the benchmark itself. Gravity differences between the base station and a benchmark measured using the North American gravity meter may therefore differ from those measured using the LaCoste and Romberg instrument. Corrections for this variation in tripod height have been made to those gravity values in the Appendix marked by an asterisk, assuming a change of 3.1 $\mu N\ kg^{-1} m^{-1}$.

Effect of ground noise (vibrations)

Microseisms were observed when making measurements in the main production borefield and within 3 km of the (now extinct) "rogue" Bore No. 204. No published information is available on high frequency ground movements in the Wairakei geothermal area, but at Waiotapu geothermal area vertical ground movements have an amplitude of about 0.15 μm and a frequency of about 0.5 to 1 Hz (Whiteford 1970). The effect of such ground movements on gravity meter measurements may be similar to that of movements of a ship on a ship borne gravity meter which, under certain conditions, produces spurious readings resulting from "cross-coupling" (Harrison 1960; LaCoste 1967). This effect occurs when simultaneous vertical and horizontal accelerations act on the beam of a gravity meter. The error introduced by "cross-coupling" is greatest when the beam of the gravity meter is parallel to the direction of the horizontal acceleration, and orientation of the gravity meter could be important. To test if this effect was significant, measurements were made with the LaCoste and Romberg gravity meter set up on Benchmark AA21 within the main production borefield. The measurements (Table 1) show that there was no significant change in gravity readings for different orientations of the gravity meter, and hence "cross-coupling" errors are negligible in the case of the LaCoste and Romberg instrument. The North American gravity meter is no longer operational and no tests could be made using it.

Table 1: Gravity meter readings (LaCoste and Romberg, G106) for different orientations of the instrument at benchmark AA21, Wairakei Geothermal Field

Azimuth	Reading
0°	3391.70 (±0.01)
45°	3391.69
90°	3391.70
135°	3391.68
180°	3391.70
270°	3391.69

REDUCTION OF MEASUREMENTS

Calculation of gravity values

Gravity values have been computed using the method described by Reilly (1970); for each day the gravity meter readings were multiplied by the appropriate scale factor, and the gravitational attraction of the sun and moon calculated, using the method of Longman (1959), and subtracted. An instrument drift correction, derived from least squares fitting of a degree one or two curve to the gravity differences at repeat stations, was made. The differences in gravity between the base and field stations were then obtained by subtracting a base correction.

Accuracy of gravity values

A measure of the accuracy of gravity meter observations is their repeatability, within each day and from day to day. When a gravity station at Wairakei is occupied several times within a day, the individual values of gravity, corrected for instrument drift and for changes in the gravitational attraction of the sun and moon, generally differ by about 0.1 or 0.2 μN/kg from each other. The value of gravity at benchmark AA13, within the main production borefield, was measured using the LaCoste and Romberg gravity meter on five successive days and the corrected measurements differed by up to 0.6 μN/kg, although the standard error of the individual values were less than 0.3 μN/kg. It is probable that an accuracy no better than 0.3 μN/kg can be expected.

DIFFERENCES BETWEEN SURVEYS

Regional gravity changes

TAUPO FUNDAMENTAL base is situated on thick Holocene lacustrine and volcanic deposits within the central volcanic zone of the North Island in which regional mass changes could be occurring. Gravity changes resulting from mass changes at great depth (> 5 km) should cause only uniform changes in the gravity differences between the Wairakei area and TAUPO FUNDAMENTAL. To determine the size of any possible regional gravity changes in the Taupo area, gravity measurements were made on Rangitaiki Fundamental benchmark (RANGITAIKI FUNDAMENTAL), situated 25 km south-east of Taupo, on a thin (200 m) veneer of ignimbrite overlying greywacke basement rock. The gravity differences between TAUPO FUNDAMENTAL and RANGITAIKI FUNDAMENTAL at the times of the gravity surveys are shown in Table 2. The gravity difference increased between 1968 and 1971 but the amount of increase (0.5 μN/kg) is insufficient to be certain if this is actual change or measurement error. Since the distance between TAUPO FUNDAMENTAL and Wairakei (7 km) is smaller than that between TAUPO FUNDAMENTAL and RANGITAIKI FUNDAMENTAL (25 km) it is probable that the effects of regional mass changes on the Wairakei gravity surveys can be neglected.

Table 2: Gravity Differences (μN/kg) between TAUPO FUNDAMENTAL and RANGITAIKI FUNDAMENTAL

Date	Gravity Difference	Standard Error	Number of Readings Taupo	Number of Readings Rangitaiki
68 04 12	540.7	0.1	4	3
71 08 27	541.2	0.1	3	2
74 12 08	541.0	0.2	4	3

Topographic changes

Changes in the topography of the area between surveys have occurred due to road construction, mainly along State Highway 1 between Wairakei and Taupo (Fig. 1). The effects of these changes on nearby gravity stations, estimated using standard topographic correction tables

(Woodward and Ferry 1973), are less than 0.2 μN/kg and have been neglected.

Groundwater level changes

Groundwater level changes may cause gravity differences between surveys. Groundwater levels beneath the benchmarks used in the gravity surveys are not known, but levels have been measured, and monitored at infrequent intervals, in holes adjacent to some bores. Data from 26 holes (G. Hitchcock, pers. comm.) show that the greatest measured difference in groundwater level between July 1967 and March 1970 was 2 m, but in most holes the differences were less than 1 m. The groundwater levels are from 5 to 30 m below the ground surface.

Assuming the groundwater level dropped from a depth of 13 to 15 m, for a radius of 500 m about a gravity station, in rock having a connected porosity of 20%, the gravity change observed at the station would be about 0.16 μN/kg. It is inferred that groundwater level changes between surveys may cause local gravity differences of about 0.2 μN/kg.

ACKNOWLEDGMENTS

I thank W. I. Reilly for criticism of the manuscript, and various members, past and present, of the Geophysical Survey for the field measurements made in 1961 and 1962. P. C. Whiteford made some of the 1971 measurements and H. Rayner assisted in 1974. J. Tawhai located benchmarks and provided elevation data, and G. Hitchcock provided groundwater level data.

REFERENCES

COWAN, M.; ROBERTSON, E. I. 1964: Principal pendulum and airport gravity stations in New Zealand. N.Z. J. Geol. Geophys. 7: 543-53.

HARRISON, J. C. 1960: Measurements of gravity at sea, in "Methods and Techniques in Geophysics" 1: 211-229, Interscience Publishers, New York.

HUNT, T. M. 1970: Gravity changes at Wairakei Geothermal Field, New Zealand. Geol. Soc. Amer. Bull. 81: 529-36.

LACOSTE, L. J. B. 1967: Measurement of gravity at sea and in the air. Rev. Geophys. 5: 477-526.

LONGMAN, I. M. 1959: Formulas for computing the tidal accelerations due to the sun and moon. J. Geophys. Res. 64: 2351-55.

REILLY, W. I. 1970: Adjustment of gravity meter observations. N.Z. J. Geol. Geophys. 13: 697-702.

WHITEFORD, P. C. 1970: Ground movement in the Waiotapu Geothermal Region, New Zealand. Geothermics 2: 478-86.

WOODWARD, D. J.; FERRY, L. M. 1973: Gravity terrain correction tables. Technical Note 66, Geophysics Division, Department of Scientific and Industrial Research, Wellington, New Zealand.

APPENDIX

Summary of repeat gravity measurements in the vicinity of Wairakei geothermal area

Date: Day on which the measurements were made.

g: Value of gravity (μN/kg), calculated using the method of Reilly (1970), relative to TAUPO FUNDAMENTAL base having a gravity value of 1000 μN/kg. An asterisk indicates that a correction has been made for the height of the North American instrument above the survey point being different from 0.58 m.

s.e. Standard error of gravity value.

Stability: An indication of the precision of the gravity meter reading, which is related to the ground noise conditions.

Excellent = no microseisms, readings ± 0.01 dial div.

Good = intermittent ground noise, readings ±0.02 dial div.

Fair = continuous ground noise. Balance position of the gravity meter beam estimated from swings. Readings can be obtained to ±(0.03 - 0.05) dial div.

Unreadable = gravity meter beam swinging erratically or hitting stops.

Instrument: North American gravity meter AG1-96 listed as 1-96, LaCoste and Romberg G106 gravity meter listed as 106.

Elevation: Elevation (metres) of the survey point at about the time of the gravity survey. The elevations given for the 1961 survey were obtained from Ministry of Works and Development Chart WG 2579/1. The elevations given for the 1967 survey were determined by extrapolating the 1956-1966 levelling data shown on chart WG 2579/1 to 1967. Most benchmarks have shown a constant change in level with time over the period 1956-66 and so extrapolation to obtain the values for 1967 is considered to be valid. The levels for the 1971 survey were obtained from M.W.D. levelling measurements made in May-August 1971 (J. Tawhai, pers. comm.). All elevations are orthometric heights, in terms of Maraetai Datum, based on the level of BM A 93 near Aratiatia being constant at 363.724 m (1193.320 ft).

BM	Date	g	n	s.e.	Stability	Inst.	Observer	Elevation
A 92/1	61.08.14	877.5*	1	0.2		1-96	Reilly	
	61.08.15	878.2*	1	0.3		1-96	Reilly	
	61.08.16	878.5*	6	0.2		1-96	Reilly	
	62.11.09	878.5*	1	1.8		1-96	Dawson	
	62.11.24	876.9*	1	0.6		1-96	Coggon	
	62.11.25	877.8*	1	0.2		1-96	Coggon	
	67.03.31	877.9	1	0.7	Excellent	106	Hunt	
	68.04.11	877.9	3	0.1	Excellent	106	Hunt	
	71.09.16	877.8	3	0.2	Good	106	Whiteford	
	74.12.13	877.8	3	0.1	Excellent	106	Hunt	
A 93	61.08.14	938.9	1	0.1		1-96	Reilly	363.724
	67.03.31	938.8	1	0.8	Excellent	106	Hunt	
	68.04.14	938.6	3	0.1	Good	106	Hunt	
	74.12.13	938.8	3	0.1	Excellent	106	Hunt	
A 95	61.08.05	977.3*	1	0	Fair	1-96	Reilly	350.89
	62.11.08	976.3*	1	1.3	Fair	1-96	Dawson	
	67.04.09	976.9	2	0.1	Excellent	106	Hunt	350.87
	68.04.14	976.9	3	0.1	Good	106	Hunt	
	71.09.04	977.3	2	0.2	Excellent	106	Hunt	350.867
	74.12.06	977.3	3	0.2	Excellent	106	Hunt	
A 96	61.08.05	967.7*	1	0	Good	1-96	Reilly	348.90
	62.11.08	966.9*	1	1.2		1-96	Dawson	
	67.04.09	967.4	2	0.1	Good	106	Hunt	348.75
	68.04.14	967.5	3	0.1	Good	106	Hunt	
	71.09.04	968.1	2	0.2	Excellent	106	Hunt	348.684
	74.12.06	968.3	3	0.2	Good	106	Hunt	
A 97	61.08.03	907.5*	1	0.1	Fair	1-96	Reilly	380.73
	62.11.06	904.0*	1	2.3	Fair	1-96	Dawson	
	67.04.02	904.3	3	0.2	Fair	106	Hunt	380.16
	68.06.10	904.8	3	0.1	Good	106	Hunt	
	71.08.30	905.8	4	0.1	Good	106	Hunt	379.580
	74.12.07	906.9	4	0.1	Good	106	Hunt	

BM	Date	g	n	s.e.	Stability	Inst.	Observer	Elevation
A 98	61.08.02	874.4*	1	0.2		1-96	Reilly	392.50
	62.11.04	885.9*	1	0.7	Fair	1-96	Banwell	
	67.03.30	874.2	4	0.1	Good	106	Hunt	392.28
	68.04.13	874.9	3	0.2	Good	106	Hunt	
	71.08.30	874.7	3	0.1	Good	106	Hunt	392.174
	74.12.05	874.6	3	0.2	Good	106	Hunt	
A 99	61.08.02	897.5*	1	0.3		1-96	Reilly	392.38
	62.11.04	898.2*	1	0.7	Fair	1-96	Banwell	
	62.11.09	898.9*	1	1.7		1-96	Dawson	
	67.04.05	897.5	2	0.1	Good	106	Hunt	392.16
	68.04.13	897.7	1	0.7	Good	106	Hunt	
	71.08.28	897.5	4	0.2	Fair	106	Hunt	
	71.08.30	897.0	3	0.1	Good	106	Hunt	392.085
	74.12.05	897.9	3	0.2	Good	106	Hunt	
AA 1	61.08.02	982.9*	1	0.3		1-96	Reilly	364.39
	62.11.07	984.0*	1	0.6		1-96	Dawson	
	62.11.08	985.4*	1	1.0		1-96	Dawson	
	67.03.30	984.5	4	0.1	Good	106	Hunt	364.28
	68.04.13	984.5	3	0.4	Fair	106	Hunt	
	71.08.28	984.8	4	0.2	Excellent	106	Hunt	364.22
	Destroyed							
AA 1/14	68.04.13	947.1	3	0.4	Good	106	Hunt	
	71.08.28	947.3	3	0.3	Excellent	106	Hunt	377.106
	74.12.05	948.1	4	0.1	Excellent	106	Hunt	
AA 2	61.08.03	865.1*	1	0.1		1-96	Reilly	
	62.11.07	864.5*	1	0.6		1-96	Reilly	
	67.04.03	864.4	3	0.1	Good	106	Hunt	
	68.04.13	864.6	2	0.3	Good	106	Hunt	
	71.08.28	863.9	3	0.1		106	Hunt	413.258
	Destroyed							
AA 3/1	61.08.02	890.6*	1	0.3		1-96	Reilly	
	62.11.07	890.3*	1	0.6		1-96	Dawson	
	67.03.30	890.9	4	0.1	Good	106	Hunt	
	68.04.13	890.7	1	0.3	Fair	106	Hunt	
	71.08.28	890.4	2	0.1	Fair	106	Hunt	415.347
	74.12.05	890.6	3	0.2	Excellent	106	Hunt	

BM	Date	g	n	s.e.	Stability	Inst.	Observer	Elevation
AA 5	61.08.16	674.9*	1	0.4		1-96	Reilly	
	68.06.11	675.6	2	0.2	Excellent	106	Hunt	
	71.09.16	674.9	3	0.2	Excellent	106	Whiteford	
	74.12.13	675.4	3	0.1	Excellent	106	Hunt	
AA 6	68.06.11	577.2	3	0.1	Excellent	106	Hunt	
	71.09.16	577.0	3	0.2	Good	106	Whiteford	485.702
	74.12.13	577.0	3	0.1	Excellent	106	Hunt	
AA 7	71.09.16	719.2	3	0.2	Good	106	Whiteford	447.413
	74.12.13	719.1	3	0.1	Excellent	106	Hunt	
AA 8	61.08.15	813.4*	1	0.1		1-96	Reilly	415.79
	67.03.31	813.4	1	0.6	Excellent	106	Hunt	415.67
	68.06.09	813.6	2	0.1	Excellent	106	Hunt	
	71.09.17	813.4	2	0.2	Good	106	Whiteford	415.595
	74.12.13	813.5	3	0.1	Excellent	106	Hunt	
AA 9	61.08.03	987.0	1	0.1		1-96	Reilly	355.49
	62.11.25	987.6	1	0.2		1-96	Coggon	
	67.03.30	987.1	4	0.1	Good	106	Hunt	355.38
	68.04.13	987.3	3	0.7	Excellent	106	Hunt	
	71.08.28	987.7	3	0.2	Fair	106	Hunt	355.316
	74.12.05	987.9	3	0.2	Excellent	106	Hunt	
AA 11	61.08.14	893.1*	1	0.1	Fair	1-96	Reilly	385.48
	62.11.23	893.5*	1	0.3		1-96	Coggon	
	67.04.02	893.2	3	0.2	Excellent	106	Hunt	385.39
	68.04.14	893.3	3	0.1	Good	106	Hunt	
	71.08.31	893.7	2	0.2	Good	106	Hunt	385.322
	74.12.12	893.5	2	0.1	Good	106	Hunt	
AA 12	61.08.14	783.1*	1	0.1		1-96	Reilly	425.56
	67.04.04	782.2	1	0.1	Excellent	106	Hunt	425.53
	68.06.06	782.1	1	0.0	Good	106	Hunt	
	71.09.16	782.3	2	0.2	Good	106	Hunt	

BM	Date	g	n	s.e.	Stability	Inst.	Observer	Elevation
AA 13	61.08.03	875.3	1	0.1		1-96	Reilly	403.43
	62.11.03	874.0	1	0.9	Fair	1-96	Banwell	
	62.11.06	872.2	1	2.3	Fair	1-96	Dawson	
	67.04.02	872.9	3	0.1	Fair	106	Hunt	403.04
	68.04.14	873.2	3	0.1	Fair	106	Hunt	
	71.08.30	873.6	2	0.1	Good	106	Hunt	402.772
	71.08.31	873.2	5	0.2	Good	106	Hunt	
	71.09.02	873.1	2	0.1	Good	106	Hunt	
	71.09.03	873.2	3	0.2	Good	106	Hunt	
	71.09.04	873.5	3	0.1	Good	106	Hunt	
	74.12.07	874.4	3	0.1	Good	106	Hunt	
AA 14	61.08.03	755.6	1	0.1		1-96	Reilly	454.76
	62.11.03	755.6	1	0.9	Fair	1-96	Banwell	
	62.11.06	752.9	1	2.2	Fair	1-96	Dawson	
	67.04.03	753.2	2	0.1	Good	106	Hunt	454.58
	68.04.15	753.0	2	0.2	Good	106	Hunt	
	71.09.02	752.2	3	0.1	Good	106	Hunt	454.484
	74.12.14	752.2	3	0.1	Excellent	106	Hunt	
AA 15	61.08.03	615.7	1	0.1		1-96	Reilly	510.24
	62.11.06	613.9	1	2.1	Fair	1-96	Dawson	
	67.04.03	614.5	3	0.1	Good	106	Hunt	510.10
	68.04.15	614.6	3	0.1	Good	106	Hunt	
	71.09.02	613.7	3	0.1	Good	106	Hunt	510.017
	74.12.14	614.3	3	0.1	Excellent	106	Hunt	
AA 18	61.08.03	581.6	1	0.1		1-96	Reilly	504.72
	62.11.06	583.2	1	2.1	Fair	1-96	Dawson	
	67.04.01	580.1	3	0.1	Excellent	106	Hunt	504.61
	68.06.10	580.0	2	0.1	Good	106	Hunt	
	71.09.14	579.6	1	0.1	Fair	106	Whiteford	
	71.09.16	579.8	2	0.2	Fair	106	Whiteford	
	74.12.10	579.9	3	0.1	Good	106	Hunt	
AA 19	61.08.04	585.1	1	0.4		1-96	Reilly	517.21
	62.11.06	616.7	1	2.2	Fair	1-96	Dawson	
	67.04.09	584.1	1	0.2	Excellent	106	Hunt	517.11
	68.06.10	584.1	2	0.1	Good	106	Hunt	
	74.12.10	584.0	2	0.1	Excellent	106	Hunt	

BM	Date	g	n	s.e.	Stability	Inst.	Observer	Elevation
AA 21	61.08.04				Unreadable	1-96	Reilly	422.17
	62.11.03	855.7*	1	0.9	Fair	1-96	Banwell	
	62.11.06	895.4*	1	2.3	Fair	1-96	Dawson	
	62.11.08	853.4*	1	1.1		1-96	Dawson	
	67.04.02	850.2	3	0.2	Fair	106	Hunt	421.87
	68.06.08	850.1	3	0.1	Good	106	Hunt	
	71.08.31	849.8	3	0.2	Fair	106	Hunt	
	74.12.07	850.1	3	0.1	Excellent	106	Hunt	
AA 22	61.08.05	860.8*	1	0.0		1-96	Reilly	427.36
	62.11.04	861.4*	1	0.6	Fair	1-96	Banwell	
	62.11.09	862.1*	1	1.7		1-96	Dawson	
	67.04.04	859.9	3	0.1	Excellent	106	Hunt	427.19
	68.06.08	860.0	3	0.1	Fair	106	Hunt	
	71.09.02	859.7	3	0.1	Good	106	Hunt	427.135
	Destroyed by forestry operations							
AA 23	61.08.05	828.4*	1	0.0	Fair	1-96	Reilly	448.12
	61.08.14	822.6*	1	0.1	Good	1-96	Reilly	
	62.11.04	825.5*	1	0.6	Fair	1-96	Banwell	
	62.11.09	825.1*	1	1.7		1-96	Dawson	
	67.04.09	822.6	2	0.1	Fair	106	Hunt	447.90
	68.06.08	822.5	2	0.1	Fair	106	Hunt	
	71.09.02	822.3	2	0.1	Fair	106	Hunt	447.865
	75.01.22	822.6	3	0.2	Excellent	106	Hunt	
AA 53	61.08.03	908.5*	1	0.1	Fair	1-96	Reilly	381.39
	62.11.03	923.9*	1	0.9	Fair	1-96	Banwell	
	62.11.06	897.4*	1	2.4	Fair	1-96	Dawson	
	67.04.02	906.7	3	0.2	Fair	106	Hunt	381.06
	Destroyed during road construction							
AA 53/1	71.09.04	908.9	1	0.2	Fair	106	Hunt	380.017
	74.12.05	909.4	2	0.2	Good	106	Hunt	
AA 70	61.08.05	967.0*	1	0	Good	1-96	Reilly	353.78
	62.11.08	965.6*	1	1.2		1-96	Dawson	
	67.03.30	967.0	4	0.1	Excellent	106	Hunt	353.75
	68.04.14	967.1	3	0.1	Fair	106	Hunt	
	71.09.04	967.7	2	0.2	Good	106	Hunt	353.734
	75.01.22	967.7	3	0.2	Good	106	Hunt	

BM	Date	g	n	s.e.	Stability	Inst.	Observer	Elevation
AA 71	61.07.31	904.9*	3	0.2	Fair	1-96	Reilly	374.85
	61.08.16	905.2*	3	0.3	Fair	1-96	Reilly	
	62.11.08	904.8*	1	1.2		1-96	Dawson	
	62.11.09	904.5*	1	1.7		1-96	Dawson	
	62.11.23	904.2*	1	0.3		1-96	Coggon	
	62.11.24	904.4*	3	0.4		1-96	Coggon	
	67.04.05	905.0	2	0.5	Excellent	106	Hunt	374.57
	68.04.14	905.1	3	0.1	Good	106	Hunt	
	71.08.31	905.4	1	0.2	Good	106	Hunt	374.348
	71.08.28	905.2	1	0.4		106	Hunt	
	75.01.22	906.5	3	0.2	Good	106	Hunt	
AA 72	61.08.14	843.6*	1	0.1	Fair	1-96	Reilly	405.88
	67.04.04	843.4	3	0.1	Good	106	Hunt	405.83
	68.06.06	843.3	2	0.0	Good	106	Hunt	
	71.08.31	843.4	3	0.2	Excellent	106	Hunt	405.795
	74.12.06	843.8	3	0.2	Excellent	106	Hunt	
AA 73	61.08.03	613.6*	1	0.1		1-96	Reilly	514.43
	62.11.03	612.9*	1	0.9	Fair	1-96	Banwell	
	62.11.06	610.6*	1	2.2	Fair	1-96	Dawson	
	67.04.03	611.0	3	0.1	Good	106	Hunt	514.30
	68.04.15	610.8	3	0.1	Excellent	106	Hunt	
	71.09.02	610.1	3	0.1	Good	106	Hunt	514.225
	74.12.14	610.4	3	0.1	Excellent	106	Hunt	
AA 74	61.08.02	654.6	2	0.2		1-96	Reilly	487.65
	61.08.16	654.8	3	0.3		1-96	Reilly	
	62.11.23	654.2	2	0.2		1-96	Coggon	
	67.04.01	653.5	3	0.1	Excellent	106	Hunt	487.50
	68.04.15	653.7	3	0.1	Good	106	Hunt	
	71.09.16	653.1	3	0.1		106	Whiteford	487.450
	74.12.06	653.5	3	0.2	Excellent	106	Hunt	
AA 75	61.08.03	876.6*	1	0.1		1-96	Reilly	391.90
	62.11.03	877.5*	1	1.0	Fair	1-96	Banwell	
	62.11.06	877.2*	1	2.4	Fair	1-96	Dawson	
	67.04.05	875.5	3	0.5	Good	106	Hunt	391.70
	68.04.13	876.0	3	0.2	Good	106	Hunt	
	71.08.30	875.8	3	0.1	Good	106	Hunt	391.597
	75.01.22	876.0	3	0.1	Excellent	106	Hunt	

BM	Date	g	n	s.e.	Stability	Inst.	Observer	Elevation
AA 76	61.08.02	905.7*	1	0.3		1-96	Reilly	396.70
	62.11.04	906.7*	1	0.7	Fair	1-96	Banwell	
	62.11.09	906.1*	1	1.6		1-96	Dawson	
	67.04.04	905.7	3	0.1	Good	106	Hunt	396.39
	68.06.10	906.1	3	0.1	Excellent	106	Hunt	
	71.09.02	906.2	3	0.1	Good	106	Hunt	396.267
	75.01.23	906.5	3	0.2	Good	106	Hunt	
AA 77	61.08.02	773.5	1	0.3		1-96	Reilly	462.48
	62.11.04	774.4	1	0.7	Fair	1-96	Banwell	
	62.11.09	774.2	1	1.6		1-96	Dawson	
	67.04.04	772.5	2	0.1	Good	106	Hunt	462.20
	68.06.10	772.9	3	0.1	Excellent	106	Hunt	
	71.09.02	772.8	2	0.1	Fair	106	Hunt	462.138
	74.01.23	772.9	2	0.2	Good	106	Hunt	
AA 78	61.08.02	983.6*	1	0.3		1-96	Reilly	360.34
	62.11.07	983.9*	1	0.6		1-96	Dawson	
	67.03.30	984.0	4	0.1	Good	106	Hunt	360.24
	68.04.13	984.1	3	0.5		106	Hunt	
	71.08.28	984.3	3	0.3	Excellent	106	Hunt	360.181
	74.12.05	984.8	3	0.2	Excellent	106	Hunt	
AA 79	61.08.05	907.4*	1	0.0		1-96	Reilly	397.04
	62.11.04	907.7*	1	0.7	Fair	1-96	Banwell	
	62.11.09	908.4*	1	1.6		1-96	Dawson	
	67.04.04	907.4	3	0.1	Good	106	Hunt	396.91
	68.06.08	907.6	2	0.1	Good	106	Hunt	
	Destroyed by road construction							
AA 79/1	71.09.02	908.1	2	0.1	Fair	106	Hunt	396.528
	75.01.22	908.0	3	0.2	Good	106	Hunt	
BM 7	61.08.01	607.6	1	0.3		1-96	Reilly	512.65
	62.11.04	613.0	1	0.7	Fair	1-96	Banwell	
	62.11.09	605.5	1	1.6		1-96	Dawson	
	67.04.01	605.8	2	0.1	Good	106	Hunt	512.49
	68.04.15	606.2	3	0.1	Fair	106	Hunt	
	71.09.14	605.6	3	0.1	Fair	106	Whiteford	512.446
	74.12.07	605.9	3	0.1	Excellent	106		

BM	Date	g	n	s.e	Stability	Inst.	Observer	Elevation
BM 8	62.11.04	582.4*	1	0.7	Fair	1-96	Banwell	
	67.04.01				Unreadable	106	Hunt	
	74.12.07	652.0	3	0.1	Excellent	106	Hunt	
BM 9	61.08.04	774.8	1	0.4	Fair	1-96	Reilly	466.03
	62.11.04	790.5	1	0.7	Fair	1-96	Banwell	
	67.04.01	773.0	1	0.2	Fair	106	Hunt	465.93
	68.06.05	772.6	2	0.1	Fair	106	Hunt	
	71.09.14	772.7	3	0.1	Fair	106	Whiteford	465.875
	74.12.10	772.4	3	0.1	Good	106	Hunt	
BM 15	62.11.08	902.3*	1	1.1		1-96	Dawson	
	67.04.02	901.7	3	0.2	Good	106	Hunt	398.05
	68.06.08	901.1	2	0.1	Good	106	Hunt	
BM 16	61.08.01	863.7	1	0.3	Fair	1-96	Reilly	423.32
	62.11.08	867.8	1	1.1		1-96	Dawson	
	62.11.26	870.7	1	0.6		1-96	Wellman	
	67.04.02	862.4	2	0.2	Good	106	Hunt	423.17
	68.06.08	861.7	3	0.1	Good	106	Hunt	
	71.08.31	861.7	3	0.2	Good	106	Hunt	423.10
	74.12.07	862.2	3	0.1	Excellent	106	Hunt	
BM 19	68.06.08	640.2	1	0.2	Fair	106	Hunt	
	74.12.07	640.4	3	0.1	Excellent	106	Hunt	
BM 20	61.08.15	786.9	1	0.3		1-96	Reilly	424.17
	67.03.31	787.1	1	0.0	Excellent	106	Hunt	424.08
	68.06.09	788.0	2	0.1	Excellent	106	Hunt	
	71.09.17	787.5	2	0.2	Good	106	Whiteford	424.060
	74.12.13	787.5	3	0.1	Good	106	Hunt	
BM 21	61.08.15	868.0*	1	0.3		1-96	Reilly	386.82
	62.11.25	868.1*	1	0.2		1-96	Goggon	
	67.03.31	867.7	1	0.6	Excellent	106	Hunt	386.70
	68.06.09	868.5	2	0.1	Excellent	106	Hunt	
	71.09.16	868.0	2	0.2	Good	106	Whiteford	386.664
	74.12.13	868.0	2	0.1	Good	106	Hunt	

BM	Date	g	n	s.e.	Stability	Inst.	Observer	Elevation
BM 22	61.08.15	710.9*	1	0.3		1-96	Reilly	450.53
	67.03.31	711.2	1	0	Good	106	Hunt	450.51
	68.06.11	711.2	2	0.2	Excellent	106	Hunt	
	71.09.16	710.9	3	0.2	Excellent	106	Whiteford	450.517
	Destroyed.							
BM 23	61.08.15	961.4*	1	0.3		1-96	Reilly	348.18
	67.03.31	961.8	1	0	Excellent	106	Hunt	348.07
	68.06.11	961.9	3	0.1	Excellent	106	Hunt	
	71.09.16	962.3	1	0.2	Excellent	106	Whiteford	348.043
BM 24	61.08.14	945.8*	1	0.2		1-96	Reilly	354.38
	67.03.31	945.9	1	0	Excellent	106	Hunt	354.36
	68.06.11	945.8	2	0.2	Excellent	106	Hunt	
	Destroyed.							
BM 26	61.08.04	582.4*	1	0.4		1-96	Reilly	518.68
	62.11.06	598.2	1	2.2	Fair	1-96	Dawson	
	67.04.01	581.0	3	0.1	Good	106	Hunt	518.57
	68.04.15	581.4	3	0.1	Fair	106	Hunt	
	71.09.14	580.9	3	0.1	Fair	106	Whiteford	518.545
	74.12.07	581.0	3	0.1	Excellent	106	Hunt	
BM 27	61.08.04	554.0*	1	0.4		1-96	Reilly	
	62.11.09	552.4*	1	1.6		1-96	Dawson	
	67.04.01	552.7	3	0.1	Good	106	Hunt	
	68.04.15	553.3	3	0.1	Fair	106	Hunt	
	71.09.14	552.5	3	0.1	Good	106	Whiteford	536.482
	74.12.07	552.8	3	0.1	Excellent	106	Hunt	
BM 28	61.08.04	736.0*	1	0.4	Fair	1-96	Reilly	487.23
	62.11.07	758.1*	1	0.6		1-96	Dawson	
	67.04.01	708.1	1	0.2	Fair	106	Hunt	487.10
	71.09.14	707.8	3	0.1	Fair	106	Whiteford	487.055
	74.12.10	707.5	3	0.1	Good	106	Hunt	

BM	Date	g	n	s.e.	Stability	Inst.	Observer	Elevation
BM 29	61.08.04	684.4*	1	0.4		1-96	Reilly	491.79
	62.11.07	683.2*	2	0.5		1-96	Dawson	
	67.04.09	683.7	1	0.2	Fair	106	Hunt	491.69
	68.06.05	683.0	3	0.1	Good	106	Hunt	
	71.09.14	683.1	3	0.1	Fair	106	Whiteford	491.669
	74.12.10	683.4	3	0.1	Good	106	Hunt	
BM 30	61.08.04	662.5*	1	0	Fair	1-96	Reilly	495.60
	67.04.09	661.5	1	0.2	Good	106	Hunt	495.50
	68.06.05	661.3	2	0.1	Good	106	Hunt	
	71.09.14	661.7	2	0.1	Fair	106	Whiteford	495.465
	74.12.10	661.5	3	0.1	Excellent	106	Hunt	
BM 31	67.04.03	864.9	3	0.1	Excellent	106	Hunt	
	68.06.05	865.0	3	0.1	Excellent	106	Hunt	
	71.09.06	865.0	1	0.2	Fair	106	Hunt	
	71.09.14	864.9	3	0.1		106	Whiteford	426.934
	74.12.09	864.8	3	0.1	Good	106	Hunt	
BM 32	67.04.03	804.2	3	0.1	Excellent	106	Hunt	
	68.06.05	804.3	4	0.1	Excellent	106	Hunt	
	71.09.06	804.1	2	0.2	Fair	106	Hunt	451.336
	74.12.09	804.0	3	0.1	Good	106	Hunt	
BM 33/1	71.09.06	754.0	3	0.2	Fair	106	Hunt	
	74.12.09	754.2	3	0.1	Good	106	Hunt	
BM 34	61.08.04	837.6*	1	0.4	Fair	1-96	Reilly	443.70
	62.11.07	839.0*	1	0.8		1-96	Dawson	
	67.04.01	836.2	3	0.1	Fair	106	Hunt	443.53
	68.06.05	835.9	4	0.1	Fair	106	Hunt	
	71.09.06	836.5	1	0.2	Fair	106	Hunt	443.473
	71.09.14	836.6	1	0.1		106	Whiteford	
	75.01.23	836.6	3	0.1	Excellent	106	Hunt	
BM 34/1	71.09.14	794.7	3	0.1	Fair	106	Whiteford	457.645
	74.12.07	794.5	3	0.1	Excellent	106	Hunt	

BM	Date	g	n	s.e.	Stability	Inst.	Observer	Elevation
BM 35	61.08.05	767.0*	1	0	Fair	1-96	Reilly	468.31
	61.08.14	767.3*	1	0.1		1-96	Reilly	
	62.11.08	765.6*	1	1.0		1-96	Dawson	
	67.04.01	766.0	2	0.2	Good	106	Hunt	468.17
	68.06.05	766.6	2	0.1	Good	106	Hunt	
	74.12.09	766.6	3	0.1	Good	106	Hunt	
BM 36	61.08.05	830.5*	1	0	Fair	1-96	Reilly	437.33
	61.08.14	830.4*	1	0.1		1-96	Reilly	
	62.11.08	828.9*	1	1.0		1-96	Dawson	
	67.04.09	829.8	1	0.2	Good	106	Hunt	437.25
	74.12.09	830.2	3	0.1	Good	106	Hunt	
BM 45	71.09.16	650.0	3	0.2	Good	106	Whiteford	483.820
	74.12.06	650.3	3	0.2	Excellent	106	Hunt	
BM 46	71.09.16	657.2	3	0.2	Good	106	Whiteford	478.774
	74.12.06	657.7	3	0.2	Excellent	106	Hunt	
BM 47	71.09.16	672.1	3	0.2	Good	106	Whiteford	467.392
	74.12.06	672.5	3	0.2	Excellent	106	Hunt	
BM 48	71.09.16	726.9	3	0.2	Good	106	Whiteford	444.271
	74.12.06	727.2	3	0.2	Excellent	106	Hunt	
BM 49	71.08.31	729.3	2	0.3	Good	106	Hunt	445.580
	74.12.06	729.6	3	0.2	Excellent	106	Hunt	
BM 50	71.08.31	795.8	3	0.2	Good	106	Hunt	422.935
	74.12.06	796.3	3	0.2	Excellent	106	Hunt	
BM 51	71.08.31	810.1	3	0.2	Good	106	Hunt	417.559
	74.12.06	810.6	3	0.2	Excellent	106	Hunt	
BM 53	71.09.16	817.7	2	0.2	Good	106	Whiteford	415.370
	71.09.17	817.4	1	0.2	Good	106	Whiteford	
	74.12.14	617.2	3	0.1	Excellent	106	Hunt	

BM	Date	g	n	s.e	Stability	Inst.	Observer	Elevation
P.H. 5	71.09.04	972.1	2	0.2	Excellent	106	Hunt	348.665
	74.12.06	972.2	3	0.2	Excellent	106	Hunt	
P. 1	71.09.04	971.5	2	0.2	Fair	106	Hunt	346.218
	75.01.23	971.3	3	0.2	Fair	106	Hunt	
P. 15	71.09.04	901.8	2	0.2	Good	106	Hunt	376.839
	74.12.06	901.8	3	0.2	Excellent	106	Hunt	
P. 36	71.09.03	901.7	2	0.2	Good	106	Hunt	384.532
	74.12.11	903.8	3	0.1	Good	106	Hunt	
P. 47	71.09.03	885.0	3	0.2	Good	106	Hunt	395.081
	74.12.11	886.3	3	0.1	Good	106	Hunt	
P. 112	68.06.11	905.7	1	0.2	Fair	106	Hunt	
	71.09.03	907.6	2	0.2	Good	106	Hunt	377.589
	74.12.11	910.6	3	0.1	Good	106	Hunt	
P. 115	68.06.11	903.6	1	0.2	Fair	106	Hunt	
	71.09.03	905.0	1	0.2	Good	106	Hunt	381.237
	74.12.11	907.5	2	0.1	Good	106	Hunt	
P. 120	71.09.04	927.3	2	0.2	Fair	106	Hunt	368.237
	74.12.06	928.0	3	0.2	Excellent	106	Hunt	
P. 125	68.06.11	889.6	1	0.2	Good	106	Hunt	
	71.09.04	891.2	2	0.2	Good	106	Hunt	381.792
	74.12.12	892.0	3	0.1	Good	106	Hunt	
P. 130	71.09.17	900.5	2	0.2	Good	106	Whiteford	379.536
	74.12.12	904.1	3	0.1	Good	106	Hunt	
P. 137A	71.09.03	862.9	1	0.2	Fair	106	Hunt	395.816
	74.12.11	865.1	3	0.1	Excellent	106	Hunt	
P. 144	71.09.04	908.4	2	0.2	Good	106	Hunt	375.6[illegible]
	74.12.11	910.8	3	0.1	Good	106	Hunt	

BM	Date	g	n	s.e.	Stability	Inst.	Observer	Elevation
P. 146	68.06.11	896.8	1	0.2	Good	106	Hunt	
	71.09.04	897.9	3	0.1	Good	106	Hunt	379.561
	74.12.12	898.7	3	0.1	Excellent	106	Hunt	
P. 147	68.06.11	908.3	2	0.2	Good	106	Hunt	
	71.09.04	910.8	2	0.2	Good	106	Hunt	373.562
	74.12.12	913.0	3	0.1	Good	106	Hunt	
P. 148	71.09.17	899.7	2	0.2	Good	106	Whiteford	379.744
	74.12.12	903.2	3	0.1	Excellent	106	Hunt	
Peg IX A	71.09.03	896.2	1	0.2	Good	106	Hunt	385.462
	74.12.11	898.6	3	0.1	Excellent	106	Hunt	
Plinth A 15 near P.66								
	71.09.03	866.8	2	0.2	Fair	106	Hunt	
	74.12.11	867.7	3	0.1	Fair	106	Hunt	
I.S. 128	71.09.03	799.5	2	0.2	Good	106	Hunt	434.611
	75.01.22	799.9	3	0.1	Good	106	Hunt	
I.S. 259	67.04.09	590.3	2	0.1	Excellent	106	Hunt	
	68.06.10	601.1	2	0.1	Excellent	106	Hunt	
	71.09.16	600.9	1	0.3		106	Whiteford	
	74.12.10	600.7	2	0.1	Excellent	106	Hunt	

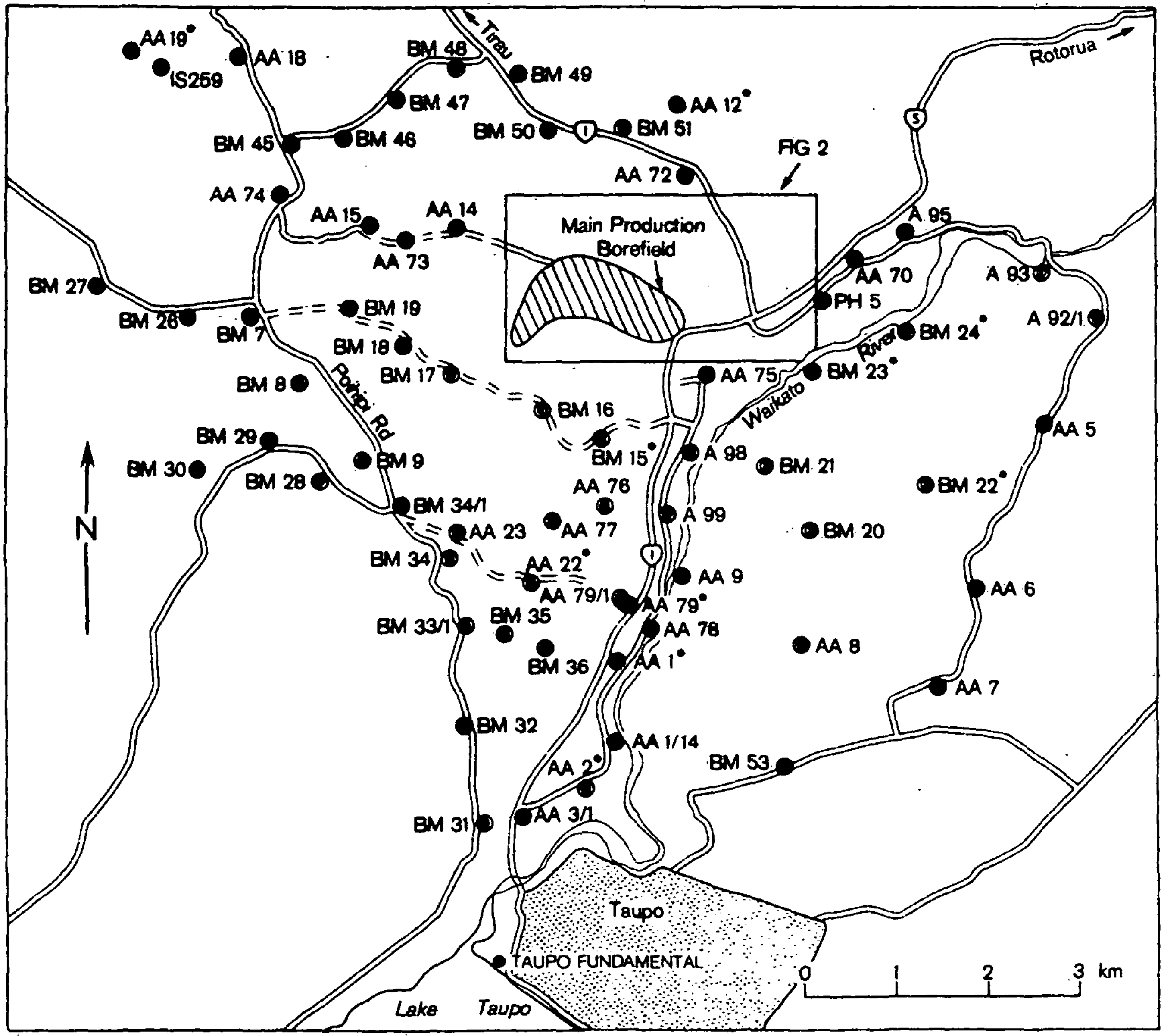

FIGURE 1: Map showing location of benchmarks used in the repeat gravity surveys. Benchmarks with an asterisk have been destroyed.

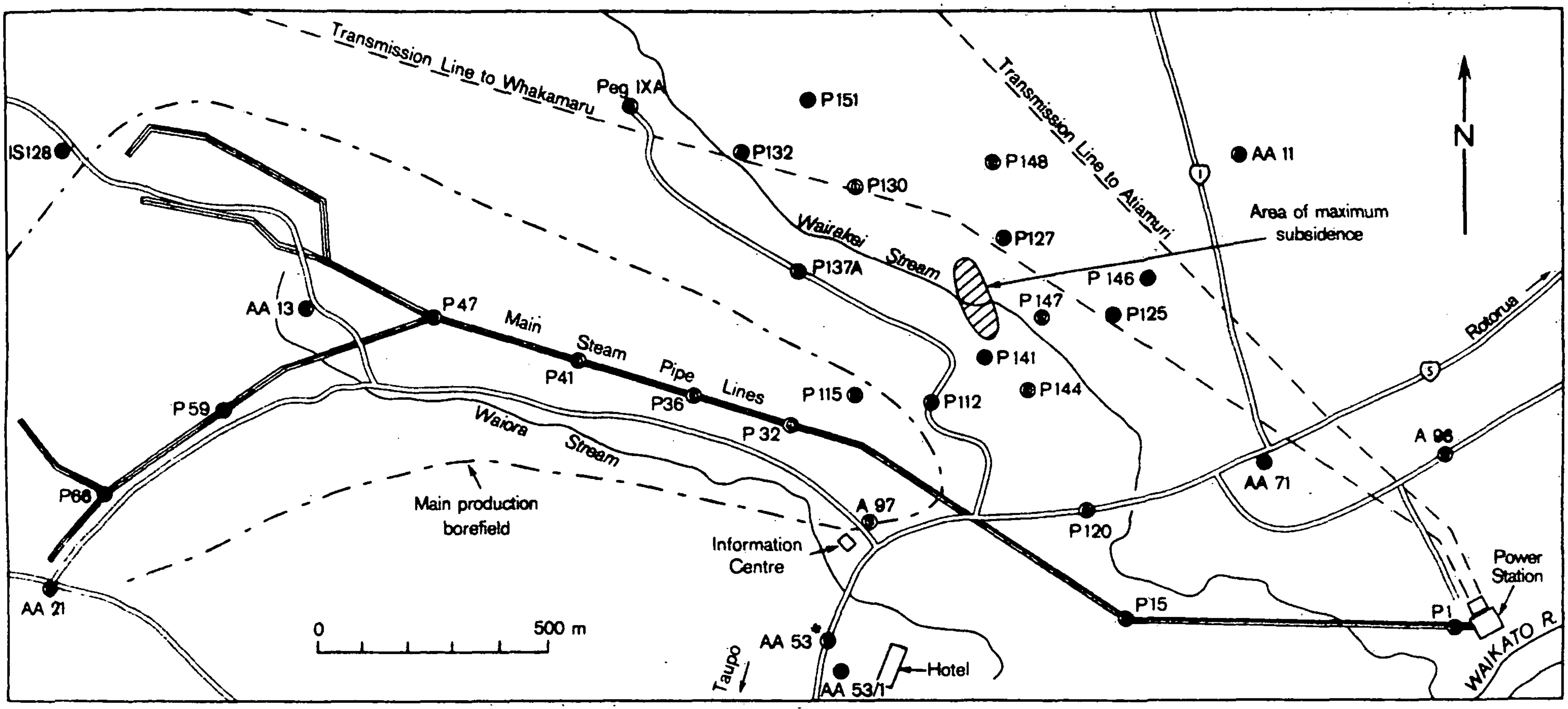

FIGURE 2: Map showing location of benchmarks in and near the main production borefield.

2

N.Z. *Journal of Geology and Geophysics Vol. 21, No. 3 (1978)*: 287–91

Hydrothermal metamorphism of the Whangakea Basalt, New Zealand

EVAN C. LEITCH

Department of Geology & Geophysics, University of Sydney, Sydney, Australia

ABSTRACT

The Cretaceous Whangakea Basalt has undergone two episodes of alteration. The earlier one pervasively affected part of the formation and produced greenschist mineral facies assemblages of the type quartz–albite–chlorite–epidote–actinolite–sphene. The later episode gave rise to zeolites, including stilbite, analcime, thomsonite, epistilbite, heulandite–clinoptilolite, and laumontite, none of which co-exist stably wth quartz. Products of the zeolitic alteration are widespread, but occur predominantly in and adjacent to veins. Calcite crystallised at a late stage in this episode. Greenschist alteration probably occurred at temperatures in excess of 320°c, whereas zeolite alteration is believed to have taken place below 165–180°c.

The Whangakea Basalt, together with an associated gabbro–peridotite body, constitute an ophiolite complex. The localised development of the greenschist alteration, the presence of relic magmatic phases, the lack of preferred orientation of the secondary minerals, and their common pseudomorphous habit suggest that this alteration resulted from hydrothermal metamorphism. Zeolitic alteration may have occurred late in this metamorphism, or may have occurred while the basaltic rocks were buried beneath some 3000 m of Tertiary strata.

INTRODUCTION

The Te Rake and Waipahirere masses comprise the more easterly of the several inliers of Cretaceous Whangakea Basalt that form the rugged headlands of northernmost New Zealand (Fig. 1). They are surrounded mainly by Tertiary and Quaternary sedimentary material and are locally intruded by middle Tertiary microdiorite bodies. I have previously described the geology of the masses and the adjacent strata (Leitch 1970). Both the Te Rake and Waipahirere masses are formed of pillowed and unpillowed basaltic flows intruded by sills and dykes of dolerite. Minor intercalations of autoclastic breccia and rare radiolarian chert occur within the dominantly extrusive piles.

This paper is concerned with the nature, origin, and significance of the alteration of the Whangakea Basalt in the two masses. Phases have been identified optically and by X-ray diffraction. Plagioclase compositions were determined with the universal stage using the curves of Slemmons (1962), and by refractive index measurements. Except where otherwise noted, zeolite identifications have been confirmed by X-ray diffraction. Refractive indices are believed accurate to ± 0·003 (± 0·002 for zeolites), and optic axial angles to ± 2°. Specimen numbers are those of the petrology collection, Department of Geology, University of Auckland.

IGNEOUS PETROGRAPHY

All of the rocks are altered, those of the Waipahirere mass almost pervasively, and those of the Te Rake mass mainly in and adjacent to veins that seam all outcrops. The following descriptions are based largely on material from the latter mass; texturally comparable rocks, believed to have had initially similar compositions, form the Waipahirere mass.

Received 17 February 1977, revised 31 October 1977

BASALT: Textures vary from perhyaline with only scattered phenocrysts of plagioclase and augite set in a dark glassy groundmass, to intersertal where glass, now usually replaced by secondary phases, occurs in interstices between subophitically intergrown augite and plagioclase. Some pillows have a variolitic texture resulting from a radial arrangement of slender labradorite laths scattered between which are small augite granules set in glass. Comb-like and aborescent clinopyroxene intergrowths with interstitial glass occur in pillow selvedges.

In most rocks plagioclase averaging about An_{60} is the most abundant magmatic phase. Phenocrysts show normal zoning from cores as calcic as An_{75} to rims of An_{50}. The phenocrysts of one specimen (9087) are spongy cores of oligoclase (An_{25}), with clear rims of labradorite, set in a hyaline groundmass containing euhedral augite phenocrysts and small clear labradorite laths. Another (9088) consists of calcic oligoclase and augite phenocrysts surrounded by an intergranular groundmass of plagioclase laths, augite granules, and opaque oxide.

Colourless clinopyroxene occurs in all little-altered basalts, typically in subhedral grains smaller than the associated plagioclase. Optical data (2V$_z$50–53°, β 1·684–1·696) indicate it is a normal augite. Specimen 9092 contains scattered microphenocrysts of bronzite (2V$_x$ 98°, $\beta < 1{\cdot}70$).

Small needles and equant grains of opaque oxide occur in most basalts and rare brown amphibole is found in the core of a variolitic pillow (9091).

DOLERITE: The dolerites, holocrystalline rocks with a hypidiomorphic-granular texture, contain the same simple primary mineral assemblage as the basalts: plagioclase, augite, and opaque oxide. Plagioclase is the most abundant phase, constituting about 60% of the rocks. The bulk of this feldspar is labradorite, with

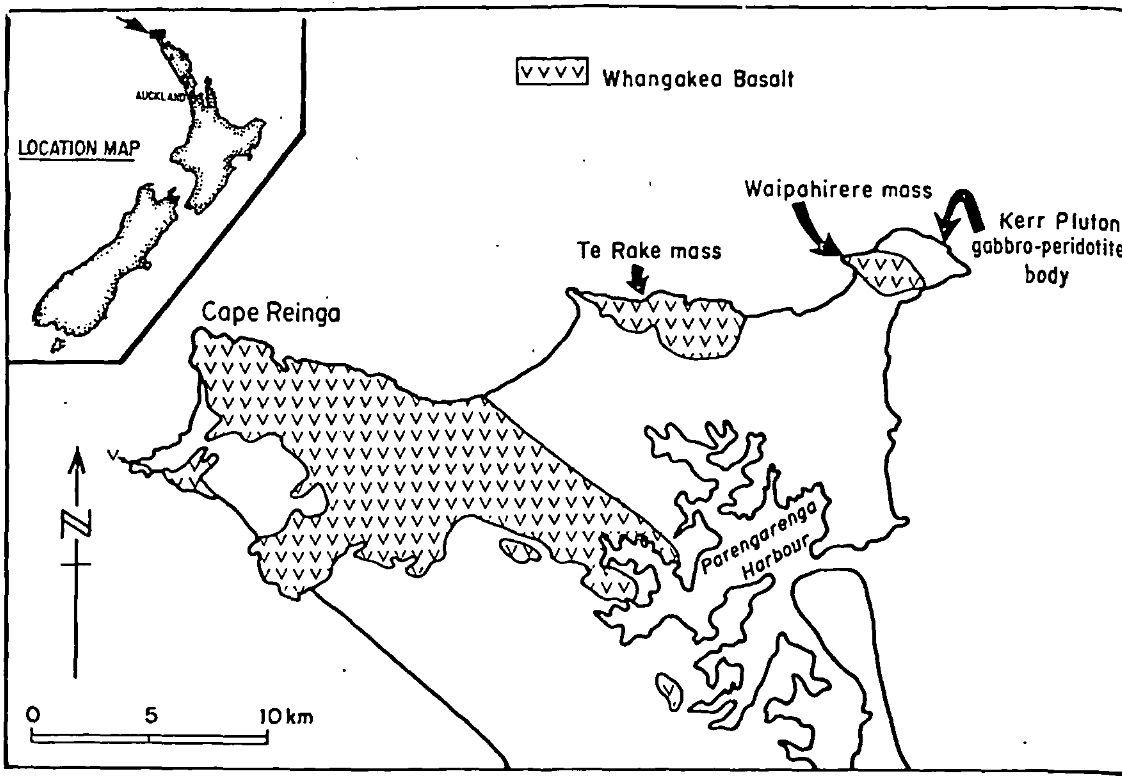

FIG. 1—Northernmost New Zealand showing location of Te Rake and Waipahirere masses.

most crystals normally zoned from cores occasionally as calcic as An_{76} to margins as sodic as An_{20}. Subhedral augite (2V$_z$ 48–52°, β 1·691–1·697) is colourless or sometimes very pale pink. Opaque oxide occurs in amounts of up to 5%, in some rocks as well-formed crystals and in others in large skeletal units. Apatite is a minor but widespread phase. Bronzite (2V$_z$ 115°, β <1·72), forms slender pale-orange to colourless pleochroic rods and constitutes 2% of specimen 9100.

Neither magmatic quartz nor olivine were found in the dolerites or basalts.

ALTERATION

Two distinct episodes of alteration of the Whangakea Basalt are recognised. The earlier episode affected only rocks of the Waipahirere mass, especially those along the northern coast of North Cape headland. It resulted in the *crystallisation of typical greenschist mineral facies* assemblages, and most rocks affected show few relic magmatic phases. Augite persists occasionally, and calcic plagioclase rarely. The textures of the rocks have, however, been little modified, except in zones of tectonic brecciation and shearing, or along major vein systems where epidosites have formed. The rocks lack schistosity or cleavage, and no preferred orientation of secondary phases has been discerned.

The second episode affected rocks of both masses. Alteration was confined largely to ramifying vein systems that criss-cross the rocks, although there was also some replacement of earlier phases found in the body of the rocks. The main products of this alteration are zeolites and calcite.

Overprinting of the zeolitic alteration on the greenschist event is clearly demonstrated by the replacement of greenschist phases, especially quartz and albite, by zeolites, and by zeolite veins cutting earlier greenschist facies veins.

Greenschist facies alteration

Typically, the products of this alteration are green rocks, composed mainly of chlorite, epidote, and actinolite. Pillow lavas frequently show a zonal arrangement of these phases, with chlorite concentrated in the cores of the pillows and epidote in the selvedges and inter-pillow interstices. In other pillows actinolite is concentrated in the outer zones.

The greenschist facies mineralogy is described below:

QUARTZ, typically in clear unstrained grains, occurs in nearly all rocks, although it has been replaced to varying degrees by zeolites during later alteration. It occupies amygdules and veins as well as being disseminated through the fabric of the rocks.

ALBITE has widely, though not completely, replaced calcium-bearing plagioclase. It has not been identified in veins or amygdules.

CHLORITE is present in most specimens, occupying amygdules and veins as well as replacing much of the bulk of the original rocks. This phase is optically negative and shows anomalous interference colours. n_{max} ranges from 1·605 to 1·612, suggesting a variation in Fe (Fe+Mg) of between about 0·28 and 0·35.

EPIDOTE occurs in all rocks. It is most common in veins, but also occupies amygdules and interpillow interstices, and occurs scattered throughout the rocks. Optical and X-ray measurements indicate it is iron-rich (Ps_{22}–Ps_{33}).

ACTINOLITE is found only in the main fabric of the rocks, where it has replaced ferromagnesium phases and glass. It is commonly intergrown with chlorite. Refractive indices (α 1·619–1·626, γ 1·646–1·650) indicate a magnesium-rich actinolite.

SPHENE is found in all rocks, generally in dark irregular aggregates.

PYRITE is a widespread, although minor, phase in veins and amygdules. It is occasionally accompanied by small amounts of chalcopyrite, the latter showing marginal replacement by digenite and chalcocite.

HEMATITE occurs mainly in narrow veins, frequently associated with pyrite.

The most common mineral assemblages, quartz–albite–chlorite–actinolite–epidote–sphene and quartz–albite–chlorite–epidote–sphene, are typical products of the greenschist facies alteration of basic igneous rocks. Alteration has mainly involved hydration of the parent rocks. The development of widespread mono-, bi-, and polymineralic veins and segregations was also undoubtedly aided by abundant hydrous fluids. Although calcite is present in some rocks, it occurs only in veins formed during or after zeolitic alteration, and the greenschist episode fluids probably contained little CO_2.

All of the greenschist phases are stable over a wide pressure interval. Only the temperature of alteration can be estimated. Replacement of calcium-bearing plagioclase by albite rather than analcime suggests temperatures exceeded 200°C (Liou 1971a). Epidote normally occurs in geothermal systems at temperatures in excess of 230°C (Muffler & White 1969; Browne & Ellis 1970; Tomasson & Kristmannsdottir 1972), although epidote in basaltic rocks from the hydrothermal system at Reykajavik is believed to have formed at temperatures as low as 135°C (Sigvaldason 1963). Keith *et al* (1968) recorded the assemblage quartz–tremolite–epidote at about 320°C in the Salton Sea geothermal system, and Browne (1969) found an amphibole he tentatively suggested was tremolite in the Broadlands field at about 275°C. The absence of prehnite and pumpellyite may be indicative of temperatures in excess of 350°C, according to the analysis of Nitsch (1971). A tentative minimum temperature of 320–350°C is thus suggested for the greenschist facies alteration.

Zeolitic alteration

The formation of zeolites and calcite are grouped together as products of zeolitic alteration, although the status of the latter phase is unclear. Calcite veins frequently cut zeolite-bearing ones, and textural relationships in calcite–zeolite veins and segregations often suggest that calcite is replacing zeolite. Thus, the crystallisation of calcite may have resulted from a third separate alteration episode, or may have occurred at a late stage during zeolitic alteration, attendant upon an increase in the mole proportions of CO_2 in the vein fluid.

Phases formed during this alteration episode are described below:

STILBITE is the most abundant zeolite and occurs both in veins and amygdules and in the fabric of the rocks. Refractive indices vary, suggesting some compositional variation (α 1·479–1·486, γ 1·487–1·497). Associated minerals are analcime, epistilbite, thomsonite, natrolite, and calcite.

ANALCIME is a common phase in amygdules and veins, and replaces earlier minerals, especially calcic plagioclase. It frequently shows low birefringence and repeated lamellar twinning. Refractive index is relatively constant (n 1·486–1·488). Associated minerals are stilbite, thomsonite, gonnardite, and calcite.

THOMSONITE is a minor, but widespread, phase. It has been found together with stilbite, analcime, gonnardite, and calcite.

GONNARDITE has been tentatively identified in specimen 9098 as a low-birefringent fibrous zeolite (α 1·499, γ 1·503) associated with analcime and thomsonite. Insufficient material was available for X-ray diffraction study.

?EPISTILBITE has been identified only from the Waipahirere mass, where an inclusion-charged zeolite replacing quartz in amygdules yields X-ray diffraction patterns appropriate to this phase. Optical properties generally support the identification, although the bifringence (α 1·492, γ 1·495) is lower than typical of epistilbite (Deer *et al* 1963, p. 377). Epistilbite is associated with heulandite–clinoptilolite and stilbite.

HEULANDITE–CLINOPTILOLITE. A zeolite yielding a diffraction pattern similar to that tabulated by Mumpton (1960) for clinoptilolite occurs occasionally in both the Te Rake and Waipahirere masses. Refractive indices (α 1·490, β 1·491, γ 1·495) are higher than those for typical clinoptilolite, and the mineral is probably an intermediate member of the heulandite–clinoptilolite series (Boles 1972). It is found associated with analcime, epistilbite, and calcite.

NATROLITE, found at only one locality, is intergrown with stilbite.

LAUMONTITE cements brecciated igneous material in both masses; it is not associated with other zeolites. Refractive indices show a small range (α 1·506–1·510, β 1·517–1·518, γ 1·519–1·521).

GREEN PHYLLOSILICATES. Moderately birefringent green and green-brown phyllosilicates are associated with other zeolitic phases, and have partially replaced ferromagnesium silicates. They have not been conclusively identified, but probably include oxidised chlorite and celadonite.

CALCITE is probably the most widespread and common secondary mineral in the Whangakea Basalt. It is found in amygdules and veins and in the fabric of the rocks replacing almost all other phases. Refractive indices indicate a composition close to pure $CaCO_3$.

Physical conditions of the zeolitic alteration are difficult to establish. Experimental data for the reaction analcime+quartz=albite are not applicable, for quartz is not a stable phase in analcime-bearing assemblages, and in silica-deficient environments analcime may exist stably to 600°C (Liou 1971a). Widespread stilbite indicates that temperatures of 165–180°C were generally not attained, for in this range stilbite dehydrates to laumontite plus quartz and water (Liou 1971b). Laumontite in the Whangakea Basalt is not associated with quartz, and the crystallisation of this phase or stilbite was probably conditioned by the activity of silica in the fluid phase present during alteration. Although these fluids appear to have been undersaturated in silica, as indicated by the instability of quartz, the presence of thomsonite, formation of which is favoured by a silica-deficient environment, and stilbite, epistilbite, and heulandite–clinoptilolite, which commonly occur associated with quartz (Coombs *et al* 1959), suggests variations in silica activity. Neither epistilbite nor heulandite–clinoptilolite have been found associated with thomsonite in the Whangakea Basalt.

Few data are available to set a minimum temperature for zeolitic alteration. The zeolite distributions found by Walker (1960a; b), in which intensity of zeolitisation decreases towards the top of thick lava piles, indicate that some elevation of temperature is necessary for the widespread development of these minerals in basaltic rocks. The distribution of laumontite in thick stratified sequences and geothermal drill holes suggests this phase forms only at temperatures above those at the Earth's surface or corresponding to shallow burial (Hay 1966).

Evidence outlined in the next section suggests that zeolitic alteration may have occurred subsequent to the Early Miocene. The lithostatic load on now-exposed Whangakea Basalt at this time is unlikely to have exceeded 0·8 kb, assuming an average density of 2·7 g/cm³ for the overlying strata.

DISCUSSION

The restricted extent of the greenschist metamorphism, the absence of a tectonic fabric, and the commonly pseudomorphous habit of secondary minerals, suggest the greenschist facies assemblages were produced by hydrothermal metamorphism in a region of highly variable heat flux. Secondary mineral assemblages very similar to those in the Whangakea Basalt have been reported from geothermal fields in California (Keith *et al* 1968) and Iceland (Sigvaldason 1963). Identical assemblages to those produced by the greenschist alteration have been recorded in rocks from the Mid-Atlantic Ridge and spreading ridges in the Indian Ocean (Bonatti *et al.* 1971; Aumento *et al.* 1971; Cann 1969; Melson & van Andel 1966). The latter are considered the result of hydrothermal alteration under a high geothermal gradient (Spooner & Fyfe 1973; Cann 1974).

Immediately east of the Waipahirere mass a grabbro–peridotite body shows a sequence from serpentinised peridotite, through layered gabbro and peridotite, to gabbro and, in its uppermost levels, sheeted dykes (Leitch 1970). This body closely resembles the well-documented Tethyan ophiolites and, although it is now in fault with Whangakea Basalt, these latter rocks would complete an ophiolite sequence (Bennett 1976). Bennett suggested that alteration of the ultramafic–mafic complex might have resulted from ocean-floor metamorphism, and drew attention to the possibility that this alteration continued up into the Whangakea Basalt. This interpretation accords with the prevalent opinion on the origin of ophiolites and is supported by the similarity of the greenschist facies assemblages to those in ocean-floor basalts and in the Lower Pillow Lavas of the Troodos Massif (Gass & Smewing 1973). However, interpretation of the Whangakea Basalt and associated mafic and ultramafic rocks as the products of early island arc magmatic activity is not precluded by the presence of hydrothermal metamorphism. Indeed, such alteration would proceed in any pervious igneous pile erupted in a marine environment, provided a heat flux sufficient to initiate and maintain convective circulation existed.

Zeolite assemblages similar to those in the Whangakea Basalt occur in basic rocks dredged from the ocean floor (Miyashiro *et al.* 1971; Aumento *et al.* 1971). It is tempting to seek the origin of the zeolitic alteration in the same hydrothermal system, with these phases forming first in the upper levels of the accreting igneous pile, and migrating deeper as the heat flux decreased. However, both analcime and laumontite occur in Miocene rocks close to the Te Rake mass, laumontite in laumontite–calcite–pyrite veins in a small microdiorite body, and analcime replacing clastic plagioclase in Lower Miocene rocks close to the edge of a similar microdiorite dyke. The zeolites may thus be the products of local phenomena arising from the cooling of the microdiorite intrusions, or alternatively may be the result of burial of the Whangakea Basalt beneath some 3000 m of sedimentary rocks in the Miocene (Leitch 1970).

CONCLUSIONS

1. The Whangakea Basalt has been affected by two episodes of alteration, the earlier producing mineral assemblages of the greenschist facies and the latter mainly zeolites and calcite.

2. Greenschist alteration occurred in a water-saturated environment at a minimum temperature of 320–350°C.

3. Zeolitic alteration took place at a temperature below 165–180°C. The accompanying fluid was undersaturated with silica, although variations occurred in the chemical potential of silica in the fluid. The mole proportion of CO_2 in the fluid remained low until towards the end of alteration.

ACKNOWLEDGMENTS

This study commenced in the Department of Geology, University of Auckland under the guidance and encouragement of Professor R. N. Brothers, to whom I am much indebted. The study continued in the Department of Geology and Geophysics, University of Sydney, and was written up during a stay in the Department of Geology, University of Cambridge. I acknowledge the use of facilities at all these institutions.

I thank Dr P. M. Black, who provided much help with X-ray diffraction; Dr D. O. Zimmerman, who aided in the identification of opaque minerals; and Dr J. R. Cann for constructive criticism of a draft of the paper.

My investigation of low-grade metamorphic rocks is supported by funds provided by the Australian Research Grants Committee.

REFERENCES

AUMENTO, F.; LONGAREVIC, B. D.; ROSS, D. I. 1971: Hudson geotraverse: geology of the Mid-Atlantic Ridge at 45°N. *Philosophical Transactions of the Royal Society, London, Series A 268*: 623–50.

BENNETT, M. C. 1976: The ultramafic-mafic complex at North Cape, northernmost New Zealand. *Geological Magazine 113*: 61–7.

BOLES, J. R. 1972: Composition, optical properties, cell dimensions and thermal stability of some heulandite group zeolites. *American Mineralogist 57*: 1463–93.

BONATTI, E.; HONNOREZ, J.; FERRARA, G. 1971: Peridotite–gabbro–basalt complex from the equatorial Mid-Atlantic Ridge. *Philosophical Transactions of the Royal Society, London. Series A, 268*: 385–402.

BROWNE, P. R. L. 1969: Sulfide mineralisation in a Broadlands geothermal drillhole, Taupo Volcanic Zone, New Zealand. *Economic Geology 64*: 156–9.

BROWNE, P. R. L.; ELLIS, A. J. 1970: The Ohaki–Broadlands hydrothermal area, New Zealand: mineralogy and related geochemistry. *American Journal of Science 269*: 97–131.

CANN, J. R. 1969: Spilites from the Carlsberg Ridge, Indian Ocean. *Journal of Petrology 10*: 1–19.

——— 1974: A model for oceanic crustal structure developed. *Geophysical Journal of the Royal Astronomical Society 39*: 169–87.

COOMBS, D. S.; ELLIS, A. J.; FYFE, W. S.; TAYLOR, A. M. 1959: The zeolite facies with comments on hydrothermal synthesis. *Geochimica et Cosmochimica 19*: 53–107.

DEER, W. A.; HOWIE, R. A.; ZUSSMAN, J. 1963: "Rock-forming minerals". Vol. 3. John Wiley & Sons, New York.

GASS, I. G.; SMEWING, J. D. 1973: Intrusion, extrusion and metamorphism at constructive margins: evidence from the Troodos Massif, Cyprus. *Nature 242*: 26–9.

HAY, R. L. 1966: Zeolites and zeolitic reactions in sedimentary rocks. *Geological Society of America, Special Paper 85*: 1–130.

KEITH, T. E. C.; MUFFLER, L. J. P.; CREMER, M. 1968: Hydrothermal epidote formed in the Salton Sea geothermal system, California. *American Mineralogist 53*: 1635–44.

LEITCH, E. C. 1970: Contributions to the geology of northernmost New Zealand: II—The stratigraphy of the North Cape district. *Transactions of the Royal Society of N.Z., Earth Sciences 8*: 45–68.

LIOU, J. G. 1971a: Stilbite-laumontite equilibrium. *Contributions to Mineralogy and Petrology 31*: 171–7.

——— 1971b: Analcime equilibria. *Lithos 4*: 389–402.

MELSON, W. G.; VAN ANDEL, TJ. H. 1966: Metamorphism in the Mid-Atlantic Ridge, 22°N latitude. *Marine Geology 4*: 165–86.

MIYASHIRO, A.; SHIDO, F.; EWING, M. 1971: Metamorphism in the Mid-Atlantic Ridge near 24° and 30° N. *Philosophical Transactions of the Royal Society, London, Series A, 268*: 589–603.

MUFFLER, L. J. P.; WHITE, D. E. 1969: Active metamorphism of Upper Cenozoic sediments in the Salton Sea geothermal field and the Salton Trough, Southeastern California. *Geological Society of America Bulletin 80*: 157–82.

MUMPTON, F. A. 1960: Clinoptilolite redefined. *American Mineralogist 45*: 351–69.

NITSCH, K. H. 1971: Stabilitätsbeziehungen von Prehnit und Pumpellyite—haltigen Paragenesen. *Contributions to Mineralogy and Petrology 30*: 240–60.

SIGVALDASON, G. E. 1963: Epidote and related minerals in two deep geothermal drillholes, Reykajavik and Hveragerdi, Iceland. *U.S. Geological Survey Professional Paper 450-E*: E77–9.

SLEMMONS, D. B. 1962: Determination of volcanic and plutonic plagioclases using a three-or-four-axis universal stage. *Geological Society of America, Special Paper 69*: 1–64.

SPOONER, E. T. C.; FYFE, W. S. 1973: Sub-sea-floor metamorphism, heat and mass transfer. *Contributions to Mineralogy and Petrology 42*: 287–304.

TOMASSON, J.; KRISTMANNSDOTTIR, H. 1972: High temperature alteration minerals and thermal brines, Reykjanes, Iceland. *Contributions to Mineralogy and Petrology 36*: 123–34.

WALKER, G. P. L. 1960a: Zeolite zones and dike distribution in relation to the structure of the basalts of eastern Iceland. *Journal of Geology 68*: 515–28.

——— 1960b: The amygdale minerals in the Tertiary lavas of Ireland. III. Regional distribution. *Mineralogical Magazine 32*: 503–27.

GEOTHERMAL

Rec'd from Isherwood Mar. 1/76

K. L. Cook

PISA 1970 IV/27 DIST. LIMITED

UNITED NATIONS SYMPOSIUM
on the
DEVELOPMENT AND UTILIZATION OF GEOTHERMAL RESOURCES

Proof

Seismic, Gravity and Magnetic Studies, Broadlands Geothermal Field, New Zealand

M. P. HOCHSTEIN * T. M. HUNT *

AREA
NZ
broad

ABSTRACT

Information about structural features within the Broadlands Field was sought using detailed seismic, gravity and magnetic surveys. Seismic measurements using the refraction method show the presence of several dome-shaped structures (rhyolite domes) but the greywacke basement could not be outlined. The gravity and magnetic surveys have been of little use in mapping structural features within the volcanic overburden. A residual gravity anomaly of up to +10 mgal covers most of the Broadlands Field and is mainly caused by densification of the rocks within the field brought about by hydrothermal alteration of various rocks. This anomaly makes it difficult to determine the basement relief beneath the Broadlands Field. Magnetic measurements give no information about the extent of the thermal area at depth. Volcanic rocks from inside the field were found to be non-magnetic.

Introduction

Exploration of geothermal areas is at present governed by various structural concepts, and those of importance for geophysical exploration are:

a) Geothermal systems in sedimentary and volcanic environments are located above fissure zones or major faults, both presumably related to basement tectonics;

b) secondary fissures and minor faults at shallow depths must be tapped for exploitation;

c) geothermal systems in a volcanic environment are associated with non-magnetic volcanic rocks.

Following these concepts seismic, gravity and magnetic methods have been used to detect basement and aquifer structures and the structure of magnetic and non-magnetic rocks of geothermal areas in Italy, Japan, Mexico, New Zealand and El Salvador. Results of such structural investigations for some geothermal regions in Italy have been presented by CASSINIS (1961), VECCHIA (1961), BATTINI and MENUT (1964) and MOUTON (1969); for thermal areas in Japan, by HAYAKAWA and MORI (1962), NOGUCHI (1966) and HAYAKAWA, TAKAKI and BABA (1967). Results of similar investigations in New Zealand have been published by BECK and Ro-

* Geophysics Division, Department of Scientific and Industrial Research, Wellington, New Zealand.

HERTON (1955), MODRINIAK and STUDT (1959) and STUDT (1959) for the Wairakei Field, by STUDT (1958) for the Kawerau Field and STUDT (1963) for the Waiotapu Field. A summary of structural investigations by geophysical methods in New Zealand has been given by STUDT (1964).

On the whole the success of these structural investigations has been limited. In some cases a generalised picture of the basement structure could be obtained from gravity and from seismic surveys but fissures and faults at shallow depths could not be detected. Magnetic surveys revealed anomalies which could be explained by the presence of non-magnetic rocks associated with thermal areas, but similar anomalies often occurred nearby. As a result of this, a swing towards more direct methods of geothermal exploration took place in New Zealand, and from 1960 onwards mapping of thermal areas has been undertaken by electrical and temperature methods (HATHERTON, MAC DONALD, THOMPSON, 1966).

The extent of the Broadlands Geothermal Field was first outlined by resistivity measurements in 1965 (also RISK, MAC DONALD, DAWSON, 1970) which led to the drilling of the first exploratory wells (BR 1, 2). Early drilling results showed that only certain areas inside the field, as defined by the resistivity low, were productive. At this point it was again thought worthwhile to use detailed seismic, gravity and magnetic measurements to find out if productive areas inside the Broadlands Field could be located.

Seismic measurements

METHOD

The structure of a few geothermal areas in New Zealand has been investigated by reflection and refraction methods, and some results of these studies have been published for the Kawerau Field (STUDT 1958) and for the Wairakei Field (MODRINIAK, STUDT 1959). In both cases the measurements were not very successful, a result which was attributed to the disturbing ground noise and the unusually high attenuation of seismic waves in these areas.

Seismic reflection tests made at the end of 1966 in the vicinity of the Broadlands Area were also discouraging. It was found that reflecting horizons had limited lateral extent, a few hundred metres at the most, and that reflecting interfaces could not be correlated. Using multiple shotpoint and geophone arrays did not significantly improve the quality of the seismic records.

On the other hand, seismic refraction measurements in the same test area showed that at least one interface could be traced, and mapping of various interfaces by the refraction method was started in 1967. The aim of this survey was to determine the structure of the volcanic rocks, to locate major faults, and to find out whether the attenuation and velocity of seismic waves in volcanic rocks within a thermal area differ from those outside (the term velocity will be used for compressional wave velocity throughout).

The main part of the seismic survey consisted of mapping volcanic interfaces down to a depth of about 0.7 km. Seismic profiles were made up by a series of 2.3 km long 'reversed lines' (spread length .775 km) which during the later part of the survey overlapped the adjacent ones by about 60%. The total length of the seismic sections was about 38 km. Shot depths and charges were 5 m and 1 kg, 15 m and 4.5 kg, and 15 m and 9 kg for shotpoint-to-receiver distances up to .775, 1.55 and 2.3 km respectively. A water table at a depth of about 3 to 4 m guaranteed good input of energy at the shotpoint. The signals were picked up by 10 Hz refraction geophones (Kipp HV-1) and recorded by an SIE PT-100 refraction-reflection unit yielding standard « wiggle-trace » seismograms. In order to determine the depth of the greywacke basement, observations were made along partly reversed segments of profiles up to 7 km long, for which shot depths of about 25 m and charges up to 50 kg were used.

Interpretation

An analysis of the seismic records showed that refracted arrivals from several interfaces had been recorded. Anticipating results discussed later, these interfaces separate velocity layers which can be correlated with geological formations as follows: velocity v_1-layer = = near surface pumice, v_2-layer = pumice-siltstone sequence, v_3-layer = rhyolites and v_4-layer = dense rhyolites (eastern part of field).

The depth and the velocity of the v_1-layer beneath each geophone were obtained using the « plus-minus » method (Hagedoorn 1959). This layer (v_1 = 0.4 to 1.2 km/s, depending on thickness) was over most of the area less than 20 m thick, except for some old channels of the Waikato River where thicknesses of up to 75 m were found. The combined effect of this low velocity layer, and of shotpoint depth and elevation was eliminated by following a procedure similar to that described by Dobrin (1960), and the resulting reduced travel times were then split into delay times (Gardner 1939). Migration of delay time vs distance profiles included various trial and error loops since the velocity of deeper layers varied laterally, and no assumptions about the extent of the refracting layers could be made.

The thickness of the v_2-layer (v_2 = 1.7 to 1.9 km/s) was obtained for each geophone position, taking into account a small increase in velocity v_2 with depth. Seismic sections similar to those shown in Figure 2 were finally constructed. For the interpretation of arrivals coming from deeper interfaces or from the greywacke basement, constant velocities and plane interfaces had to be assumed.

DISCUSSION OF RESULTS

Attenuation. Values for the attenuation constant α were calculated from energy vs distance plots, assuming that the refracted pulse of the compressional wave travelling through the water-saturated pumice cover (v_2-layer) is similar to that of a body wave, and using an empirical correction for geometrical spreading (HOWELL, KAUKONEN 1954). It was found that inside the geothermal area over distances of 0.3 to 0.6 km, the attenuation constant varies between 1 and 20×10^{-3}/m (frequency of refracted pulse between 20 and 50 Hz) with the highest values occurring in the vicinity of warm and steaming ground, and that α increases at greater distances (0.6 to 1 km), which points to an increase of attenuation with depth. Outside the thermal area α is less than $2 \times {}^{-3}$/m. Although high attenuation is characteristic of thermal areas, little use could be made of this parameter for geothermal prospecting, since a different set of values was obtained when shotpoint and receiving positions were interchanged.

A different mechanism of attenuation is apparently connected with steep subsurface scarps within or near to the Broadlands Field. For more than 60% of those profiles crossing such features no refracted arrivals could be observed. In the few cases where refracted arrivals were found, they were accompanied by a strong decrease in amplitude.

Rhyolite structure. A contour map of the depths of the refracting interface underlying the pumice-tuff-siltstone sequence was constructed from 10 seismic sections (Figure 1). This map shows that two large and two small seismic structures occur in the Broadlands region at shallow depths (0.05 to 0.5 km). Drilling has shown that the larger structures are rhyolite domes; holes drilled on top of the western dome (Ohaki Dome) produce steam, whereas only limited production has so far been obtained from holes over the eastern dome (Broadlands Dome). No vertical displacement ($>$ 45 m), indicating a major fault, has been found on the rhyolite surface; the only possible exception is a displacement between H3 and H4 (Figure 2) which, however, can also be explained by an undetected lateral change of the rhyolite velocity.

There is some disagreement between the depth of the rhyolite surface as given by core logs and that from seismic studies. The top of the v_3-layer is about 60 m deeper than the logged rhyolite surface; however, the agreement becomes much better if one takes the depth of the more solid rhyolite instead (HEALY pers. comm.).

From the seismic studies it was found that the velocity of the rhyolites increases laterally towards the centres of the domes. The highest part of the Ohaki Dome is marked by a velocity of about 3.0 km/s whereas on the lower part of the flanks the velocity drops to about 2.5 km/s; a similar, but less marked, change also occurs in the Broadlands Dome (Figure 1). The core logs indicate that rhyolites in the central parts of the domes are more thermally altered than those on the flanks. The decomposed appearance of the highly altered rhyolite samples did not suggest that the seismic velocity of such material would be higher than that of fresh rhyolite. However, subsequent measurement of velocities by an ultrasonic pulse method showed that this was the case. Tests on 5 representative samples of Ohaki Rhyolite from depths of 0.3 to 0.4 km gave a velocity of 2.6 km/s in slightly altered rhyolite, increasing to 3.65 km/s in highly altered material. Hence velocity variations as shown in Figure 1 can be explained by changes in rank of thermal alteration.

The structural interpretation as presented in Figure 1 is the result of a number of surveys, and has been successively modified. The Ohaki and Broadlands Dome were originally detected by a survey which comprised only 4 profiles. The steep scarps to the West and East of the Ohaki Dome were first interpreted as faults, into the southern extensions of which BR5 and BR6 were drilled. The failure of these holes to produce steam led to further seismic surveys. The extent of the Broadlands Dome was outlined only recently, when it was realised that refracted arrivals from the top of this structure had not been observed during the earlier studies, and that in the earlier interpretation arrivals from deeper interfaces had been picked instead. Additional seismic profiles having sufficient overlap finally allowed the identification of scarps and led to the interpretation shown in Figure 1.

Deeper Structures. On some profiles arrivals with a velocity greater than 3.0 km/s could be identified but in most cases they could not be correlated over more than two spreads, and the velocity control in each case was poor. Two interfaces at a depth of 0.65 km under the Broadlands Dome provided a solution for isolated wide angle reflections. At present we believe that the v_4-layer under the Broadlands Dome ($v_4 = 3.4$ to 4.0 km/s) is associated with dense rhyolite flows (Figure 2).

Originally it was planned to map the greywacke basement under the Broadlands Field from a profile on the Kaingaroa Plateau. Here, about 8 km East of the Broadlands Road, the near-horizontal surface of the greywacke basement (velocity 4.3 to 4.8 km/s) was found at 350 m above sea level under a 250 m thick cover of ignimbrite (velocity 3.0 to 3.4 km/s). All attempts to trace this surface westwards, beyond the Kaingaroa scarp, failed. Even under optimum conditions no refracted arrivals could be observed West of the scarp from shots fired on the eastern side, and vice versa. Similarly, no arrivals from the greywacke basement could be observed inside the geothermal field except for a small area halfway between holes BR6 and BR10. These results point to a strong attenuation of seismic waves under the Broadlands geothermal area and the Kaingaroa scarp. On the other hand, good basement arrivals were recorded along spreads to the North and South of the Broadlands Dome, the shotpoint and receiving station being separated by the geothermal field. An analysis of the basement velocities showed that the apparent dip of the greywacke in a North-South direction outside the Broadlands area does not exceed 8°; the data, however, are insufficient for any depth calculation.

Gravity measurements

Gravity anomalies

Gravity measurements have been used in New Zealand to determine the depth of the greywacke basement beneath the volcanic cover rocks at Kawerau (Studt 1958), at Wairakei (Modriniak, Studt 1959) and at Waiotapu (Studt 1965). The positive residual gravity anomalies (of up to 10 mgal), found to be associated with these geothermal areas, have been attributed to basement uplift.

In the Broadlands area, 656 gravity stations were established with a La Coste-Romberg gravimeter, and linked to base stations of the New Zealand Primary Gravity Network (Robertson, Reilly 1960). Of these stations, 371 were at benchmarks levelled to 2nd order standard, and the elevations of the remaining 285 gravity stations were determined using a tacheometer. Bouguer gravity anomalies (Figure 3) were calculated using a rock density of 2.67 g/cm^3. Topographic corrections were made to a radius of 167 km and theoretical values of gravity were obtained from the International Gravity Formula 1930. The maximum error in the Bouguer anomalies has been estimated as 0.1 mgal.

In order to separate the gravity effects of density variations within the Broadlands area from those outside, regional gravity anomalies, presumably caused by density changes at great depths ($>$ 5 km), have been subtracted from the Bouguer gravity anomalies. The regional anomalies used were those published by Modriniak and Studt (1959), but corrected by about 5 mgal to put all values on the same datum. The resultant residual gravity anomalies (Figure 4) therefore reflect lateral density variations mostly in the top 5 km within the Broadlands area.

Density variations

The mean densities of the geological rock units are shown in Table 1, and it can be seen that no individual rock unit of the volcanic cover has a significant density contrast with its neighbours, except perhaps the Broadlands Rhyolite. The gravity method is therefore of little use in determining structures within the volcanic cover.

Density measurements of cores from drillholes suggested that hydrothermal alteration causes lateral density variations within a single rock unit. At present

TABLE 1 *Mean wet density of geological rock units, Broadlands Geothermal Field.*

	Geological Unit (1)	*Lithology* (1)	*Thickness* (1) (m)	*No. of Samples*	*Mean Wet Density* (g/cm³)	(s) (g/c
Volcanic cover rocks	Taupo Pumice, Hapatangi Pumice Waiakei Breccia	pumice alluvium, ash showers sand, tuff and breccia	30-96	8	1.79	(0.[illegible]
	Huka Falls Formation	siltstone, grit, tuff beds	30-300	36	1.83	(0.[illegible]
	Ohaki Rhyolite	rhyolite	0-425	93	2.10	(0.[illegible]
	Upper Waiora Formation	tuff-breccia, lapilli, siltstone	185-275	67	2.01	(0.[illegible]
	Broadlands Rhyolite	rhyolite	0-685	58	2.44	(0.[illegible]
	Rautawiri Breccia	coarse breccia of rhyolite, pumice and	150-275	79	2.21	(0.[illegible]
	Rangitaiki Ignimbrite	ignimbrite	30-425	31	2.36	(0.[illegible]
	Upper Waikora Formation	ignimbrite and welded tuff	0-60	3	2.59	(0.[illegible]
	Lower Waiora Formation	sandstone, grit & conglomerate beds	0-105	10	2.27	(0.[illegible]
	Lower Waikora Formation	ignimbrite and welded tuff	0-90	10	2.48	(0.[illegible]
	Wairakei Ignimbrite	sandstone, grit & conglomerate	45+	2	2.37	(0.[illegible]
	Basement	massive indurated greywacke and argillite		8	2.61	(0.6

(1) After GRINDLEY, (this issue).

TABLE 2 — *Variation in Mean Wet Density with Rank of Hydrothermal Alteration of the Ohaki Rhyolite, Upper Waiora Formation, Broadlands Rhyolite, and Rautawiri Breccia, in the Broadlands Geothermal Field.*

Rock Unit	*« Unaltered »* (No or only minor hydrothermal alteration. Only partial replacement of primary materials).			*« Low Rank Alteration »* (Partial or complete replacement of primary minerals. Presence of secondary minerals such as albite, epidote, calcite, quartz, sericite & hydromica).			*« High Rank Alteration »* (Presence of secondary adularia, together with epidote, albite, wair[akite] and hydromica).		
	n	mean (g/cm³)	s. d. (g/cm³)	n	mean (g/cm³)	s. d. (g/cm³)	n	mean (g/cm³)	s. d. (g/cm³)
Ohaki Rhyolite	*(41)*	2.10	*(0.14)*	*(27)*	2.13	*(0.24)*	*(12)*	2.27	*(0.13)*
Upper Waiora Formation	*(23)*	1.85	*(0.18)*	*(29)*	2.01	*(0.15)*	*(12)*	2.28	*(0.20)*
Broadlands Rhyolite	*(10)*	2.21	*(0.07)*	*(32)*	2.42	*(0.21)*	*(4)*	2.55	*(0.09)*
Rautawiri Breccia	*(3)*	2.01	*(0.04)*	*(50)*	2.20	*(0.15)*	*(17)*	2.26	*(0.18)*

Explanation of columns: n = number of samples, mean = mean wet density, s.d. = standard deviation.

three degrees of hydrothermal alteration are recognised from examination of the mineralogy and texture of the rock. A plot of mean density against rank of hydrothermal alteration for the best sampled rock units (Figure 5, Table 2) shows that there is a significant increase in density with increase in rank of hydrothermal alteration, and that there is a density contrast of 0.3 to 0.4 g/cm³ between hydrothermally altered and unaltered rocks of the same geological rock unit. The mean density of unaltered volcanic rocks, weighted with respect to the maximum thickness of each unit, is 2.15 g/cm³, and the density contrast between the unaltered volcanic cover rocks and the greywacke basement rocks is about 0.5 g/cm³.

Residual gravity anomalies in the Broadlands Geothermal Area will therefore reflect mainly:

— changes in the depth of the greywacke basement, the volume of altered rocks within the volcanic cover rocks and their degree of hydrothermal alteration.

INTERPRETATION OF THE RESIDUAL GRAVITY ANOMALIES

Seismic measurements have provided little information about the depth of the greywacke basement beneath the Broadlands area, and only four drillholes BR7, 10, 15, 16, have reached basement. Assuming that the relief of the greywacke basement can be approximated by a simple geometrical model and that density variations within the basement can be neglected, the residual gravity anomalies can be separated into two components: first order residual anomalies reflecting mainly changes in depth of basement, and second order residual anomalies reflecting marked lateral density variations resulting from hydrothermal alteration within the volcanic rocks. The first order residual gravity anomalies (Figure 6) have been obtained by interpolating the residual gravity anomalies from the margins across the Broadlands Geothermal Field, and sesond order residual anomalies (Figure 6) determined by subtraction. The justification for the assumption that the basement topography can be approximated by a simple geometrical model is shown in Figure 7. In this figure the gravity anomaly produced by a sequence of fault-block structures, with height and width comparable to the thickness of cover rocks (model A), is about the same as that produced by a smooth basement surface (model B). It is of interest to note that although the gravity method is insensitive to such local variations in depth of the basement, it is, nevertheless, sensitive to changes in the angle of dip of the « averaged basement surface ».

The first order residual gravity anomalies can be used to determine the average slope of the greywacke basement beneath the Broadlands area, assuming the basement can be approximated by a « two-dimensional » model, and neglecting the gravitational effect of the thin (250 m) volcanic cover East of the Kaingaroa scarp. From a section (X-Y) perpendicular to the contours, the model B shown in Figure 7 has been derived, the gravity effect of which is similar to the first order residual anomalies. This suggests that the « averaged basement surface » dips at 20° (± 5°) N.W. If fault-block structures were superimposed on this averaged surface then they could have wavelengths and amplitudes as great as half the depth of the overburden without being detectable by gravity measurements. The difference at the surface of about 5 mgal between the observed and calculated anomalies is probably due to an error in the determination of the regional gravity anomaly values but this discrepancy does not affect the interpretation.

The second order residual gravity anomaly forms an elliptical high with the greatest value of + 10 mgal between drillhole BR7 and Broadlands Road (Figure 6). This anomaly may be due in part to the Broadlands Rhyolite Dome and to the basement surface being close to the surface in this area, or to a local increase in the density of the volcanic rocks or the basement rocks. Drillholes (BR7, 10) in the vicinity of the anomaly show that the anomaly cannot be explained by the basement being close to the surface, nor can the anomaly be entirely accounted for by density variations within the basement without assuming unreasonably high densities (3.7 g/cm³). Calculations have shown that only about 2 mgal of the second order residual anomaly can be attributed to the Broadlands Rhyolite Dome as detailed by the seismic measurements (Figure 1). Hence the major part of the second order residual gravity anomaly must be due to a local increase in density within the volcanic cover rocks resulting from hydrothermal alteration. The shape of the anomaly contours suggests that they result from bodies having nearly radial symmetry, which have been approximated by three vertical cylinders. Taking a density contrast of + 0.4 g/cm³ between hydrothermally altered and unaltered volcanic cover rocks, as suggested by the density measurements, gravity anomalies (due to this pattern of regular bodies) were calculated using the method of REILLY (1969) and are shown in Figure 8. The reasonably close fit between the observed and calculated anomalies implies that the volume occupied by the hydrothermally altered rocks at Broadlands can be approximated by three vertical cylinders, one of radius 1 km, centred near drillhole BR16, and two smaller cylinders of radius 0.5 km, centred near drillhole BR9 and South of BR5, extending between the basement and the surface. The total volume of hydrothermally altered rocks suggested by these models is about 5 km³.

Magnetic measurements

Magnetic measurements were used in geothermal exploration in New Zealand as early as 1937 (WATSON-MUNRO 1938). These studies together with later, more detailed surveys (STUDT 1958, 1959; MODRINIAK, STUDT 1959) have shown that areas of negative magnetic anomalies often coincide with thermal areas, but a direct relationship between magnetic anomalies and the occurrence of geothermal steam has not been established.

TOTAL FORCE ANOMALIES

Total magnetic force (F) measurements were made at each gravity station in the Broadlands area using a proton-precession magnetometer. Diurnal correlations were obtained by repeating measurements at two base station and the accuracy of the reduced measurements is about ± 20 gamma. In order to obtain total force magnetic anomalies normal field values derived from BURROWS (1967) were subtracted from the reduced measurements.

It can be seen from a profile across the northern part of the Broadlands area (AB, Figure 9) that the magnetic anomalies can be separated into two parts: a smooth first order anomaly of long wave length ([illegible] 1 km) with an amplitude of several hundred gamma and an irregular second order anomaly of short wave-length (up to 200 m) with amplitudes of up to one hundred gamma. A map of the first order component is shown in Figure 10, which was constructed from smoothed profiles such as that shown in Figure 9.

Magnetic properties of rocks from the Broadlands Geothermal Field

The volume susceptibility of cores obtained from deep drillholes has been measured and the distribution of volume susceptibility with depth is summarised in Figure 11, which clearly shows that the bulk of the rocks so far sampled within the geothermal field have practically no susceptibility. Although magnetic rocks have been encountered in drillhole BR5, samples of these formations from other bores have no magnetisation, and hence none of the geological formations so far encountered in the Broadlands Field can be mapped by magnetic methods.

In order to investigate the short wavelength magnetic anomalies, several shallow holes were drilled from which cores were obtained down to a depth of about 20 m. Most of the cores measured have volume susceptibilities greater than 100×10^{-6}, and the intensity of remanent magnetisation varies between 0 and 200×10^{-6} e.m.u. These measurements show that there is considerable variation in the magnetisation of the soil and tephra in the upper 20 m, and that this material has a much greater magnetisation than the rocks below.

Interpretation of first order magnetic anomalies

The map of the first order total force magnetic anomalies (Figure 10) reveals two magnetic highs and one magnetic low. The magnetic high West of the Broadlands area suggests the presence of magnetic rocks West of State Highway No. 5, but no information is yet available on the magnetic properties of rocks in this area.

There is no surface expression that might account for the second magnetic high, between Broadlands Road and Allen Road, and subsurface information is limited. There does not appear to be any direct relationship between the second order residual gravity anomaly centred near drillhole BR7 and this magnetic high. However it is possible that this high may be caused by a portion of the Broadlands Rhyolite Dome which has retained its magnetisation. Assuming that the bulk of the source rock has a total magnetisation of 2.3×10^{-3} e.m.u., a representative mean for rhyolites according to MOHRSAM and STEDE (1959), magnetic effects of various vertical cylinders were computed (REILLY 1969). These calculations show that a vertical cylinder of radius 1 km, having an upper surface at a depth of 0.2 km and a lower surface at 1.2 km, would produce a magnetic anomaly similar to that observed.

It is possible that the magnetic anomaly could be due to a thinner, disk-like body if the magnetisation of the source rocks was greater than that assumed above. High magnetisations have been found in rhyolites taken from a depth of 1.2 km in drillhole BR16. These rocks have a low volume susceptibility of 50×10^{6} but an unusually high intensity of remanent magnetisation of 5.7×10^{2} e.m.u.

The magnetic low between the two magnetic highs is probably due to the absence of magnetic rocks. Model calculations have shown that the magnetic low cannot be caused entirely by non-magnetic material within the Broadlands Geothermal Field itself (as defined by resistivity boundary (RISK, MACDONALD, DAWSON 1970)) and that non-magnetic material extends well beyond the field. Although part of this negative magnetic anomaly may result from hydrothermal alteration of magnetic rock to non-magnetic rock, the magnetic low is of little value in outlining the hydrothermal system at depth because it is not confined to the present field.

INTERPRETATION OF SECOND ORDER MAGNETIC ANOMALIES

There were insufficient magnetic measurements to enable a map of the second order anomalies to be drawn. The presence of magnetic material in the top 20 m, as shown by samples from shallow drillholes, suggests that these rocks are responsible for the irregular second order anomalies, and theoretical calculations have confirmed this.

Conclusion

Seismic refraction measurements in the Broadlands Geothermal Area have shown the presence of several rhyolite domes covered by a pumice-tuff-siltstone sequence. No major faults (throw > 45 m) could be identified. Features initially thought to be major faults are most likely steep scarps over which there is a high loss of seismic energy. No coherent structures inside the field at depths greater than 1 km could be mapped because of high attenuation which, in the vicinity of thermal ground, increases with depth. Observed changes in compressional wave velocity of rhyolites can be explained by changes in rank of hydrothermal alteration.

The gravity method is of little use in mapping the geological formations within the volcanic overburden. A generalised picture of the basement relief was derived from first order residual gravity anomalies but details of the postulated basement fault-block structure could not be obtained because of the insensitivity of the method in outlining structures of small lateral extent. The detection of basement relief under the field is also prevented by the masking effect of second order anomalies (up to + 10 mgal) caused by lateral density variations within the volcanic rock sequence. These anomalies are centred above the rhyolite domes as mapped by the seismic measurements. Core studies have shown that there is an increase in density of up to 0.4 g/cm^3 with increase in rank of hydrothermal alteration in the volcanic rocks. After subtracting the small effect of the rhyolite domes, it was found that the second order residual gravity anomalies can be entirely explained by the presence of hydrothermally altered rocks within the volcanic cover. This interpretation differs from that of earlier studies of other geothermal areas in New Zealand, in which positive residual gravity anomalies were attributed to basement uplifts. The distribution of altered rocks, as defined by the second order anomalies, presumably outlines centres where mineral deposition, and hence upflow, has been a maximum, and since present day surface discharge still takes place in the vicinity of these centres, the results imply stable conditions for the Broadlands hydrothermal system throughout the past.

There is good evidence from core studies that volcanic rocks inside the field are non-magnetic. A northwest-Southeast aligned negative magnetic anomaly in the vicinity of the Broadlands Area is of little value in outlining hydrothermally altered non-magnetic rocks at depth; a positive anomaly to the East is probably connected with unaltered rhyolites on the eastern flank of the Broadlands Dome. A thin nearsurface magnetic layer occurs throughout the field.

Interpretation of seismic, gravity and magnetic measurements has shown that within the Broadlands Geothermal Field, as defined by resistivity boundaries, productive areas cannot be outlined by these methods. However, the studies suggest that there is a « direct » connection between the volcanic structure (rhyolite extrusions) and secular rising of thermal waters. These results give little support to the structural concepts outlined in the introduction, and cast doubts on the utility of these concepts as a guide to the finding of geothermal steam.

Acknowledgements

The assistance of various members of the Geophysical Survey, Geophysics Division, D.S.I.R., in making the measurements in the field and in the laboratory is acknowledged.

REFERENCES

BATTINI F., MENUT P. 1964 — Étude structurale de la zone de Roccastrada en vue de la recherche de vapeur par les méthodes géophysiques, gravimétriques et électriques. *U.N. Conf. New Sources Energy, Rome*, *73*.

BECK A. C., ROBERTSON E. I. 1955 — Geothermal steam for power in New Zealand (Compiled by L. I. Grange). Chapter II: Geology and Geophysics. *Bull. N.Z. Dep. sci. industr. Res.*, 117, *15*.

[illegible] A. J. 1967 — The geomagnetic field in New Zealand at epoch 1965.5. *Bull. N. Z. Dep. sci. industr. Res.,* 175.

Cataldi R. 1961 — Application of seismic methods to geothermal energy exploration. *Quaderni Geofis. appl.,* 21, 28.

Dobrin M. B. 1960 — Introduction to geophysical prospecting. *McGraw Hill, New York.*

Gardner L. W. 1939 — An areal plan of mapping subsurface structure by refraction shooting. *Geophysics,* 4, 247.

Grindley G. W. 1970 — Subsurface structures and relation to steam production, Broadlands Geothermal Field, New Zealand. *U. N. Symp. Development Utilization Geothermal Resources, Pisa.*

Hagedoorn J. G. 1959 — The plus-minus method of interpreting seismic refraction sections. *Geophys. Prosp.,* 7, 158.

Hatherton T., Macdonald W. J. P., Thompson G. E. K. 1966 — Geophysical methods in geothermal prospecting in New Zealand. *Bull. volcan.,* 29, 485.

Hayakawa M., Mori K. 1962 — Seismic prospecting at Matsukawa geothermal area, Iwate Prefecture (in Japan.). *Bull. geol. Surv. Japan,* 13, 643.

Hayakawa M., Takaki S., Baba K. 1967 — Geophysical study of Matsukawa geothermal area, Northeast Japan. *Bull. Geol. Surv. Japan,* 18, 147.

Howell B. F., Kaukonen E. H. 1954 — Attenuation of seismic waves near an explosion. *Bull. seism. Soc. Amer.,* 44, 481.

Modriniak N., Studt F. E. 1959 — Geological structure and volcanism of the Taupo-Tarawera district. *N. Z. J. Geol. Geophys.,* 2, 654.

Mouton J. 1969 — Contribution des méthodes des prospectiones géothermiques et géophysiques à l'étude des champs géothermiques de Toscane, Italy. *Bull. volcan.,* 33, 165.

Noguchi T. 1966 — Exploration of Otake Steam Field. *Bull. volcan.,* 29, 529.

Reilly W. I. 1969 — Gravitational and magnetic effects of a right circular cylinder. *N. Z. J. Geol. Geophys.,* 12, 497.

Risk G. F., Macdonald W. J. P., Dawson G. B. 1970 — D. C. resistivity surveys, Broadlands Field, New Zealand. *U. N. Symp. Development Utilization Geothermal Resources, Pisa.*

Robertson E. I., Reilly W. I. 1960 — The New Zealand primary gravity network. *N. Z. J. Geol. Geophys.,* 3, 41.

Studt F. E. 1958 — Geophysical reconnaissance at Kawerau, New Zealand. *N. Z. J. Geol. Geophys.,* 1, 219.

Studt F. E. 1959 — Magnetic survey of the Wairakei Hydrothermal Field. *N. Z. J. Geol. Geophys.,* 2, 746.

Studt F. E. 1963 — Waiotapu Geothermal Field, Chapter IV: Geophysics of Waiotapu Area. *Bull. N. Z. Dep. sci. industr. Res.,* 155, 35.

Studt F. E. 1964 — Geophysical prospecting in New Zealand's hydrothermal fields. *U. N. Conf. New Sources Energy, Rome,* 2, 380.

Vecchia O. 1961 — Gravimetric exploration for natural steam in Tuscany. *Quaderni Geofis. appl.,* 21, 18.

Watson-Munro C. N. 1938 — Reconnaissance survey of the variation of magnetic force in the New Zealand Thermal Regions. *N. Z. J. Sci. Techn.,* B20, 99.

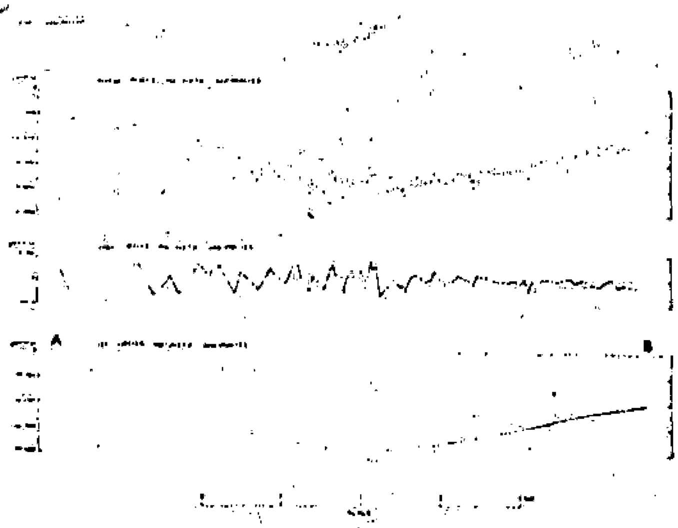

FIG. 9. — *Total Force Magnetic Anomaly Profile across the northern part of the Broadlands Geothermal Area, showing the separation into First and Second Order Anomalies. Section line AB is shown in Figure 10.*

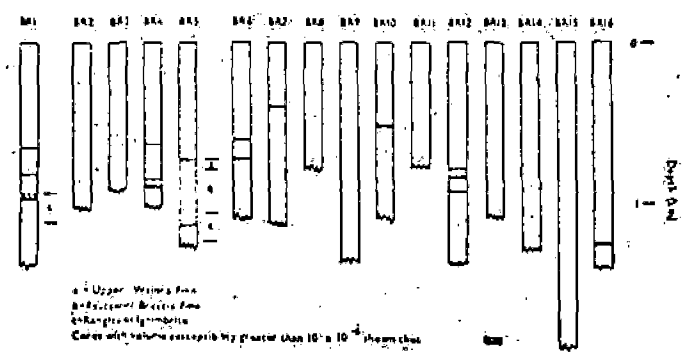

FIG. 11. — *Distribution of Magnetic Susceptibility with depth in drillholes, Broadlands Geothermal Area. (Note: in general only 2 m every 30 m is cored).*

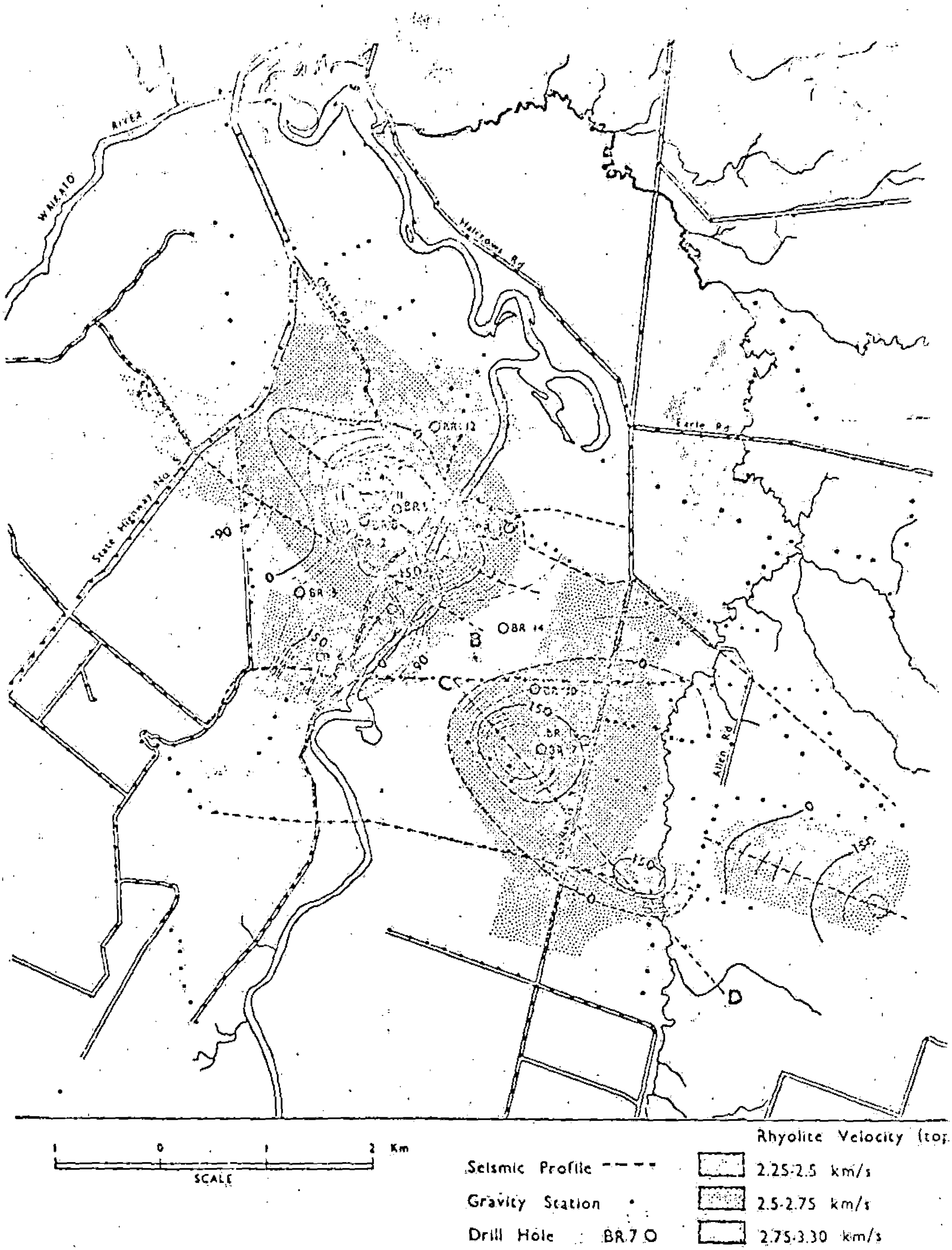

FIG. 1. - *Contour map of surface of rhyolites, Broadlands Geothermal Area. The figures beside the contours give elevation metres above sea level (contour interval 30 m); location of seismic profiles is shown by dashed lines.*

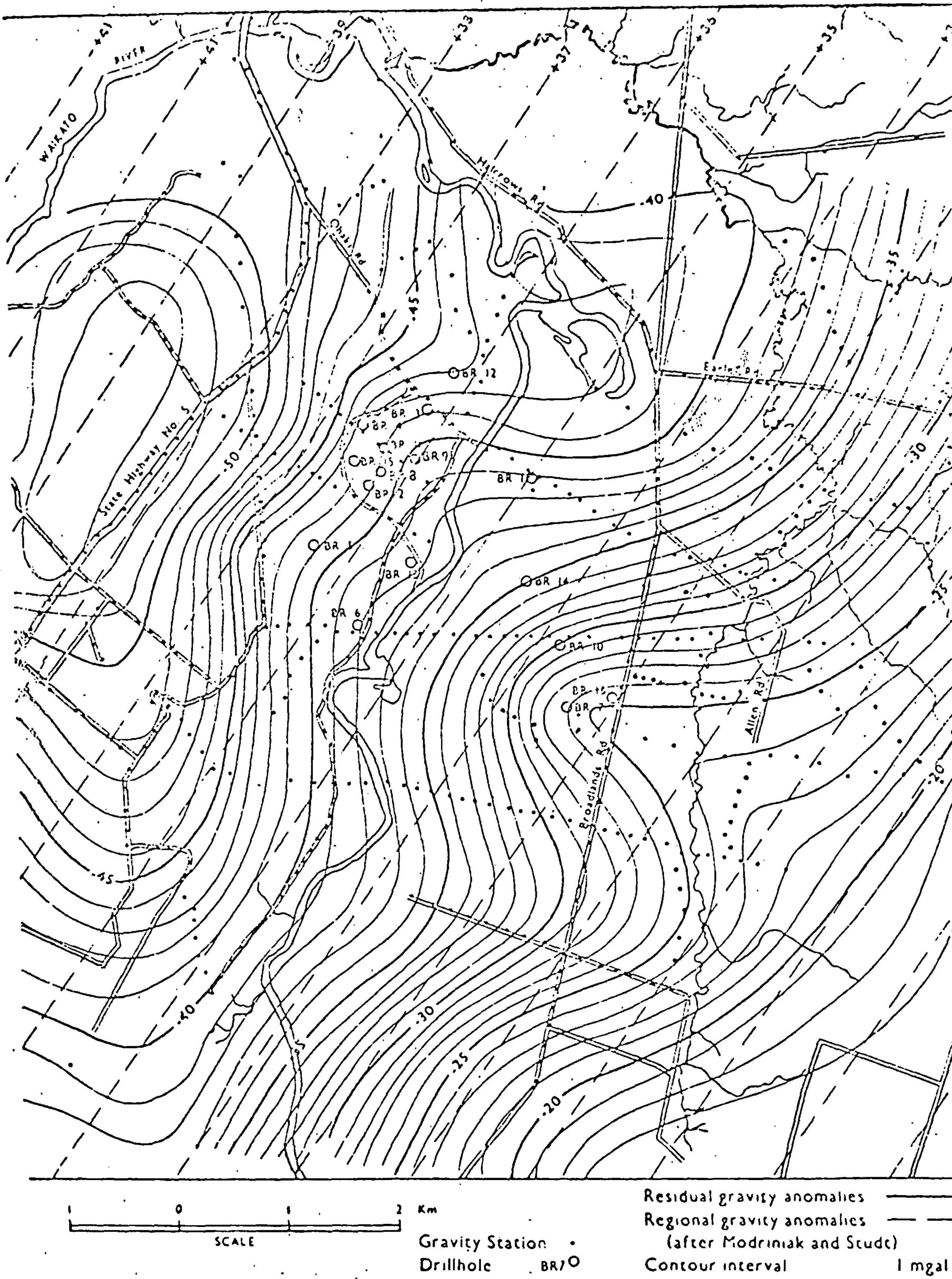

FIG. 3. — *Bouguer Gravity Anomalies, Broadlands Geothermal Area. To prevent overcrowding of the figure only a small nun of the gravity stations made along profile lines are shown.*

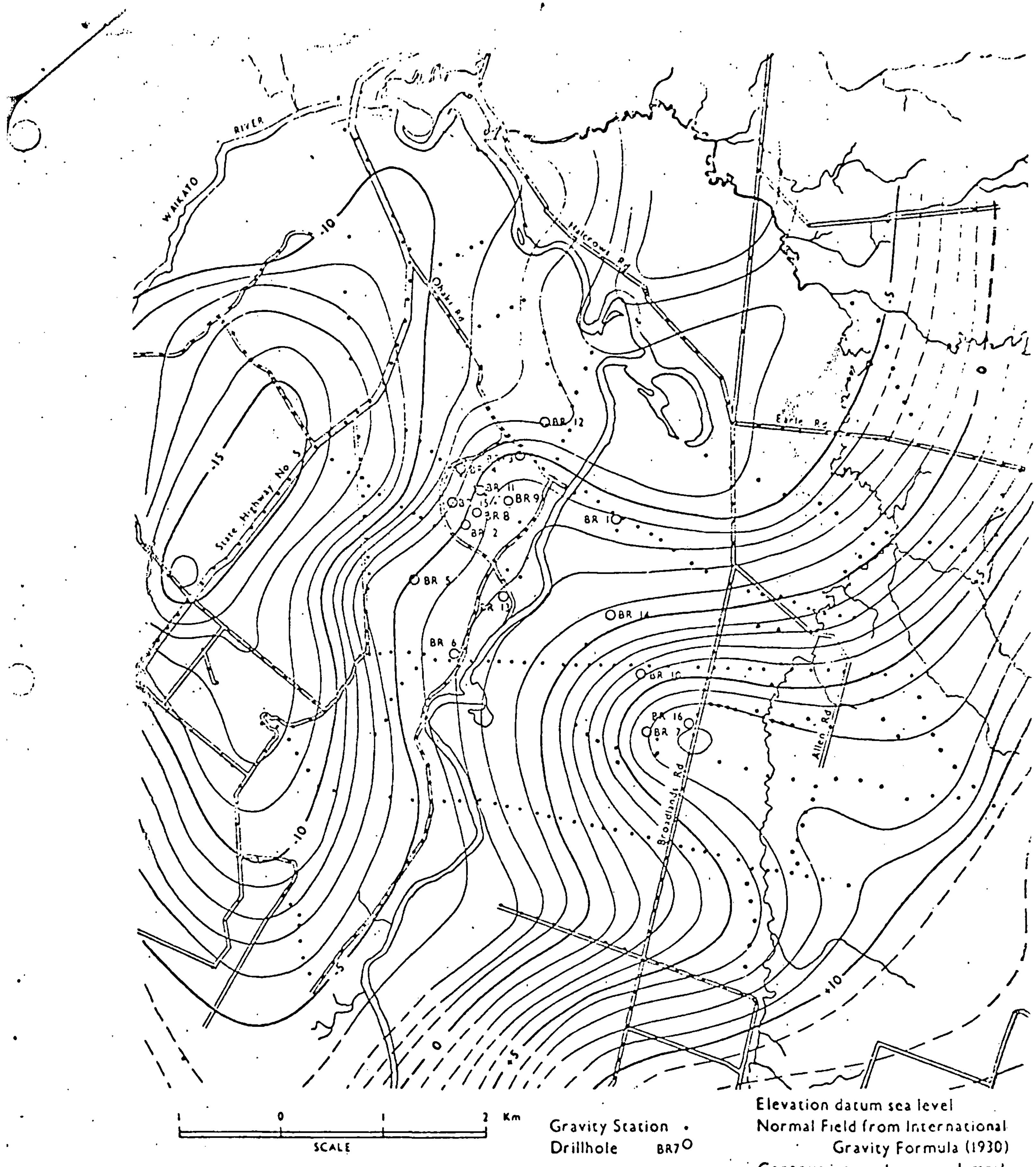

FIG. 4. — *Residual Gravity Anomalies, Broadlands Geothermal Area.*

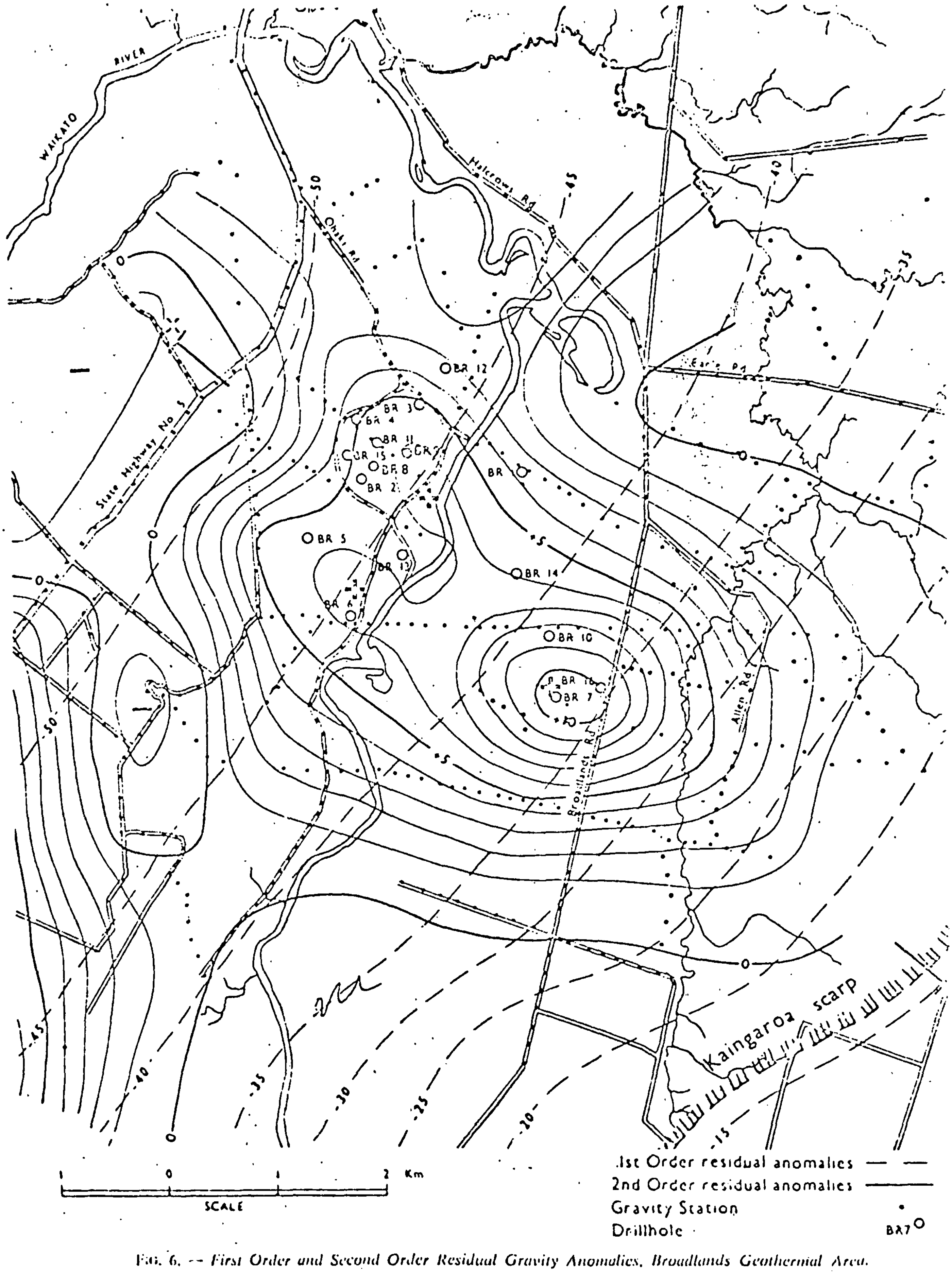

FIG. 6. -- First Order and Second Order Residual Gravity Anomalies, Broadlands Geothermal Area.

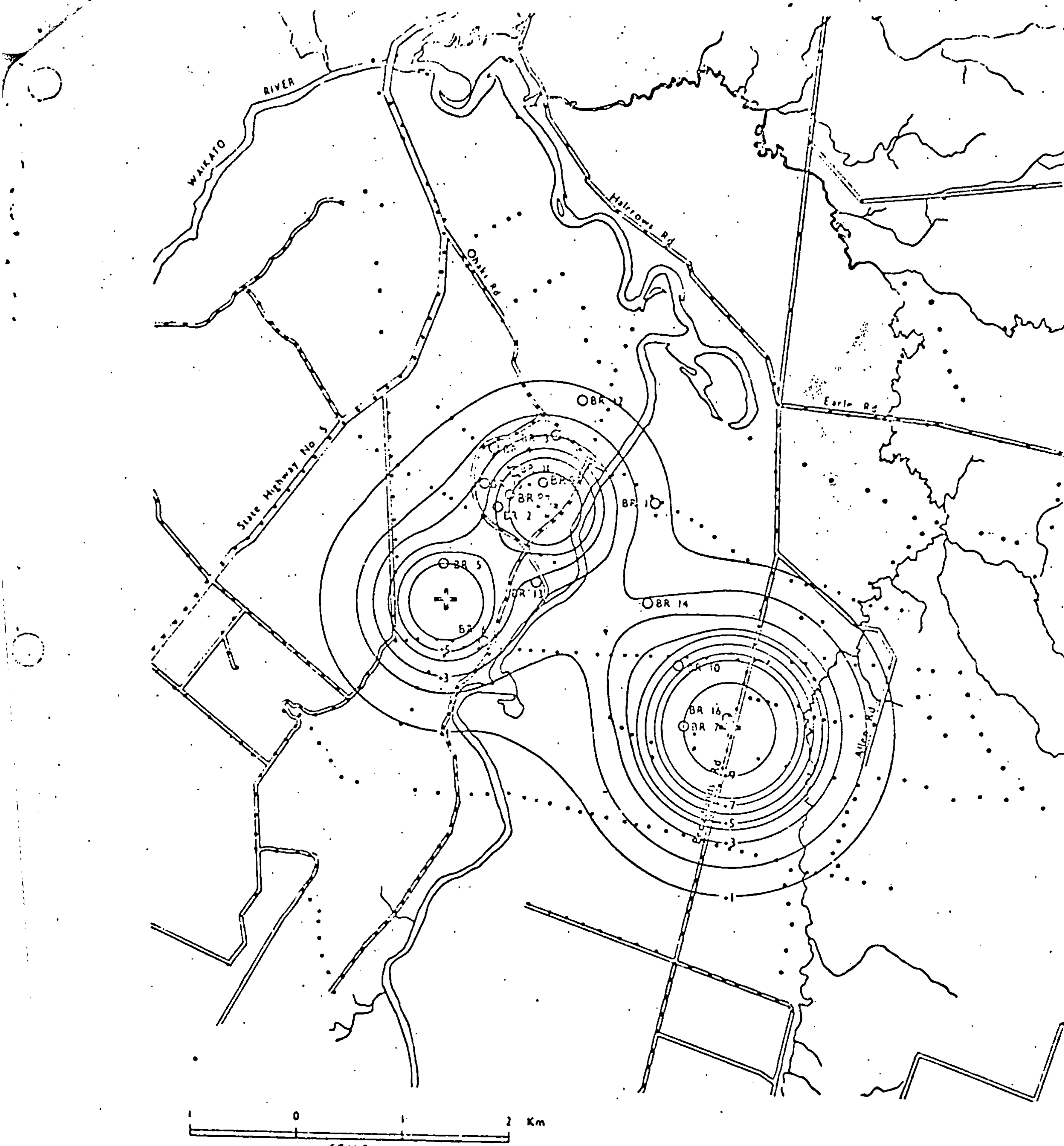

FIG. 8. – Interpretation of the Second Order Residual Gravity Anomalies, Broadlands Geothermal Area.

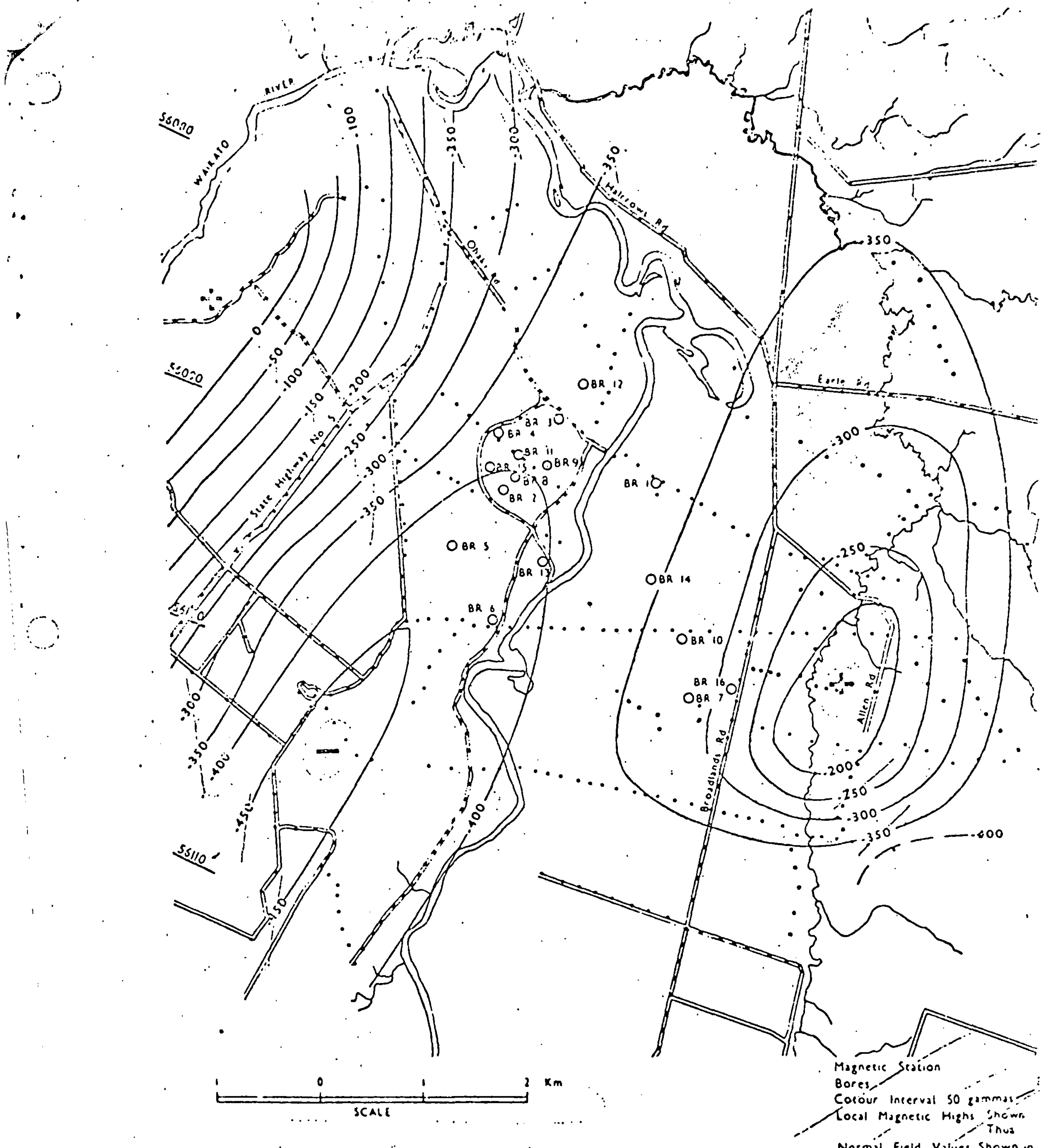

FIG. 10. - - *First Order Total Force Magnetic Anomalies in the Broadlands Geothermal Area. To prevent overcrowding figure only a small number of the magnetic stations made along profile lines are shown.*

First order total
Magnetic

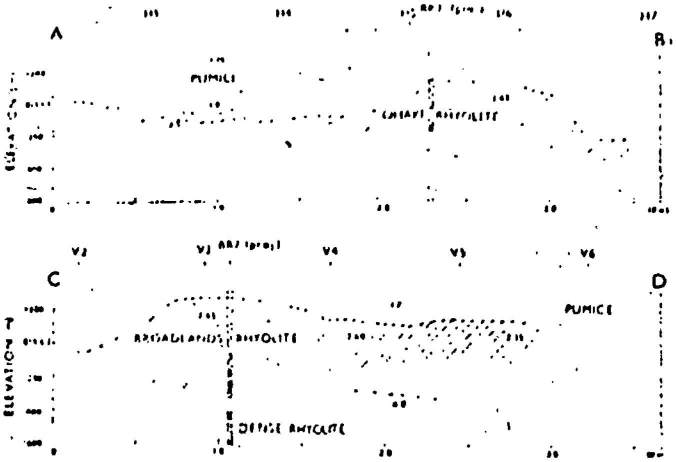

FIG. 2. · *Seismic cross sections along lines AB and CD (location of section lines shown in Figure 1), Broadlands Geothermal Area. Figures inside sections indicate velocity in km/s; seismic interfaces with poor energy return are shown by dashed lines.*

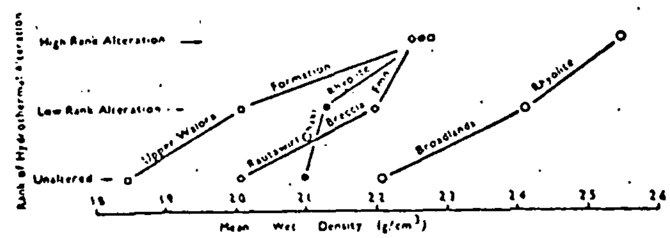

FIG. 5. — *Variation of density with rank of hydrothermal alteration, Broadlands Geothermal Area.*

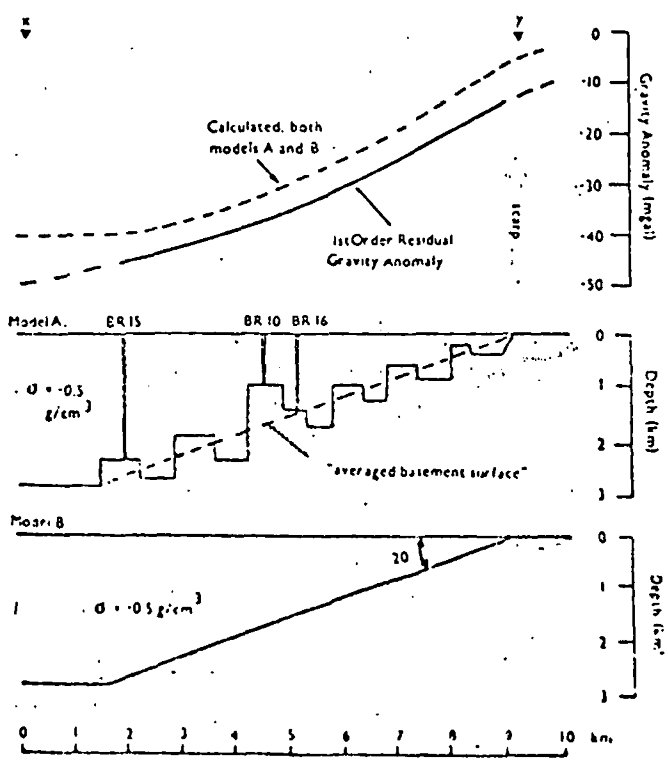

FIG. 7. — *Interpretation of the First Order Residual Gravity Anomalies, Broadlands Geothermal Area.*

AREA
NZ
Broad

Ward

REPEAT GRAVITY MEASUREMENTS AT BROADLANDS GEOTHERMAL FIELD, 1967-1974

by

T. M. HUNT and S. R. HICKS

GEOPHYSICS DIVISION

REPORT NO. 113

Geophysics Division,
Department of Scientific and Industrial Research,
Wellington, New Zealand

1975 OCTOBER

CONTENTS

REPEAT GRAVITY MEASUREMENTS AT BROADLANDS GEOTHERMAL FIELD, 1967-1974

by T. M. HUNT and S. R. HICKS

ABSTRACT

Measurements at Broadlands Geothermal Field show that there are no significant gravity differences (when corrected for known ground subsidence) between surveys in 1967 and 1974 attributable to the withdrawal of 35×10^9 kg of water from the area. Examination of several models for the withdrawal indicates that at least 75% of the water discharged has been replaced.

INTRODUCTION

Broadlands is situated close to the Waikato River about 25 km north-east of Wairakei. Resistivity measurements in the Ohaki and Broadlands areas led to the investigation for geothermal steam in 1967-68 and the finding of a large area (10-13 km^2) of low ($<5\,\Omega$m) resistivity (Risk et al. 1970) known as the Broadlands Geothermal Field. Since then 28 bore holes have been drilled and, up to March 1975, about 35.6×10^9 kg of water (liquid and gas phases) discharged from the bores during testing (G. W. Hitchcock, pers. comm.).

The use of repeat gravity measurements to determine the net mass loss from, and hence the amount of recharge in, geothermal fields is described by Hunt (1970). During the investigations at Broadlands, gravity measurements were made at a large number of benchmarks in and about the low resistivity area (Hochstein and Hunt 1970) to determine the geological structure within the geothermal field. Repeat gravity measurements at 88 selected bench-marks were made in 1974 to determine any net mass changes associated with testing of the bores. This report describes and discusses the gravity differences between the two surveys.

GRAVITY MEASUREMENTS

Gravity observations were made in August-October 1967 by A. Doone (nee Cuthbert), I. Ferry, and T. M. Hunt, and in July 1974 by S. R. Hicks. Values of gravity determined from these observations are given in Appendix 1, and the locations of the benchmarks used are given in Fig. 1.

Gravity meter and calibration

Both surveys were made using LaCoste and Romberg gravity meter G106. For some stations in the 1967 survey and all stations in the 1974 survey a looping technique was used to minimise instrument reading errors and to determine instrument drift; most stations were occupied three times.

Gravity observations were made over the Wellington Calibration Interval (Cowan and Robertson 1964) after each survey to determine the calibration correction factor. The manufacturers calibration curve, adjusted on the basis of this correction factor, was used in the calculation of gravity values.

Gravity base stations

During the 1967 survey observations were made at the beginning, middle, and end of each day at benchmark H346 or H383 within the Broadlands area. These stations were later linked to TAUPO FUNDAMENTAL situated on Taupo Fundamental benchmark. In the 1974 survey TAUPO FUNDAMENTAL was occupied twice each day for the whole survey. The values of gravity in the Broadlands area, given in Appendix 1, have been calculated relative to, and are within 200 µN/kg of that at TAUPO FUNDAMENTAL. The value of gravity at TAUPO FUNDAMENTAL is 9 799 883.1 µN/kg in the N.Z. Potsdam System (1959) (Robertson and Reilly 1960) and 9 799 849.0 µN/kg in the International Gravity Standardisation Net (1971) (Morelli 1974).

Ground noise

The effects of ground vibrations were observed when making measurements near the Ohaki and Broadlands thermal areas. However, tests using the same instrument, in the main production borefield at Wairakei, show (Hunt 1975) that these movements do not cause cross-coupling errors.

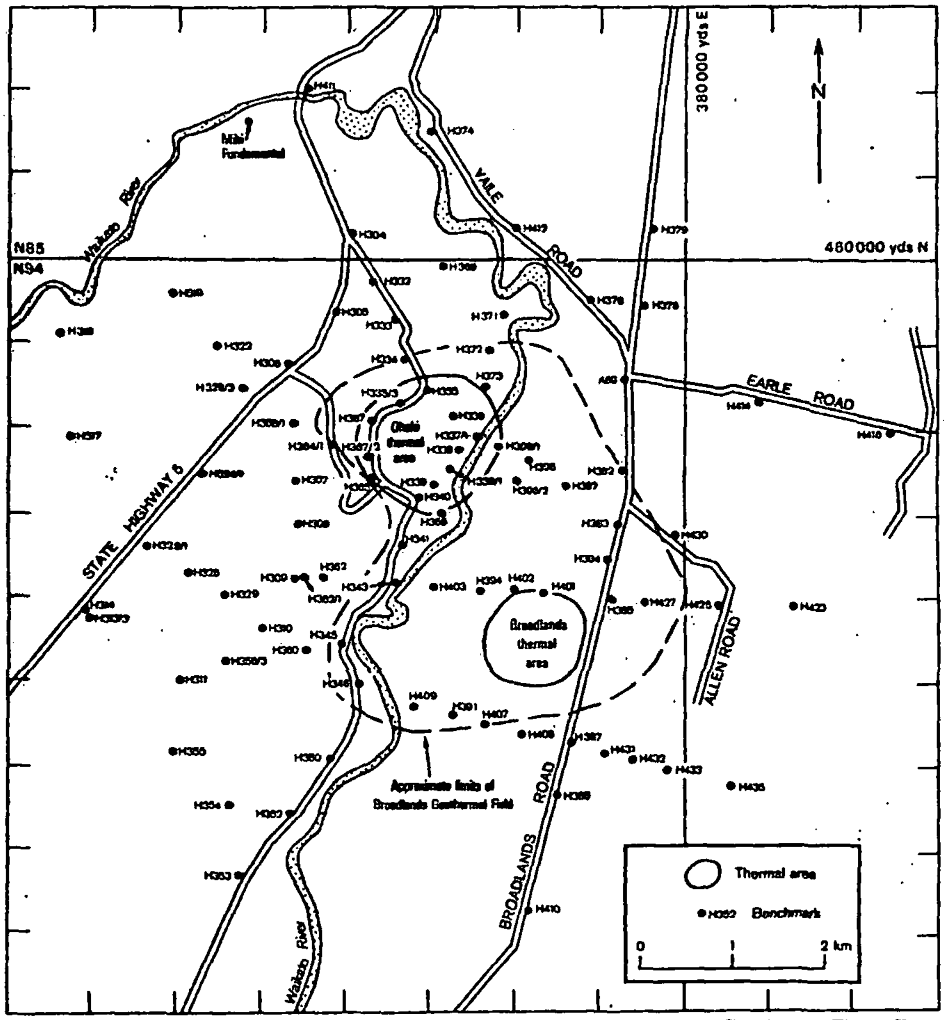

Fig.1 – Location of benchmarks used in the repeat gravity surveys at Broadlands Geothermal Field. The grid co-ordinates shown are for the National Yard Grid.

REDUCTION OF MEASUREMENTS

Calculation of gravity values

Gravity values were computed using the method described by Reilly (1970); for each day the gravity meter readings were multiplied by the appropriate scale factor, and the gravitational attraction of the sun and moon calculated, using the method of Longman (1959), and subtracted. An instrument drift correction, derived from least squares fitting of a degree one or two curve to the gravity differences at repeated stations, was made. The differences in gravity between the base and field stations were then obtained by subtracting a base correction.

Accuracy of gravity values

When a gravity station at Broadlands was occupied several times within a single day, the values of gravity, calculated in the manner described above, generally differed by 0.1 or 0.2 μN/kg. However when the same station was occupied several times a day, on different days, the mean values of gravity for each day differed by up to 0.7 μN/kg, as shown by the observations made for eight days at benchmark A69, given in Table 1. It is probable that an accuracy of about ±0.3 μN/kg can be expected.

Table 1: Gravity values at Lands and Survey Dept benchmark A69 near Broadlands. Values determined from observations in July 1974 by S. Hicks using LaCoste and Romberg gravity meter G106

Date	g	n	s.e.	stability
08	1014.1	3	0.2	Good
10	1014.8	2	0.1	Fair
11	1014.6	3	0.1	Fair
12	1014.3	3	0.1	Good
13	1014.5	2	0.2	Fair
14	1014.7	2	0.1	Fair
15	1014.2	2	0.1	Excellent
24	1014.6	2	0.2	Good

g — Mean value of gravity for the day (μN/kg).
n — Number of observations.
s.e. — Standard error.
stability — Stability of the reading as explained in Appendix 1.

DIFFERENCES BETWEEN SURVEYS

Differences between the values of gravity at a benchmark, between surveys, may be caused by regional gravity changes, topographic changes, variations in groundwater level, and vertical ground movements, as well as net mass changes associated with the discharge of water from the geothermal field.

Regional gravity changes

Data given by Hunt (1975) suggest that regional gravity changes in the Taupo area, between April 1968 and December 1974, are less than 0.5 μN/kg. The changes in gravity at benchmarks outside the Broadlands Geothermal Field between 1967 and 1974, given in Appendix 1, are generally less than 0.3 μN/kg, indicating that regional gravity changes in the Broadlands area can be neglected.

Topographic changes

Changes in topography of the Broadlands area between surveys have occurred due to road construction along State Highway 5, and drilling operations in the Ohaki thermal area. The effects of these changes on nearby gravity stations, estimated using standard topographic correction tables (Woodward and Ferry 1973), are generally less than 0.2 μN/kg and have been neglected.

Groundwater level changes

Groundwater levels beneath benchmarks used in the surveys are not known, but levels measured at about the time of the surveys, in shallow monitor holes (/0) adjacent to some deep bores are given in Table 2. These data suggest that, with the exception of the area near bore BR 4 in the Ohaki area, there have been no large groundwater level changes in the Broadlands area.

Table 2: Groundwater levels at Broadlands. Values given (in metres) are depths below ground level. Data from G. W. Hitchcock (pers. comm.)

Borehole	Total depth of hole	Ground water level	
		August-Sept 1967	August 1974
1/0	139	4.3	3.8
2/0	30	3.2	6.1
3/0	34	7.6	8.8
4/0	37	10.2	18.0
5/0	32	6.1	5.6
6/0	34	5.7	4.7
7/0	37	10.4	11.0

Vertical ground movement

Level of benchmarks in the Broadlands area were measured (to 2nd order standard) by Ministry of Works and Development in March-June 1968 and in April-May 1974. The differences in elevation of the benchmarks between these surveys (A. Johnston, M.W.D., pers. comm.) are shown in Fig. 2. It can be seen from this map that the only significant ground level movements have been in the Ohaki thermal area. This is the area in which most of the bores are situated and from which most of the mass discharged has come (Table 3). The gravity effect of vertical ground movement is about +3.1 $\mu N\ kg^{-1}\ m^{-1}$ of subsidence. Most of the water discharged from the Ohaki area was removed between 1969 and 1971, therefore it is assumed that the gravity effects of the vertical ground movements between March 1968 and April 1974 (times of the levelling surveys) will be the same as between August 1967 and July 1974 (times of the gravity surveys).

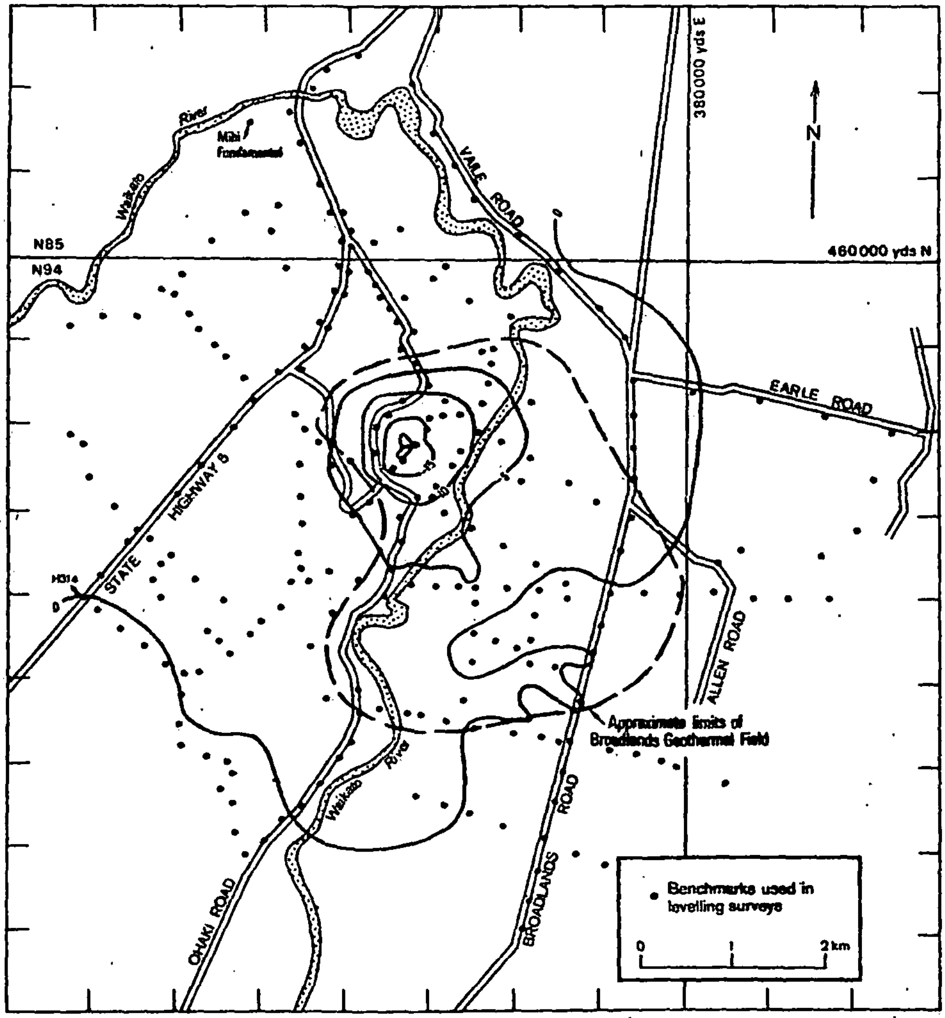

Fig.2 – Vertical ground movements at Broadlands Geothermal Field between March 1968 and April 1974. Contour values shown are in centimetres, contour interval 5cm. Not all benchmarks used in the levelling surveys are shown.

Table 3: Cumulative discharge from bores at Broadlands Geothermal Field, March 1975. Data from G. Hitchcock (pers. comm.). Location of the bores is given in Fig. 1.

Bore	Area	Mass discharged x 10^9 kg	Bore	Area	Mass discharged x 10^9 kg
1			15	Ohaki	
2	Ohaki	7.66	16	Broadlands	
3	Ohaki	4.19	17	Ohaki	1.12
4	Ohaki	0.62	18	Ohaki	0.44
5			19	Ohaki	1.70
6		0.42	20	Ohaki	2.02
7	Broadlands	1.04	21	Ohaki	0.37
8	Ohaki	3.48	22	Ohaki	1.58
9	Ohaki	1.86	23	Ohaki	0.49
10	Broadlands	0.04	24		0.03
11	Ohaki	4.45	25	Broadlands	1.64
12			26	Not drilled	
13	Ohaki	2.09	27	Broadlands	0.16
14		0.16	28	Broadlands	
			29		

Net mass loss

Gravity differences in the Broadlands area, corrected for the effects of vertical ground movements, are given in Fig. 3 and in Appendix 2. The large (-15.4 µN/kg) gravity difference at benchmark H 411 is probably due to a failure to reoccupy the point measured in 1957. The gravity difference of + 2.1 µN/kg at benchmark H 337/1 may be caused partly by topographic changes made during construction of the nearby drain from bore BR 3 to the Waikato River.

A histogram showing the frequency distribution of gravity differences, given in Fig. 4, suggests that the differences have a normal (Gaussian) distribution about zero change. The mean of the differences, excluding

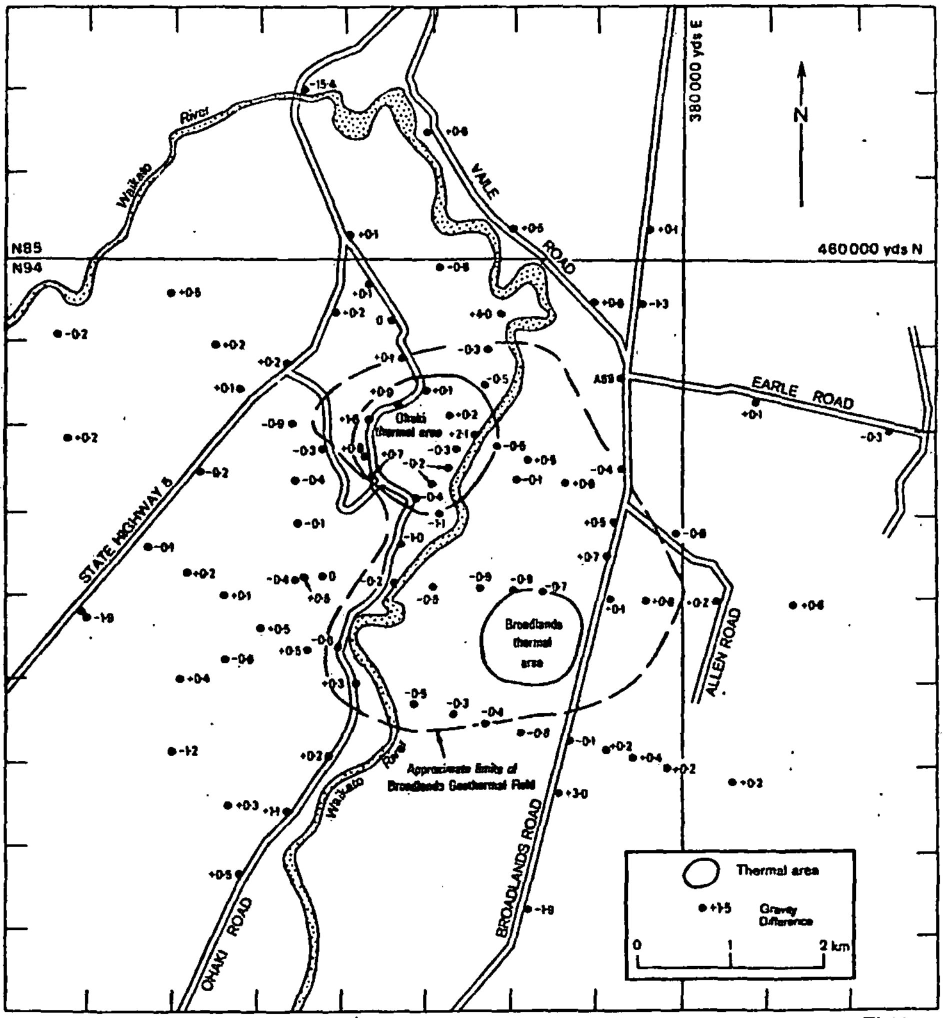

Fig. 3 – Gravity differences (corrected for vertical ground movements) at Broadlands Geothermal Field for the period 1967–1974. Gravity differences are in μN/kg. A negative difference indicates the value of gravity in 1974 was less than in 1967.

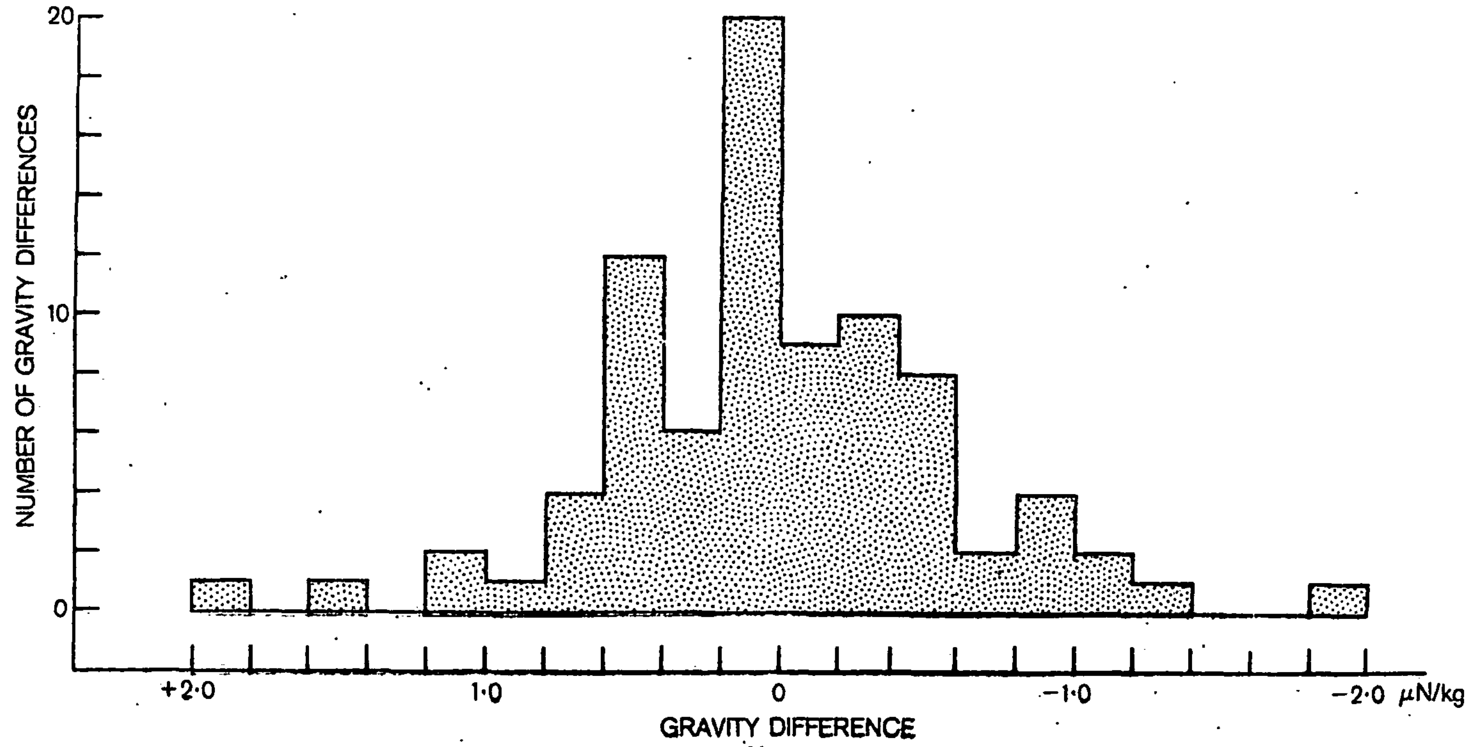

Fig. 4 – Histogram showing the frequency distribution of gravity differences (corrected for vertical ground movements) at Broadlands Geothermal Field for the period 1967–1974. A negative difference indicates the value of gravity in 1974 was less than in 1967.

those at benchmarks H 411 and H 337/1, is close to zero (+0.05 μN/kg), and the frequency distribution has a standard deviation of 0.62 μN/kg. The distribution of gravity differences (Fig. 4) shows little sign of the positive skewness which would be expected if a significant number of differences were due to a large net mass loss from the geothermal field.

Measurements by M.W.D. (G. Hitchcock, pers. comm.) show that, of the total mass of water discharged, most (32×10^9 kg) has been drawn from beneath the Ohaki thermal area, yet the gravity differences in this area are not consistently negative: there are no differences more negative than -0.5 μN/kg. Larger negative differences (-0.8 to -1.1 μN/kg) occur near the Broadlands thermal area, and between it and the Ohaki area, but it is not certain whether these differences are due to net mass losses or to random observational errors.

DISCUSSION

The lack of any large negative gravity differences associated with the Broadlands Geothermal Field suggests that there has been little or no net mass lost from the area. Because the differences are small and variable it was not possible to contour the differences and find the net mass loss and the amount of recharge, as was done at Wairakei (Hunt 1970). Instead the gravity effects of complete withdrawal (without recharge) from the area are examined and estimates of the minimum amount of recharge made.

Models for withdrawal from the Ohaki area

Since most of the mass withdrawn from the Broadlands Geothermal Field was taken from beneath the Ohaki thermal area, only this region is examined. In this area the water was drawn mainly from a zone (withdrawal zone) at a depth of between 600 and 750 m below ground level. In order to calculate the effects of the withdrawal several models are considered:

A. <u>Complete removal of water from an area about the withdrawal zone</u>

Measurements by M.W.D., given in Appendix 3, show that in the withdrawal zone beneath the Ohaki area, the mean pressure is about 6.33 MPa, and the temperature is about 265°C, which is close to boiling point for that pressure. Boiling water at a temperature of 265°C has a density of 0.78 Mg/m^3, and steam at the same temperature and pressure has a density of 0.03 Mg/m^3 (Bain 1964). If boiling water was extracted from the withdrawal zone, and replaced by steam, at the same temperature and pressure, there would be a density change of about -0.75 Mg/m^3 within the pore spaces. Measurements by Leopard (1968 a,b) show that the porosity of rocks in this zone varies between about 10 and 40%. Assuming that the rocks have an average porosity of 20%, the minimum volume of rock from which the water could be drawn is 2.13×10^8 m^3. In order to calculate the gravity effects of withdrawal of water, this volume is approximated by a cylinder of height 150 m and radius 672 m. The gravity effects of this cylinder, at the ground surface calculated using the method of Reilly (1969), are given by curve A in Fig. 5.

B. <u>Partial removal of water from a large area about the withdrawal zone</u>

If (say) half the water in an area about the withdrawal zone was removed (and not replaced) the volume of rock from which 32×10^9 kg is taken would be 4.27×10^8 m^3 (assuming a density of water of 0.75 Mg/m^3 and a porosity of 20%, as explained above). This model can be approximated by the removal of water from a cylinder of height 150 m and radius 952 m. The gravity effects of this cylinder, at the ground surface, calculated using the method of Reilly (1969), are given in curve B in Fig. 5.

C. <u>Draining of near surface water</u>

Macdonald (1975) suggests that in the Ohaki area the Broadlands geothermal field consists of a vertical column of hot (150 - 300°C) water which is capped by an impermeable layer at a depth of about 150 m. If

ıne
withdrawal
IPa, and
; for that
ıity of .
ı a density
rom the
re and
within
ıat the
ı.
ıinimum
0^8 m^3.
ıer, this
ıs 672 m.
ılculated
ı. 5.
ıl zone
ras removed
ıs taken
$/m^3$ and
proximated
. radius
urface,
ve B in

s geo-
C) water
O m. If

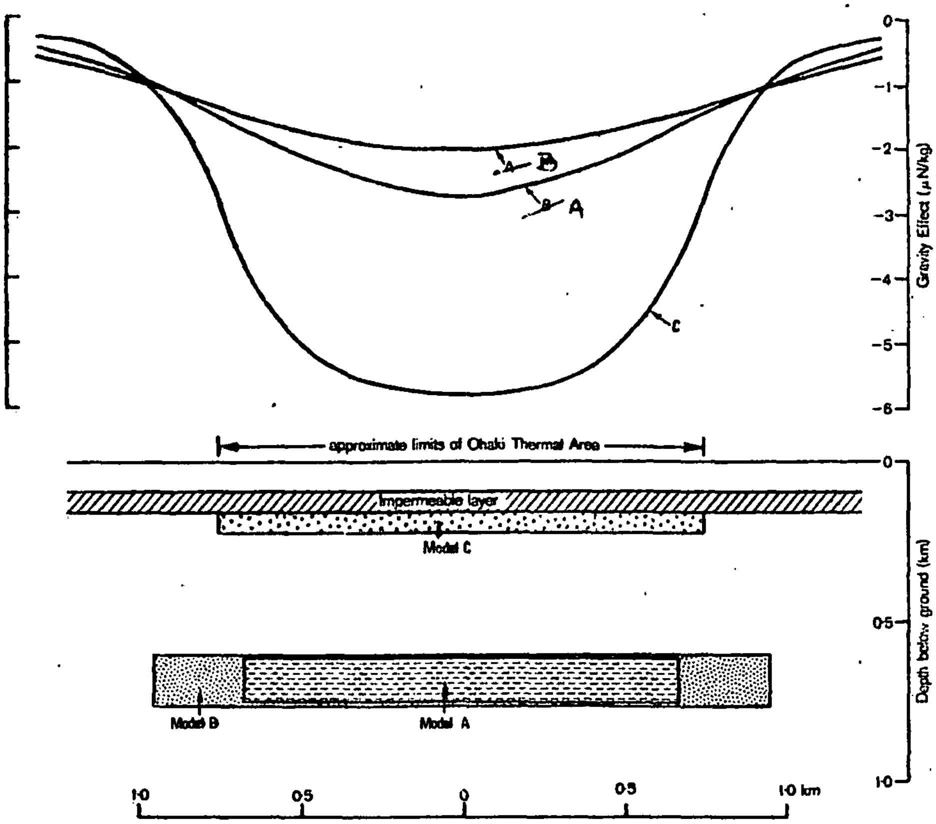

Fig. 5 – Gravity effects of models for the withdrawal of 35×10^9 kg of water from beneath the Ohaki Thermal Area, Broadlands Geothermal Field.

the permeability below this layer is sufficient to allow substantial vertical movement, water removed by the bores from rocks in the withdrawal zone may be replaced by water from above and lead to a falling of the water level beneath the impermeable layer. If this water is not replaced by horizontal inflow a net mass loss will occur just beneath the impermeable layer. The groundwater level measured in the shallow /O holes adjacent to some bores is probably that of a perched groundwater table and will not be affected. Measurements by M.W.D., given in Appendix 3, show that the temperature at a depth of 150 m beneath the Ohaki area, is about 165°C. The density of water at this temperature will be about 0.90 Mg/m^3 (Bain 1964). Assuming that the area over which the water level falls is about the same as that of the Ohaki thermal area (approx. 1.76 km^2), the rocks have a porosity of 30% (Leopard 1968 a,b), and the water has a density of 0.90 Mg/m^3, then the volume of rock from which the water has drained will be about 1.19×10^8 m^3. This volume can be approximated by a cylinder of radius 750 m and height 67 m. The gravity effects at the surface of completely removing the water from a cylinder of these dimensions and porosity, centred at a depth of 180 m, are given by curve C in Fig. 5.

Interpretation

In all the above cases the gravity effects of withdrawing 32×10^9 kg of water from the Ohaki area, without replacement, are about 2 - 6 times greater than those observed, and much greater than the errors of measurement (approx. 0.5 μN/kg).

If there has been partial replacement of the water the observed gravity difference will be proportional to the percentage not replaced:

$$\Delta g_{(\text{observed})} \sim \Delta g_{(\text{calculated for no recharge})} \times \frac{\text{total mass withdrawn} - \text{mass replaced}}{\text{total mass withdrawn}}$$

It can be seen from Fig. 3 that all negative gravity differences in the Ohaki area are smaller than -0.5 μN/kg, therefore the minimum amounts of recharge are:

Model A: about 80%

Model B: about 75%

Model C: about 90%.

These values may alter slightly if the adopted values for porosity and water density are changed, but it is clear that for all likely models, at least 75% of the water withdrawn from the Broadlands Geothermal Field since 1967 has been replaced.

ACKNOWLEDGMENTS

We thank W. J. P. Macdonald and G. F. Risk for criticism of the manuscript, G. W. Hitchcock (M.W.D., Wairakei) for groundwater level and borehole data, and A. Johnston (M.W.D., Wellington) for levelling data.

REFERENCES

BAIN, R. W. 1964: Steam Tables, Her Majesty's Stationery Office, Edinburgh, 147 pp.

COWAN M.; ROBERTSON, E. I. 1964: Principal pendulum and airport gravity stations in New Zealand. N.Z. Journal of Geology and Geophysics, 7: 543-53.

HOCHSTEIN M. P.; HUNT, T. M. 1970: Seismic, gravity and magnetic studies, Broadlands Geothermal Field, New Zealand. Geothermics, 2: 333-46.

HUNT, T. M. 1970: Net mass loss from the Wairakei Geothermal Field, New Zealand. Geothermics, 2: 487-491.

———— 1975: Repeat gravity measurements at Wairakei, 1961-1974. Report No. 111, Geophysics Divsion, Department of Scientific and Industrial Research, Wellington, New Zealand.

LEOPARD, A. E. 1968a: Measurements of Rock Properties in Broadlands Geothermal Area, Geophysical Survey, Further Results (W.J.P. Macdonald, compiler), Report No. 49, Geophysics Division, Department of Scientific and Industrial Research, Wellington.

———— 1968b: Further measurements of rock properties of cores from the Broadlands Field in Broadlands Geothermal Area, Geophysical Survey, Third Report, Report No. 53, Geophysics Division, Department of Scientific and Industrial Research, Wellington.

LONGMAN, I. M. 1959: Formulas for computing the tidal accelerations due to the sun and moon. Journal of Geophysical Research, 64: 2351-55.

MACDONALD, W.J.P. 1975: The useful heat contained in the Broadlands Geothermal Field in Geophysical papers submitted to the 2nd U.N. Symposium on the development and use of geothermal resources, at San Francisco, U.S.A., 1975 May 20-29 (G. F. Risk, compiler). Report No. 102: 20-35. Geophysics Division, Department of Scientific and Industrial Research, Wellington, New Zealand.

MORELLI, C. 1974: The International Gravity Standardisation Net 1971 International Association of Geodesy Special Publication 4.

REILLY, W. I. 1969: Gravitational and magnetic effects of a right circular cylinder. N.Z. Journal of Geology and Geophysics, 12: 497-506.

———— 1970: Adjustment of gravity meter observations. N.Z. Journal of Geology and Geophysics, 13: 697-702.

RISK, G. F.; MACDONALD, W.J.P.; DAWSON, G. B. 1970: D.C. resistivity surveys of the Broadlands geothermal region, New Zealand. Geothermics, 2: 287-294.

ROBERTSON, E. I.; REILLY, W. I. 1960: The New Zealand Primary Gravity Network. N.Z. Journal of Geology and Geophysics, 3: 41-68.

WOODWARD, D. J.; FERRY, L. M. 1973: Gravity terrain correction tables. Technical Note No. 66. Geophysics Division, Department of Scientific and Industrial Research, Wellington, New Zealand.

APPENDIX 1

Gravity and elevation data, Broadlands Geothermal Field

BM	Ministry of Works and Development (Power Division) benchmark number.
Date	Date of gravity observations.
g	Mean value of gravity (μN/kg), calculated from the gravity observations, relative to TAUPO FUNDAMENTAL having a gravity value of 1000.00 μN/kg.
n	Number of gravity observations.
s.e.	Standard error of the calculated value of gravity.
Stability	An indication of the precision of the gravity meter reading, which is related to ground noise conditions. Excellent = no ground noise, readings ± 0.01 dial div. Good = intermittent ground noise, readings ±0.02 dial div. Fair = continuous ground noise. Balance position of the gravity meter beam estimated from swings. Readings ±(0.03 - 0.5) dial div. Gravity meter scale factor is approximately 0.1 μN/kg per dial div.
Elevation	Elevation (m) of the benchmark. Elevations given for 1967 survey were obtained from 2nd order levelling by M.W.D. assuming Mihi Fundamental benchmark to have an elevation of 290.492 m. Elevations given for the 1974 were obtained from 2nd order levelling by M.W.D. assuming benchmark H 314 to have the same elevation as in the 1967 survey (361.378 m). All elevations are orthometric heights.

BM	Date	g	n	s.e.	Stability	Observer	Elevation
H 304	67 08 31	934.2	2	0.2		Doone	310.912
	74 07 22	934.3	2	0.1	Good	Hicks	.906
H 305	67 10 16	913.0	1			Ferry	322.552
	74 07 23	913.2	3	0.2	Good	Hicks	.544
H 306	67 10 13	841.5	1		Excellent	Ferry	348.382
	74 07 23	841.7	3	0.2	Good	Hicks	.371
H 307	67 10 13	881.9	1		Excellent	Ferry	348.858
	74 07 18	881.6	3	0.1	Excellent	Hicks	.835
H 308	67 10 13	921.7	1		Excellent	Ferry	353.268
	74 07 18	921.7	3	0.1	Excellent	Hicks	.253
H 309	67 09 01	933.0	3	0.2		Doone	344.766
	74 07 18	932.6	3	0.1	Good	Hicks	.754
H 310	67 09 01	895.9	3	0.2		Doone	344.624
	74 07 18	896.4	3	0.1	Good	Hicks	.613
H 311	67 09 01	881.8	3	0.2		Doone	346.925
	74 07 23	882.2	3	0.2	Fair	Hicks	.923
H 313/3	67 10 27	869.8	1			Ferry	357.999
	74 07 16	867.9	4	0.1	Good	Hicks	358.003
H 317	67 10 12	887.2	1		Excellent	Ferry	340.270
	74 07 18	887.4	3	0.1	Excellent	Hicks	.266
H 318	67 10 12	949.2	1			Ferry	303.473
	74 07 23	949.0	3	0.2	Good	Hicks	.467
H 319	67 10 12	915.1	1		Excellent	Ferry	310.112
	74 07 23	915.6	3	0.2	Good	Hicks	.105
H 322	67 10 12	809.1	1		Excellent	Ferry	354.366
	74 07 23	809.3	3	0.2	Good	Hicks	.357
H 324/1	67 10 16	828.2	1			Ferry	350.445
	74 07 18	828.0	3	0.1	Good	Hicks	.439
H 326/3	67 10 12	823.2	1		Good	Ferry	349.278
	74 07 23	823.3	3	0.2	Good	Hicks	.268
H 328	67 08 31	861.0	3	0.2		Doone	348.868
	74 07 18	861.2	3	0.1	Fair	Hicks	.862
H 328/1	67 10 13	841.9	1			Ferry	350.439
	74 07 18	841.8	3	0.1	Good	Hicks	.436
H 332	67 08 31	964.1	3	0.2		Doone	302.911
	74 07 22	964.2	2	0.1	Excellent	Hicks	.903

BM	Date	g	n	s.e.	Stability	Observer	Elevation
H 329	67 09 01	875.5	3	0.2		Doone	347.045
	74 07 18	875.6	3	0.1	Good	Hicks	.040
H 333	67 08 30	979.1	3	0.1		Doone	299.930
	74 07 22	979.1	3	0.1	Good	Hicks	.918
H 334	67 08 30	993.3	3	0.1		Doone	298.366
	74 07 21	993.5	3	0.1	Good	Hicks	.335
H 335	67 08 29	1019.0	3	0.3		Doone	295.257
	74 07 20	1019.4	3	0.1	Good	Hicks	.162
H 335/3	67 08 29	1008.7	3	0.3		Doone	303.957
	74 07 20	1010.0	4	0.1	Good	Hicks	.829
H 336	67 08 28	1041.2	3	0.3		Doone	293.508
	74 07 20	1041.9	3	0.1	Good	Hicks	.347
H 337/1	67 08 28	1051.2	3	0.2	Fair	Doone	289.734
	74 07 20	1053.6	3	0.1	Good	Hicks	.643
H 338	67 10 17	1052.5	1			Ferry	292.960
	74 07 20	1052.6	3	0.1	Good	Hicks	.842
H 338/1	67 10 17	1060.5	1			Ferry	293.215
	74 07 20	1060.7	3	0.1	Excellent	Hicks	.095
H 339	67 10 17	1060.6	1			Ferry	293.153
	74 07 20	1060.8	3	0.1	Good	Hicks	.019
H 340	67 09 04	1057.0	3	0.2		Ferry	293.204
	74 07 20	1057.0	3	0.1	Good	Hicks	.091
H 341	67 10 26	1068.6	1	1.4		Ferry	292.163
	74 07 20	1067.8	3	0.1	Excellent	Hicks	.094
H 343	67 09 24	1077.2	2	0.1	Excellent	Ferry	292.212
	74 07 19	1077.1	3	0.1	Good	Hicks	.190
H 345	67 10 26	1064.1	1	1.3		Ferry	293.235
	74 07 19	1063.6	3	0.1	Excellent	Hicks	.218
H 346	67 09 24	1065.6	4	0.1	Excellent	Hunt	293.394
	74 07 19	1066.0	3	0.1	Good	Hicks	.379
H 350	67 10 26	1064.2	1	1.2		Ferry	295.227
	74 07 16	1064.4	3	0.1	Good	Hicks	.224
H 352	67 10 26	1065.5	1	1.3		Ferry	295.886
	74 07 16	1066.6	3	0.1	Good	Hicks	.885
H 353	67 10 26	1051.8	1	1.3		Ferry	304.081
	74 07 16	1052.3	3	0.1	Good	Hicks	.084
H 354	67 10 26	1027.1	1	1.4		Ferry	302.694
	74 07 16	1027.4	3	0.1	Excellent	Hicks	.691

BM	Date	g	n	s.e.	Stability	Observer	Elevation
H 355	67 10 27	898.9	1			Ferry	350.489
	74 07 16	897.7	3	0.1	Excellent	Hicks	.485
H 356/3	67 10 27	957.4	1			Ferry	312.721
	74 07 18	956.8	3	0.1	Good	Hicks	.712
H 358/1	67 10 16	849.6	1			Ferry	349.779
	74 07 18	848.8	3	0.1	Excellent	Hicks	.752
H 360	67 10 27	1031.1	1			Ferry	298.986
	74 07 19	1031.6	3	0.1	Fair	Hicks	.972
H 361	67 09 04	964.9	3	0.2		Ferry	320.313
	74 07 21	965.2	3	0.1	Excellent	Hicks	.234
H 362	67 09 01	970.0	3	0.2		Doone	334.815
	74 07 19	970.1	3	0.1	Good	Hicks	.799
H 362/1	67 09 01	929.0	1	0.3		Doone	348.189
	74 07 18	929.5	3	0.1	Good	Hicks	.176
H 364/1	67 10 16	894.5	1			Ferry	341.063
	74 07 19	894.4	3	0.1	Excellent	Hicks	.012
H 365	67 09 04	1016.5	3	0.2		Ferry	306.395
	74 07 21	1017.4	3	0.2	Excellent	Hicks	.281
H 366	67 09 04	1072.0	2	0.2		Ferry	
	74 07 20	1071.2	4	0.1	Good	Hicks	
H 367	67 10 17	990.6	1			Ferry	306.877
	74 07 21	992.2	3	0.1	Excellent	Hicks	.738
H 367/2	67 10 17	1002.4	1			Ferry	308.144
	74 07 21	1003.6	2	0.2	Good	Hicks	.029
H 369	67 10 18	1004.3	1			Ferry	292.687
	74 07 22	1003.7	3	0.1	Good	Hicks	.679
H 371	67 10 18	1023.8	1			Ferry	291.211
	74 07 22	1024.2	3	0.1	Good	Hicks	.197
H 372	67 10 18	1018.0	1			Ferry	291.297
	74 07 22	1017.8	3	0.1	Good	Hicks	.273
H 373	67 10 18	1021.5	1			Ferry	290.974
	74 07 22	1021.2	3	0.1	Good	Hicks	.924
H 374	67 10 28	994.9	1			Ferry	291.375
	74 07 12	995.7	3	0.1	Excellent	Hicks	.369
H 376	67 10 28	1016.3	1			Ferry	296.758
	74 07 12	1016.9	3	0.1	Excellent	Hicks	.756
H 378	67 10 28	1011.0	1			Ferry	
	74 07 12	1009.7	3	0.1	Good	Hicks	

BM	Date	g	n	s.e	Stability	Observer	Elevation
H 379	67 10 28	1025.0	1			Ferry	
	74 07 24	1025.1	3	0.2	Good	Hicks	
H 382	67 10 28	1042.3	1			Ferry	296.659
	74 07 08	1041.9	3	0.2	Good	Hicks	.649
H 383	67 09 24	1079.0	3	0.1		Ferry	297.819
	74 07 10	1079.5	3	0.1	Good	Hicks	.809
H 384	67 10 31	1099.0	1			Ferry	299.468
	74 07 10	1099.7	3	0.1	Good	Hicks	.460
H 385	67 09 25	1134.1	3	0.2	Excellent	Ferry	300.235
	74 07 10	1134.2	3	0.1	Good	Hicks	.238
H 386	67 10 31	1174.0	1			Ferry	302.971
	74 07 10	1173.2	3	0.1	Excellent	Hicks	.971
H 387	67 09 30	1126.5	3	0.2	Excellent	Hunt	308.682
	74 07 15	1126.4	3	0.1	Good	Hicks	.686
H 388	67 10 31	1119.3	1			Ferry	309.846
	74 07 14	1122.3	3	0.1	Good	Hicks	.851
H 391	67 09 29	1086.4	3	0.2	Good	Ferry	302.969
	74 07 15	1086.1	3	0.1	Excellent	Hicks	.966
H 394	67 09 23	1085.4	3	0.1	Good	Hunt	301.716
	74 07 10	1084.7	3	0.1	Good	Hicks	.667
H 396	67 09 05	1045.6	2	0.5		Ferry	294.312
	74 07 08	1046.3	4	0.2	Excellent	Hicks	.265
H 396/2	67 09 05	1051.5	1	0.5		Ferry	295.264
	74 07 24	1051.5	3	0.2	Good	Hicks	.219
H 397	67 09 05	1058.1	2	0.6		Ferry	293.708
	74 07 08	1058.6	2	0.2	Excellent	Hicks	.682
H 399/1	67 10 31	1053.6	1			Ferry	
	74 07 08	1053.3	3	0.2	Good	Hicks	
H 401	67 09 23	1112.4	3	0.1	Excellent	Hunt	301.419
	74 07 11	1111.7	3	0.1	Good	Hicks	.424
H 402	67 09 23	1100.1	3	0.1	Good	Hunt	301.072
	74 07 11	1099.2	3	0.1	Good	Hicks	.063
H 403	67 09 23	1081.5	3	0.1	Excellent	Hunt	295.904
	74 07 10	1081.1	3	0.1	Excellent	Hicks	.864
H 406	67 09 29	1102.8	4	0.2	Good	Ferry	309.543
	74 07 15	1102.0	3	0.1	Good	Hicks	.545
H 407	67 09 29	1099.4	3	0.2	Good	Ferry	304.499
	74 07 15	1099.0	3	0.1	Excellent	Hicks	.501

BM	Date	g	n	s.e.	Stability	Observer	Elevation
H 408	67 09 29	1092.9	3	0.2	Good	Ferry	293.492
	74 07 15	1092.4	3	0.1	Excellent	Hicks	.489
H 410	67 10 31	1171.8	1			Ferry	314.978
	74 07 14	1173.7	3	0.1	Excellent	Hicks	.987
H 411	67 10 28	957.4	1			Ferry	299.411
	74 07 24	942.0	3	0.2	Good	Hicks	.401
H 412	67 10 28	1022.9	1			Ferry	291.412
	74 07 12	1023.4	3	0.1	Good	Hicks	.408
H 414	67 10 28	1046.4	1			Ferry	299.454
	74 07 12	1046.5	3	0.1	Good	Hicks	.457
H 416	67 10 28	1109.0	1			Ferry	303.665
	74 07 12	1108.7	3	0.1	Good	Hicks	.669
H 423	67 09 25	1142.9	3	0.2	Excellent	Ferry	303.429
	74 07 13	1143.7	3	0.1	Good	Hicks	.436
H 425	67 09 25	1129.4	3	0.2	Excellent	Ferry	301.330
	74 07 13	1129.6	3	0.1	Good	Hicks	.334
H 427	67 09 25	1130.9	4	0.2	Good	Ferry	300.086
	74 07 10	1131.5	3	0.1	Excellent	Hicks	.087
H 430	67 09 28	1089.9	3	0.1		Hunt	298.608
	74 07 13	1089.5	3	0.1	Good	Hicks	.606
H 431	67 09 30	1145.9	3	0.2	Good	Hunt	305.302
	74 07 14	1146.1	3	0.1	Excellent	Hicks	.307
H 432	67 09 30	1144.8	4	0.2	Good	Hunt	308.405
	74 07 14	1145.2	3	0.1	Excellent	Hicks	.411
H 433	67 09 30	1148.2	1	0.3		Hunt	309.823
	74 07 14	1146.4	3	0.1	Excellent	Hicks	.829
H 435	67 09 22	1147.2	2	0.1		Hunt	317.868
	74 07 14	1147.4	3	0.1	Excellent	Hicks	.874

APPENDIX 2

Calculations of gravity differences, Broadlands Geothermal Field

BM	Ministry of Works and Development (Power Division) benchmark number.
Δg	Difference in the value of gravity between the 1967 and 1974 surveys. Values given are gravity value in 1974 minus gravity value in 1967; negative values indicate that the value of gravity at the benchmark decreased between 1967 and 1974.
Δh	Difference in elevation between the 1968 and 1974 surveys. Values given are elevation in 1974 minus elevation in 1968; negative values indicate subsidence has occurred. Values marked by an asterisk were not measured and were estimated from the contour map given in Fig. 2.
$g_{\Delta h}$	The gravity effect of the difference in elevation assuming a normal free air change of +3.1 μN kg^{-1} m^{-1} of subsidence.
$\Delta g - g_{\Delta h}$	Difference in gravity corrected for the change in elevation. Negative values indicate a decrease between 1967 and 1974.

BM	Δg ($\mu N/kg$)	Δh (m)	$g_{\Delta h}$	$\Delta g - g_{\Delta h}$
H 304	+0.1	−0.006	0	+0.1
H 305	+0.2	−0.008	0	+0.2
H 306	+0.2	−0.011	0	+0.2
H 307	−0.3	−0.023	+0.1	−0.4
H 308	0	−0.015	+0.1	−0.1
H 309	−0.4	−0.012	0	−0.4
H 310	+0.5	−0.011	0	+0.5
H 311	+0.4	−0.002	0	+0.4
H 313/3	−1.9	+0.004	0	−1.9
H 317	+0.2	−0.004	0	+0.2
H 318	−0.2	−0.006	0	−0.2
H 319	+0.5	−0.007	0	+0.5
H 322	+0.2	−0.009	0	+0.2
H 324/1	−0.2	−0.006	0	−0.2
H 326/3	+0.1	−0.010	0	+0.1
H 328	+0.2	−0.006	0	+0.2
H 328/1	−0.1	−0.003	0	−0.1
H 329	+0.1	−0.005	0	+0.1
H 332	+0.1	−0.008	0	+0.1
H 333	0.	−0.012	0	0
H 334	+0.2	−0.031	+0.1	+0.1
H 335	+0.4	−0.095	+0.3	+0.1
H 335/3	+1.3	−0.128	+0.4	+0.9
H 336	+0.7	−0.161	+0.5	+0.2
H 337/1	+2.4	−0.091	+0.3	+2.1
H 338	+0.1	−0.118	+0.4	−0.3
H 338/1	+0.2	−0.120	+0.4	−0.2

BM	Δg (μN/kg)	Δh (m)	$g_{\Delta h}$	$\Delta g - g_{\Delta h}$
H 339	+0.2	−0.134	+0.4	−0.2
H 340	0	−0.113	+0.4	−0.4
H 341	−0.8	−0.069	+0.2	−1.0
H 343	−0.1	−0.022	+0.1	−0.2
H 345	−0.5	−0.017	+0.1	−0.6
H 346	+0.4	−0.015	+0.1	+0.3
H 350	+0.2	−0.003	0	+0.2
H 352	+1.1	−0.001	0	+1.1
H 353	+0.5	+0.003	0	+0.5
H 354	+0.3	+0.003	0	+0.3
H 355	−1.2	+0.004	0	−1.2
H 356/3	−0.6	−0.009	0	−0.6
H 358/1	−0.8	−0.027	+0.1	−0.9
H 360	+0.5	−0.014	0	+0.5
H 361	+0.3	−0.079	+0.2	+0.1
H 362	+0.1	−0.016	+0.1	0
H 362/1	+0.5	−0.013	0	+0.5
H 364/1	−0.1	−0.051	+0.2	−0.3
H 365	+1.1	−0.114	+0.4	+0.7
H 366	−0.8	−0.080*	+0.3	−1.1
H 367	+2.0	−0.139	+0.4	+1.6
H 367/2	+1.2	−0.115	+0.4	+0.8
H 369	−0.6	−0.008	0	−0.6
H 371	+0.4	−0.014	0	+0.4
H 372	−0.2	−0.024	+0.1	−0.3
H 373	−0.3	−0.050	+0.2	−0.5

BM	Δg ($\mu N/kg$)	Δh (m)	$g_{\Delta h}$	$\Delta g - g_{\Delta h}$
H 374	+0.6	-0.006	0	+0.6
H 376	+0.6	-0.002	0	+0.6
H 378	-1.3	0*	0	-1.3
H 379	+0.1	0*	0	+0.1
H 382	-0.4	-0.010	0	-0.4
H 383	+0.5	-0.010	0	+0.5
H 384	+0.7	-0.008	0	+0.7
H 385	+0.1	+0.003	0	+0.1
H 386	+1.1	0	0	+1.1
H 387	-0.1	+0.004	0	-0.1
H 388	+3.0	+0.005	0	+3.0
H 391	-0.3	-0.003	0	-0.3
H 394	-0.7	-0.049	+0.2	-0.9
H 396	+0.7	-0.047	+0.2	+0.5
H 396/2	0	-0.045	+0.1	-0.1
H 397	+0.7	-0.026	+0.1	+0.6
H 399/1	-0.3	-0.057*	+0.2	-0.5
H 401	-0.7	+0.005	0	-0.7
H 402	-0.9	-0.009	0	-0.9
H 403	-0.4	-0.040	+0.1	-0.5
H 406	-0.8	+0.002	0	-0.8
H 407	-0.4	+0.002	0	-0.4
H 408	-0.5	-0.003	0	-0.5
H 410	+1.9	+0.009	0	+1.9
H 411	-15.4	-0.010	0	-15.4
H 412	+0.5	-0.004	0	+0.5

BM	Δg (μN/kg)	Δh (m)	$g_{\Delta h}$	$\Delta g - g_{\Delta h}$
H 414	+0.1	+0.003	0	+0.1
H 416	-0.3	+0.004	0	-0.3
H 423	+0.8	+0.007	0	+0.8
H 425	+0.2	+0.004	0	+0.2
H 427	+0.6	+0.001	0	+0.6
H 430	-0.6	-0.002	0	-0.6
H 431	+0.2	+0.005	0	+0.2
H 432	+0.4	+0.006	0	+0.4
H 433	+0.2	+0.006	0	+0.2
H 435	+0.2	+0.006	0	+0.2

APPENDIX 3

Temperatures and pressures in boreholes in the Ohaki area, Broadlands Geothermal Field

Bore	(A) 150 m below ground level T	Run	P	Run	(B) 750 m below ground level T	Run	P	Run
2	188	15 126	2.17	A1407P	265	15 168	5.90	32 521
3	170	15 224	2.03	3 160	260	14 659	6.86	31 845
4	186	16 070	1.34	33 567	265	14 736	7.14	31 866
8	192	15 849	2.10	33 378	270	15 169	5.90	32 604
9	186	15 530	2.17	32 366	278	15 176	7.14	32 564
11	184	16 224	0.86	33 031	265	16 224	5.48	33 714
13	126	16 223	2.03	32 661	266	16 223	6.10	33 713
15	192	16 293	2.86	33 762	272	16 293	7.83	33 762
17	180	15 726	1.38	33 838	270	16 226	6.03	33 716
18	178	16 110	*		257	16 225	5.96	33 715
19	86	16 275	*		277	16 275	6.00	33 753
20	156	16 160	1.28	33 718	275	16 228	6.03	33 718
21	133	16 111	*		270	16 111	6.03	33 615
22	186	16 106	2.45	33 842	275	16 106	6.34	33 842
23	115	16 108	0.93	33 839	225	16 377	6.17	33 839
Mean	164°C		1.80 MPa		226°C		6.33 MPa	

T = temperature (°C).

P = pressure (MPa). Asterisk indicates well-head pressure due to gas in the bore.

P = $P_{absolute} = P_{gauge} + 0.10$ MPa (1 MPa = 10^6 N/m^2 = 145.038 lbf/in^2).

Run = Ministry of Works and Development measurement run number. Data has been taken from those runs which have the longest standing times. Refer to unpublished M.W.D. Temperature and Pressure Graphs WG 3932/Bore Number.

CONCLUSIONS

The validity of the conclusion that the Florida Peninsula is differentially subsiding, and the reliability of phytogeography and plant succession as criteria leading to this conclusion depend upon additional radiometric data from the eastern and western coasts of the state. Substantiation of these inferences would underscore the pertinence of Laporte's (1968, p. 249) statement emphasizing that failure to regard lateral as well as vertical distribution of facies has usually resulted ". . . in hypotheses of multiple eustatic sea-level fluctuations which strain geologic credulity." Confirmation would also enable application of the criteria to fossil marine communities. Providing the communities are studied ... to the shore, and providing both the temporal succession and geographic distribution of the communities could be determined, it should be possible to determine the importance of coastal subsidence and uplift relative to eustatic fluctuations of sea level.

ACKNOWLEDGMENTS

I am grateful for the insight into this paper offered by Dr. Clarence A. Hall, Jr., Dr. J. William Schopf, Dr. Ronald Shreve, Bob Horodyski, and John C. Grimmer. I am also indebted to Dr. David Scholl for his encouragement. I must assume full responsibility, however, for any errors in this investigation. Julie Guenther prepared the illustrations.

REFERENCES CITED

Bromley, S. W., 1935, The original forest types of southern New England: Ecol. Mon., v. 5, p. 61–89.

Cooke, C. Wythe, 1939, Scenery of Florida, interpreted by a geologist: Florida Geol. Survey Bull., v. 17, 111 p.

Davis, John H., Jr., 1943, The natural features of southern Florida, especially the vegetation, and the Everglades: Florida Geol. Survey Bull., v. 25, 301 p.

Harshberger, John W., 1911, Phytogeographic survey of North America: New York, G. E. Stechert and Co., 704 p.

Laporte, Léo F., 1968, Recent carbonate environments and their paleoecologic implications, *in* Drake, Ellen T., *Editor*, Evolution and Environment, New Haven, Yale Univ. Press, 439 p.

Monk, Carl D., 1968, Successional and environmental relationships of the forest vegetation of North Central Florida: Am. Midland Naturalist, v. 78, p. 441–457.

Redfield, A. C., 1967, The post-glacial change in sea level in the western North Atlantic Ocean: Science, v. 157, p. 687–692.

Scholl, David W., 1964, Recent sedimentary record in mangrove swamps and rise in sea level over the southwestern coast of Florida, part 2: Marine Geology, v. 2, p. 343–364.

Scholl, David W., Craighead, Frank C., and Stuiver, Minze, 1969, Florida submergence curve revised: Its relation to coastal sedimentation rates: Science, v. 163, p. 562–564.

Manuscript Received by The Society August 11, 1969

TREVOR M. HUNT *Geophysics Division, Department of Scientific and Industrial Research, Wellington, New Zealand*

Geothermal Rm.

AREA NZ Wairakei

Gravity Changes at Wairakei Geothermal Field, New Zealand

ABSTRACT

Measurements of the value of gravity at 50 bench marks at Wairakei Geothermal Field, New Zealand, show that differences of up to 0.5 mgal have occurred between 1961 and 1967 and up to 0.1 mgal between 1967 and 1968. These differences, corrected for known changes in elevation, are interpreted as reflecting the net mass of water lost from the aquifer. The net loss between 1961 and 1967 is determined to be about 2.9×10^{14}g and hence only about 20 percent of the water drawn off was replaced, but between 1967 and 1968 there was little or no net loss.

INTRODUCTION

The Wairakei Geothermal Field is one of the larger hydrothermal areas in the active volcanic belt of New Zealand (Fig. 1). The geothermal field is underlain by a near-flat, Quaternary, acid volcanic rock sequence (Grindley, 1965) and the bulk of the steam production is obtained from a thick aquifer of pumice breccias (Waiora Formation) that is capped by lacustrine shales (Huka Falls Formation).

Since the opening of the Wairakei Geothermal Power Scheme in 1950 more than 5.6×10^{14}g of water (both liquid and gas phases) have been drawn from the ground for generating electricity, neglecting the small amount discharged into the atmosphere from natural geysers and fumaroles nearby. Extensive ground subsidence in the area was revealed by repeated releveling of bench marks and drew attention to the consequences of this substantial mass loss. Precise gravity measurements were made in August 1961, followed by remeasurements in April 1967 and May 1968 to see whether or not this mass loss could be detected and, if so, from what areas it was being drawn and to what extent it was being replaced. No previous measurements of gravity changes resulting from the exploitation of a geothermal field appear to have been made, although gravity changes resulting from volcanic eruptions (Iida and others, 1952) and earthquakes (Barnes, 1966) have been studied.

GRAVITY MEASUREMENTS

Gravity measurements were made on concrete bench marks in and about the Wairakei Geothermal Field using North American gravimeter AG1–96 (1961 survey) and La Coste Romberg gravimeter G-106 (1967 and 1968 surveys). The measurements were made under optimum ground-noise conditions, and a looping technique (Nettleton, 1940) was used to minimise instrumental drift errors. The gravimeter readings were corrected for instrument drift and for changes in the gravitational attraction of the sun and moon. The instrument drift correction was obtained from the quadratic curve of best fit (least-squares method) through the differences in gravity measured at repeated stations. The correction for changes in the gravitational attraction of the sun and moon was that of Longman (1959) multiplied by 1.2 (to account for deformation of the Earth). All computations were made by a digital computer and the measurements were reduced in terms of a base station on Taupo Fundamental bench mark, 7.2 km from Wairakei, considered to be outside the area affected by mass changes associated with the Wairakei Geothermal Field. Gravity measurements could not be made at bench marks in the vicinity of the uncontrolled "rogue" bore number 204 because of continuous strong microseisms.

GRAVITY CHANGES

In many cases there are differences in the value of gravity at the same point between 1961, 1967, and 1968 that are much greater than the standard error of the measurements. These differences can result from topographic changes adjacent to the points of measurement.

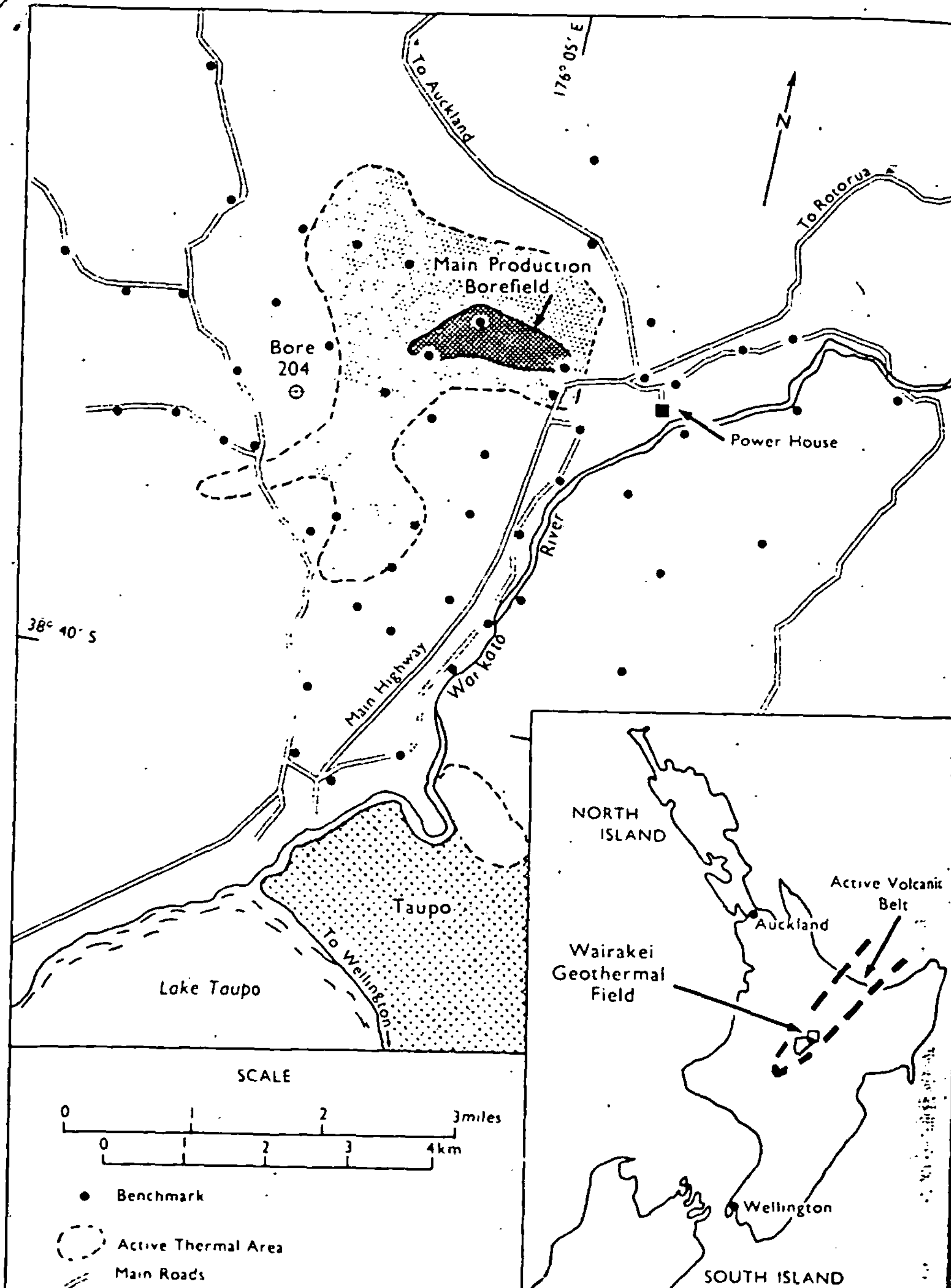

Figure 1. Location of Wairakei Geothermal Field, New Zealand, and bench marks used in the survey.

...cal changes in the ground-water level, changes in the elevation of the points of measurement relative to one another or to the base station, and net loss of water from the aquifer.

Small topographic changes associated with development of the geothermal power scheme have occurred adjacent to a few points, but in all cases the resulting gravitational change is estimated as being less than or equal to 0.01 mgal.

Measurements of water levels in 14 shallow drill holes in the Wairakei area between 1961 and 1966 showed that there was no continuous rise or fall of ground-water level, but local variations having an average fluctuation of 2 m occurred, which might cause variations of about 0.03 mgal. The bench marks were levelled in 1956, 1961, 1962, and 1966, and graphs of change of level with time for each bench mark have been drawn from which differences in elevation between 1961, 1967, and 1968 were determined (Figs. 2a, 3a). Bench-mark levels for April 1967 and May 1968 had to be obtained by extrapolation of the level-change graphs, but individual values are unlikely to be in error by more than 0.03 m. The bench marks were levelled in terms of bench mark A93, which was not a suitable gravity base station, and unfortunately Taupo Fundamental bench mark was not included in these levellings. Bench marks close to the Taupo Fundamental gravity base show little or no change in elevation relative to A93, however, and it has been assumed that elevation changes relative to Taupo Fundamental are equal to those relative to BM A93.

Assuming that no horizontal mass change took place in the subsidence, the gravity change would be approximately 0.31 mgal/m, the normal "free-air" gradient. Gravity differences for the periods 1961 to 1967 and 1967 to 1968 corrected for the elevation changes using a factor of 0.31 mgal/m are shown in Figures 2b and 3b. The mean standard error of the corrected gravity differences between August 1961 and April 1967 is 0.04 mgal and 0.03 mgal between April 1967 and May 1968. Contouring the gravity differences involved adjusting individual values by up to 0.1 mgal to obtain smooth contours. These corrected gravity differences are likely to represent the net mass differences in the aquifer of the Wairakei hydrothermal field for the periods 1961 to 1967 and 1967 to 1968.

The removal of a known mass of water from ... approximated by a change in density σ of a cylindrical disc for which the corresponding gravitational change can be computed. The change is given by:

$$\sigma = m/r^2h,$$

where m = mass of water withdrawn, r = radius to which withdrawal occurs, and h = thickness of aquifer. This assumes a uniform high permeability within a radius r about a central point and low permeability beyond.

At Wairakei the Waiora Formation has an average thickness of 0.5 km and over most of the geothermal field is at a depth of about 0.2 km. Using the cylindrical disc model and taking the measured mass loss of 3.6×10^{14}g for the period August 1961 to April 1967, I computed the change in gravity at the surface for various values of r (Fig. 4). If the water drawn off came solely from that portion of the aquifer below the main production bore field and was not replaced, a maximum gravity change of about -2.7 mgal would be expected. If the water was completely replaced there should be no gravity change, and if there was partial replacement or the water was extracted from a greater volume there would be corresponding gravity changes smaller than -2.7 mgal.

The gravity differences between August 1961 and April 1967 corrected for changes in elevation (Fig. 2b) show that:

(1) in all but one case there was a decrease in the value of gravity with a maximum change of -0.51 mgal;
(2) the greatest decrease in gravity measured occurred within the main production bore field and the gravity differences become smaller farther away from the bore field;
(3) the decrease in the value of gravity is not symmetrical about the main production bore field but extends in a westerly direction, roughly coincident with the level changes.

It follows from Gauss's potential theorem that the total anomalous mass m (in this case the net loss of water) can be determined by integrating the gravity anomaly (in this case the gravity differences) over the plane of measurement without assuming or calculating the shape and depth of the source (Hammer, 1945; Parasnis, 1962). The integration can be approximated by a summation

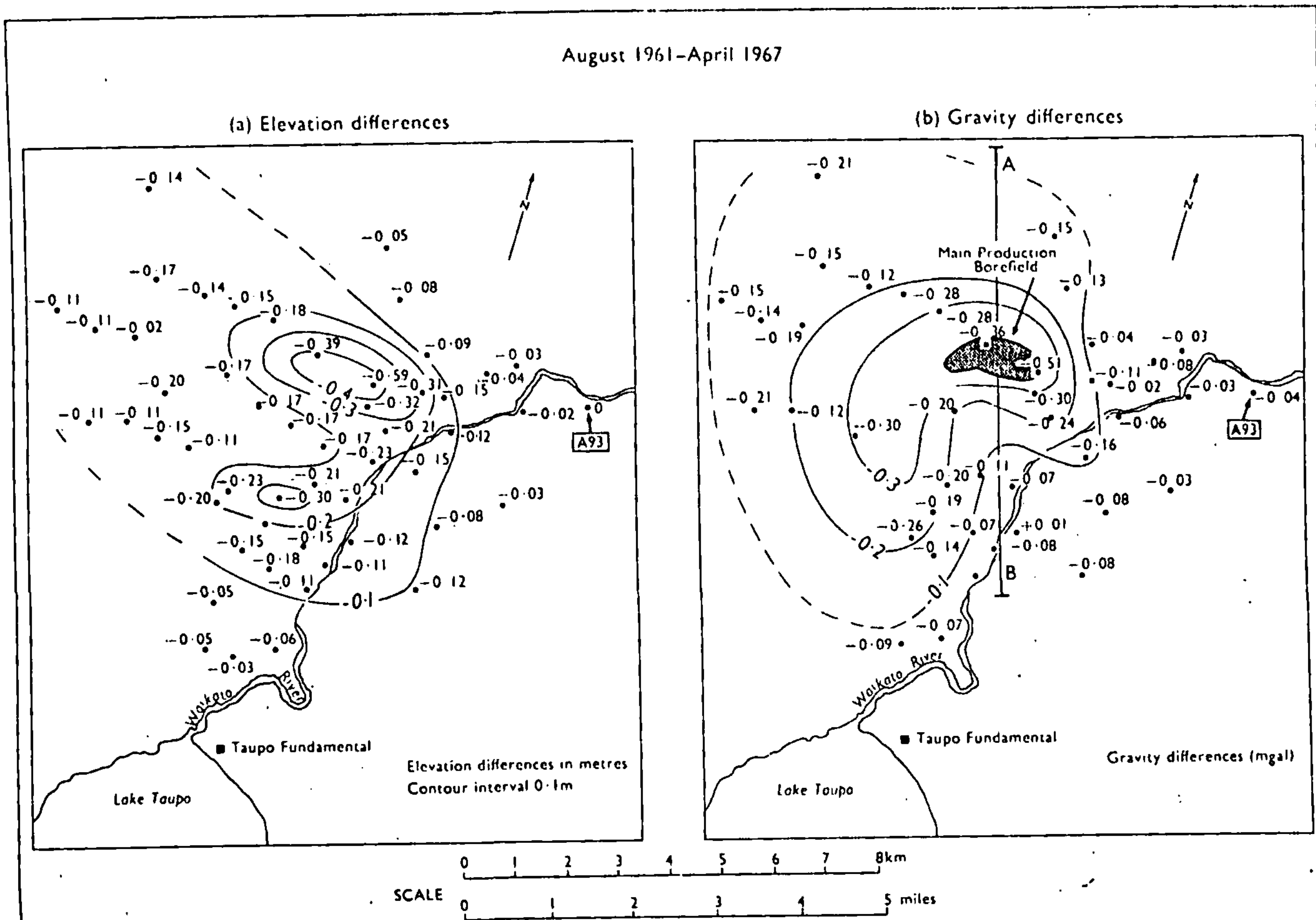

Figure 2. Elevation differences and gravity differences corrected for elevation differences, between August 1961 and April 1967, Wairakei Geothermal

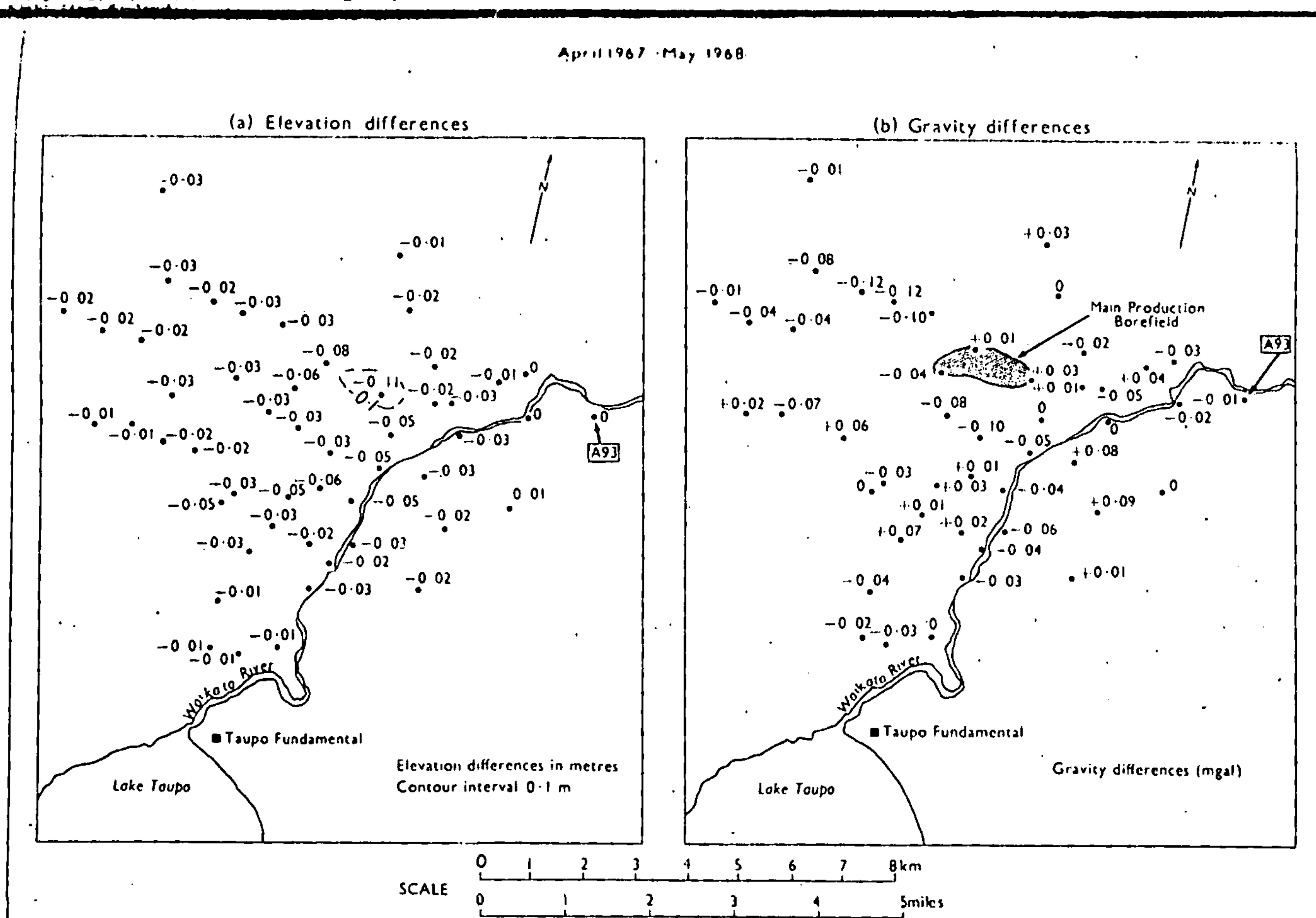

Figure 3. Elevation differences and gravity differences corrected for elevation differences, between April 1967 and May 1968, Wairakei Geothermal Field, New Zealand.

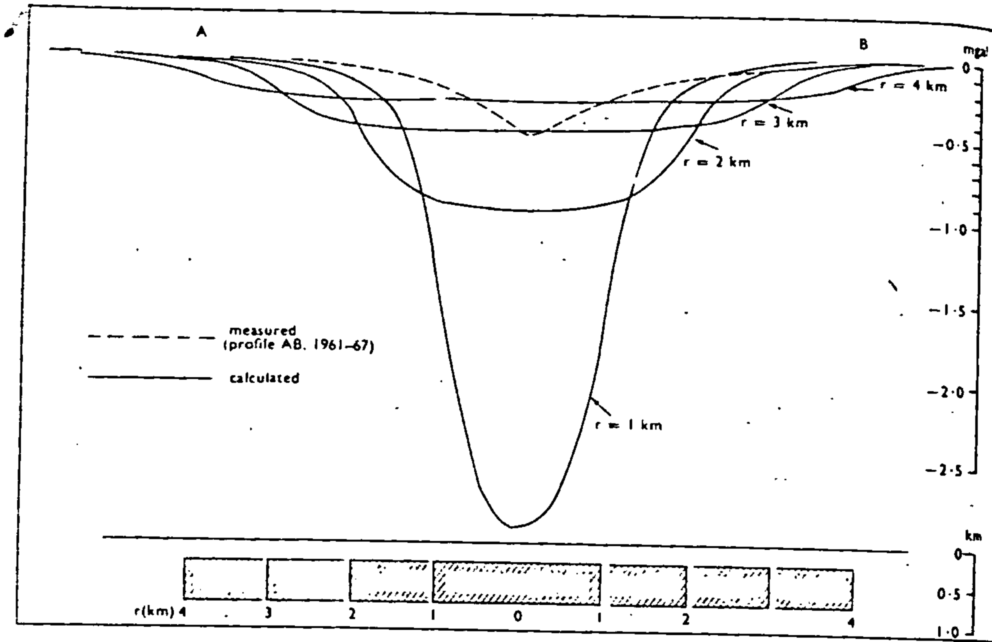

Figure 4. Gravity profiles over cylinders of different radius representing the mass loss between August 19[61] and April 1967 (3.6×10^{14}g).

where G = universal gravitational constant and Δg = local gravity anomaly associated with an areal element Δs of the plane P.

The sum of the gravity differences between 1961 and 1967, obtained from the contours in Figure 2b, is about -12 mgal km², which corresponds to an anomalous mass of -2.9×10^{14}g or 80 percent of the mass of water actually withdrawn. This means that between August 1961 and April 1967 about 20 percent of the water removed from the aquifer was replaced. However, this value is only approximate because of the errors involved in obtaining the summation, as discussed by Hammer (1945), and the uncertainty of the 0.1-mg[al] change contour west of the main productio[n] bore field.

Despite a mass draw-off of 0.5×10^{14}g be[tween] April 1967 and May 1968, the correcte[d] gravity differences (Fig. 3b) are generall[y] small, and no consistent pattern can be see[n] except for a small area of decrease in gravi[ty] west of the main production bore field. Th[is] suggests that either the water is being draw[n] from a much greater area than was surveyed o[r] what is more likely, the mass inflow equalle[d] the mass draw-off. Between December 19[6?] and April 1968 about 60 percent of the ma[ss] ...

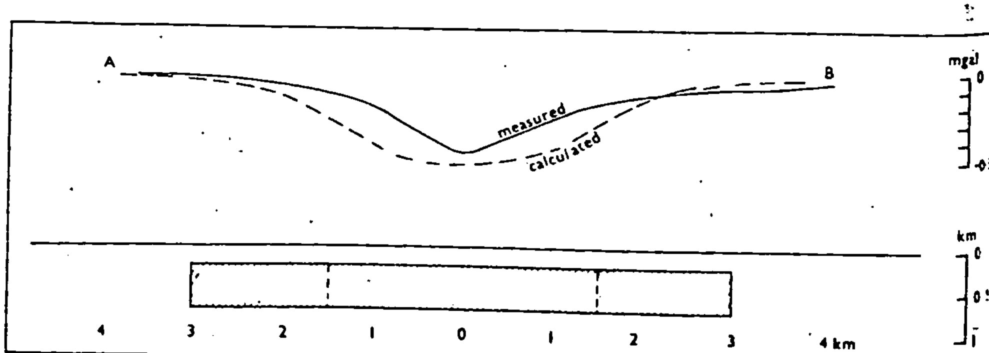

Figure 5. Comparison of gravity differences (August 1961 to April 1967) along profile AB with the grav[ity] ...

...duction bore field was shut down, and this ...uld have assisted recharging.

The asymmetry of the gravity differences between August 1961 and April 1967 suggests that the aquifer is not of uniform effective porosity and that either:

(1) water is being drawn from areas west of the main bore field in preference to the east; or

(2) the aquifer has high effective porosity in areas east of the main bore field, allowing rapid replacement of water drawn from those areas.

Measurements made in drill holes have shown that east of the main bore field the aquifer pressures do not respond to pressure changes originating in the main bore field as do those to the west, indicating low effective porosity to the east. This would suggest that water has been drawn from western areas at a greater rate than it has been replaced. There does not appear to be any geological explanation for this.

A comparison of a section AB (Fig. 2b) through the measured gravity differences for the period 1961 to 1967 with the theoretical curves is given in Figure 4. The measured anomaly profile is difficult to reconcile with those of the various theoretical models, but a closer fit is obtained if a double cylinder model (Fig. 5) is taken, in which half the mass loss comes from an inner cylinder of radius 1.5 km and half from an annulus of inner radius 1.5 km and outer radius 3 km. This suggests that in any one direction the net amount of water lost is an inverse function of the distance from the centre of the bore field.

The mean temperature between 0.3 km and 0.6 km beneath the geothermal field has been averaged for all drill holes at two-monthly intervals since 1953, and in the period 1955 to 1962 the temperature in that zone has remained within the range 240° to 250° C (Grindley, 1965) in which water has a density of about 0.8 g/cm³ (Forsythe, 1954). Taking this value for density, the water lost (net) from the geothermal system in the period August 1961 to April 1967 would have a volume of about 4×10^{14} cm³. The volume of surface subsidence between August 1961 and April 1967, obtained by integrating the elevation differences shown in Figure 2a over the area, is about 1×10^{13} cm³, which is only about 3 percent of the volume of water lost from the geothermal system.

CONCLUSIONS

The gravity method can be used to monitor the net mass loss from a geothermal field under exploitation and can also give an indication of the area from which the water has been drawn.

ACKNOWLEDGMENTS

Credit must be given to C. J. Banwell and W. I. Reilly for proposing the idea and making the original measurements in 1961. I am grateful for unpublished material and assistance provided by engineers John W. Hatton (Wairakei) and Neville D. Dench (Wellington) from the New Zealand Ministry of Works. John Tawhai (Wairakei) gave me valuable assistance by locating bench marks during the field work. R. Boulton, T. Hatherton, M. P. Hochstein, and W. I. Reilly critically reviewed the manuscript.

REFERENCES CITED

Barnes, D. F., 1966, Gravity changes during the Alaska Earthquake: Jour. Geophys. Research, v. 71, no. 2, p. 451–456.

Forsythe, W. E., 1954, Smithsonian physical tables (9th ed.): Washington, Smithsonian Institute, 827 p.

Grindley, G. W., 1965, The Geology, structure, and exploitation of the Wairakei Geothermal Field, Taupo, New Zealand: New Zealand Geol. Survey Bull. n.s. 75, Wellington, Govt. Printer, 131 p.

Hammer, S., 1945, Estimating ore masses in gravity prospecting: Geophysics, v. 10, no. 1, p. 50–62.

Iida, K., Kayakawa, M., Katayose, R., 1952, Gravity survey of Mihara Volcano, Ooshima Island, and changes in gravity caused by eruption: Geol. Survey Japan; Rept. 152, p. 1–23 (in Japanese, but has English summary).

Longman, I. M., 1959, Formulas for computing the tidal accelerations due to the sun and moon: Jour. Geophys. Research, v. 64, no. 12, p. 2351–2355.

Nettleton, L. L., 1940, Geophysical prospecting for oil: New York, McGraw-Hill Book Co.

Parasnis, D. S., 1962, Principles of applied geophysics: London, Methuen, 176 p.

AREA
NZ
Wairakei

A Galerkin-Finite Element Analysis of the Hydrothermal System at Wairakei, New Zealand

JAMES W. MERCER

U.S. Geological Survey, Reston, Virginia 22092

GEORGE F. PINDER

U.S. Geological Survey and Department of Civil Engineering, Princeton University, Princeton, New Jersey 08540

IAN G. DONALDSON

New Zealand Department of Scientific and Industrial Research, Lower Hutt, New Zealand

A single-phase simulation model was applied to the hot-water hydrothermal field at Wairakei, New Zealand. A two-dimensional areal analysis was made of the production aquifer under steady state and transient flow conditions, allowing vertical flow of heat and fluid through an overlying confining bed. Calculated temperature and pressure patterns correlate well with observed patterns until approximately 1963, when increasing quantities of steam in the production aquifer invalidated the assumption of single-phase flow. For further simulation of the Wairakei reservoir the numerical model will need to be extended to incorporate phase change and three-dimensional flow. Preliminary results, however, indicate that the response of hot-water hydrothermal systems to exploitation can be simulated by using a mathematical reservoir model based on a Galerkin-finite element approach.

INTRODUCTION

Current interest in geothermal energy has stimulated increased research in the area of heat transport in porous media. Many of these investigations are concerned with understanding the physics and chemistry of both vapor-dominated and hot-water geothermal systems in order to aid exploration and help predict exploitation effects. In this study we consider only hot-water geothermal systems and present a mathematical analysis designed to compute the spatial (horizontal cross section only) and temporal distribution of pressure and temperature in saturated porous media.

The partial differential equations which describe the flow of liquid and the transport of heat in porous media are presented. Assuming the problem to be two-dimensional, we then use Galerkin's criterion to generate approximate integral equations. These equations are solved temporally by using finite difference techniques and spatially by using the method of finite elements.

The applicability of this approach to solving field problems is demonstrated by simulating over a 10-year period (1953-1962) the response to development of a hot-water hydrothermal (geothermal) system located at Wairakei, New Zealand. The Wairakei field was the first hot-water hydrothermal system to be utilized for the generation of electricity. Exploitation has caused decreased pressures and the formation of large quantities of steam in the production aquifer. The field, however, remained a hot-water system for approximately 10 years, and there are sufficient data available to formulate a numerical model.

Previous Investigations

Investigations of the simultaneous flow of fluid and heat in porous media may be classed into three groups: (1) those made in hydrological research, (2) those made in research related to the petroleum industry, and (3) those made in research associated with geothermal studies. Early work in the first group was conducted by *Philip and DeVries* [1957] and *DeVries* [1958], who developed the differential equations for heat and moisture transfer in porous media and examined the conditions of steady state heat conduction. More recently, *Stallman* [1963] and *Bredehoeft and Papadopulos* [1965] examined heat flow in porous media as a means of calculating rates of groundwater movement.

In the petroleum industry, most of the work concerned with heat and fluid flow in porous media is associated with the secondary recovery of oil by hot fluid injection and in situ combustion. Although these processes were used in the field as early as the 1930's, theoretical studies were not made until the 1950's [e.g., *Lauwerier*, 1955; *Marx and Langenheim*, 1959]. Most of the early theoretical studies considered heat flow by conduction only and ignored liquid flow. More recent studies consider both conduction and convection. Typical equations used in this work are given by *Shutler* [1970] and *Chappelear and Volek* [1968].

Most fluid flow research relating to geothermal studies involves two-dimensional models of a vertical cross section. In most cases the authors consider such problems as the source of the hydrothermal liquid and its mechanism of transport. One early modeling effort by *Einarsson* [1942] involved the use of a pipe model to study the hot springs of West Iceland. This work was extended and further developed by *Bodvarsson* [1948, 1949, 1950, 1954, 1961]. Other authors who have used pipe models include *White* [1957, 1961], *Elder* [1966], and *Donaldson* [1968*a*, 1968*b*, 1970]. Another popular vertical model consists of a saturated homogeneous porous medium heated from below. Examples of this type of model are given by *Wooding* [1957, 1958, 1959, 1960*a*, 1960*b*, 1962, 1963], *Donaldson* [1962], *Elder* [1957, 1966], *McNabb* [1965], *Aziz et al.* [1968], and *Cady* [1969].

Although the above models are useful in understanding hydrothermal systems, in general they cannot be used to predict the response of a hydrothermal field to the stresses of exploitation. An early attempt to do this was made by *Whiting and Ramey* [1969], who used concepts generally applied in reservoir engineering to model the Wairakei hydrothermal field as a lumped parameter system. Another lumped parameter approach was made by *Marshall* [1966, 1970] using a vertical flow model with allowance for lateral inflow. These types of models are useful in examining the general trends of a system; however, they do not account for the spatial dependence of the solution. What is needed is a deterministic model which treats the hydrothermal field as a distributed parameter system.

Such a model is presented in this paper and consists of a digital computer program which solves the liquid flow and heat transport equations, given appropriate boundary and initial conditions. The model is currently constrained by economic considerations to two dimensions in space and one in time. The question arises as to which two spatial dimensions to consider. The vertical cross section would provide the more interesting scientific problem, since this model would allow free convection to be simulated. However, to consider the practical problem of simulating the response of the hydrothermal system to development (including well location and withdrawal distribution), it is necessary that we consider an areal model similar to those used for simulation in groundwater hydrology [e.g., *Pinder and Bredehoeft*, 1968; *Bredehoeft and Pinder*, 1973].

DESCRIPTION OF NUMERICAL MODEL

A detailed development of the governing equations is given by *Mercer et al.* [1975]. Only the major assumptions and final equations are presented here.

Assumptions

Although there are many assumptions involved in this development, only the major ones are listed below:

1. Density is assumed to be related to temperature and pressure by a first-order Taylor series. This assumption is only valid when there are small density variations about some initial density distribution ρ_0. Since temperatures, and hence densities, vary only slightly throughout the early period of exploitation at the Wairakei field, this assumption appears reasonable. The problem is to determine accurate initial densities based on initial temperatures and pressures. An examination of the variation of water density with temperature and pressure [*Meyer et al.*, 1968, p. 42] shows that density varies with pressure (1.0×10^6 to 50.0×10^6 N/m^2 at various temperatures) only about 3.0%, whereas density varies with temperature (0.0° to 250.0°C at various pressures) approximately 20.0%. Because of the larger temperature dependence, we decided to use the following empirical formula developed by I. G. Donaldson (written communication, 1972) which relates initial density to temperature alone:

$$\rho_0 = 1.00606 \times 10^3 - 2.46020 \times 10^{-1} T_0 - 2.31633 \times 10^{-3} T_0^2 \quad (1)$$

where T_0 is the initial temperature in degrees Celsius and ρ_0 has the dimensions kg/m^3. This equation is valid for liquid saturation temperatures between 100° and 280°C.

2. Although viscosity is both temperature- and pressure-dependent, it varies with temperature to a much greater extent than it does with pressure [*Meyer et al.*, 1968, p. 73]. We therefore assume that viscosity is related to temperature by the empirical equation (A. McNabb, written communication, 1967)

$$\frac{1}{\mu} = 5.38 \times 10^3 + 3.8 \times 10^3 A - 2.6 \times 10^2 A^3 \quad (2)$$

where $A = (T - 150)/100$, T is in degrees Celsius, and μ is in kg/m s. This equation is valid in the liquid saturation temperature range of 0°–300°C.

3. Heat transport is assumed to occur in both the liquid phase and the solid matrix. Further, it is assumed that thermal equilibrium between the liquid and solid matrix is achieved instantaneously.

4. Conductive heat flow in the solid phase is given by

$$h_i^s = -(1 + \phi) K_{ij}^s \, \partial T / \partial x_j \quad (3)$$

where K_{ij}^s is the thermal diffusion tensor of the solid phase and ϕ is the porosity.

5. Heat transfer in the liquid phase is somewhat more complicated, since in addition to molecular diffusion, heat transfer by mechanical dispersion may be important. The heat flux associated with these mechanisms is given by

$$h_i = -\phi K_{ij} \, \partial T / \partial x_j \quad (4)$$

where

$$K_{ij} = K_{ij}^m + K^d \psi_{ij} \quad (5)$$

K_{ij} is the hydrodynamic thermal dispersion tensor, K_{ij}^m is the mechanical thermal dispersion tensor, K^d is the molecular thermal diffusion coefficient, and ψ_{ij} is the porous medium 'tortuosity' tensor.

The hydrodynamic thermal dispersion tensor is analogous to the hydrodynamic dispersion tensor used in mass transport work and is subject to a similar analysis. Following a development analogous to that used by *Reddell and Sunada* [1970, p. 10] for the hydrodynamic dispersion tensor, we obtain the nine components of the hydrodynamic thermal dispersion tensor. The main diagonal terms have the form

$$K_{xx} = K_l \frac{v_x v_x}{v^2} + K_t \frac{v_y v_y}{v^2} + K_t \frac{v_z v_z}{v^2} + K^d \psi \quad (6)$$

where K_l and K_t are the longitudinal and transverse mechanical thermal dispersion coefficients and ψ is the tortuosity factor. The off-diagonal terms are of the form

$$K_{xy} = K_{yx} = (K_l - K_t) \frac{v_x v_y}{v^2} \quad (7)$$

6. Heat capacity c_v, vertical compressibility α, liquid compressibility β, liquid thermal volume expansion λ, and the solid density ρ_s are treated as constants. Although the above parameters are functions of temperature and pressure, their variation is relatively small. Consequently, treating these as constants does not significantly reduce the accuracy of the model.

7. It is assumed that flow within a confined aquifer can be considered essentially horizontal, so that only the two horizontal dimensions need be considered.

8. Finally, we assume a chemically inert single-phase (hot-water) system.

Equations

On the basis of these assumptions, the liquid flow equation and heat transport equation can be written

$$\frac{\partial}{\partial x_i} b\left(\frac{\rho k_{ij}}{\mu} \frac{\partial p}{\partial x_j}\right) = b(\rho\alpha + \phi\rho_0\beta) \frac{\partial p}{\partial t} - b\phi\rho_0\lambda \frac{\partial T}{\partial t} - rb - \frac{\rho k_{zz}}{\mu}\left(\frac{\partial p}{\partial z} + \rho g\right)\Big|_{z_2} + \frac{\rho k_{zz}}{\mu}\left(\frac{\partial p}{\partial z} + \rho g\right)\Big|_{z_1} \quad (8)$$

and

$$b[\gamma c_w + (1 - \phi)\rho_s c_{ss}] \frac{\partial T}{\partial t} + b\gamma c_w v_i \frac{\partial T}{\partial x_i} = \frac{\partial}{\partial x_i} b[\phi K_{ij} + (1 - \phi) K_{ij}'] \frac{\partial T}{\partial x_j} + b\gamma Q + b(1 - \phi)\rho_s Q_s + [\phi K_{zz} + (1 - \phi) K_{zz}'] \frac{\partial T}{\partial z}\Big|_{z_2} - [\phi K_{zz} + (1 - \phi) K_{zz}'] \frac{\partial T}{\partial z}\Big|_{z_1} + \gamma c_w v_z (T - T')\big|_{z_2} - \gamma c_w v_z (T - T')\big|_{z_1} \quad (9)$$

where the equation parameters have been vertically averaged between the top of the aquifer z_2 and the bottom z_1 and where $b = b(x_i)$ is the saturated thickness of the aquifer. The vertical bars indicate terms which are evaluated at either the top or the base of the aquifer. In obtaining these terms it was assumed that the mass and heat flow entering the top and bottom of the aquifer are vertical and colinear with the z axis. These terms depend on observed field conditions and will be evaluated later. The sink term r in (8) represents a discharging well or wells and is defined by

$$rb = \rho q = -\rho \sum_{k=1}^{n} \hat{q}(x_k, y_k)\delta(x - x_k)(y - y_k) \quad (10)$$

where $\hat{q}$ is the discharge from the aquifer, δ is the Dirac delta function, and n is the number of sinks. The source terms Q and Q_s in the heat transport equation also represent point sources and are assumed to be zero.

The system of (8) and (9) cannot in general be solved analytically, and a numerical approach is required. The numerical scheme chosen for the spatial solution is a combination of the finite element concept and the Galerkin method of weighted residuals. Finite difference techniques are used to approximate the time derivatives. Details of this approach are given by *Mercer et al.* [1975]. General references on the application of the Galerkin-finite element method to field equations include *Zienkiewicz and Parekh* [1970] and *Pinder and Frind* [1972].

WAIRAKEI HYDROTHERMAL SYSTEM

Location and History of Development

The Wairakei field is located 8 km north of Lake Taupo and is situated on the west bank of the Waikato River (see Figure 1). At this location the river acts as a groundwater discharge area. The Wairakei region, generally considered to occupy a surface area of approximately 15 km² [*Grindley*, 1965, p. 85], extends westward from the river approximately 5 km over relatively flat valleys floored with Taupo pumice alluvium. It is bordered on the west by hills of Wairakei breccia that rise 90–150 m above the valleys and serve as a groundwater recharge area.

Centered in an active volcanic belt, Wairakei is one of many geothermal regions located between the Tongariro and White Island volcanoes. This volcanic belt appears to be a surface manifestation of a landward extension of the Pacific trench system found north of New Zealand. This hypothesis is supported by gravity, magnetic, and seismic studies which indicate that this volcanic belt is a structural depression approximately

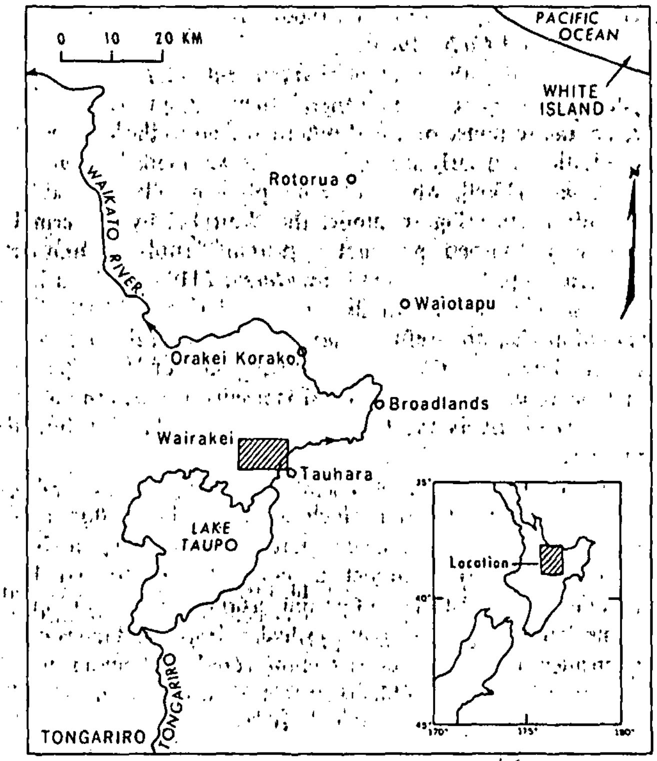

Fig. 1. Index map showing location of Wairakei, New Zealand; inset is of North Island.

5 km deep filled with broken block structure and penetrated by rhyolitic complexes [*Modriniak and Studt*, 1959].

Power generation began at Wairakei in 1958, and by 1968 the power stations at Wairakei were providing 192 MW, or approximately 18% of the total electrical requirements of New Zealand's North Island. Wairakei is considered to have been a hot-water system prior to exploitation [*White et al.*, 1971, p. 76] and to have remained so until approximately 1963. Utilizing steam (which flashes in the wells) to drive turbines, Wairakei became the first hot-water system to be developed for the purpose of generating electricity. The original hot-water nature of the field and the documentation of its response to development make Wairakei a logical choice for demonstrating the application of the simulation model. Once tested, this model can be used in research and development of other hot-water hydrothermal fields, such as those found in Iceland, Mexico, Japan, USSR, El Salvador, the Philippines, and the United States.

Geohydrology

The Wairakei hydrothermal field is underlain by a nearly horizontal Quaternary acidic volcanic rock sequence consisting of the following formations (in ascending order) [*Grindley*, 1965, p. 11]: Holocene pumice cover, Wairakei breccia, Huka Falls formation, Haparangi rhyolite, Waiora formation, Waiora Valley andesite, Wairakei ignimbrites, and the Ohakuri group. There are at least two aquifers in the above sequence, the Wairakei breccia and the Waiora formation. Although a deeper third aquifer may also exist in the Ohakuri group, it has been found in only one well, and its lateral extent is unknown.

The bulk of steam and hot water discharged by Wairakei wells comes from the Waiora aquifer. This unit consists of pumice breccias and vitric tuffs, ranging in thickness from

TABLE 1. Properties of the Waiora Aquifer and Huka Falls Aquitard

Property	Value	Reference
Aquifer permeability (horizontal)	$k_{xx} = k_{yy} = 1.0 \times 10^{-13}$ m^2	*Elder* [1966, p. 12]
Aquifer porosity	$\phi = 0.20$	McNabb (written communication, 1967)
Vertical compressibility of aquifer	$\alpha = 2.90 \times 10^{-10}$ m^2/N	*Jacob* [1950, p. 334]*
Heat capacity of solid phase	$c_{vs} = 0.22$ kcal/kg °C	Donaldson (oral communication, 1972)
Density of solid phase	$\rho_s = 2187$ kg/m^3	*Barwell* [1955, p. 46]*
Thermal diffusion coefficient of solid phase	$K_s = 5.2 \times 10^{-4}$ kcal/m s °C	McNabb (written communication, 1967)
Confining bed permeability (vertical)	$k' = 1.0 \times 10^{-14}$ m^2	*Wooding* [1963, p. 530]*
Confining bed porosity	$\phi' = 0.25$	McNabb (written communication, 1967)
Confining bed specific storage	$S_s = 1.0 \times 10^{-3}$/m	*Domenico and Mifflin* [1965, p. 566]*

*Estimated from given reference.

about 600 m in the western part of the production zone to more than 800 m in the eastern part. The permeability of the Waiora aquifer varies spatially depending on the amount of brecciation and is highest at fault zones and near a lower unconformable contact. Although productive wells at Wairakei are nearly always located in zones of locally high permeability associated with major faults, the reservoir as a whole responds as a porous medium defined in a continuum sense and is treated as such in this model. This assumption leads to a value of permeability which probably lies between that of the intergranular matrix and the fracture permeability. While in general the Waiora aquifer is assigned an average permeability of 1.0×10^{-13} m^2, a value of 1.0×10^{-14} m^2 was assigned to the eastern part of the production area because of fewer fault zones and generally lower calculated permeabilities. Other properties of the Waiora aquifer are given in Table 1, and associated fluid properties are given in Table 2.

The Waiora aquifer is overlain by lacustrine shales of the Huka Falls formation which range in thickness from 30 to 300 m and act as confining beds. In some locations the shales are interbedded with breccia. These confining beds are also treated as a porous medium defined in a continuum sense. Properties of the Huka Falls formation pertinent to this analysis are shown in Table 1.

The Wairakei ignimbrite, a welded rock of low primary permeability, underlies the Waiora aquifer. The base of the Waiora aquifer is not well defined because of secondary permeability afforded by fracture zones and the irregular surface of the unconformity between the ignimbrites and the aquifer. The problem of determining the base of the aquifer is further complicated in the south and southwest, where rhyolite overlies the ignimbrite and progressively cuts out the Waiora aquifer from below. The rhyolite also displays secondary permeability in its upper layers [*Studt*, 1958, p. 708].

The stratified volcanic sequence at Wairakei is complexly faulted and draped over a basement horst. Most of the major fault zones are well-defined through drilling and strike in a southwest-northeast direction [*Bolton*, 1970]. It is generally thought that such fault zones in the underlying ignimbrites are the source of the hot water in the Waiora aquifer.

Heat and Mass Flows and Temperatures at Wairakei

The natural heat flow at Wairakei has been measured several times beginning in 1951. *Fisher* [1964] gives a summary of results obtained by various authors over the period from 1951–1959, and his tabulations are shown in Table 3. As may be seen, the values range from 82,000 kcal/s [*Ellis and Wilson*, 1955] obtained by using chemical methods to 163,000 kcal/s [*Thompson et al.*, 1961] measured by using physical methods. *Elder* [1966, p. 68, 1965, p. 224] interpreting data from *Ellis and Wilson* [1955] and *Thompson et al.* [1961] estimates that the preexploitation heat flow at Wairakei was 252,000 kcal/s.

One common conclusion of all the heat flow surveys is that the majority of the natural heat flow is due to convection and is thus associated with a natural mass discharge. Although the total mass discharge was not measured, it can be estimated

TABLE 2. Properties of the Liquid

Property	Value	Reference
Compressibility coefficient of the liquid phase	$\beta = 4.78 \times 10^{-10}$ m^2/N	*Jacob* [1950, p. 334]*
Coefficient of thermal volume expansion for the liquid phase	$\lambda = 5.0 \times 10^{-4}$/°C	*Harlow and Pracht* [1972, p. 7044]
Heat capacity of the liquid phase	$c_v = 1.0$ kcal/kg °C	*Weber et al.* [1959, p. 206]
Thermal diffusion coefficient (thermal conductivity of the liquid phase)	$K^d = 1.553 \times 10^{-4}$ kcal/s m °C	*Elder* [1966, p. 26]

*Estimated from given reference.

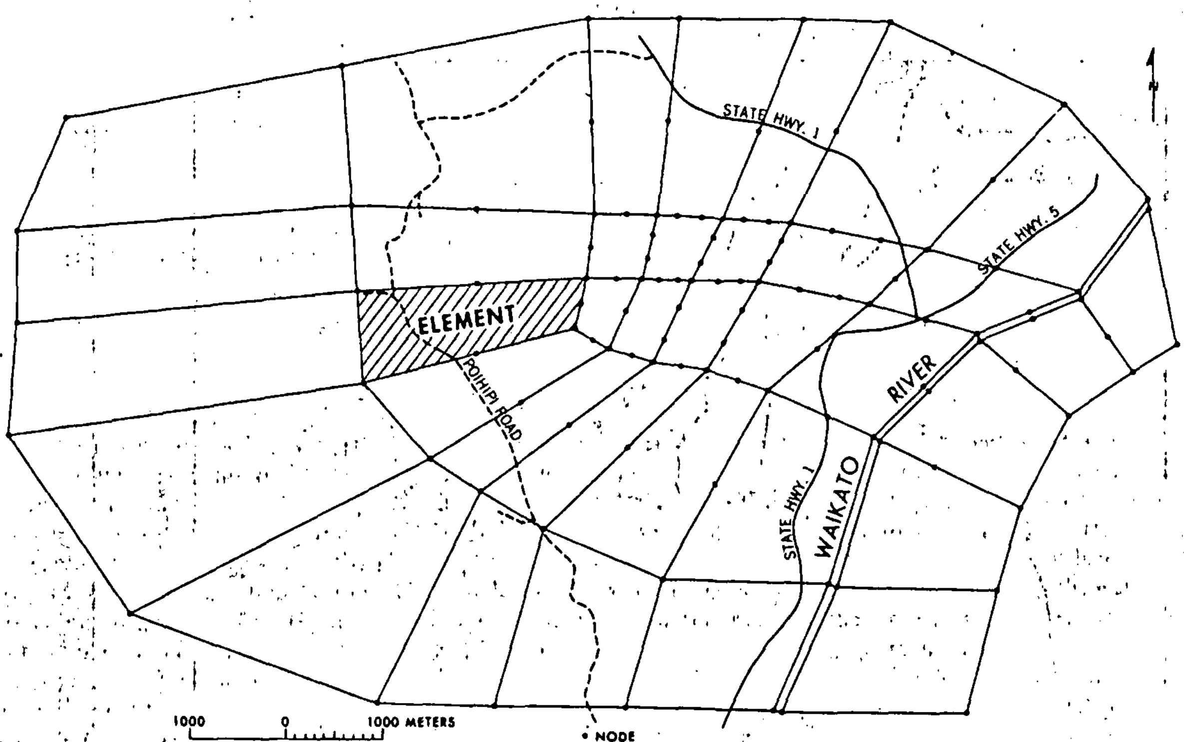

Fig. 3. Wairakei element configuration for Galerkin-finite element analysis.

clude terms which account for vertical mass and heat flows at the top and base of the aquifer (these are sometimes referred to as leakage terms). These terms need to be evaluated in order to model the Wairakei system.

The conceptual model of Wairakei consists of a layered system as shown in the idealized geologic cross section in Figure 4. Mass and heat are allowed to flow vertically through the confining beds (i.e., the Huka Falls formation). The direction of flow is determined by the potential and thermal gradients across the confining beds and may vary spatially and temporally. To determine the direction and magnitude of these flows, the pressure and temperature distributions at the top of the Huka Falls formation are required. To obtain the pressure distribution, the Wairakei breccia and the Holocene pumice are treated as a single aquifer ranging in thickness from 520 m in the west to 160 m in the east, where they are cut by the Waikato River. It is assumed that recharge (rainfall) is sufficient in this upper aquifer to maintain a water table near land surface. Head values in this upper aquifer can be estimated by using a topographic map of the Wairakei region, and pressures at the top of the Huka Falls formation can be calculated. The temperature distribution for the top of the Huka Falls formation was obtained from data of *Grindley* [1965, Table 1, p. 109] and is presented in Figure 5.

Using these assumptions, we can evaluate the vertical flow terms in (8) and (9) for the top of the aquifer. For the flow equation,

$$\frac{\rho k_{zz}}{\mu}\left(\frac{\partial p}{\partial z} + \rho g\right)\bigg|_{z_2} = \rho q' \tag{11}$$

where q' represents vertical liquid flow through the Huka Falls formation. For the steady state case, q' becomes

$$q' = (k'/\mu b')(p' - p + \rho g b') \tag{12}$$

where k' is the permeability and b' is the thickness of the Huka Falls formation, p' is the pressure distribution above the Huka Falls formation, and p is the pressure in the Wairoa formation. It is assumed that transient flow in the Huka Falls formation is due to a stepwise change in pressure in the Waiora aquifer and for the transient case q' may be approximated by [*Bredehoeft and Pinder*, 1970]

$$q' = (p_0 - p)\frac{K'}{\rho g b'(\pi K' t'/2b'^2 S_s)^{1/2}} \cdot\left\{1 + 2\sum_{n=1}^{\infty} \exp\left[-\frac{n^2}{(K't'/2b'^2 S_s)}\right]\right\} + \frac{K'}{\rho g b'}(p' - p_0) + K' \tag{13}$$

where $K' = k'\rho g/\mu$ is the hydraulic conductivity and $S_s = \rho g(\alpha + \phi'\lambda)$ is the specific storage of the Huka Falls formation and

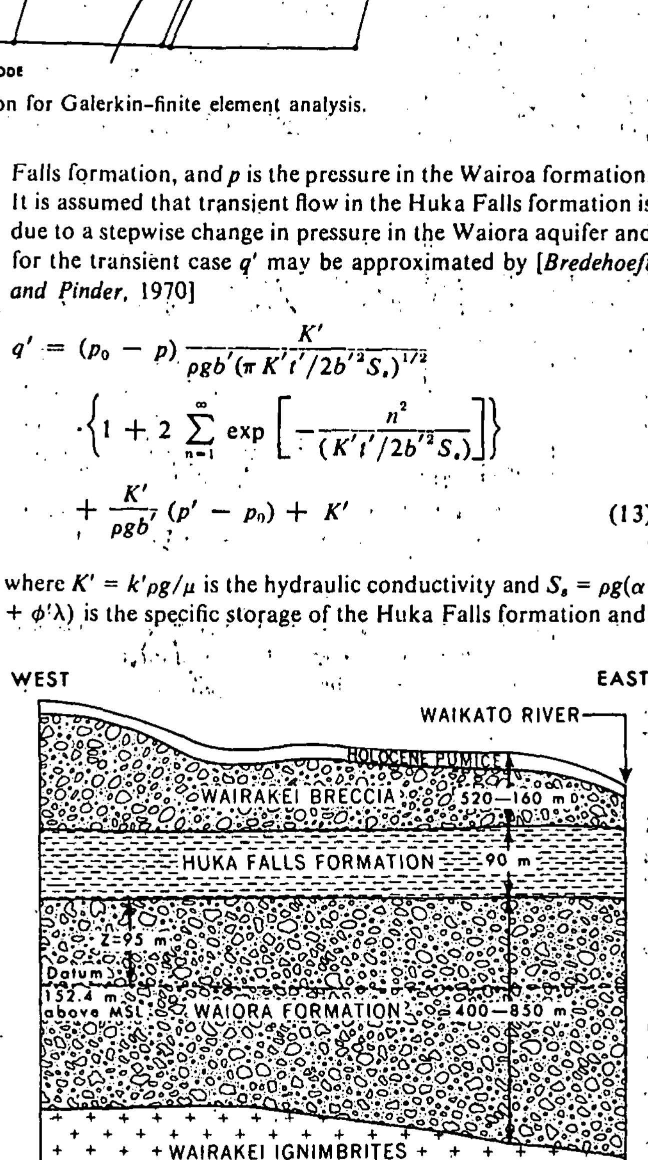

Fig. 4. Idealized geologic cross section of Wairakei, New Zealand.

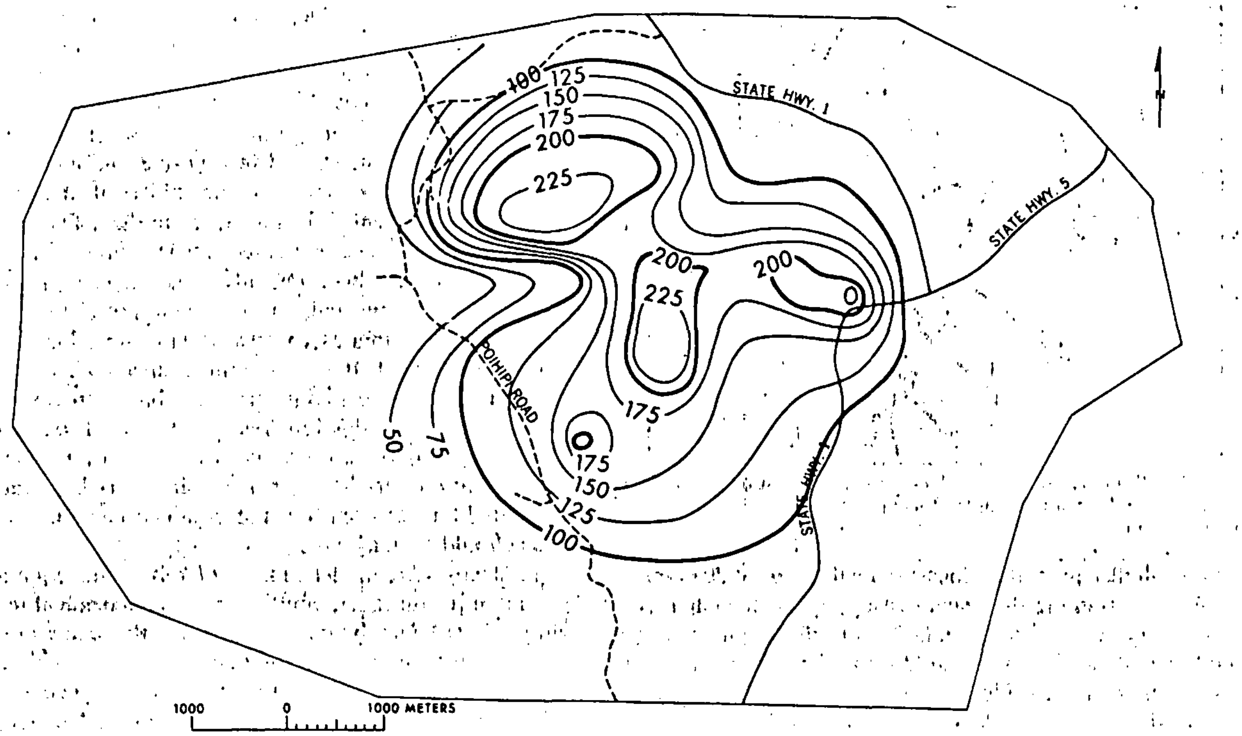

Fig. 5. Temperature distribution in degrees Celsius above the Huka Falls formation; contour interval is 25°C.

p_0 is the initial pressure in the Waiora aquifer. As was indicated in Table 1, the Huka Falls formation is considered to have an average vertical permeability of 1.0×10^{-14} m² except under the Waikato River, where it is estimated to be 5.0×10^{-14} m². Although this increase in permeability under the Waikato River was required to obtain a satisfactory pressure solution, the increase may be justified physically, since in the Wairakei area the Waikato River trends in the same direction as the regional faults and may be fracture-controlled.

For the heat transport equation (9) there are two vertical flow terms which must be evaluated at the top of the aquifer, one for conduction and one for convection. These terms are

$$[\phi K_{lz} + (1 - \phi) K_{sz}'] \frac{\partial T}{\partial z}\bigg|_{z_2} = [\phi' K_{lz} + (1 - \phi') K_{sz}'] \frac{T' - T}{b'} \qquad (14)$$

$$\gamma c_v v_z (T - T')|_{z_2} = \rho q' c_v (T - T') \qquad (15)$$

where K_l' and K_s' are the vertical components of the liquid thermal dispersion and solid thermal diffusion coefficient for the Huka Falls formation, T' is the temperature distribution above the Huka Falls formation, and T is the temperature distribution in the Waiora aquifer. As can be seen, convective heat flow depends on q' as defined earlier. For conductive heat flow a Fourier-type equation is used for both steady state and transient conditions. An approach similar to that used for pressure could have been used for calculating temperatures under transient conditions, but for the Wairakei system, temperature changes are small, and the simpler approximation is considered adequate.

Vertical flow at the base of the aquifer (through the Wairakei ignimbrites) is not well understood. As was stated earlier, it is assumed that the Wairakei ignimbrites are impermeable relative to the Waiora formation. Consequently, liquid flow and convective heat flow are assumed not to occur at the base of the aquifer. Since only the heat flow at the surface of the Wairakei area is known, a spatially distributed (conductive) heat function is used in the steady state model to reproduce the observed temperature distribution. Applying a trial and error approach, we adjust the distributed heat function until the calculated temperature distribution matches the observed temperature distribution and the calculated heat flow leaving the top of the model reproduces that measured at the Wairakei field. The vertical flow terms in (8) and (9) for the bottom of the Waiora aquifer are

$$\frac{\rho k_{zz}}{\mu_l}\left(\frac{\partial p}{\partial z} + \rho g\right)\bigg|_{z_1} = 0 \qquad (16)$$

$$[\phi K_{lz} + (1 - \phi) K_{sz}'] \frac{\partial T}{\partial z}\bigg|_{z_1} = -Q' \qquad (17)$$

$$\gamma c_v v_z (T - T')|_{z_1} = 0 \qquad (18)$$

where Q' is an areally distributed (conductive) heat source.

Initial Conditions

The Wairakei hydrothermal system is considered to have been at steady state prior to exploitation. The first step in modeling the Wairakei system is therefore the reproduction of the observed virgin or steady state conditions. These results will be used as the initial conditions for the transient model of exploitation. Inasmuch as wells drilled in the early 1950's had little discharge, temperature and pressure measurements made in these original wells are considered representative of steady state conditions. Figure 6, taken from *Studt* [1958, p. 712], is a 1955 potentiometric surface of the main production area. The early wells were shallow, and an upper datum of 152.4 m above sea level was chosen, since more data are available for this level. Nevertheless, the observed potentiometric surface is limited in extent, and few data are left on which to calibrate a simulation model.

Studt's head values were calculated from wellhead pressures

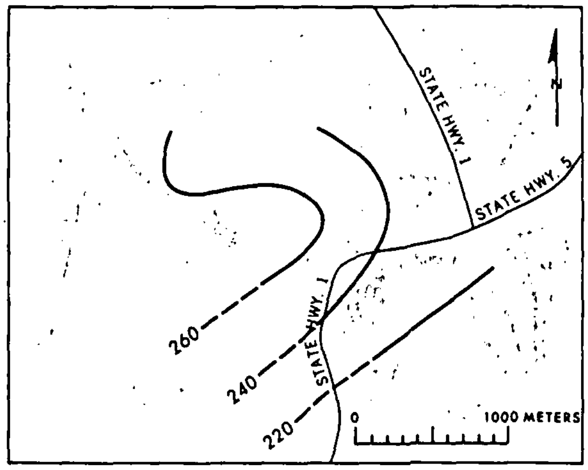

Fig. 6. Wairakei measured steady state potentiometric surface, 1955 [after *Studt*, 1958]. Datum is 152.4 m above sea level; contour interval is 20 m.

and downhole temperature measurements made at 30.48-m intervals. By assuming that each density value calculated from the recorded temperatures could be considered constant over an interval of 15.24 m above and below where the temperature was measured, he was able to estimate pressures from which he calculated equivalent or 'cold water' head values.

The observed steady state temperature distribution is shown in Figure 7. This surface is more extensive than the observed steady state potentiometric surface because it is based not only on measurements made in the early 1950's but also on recent temperature measurements. These recent values were utilized in preparing Figure 7 because temperatures have changed only slightly since exploitation began and the recent measurements still represent near steady state conditions. It should be pointed out that although temperatures vary with depth in the Waiora aquifer, vertically averaged temperature values must be used because the problem is treated as two-dimensional in the areal plane. These average temperatures are based on data collected from wells which penetrate the top and bottom of the Waiora aquifer [*Grindley*, 1965, pp. 123, 109].

The finite element configuration selected for modeling the Wairakei system is illustrated in Figure 3 and consists of 41 elements and 109 nodes. The flexibility of the irregular isoparametric element is demonstrated in the definition of the Waikato River, where increased vertical flow is permitted through the stream bed. The advantage of using mixed elements is apparent through an examination of elements in the main production area as contrasted with those located away from the main field. It is important to have higher-order elements and their associated higher-order basis functions in and around the main production area in order to approximate better the more pronounced changes which will occur there during exploitation. On the other hand, since very little change is anticipated farther from the main production area, linear elements should be adequate.

The steady state model consists of solving the equations of flow and heat transport, omitting the time-dependent terms. A solution is obtained by iterating between the temperature and pressure equations and using updated densities and viscosities. Although temperature and pressure are obtained for each node, corresponding head values can also be calculated, since the average densities are constant in the vertical direction. The simulated potentiometric surface with datum 152.4 m above sea level is shown in Figure 8, where the insert is the main production area and is shown in Figure 9. To facilitate comparing the observed and calculated surfaces, Figure 9 has the same border as the observed potentiometric surface in Figure 6. The calculated temperature distribution is shown in Figure 10 and is based on a dispersivity coefficient of 10 m in both the X and the Y direction.

Comparison of the calculated potentiometric surface in

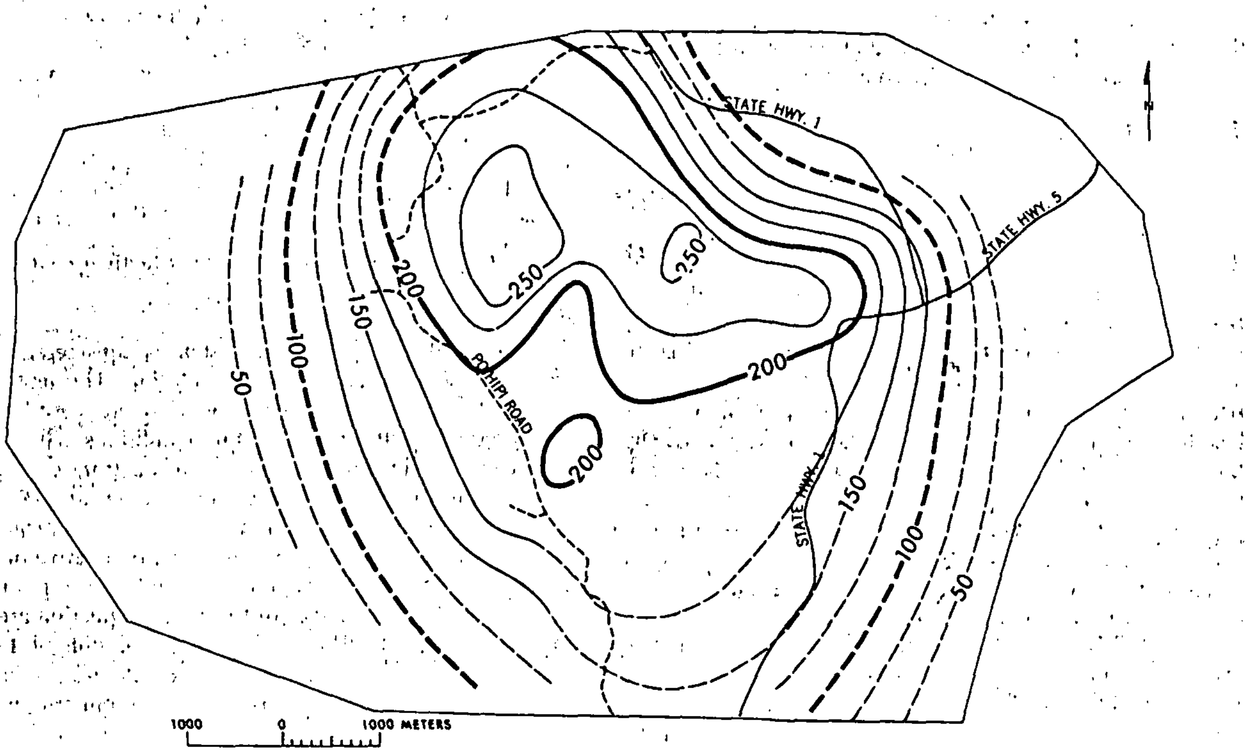

Fig. 7. Measured Wairakei steady state (vertically averaged) temperature distribution in degrees Celsius; contour interval is 25°C.

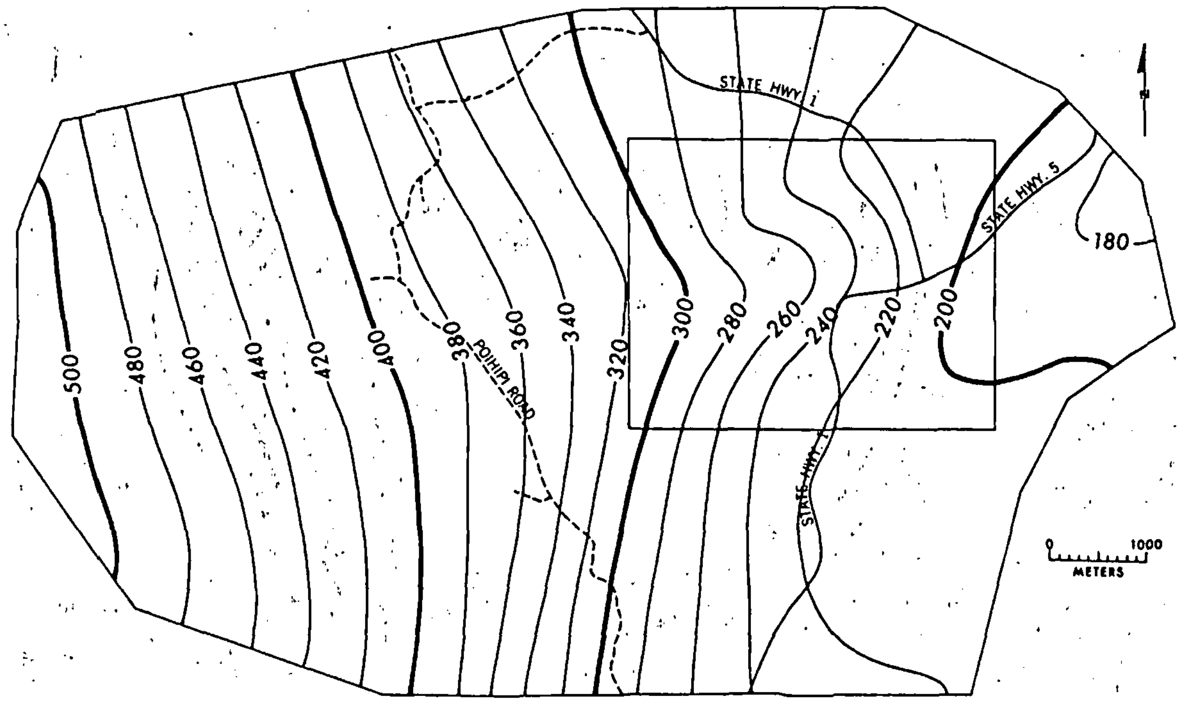

Fig. 8. Wairakei calculated steady state potentiometric surface. Datum is 152.4 m above sea level; contour interval is 20 m.

Figure 9 with the measured surface in Figure 6 reveals that both surfaces show a flow pattern which is basically from west to east. The observed potentiometric surface shows a distinct 'ridge' and 'valley' which is less pronounced in the calculated surface. This could possibly be the effect of 3 years of discharge from the field or the result of treating the Wairakei field as a porous medium and neglecting fault zones. The existence of a fault or an implied fault in the axes of both the valley and the ridge supports this latter hypothesis. Whatever the case, the surfaces still compare well, and the general trends are the same.

The computed temperature distribution in Figure 10 compares favorably with the observed temperature distribution in Figure 7. The most difficult task in obtaining a satisfactory temperature solution was adjusting the unknown heat source at the base of the aquifer. Another difficulty involved the selection of the element configuration. As was indicated earlier, the element configuration used in this problem was designed for the pressure solution, and consequently high nodal density and higher-order elements do not necessarily coincide with regions having large temperature gradients.

To test the accuracy of the model, mass and heat balances were made on the steady state results, and the 'mass out' compared to the 'mass in' of the model had a 0.023% error, while the heat difference had a 0.003% error. Since the boundaries of the model are impermeable, the balances were made on the vertical flow of fluid and heat entering and leaving the aquifer.

The heat flow calculated in the model was 214,700 kcal/s by convection and 18,380 kcal/s by conduction. As can be seen, convective heat flow is approximately an order of magnitude larger than conductive flow, which is consistent with what is observed at Wairakei [*Fisher*, 1964, p. 173]. The total calculated heat flow is 233,000 kcal/s (using a reference temperature of 0°C), which is higher than most of the observed values discussed earlier. Examination of Figures 2 and 3 suggests that the larger calculated value may be due to the larger area considered in the model. Further, using a constant heat capacity of 1.0 kcal/kg °C (Table 2) may have caused the calculated value to be high. The mass discharge calculated in the model amounted to 1,133 kg/s, which is higher than the estimated values. The estimated values, however, are generally based on a single mean enthalpy and consequently a single mean temperature, whereas the model considers the wide range of temperatures shown in Figure 10. If the assumed mean enthalpy is high, then the observed mass flux will be underestimated. Using an average enthalpy instead of an areally distributed one could account in part for the difference in mass flows. The larger area used in the model may also have contributed to the larger calculated mass flux.

A sensitivity analysis was performed on selected parameters in the steady state model. One of the parameters varied was the permeability of the Huka Falls confining bed. Reducing only the permeability of the confining bed produced a decrease in

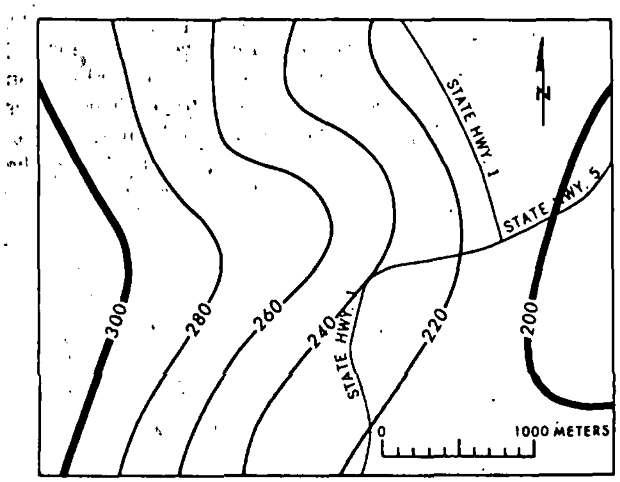

Fig. 9. Wairakei calculated steady state potentiometric surface of the production area. Datum is 152.4 m above sea level; contour interval is 20 m.

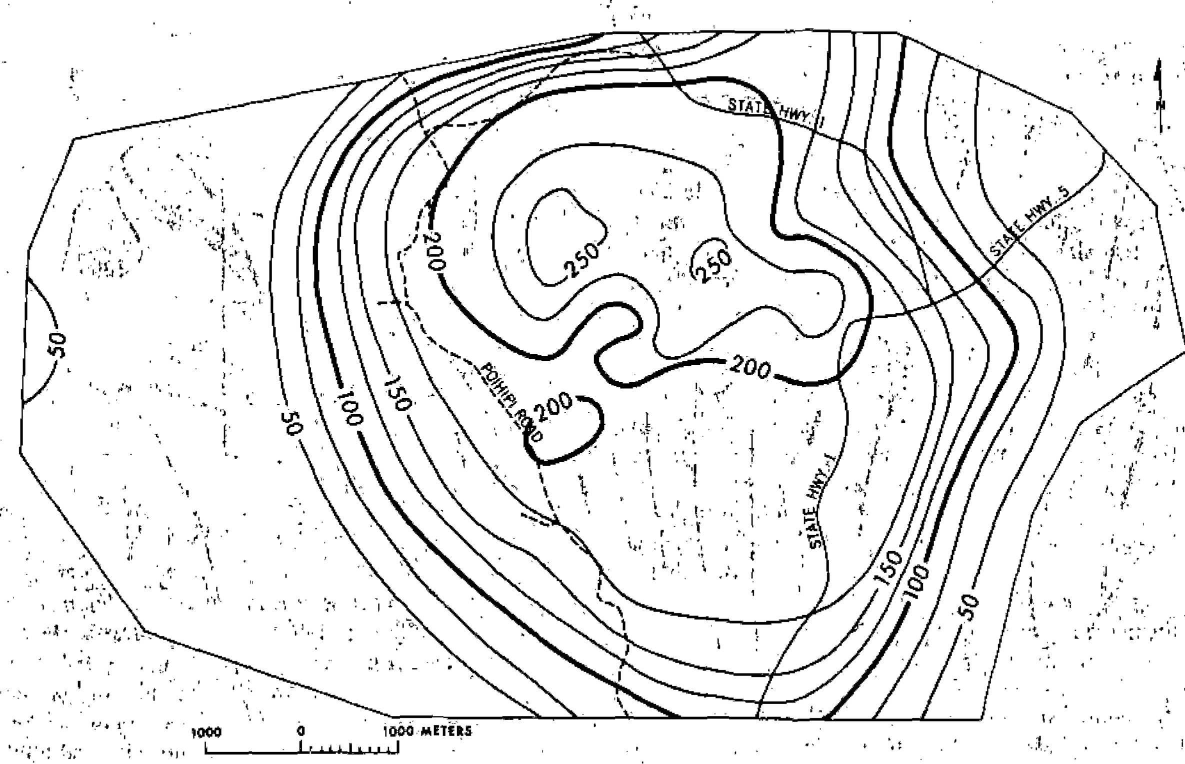

Fig. 10. Calculated Wairakei steady state temperature distribution in degrees Celsius; contour interval is 25°C.

mass discharge through the confining bed and an increase in the temperatures in the aquifer, while increasing permeability of the confining bed produced the opposite effect. It appears that for this particular application the confining bed permeability has a considerable effect on the temperature distribution.

The dispersivity coefficient was also varied in an attempt to examine the sensitivity of the temperature solution to this parameter. When this coefficient was increased from 10 to 100 m, the temperature changes were insignificant. When the dispersivity coefficient was increased to 1000 m, temperature changes were usually less than 10°C. Thus it appears that in contrast to point source problems where the dispersivity coefficient plays an important role, for this areal simulation the dispersivity influences the temperature distribution only slightly.

Transient Simulation

By using the steady state temperature and pressure solutions as initial conditions, well discharge rates were incorporated into the model and the transient effects of exploitation simulated. Discharge rates were averaged for each well over 30-day intervals. Since the locations of the nodes in the model do not correspond exactly with the locations of the wells in the field, the temporally averaged discharge rates were distributed to adjacent nodes using linear interpolation. For example, a well located in an element with 10 nodes would have its discharge distributed to those 10 nodes, the nearest node having the largest fraction of the discharge. The discharge for the entire field may be obtained by summing the discharge for each well and is presented in Figure 11. As may be seen, little discharge took place before power generation began in 1958. By estimating the enthalpy of the mass discharged, the approximate heat output may be calculated and is also presented in Figure 11.

Since the simulation is over an extended period of time, a time step of 1 month was utilized. The 1-month time step in conjunction with a backward difference scheme was found to provide a satisfactory solution.

Measured potentiometric surfaces of the main production area are shown in Figures 12 and 13 for 1958 and 1962, respectively. The 1958 surface [after *Studt*, 1958, p. 709] was constructed in the same fashion as Figure 6. The 1962 surface was contoured by using data from *Grindley* [1965, p. 124, Table 20]. Grindley gives downhole pressure values at sea level datum for several wells. These pressure values were converted to head values at a datum of 152.4 m above sea level by using

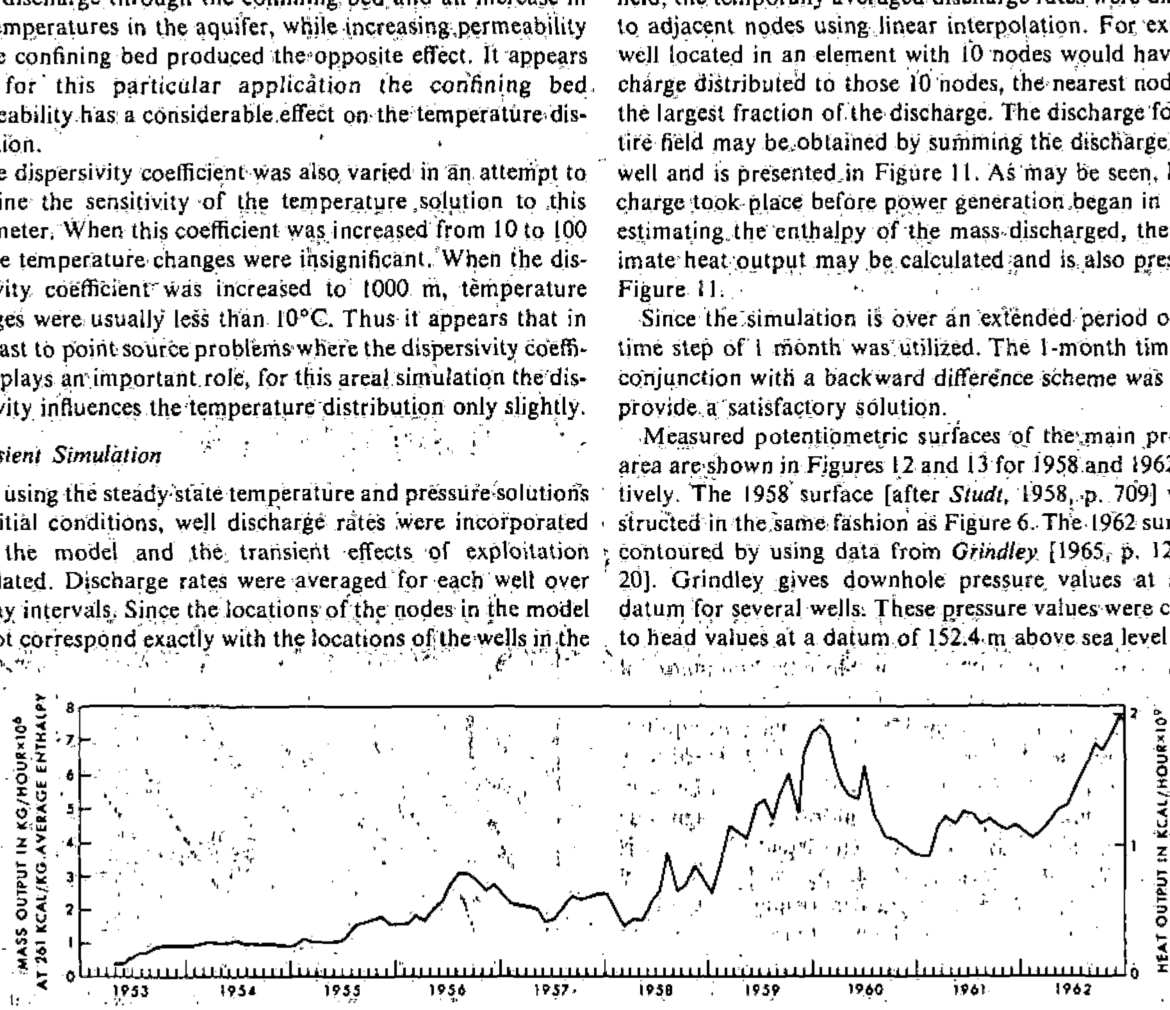

Fig. 11. Mass and heat discharged through Wairakei wells, 1953–1962; 200 series wells excluded [after *Grindley*, 1965].

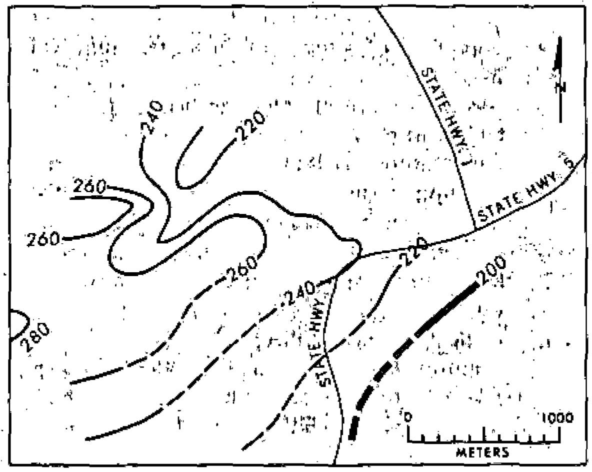

Fig. 12. Wairakei measured potentiometric surface, 1958 [after *Studt*, 1958]. Datum is 152.4 m above sea level; contour interval is 20 m.

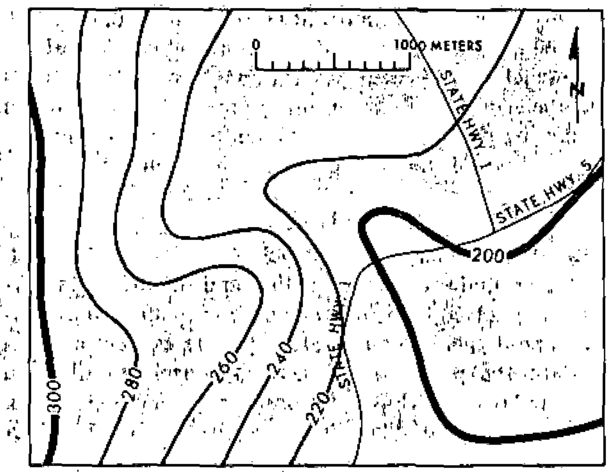

Fig. 14. Wairakei calculated 1958 potentiometric surface of the production area. Datum is 152.4 m above sea level; contour interval is 20 m.

density values computed from the average temperature data in Figure 7. As is indicated by the dashed lines, there is a considerable amount of uncertainty in the 1962 potentiometric surface. As exploitation continues, pressures decrease sufficiently to cause the formation of steam in the aquifer. This leads to inaccurate calculation of densities, and water levels in the wells can no longer be accurately measured. Thus potentiometric surfaces for periods after 1958 are difficult to calculate, and no contoured surfaces could be found in the published literature. Since the observed temperature distributions for 1958 and 1962 are approximately the same as the one given in Figure 7, no new temperature surfaces are presented.

The computed potentiometric surfaces of the main production area for August 1958 and December 1962 are presented in Figures 14 and 15, respectively. Computed temperatures showed a slight decrease throughout the field, a maximum decrease of approximately 4°C in December 1962 coinciding with the maximum drawdown. Since the change in the calculated temperature distribution is very small, once again no new surfaces are presented.

The major changes in the potentiometric surface occur in the vicinity of the main production area and consist of a general decline in head due to the withdrawal of water and heat. A comparison of computed and observed surfaces for this area can be made for 1958 by using Figures 12 and 14 and for 1962 by using Figures 13 and 15. The maximum drawdown has increased from approximately 40 m in 1958 to approximately 80 m by 1962. In general, flow is still from west to east with exploitation effects causing a local flow toward the production area. Possible causes for differences between the observed and computed surfaces include the way in which the discharge data was distributed to the nodes, steam forming in the aquifer causing errors in either the model (which is single phase) or the observed data, error in the original steady state conditions, error in not giving fault zones special attention, and error in treating a three-dimensional problem as two-dimensional.

The single-phase model was not adequate to reproduce historical data after 1962 because of the considerable quantity of steam that had formed in the Waiora formation [*Grindley*, 1965; *Bolton*, 1970, 1973]. Results of simulations from 1953 to 1962, however, indicate that hot-water hydrothermal systems can be modeled and evaluated. In the case of the Wairakei model the mass and heat outputs due to exploitation were known. This information was used to calibrate the simulation model by comparing observed and computed temperature and potentiometric surfaces. To apply this basic model to forecast

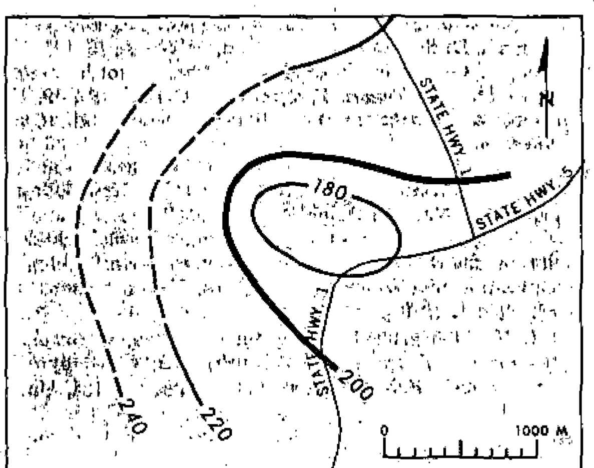

Fig. 13. Wairakei measured potentiometric surface, 1962 [data from *Grindley*, 1965]. Datum is 152.4 m above sea level; contour interval is 20 m.

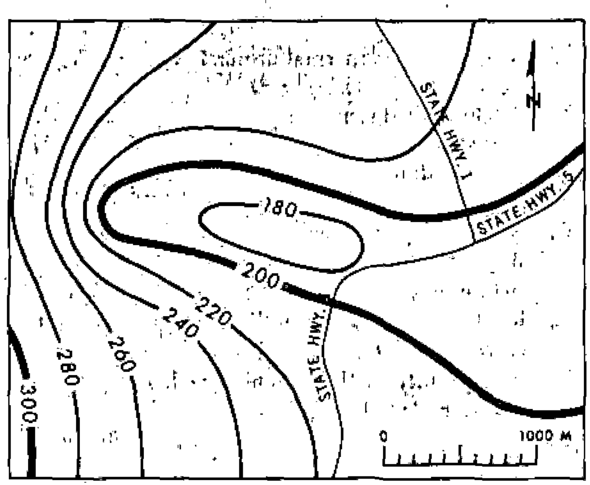

Fig. 15. Wairakei calculated 1962 potentiometric surface of the production area. Datum is 152.4 m above sea level; contour interval is 20 m.

the performance of other hot-water systems, mass outputs will need to be assumed, perhaps using economic considerations. Such a model will indicate, within the accuracy of the description of the geothermal system, the amount and rate at which mass may be withdrawn and if the enthalpy of the mass is known, will permit the heat output to be estimated.

CONCLUSIONS

A two-dimensional (areal) model has been developed in which the groundwater flow equation and the heat transport equation are solved by using finite difference approximations for the time derivatives and Galerkin-finite element approximations for the space derivatives. The approach is flexible and efficient, and once developed, the basic program can be reused, possibly with some modification, for a variety of groundwater problems involving heat transport.

The study of the Wairakei hydrothermal system described in this paper illustrates the potential of this approach for simulating both the predevelopment conditions (assumed steady state) of a hot-water geothermal system and its response over a development period (assuming that steam within the aquifer plays a relatively minor role in the field behavior). It has been shown that the initial patterns of, and changes in, temperature and pressure in such a system can be reproduced using basic field and well information. Thus the amount of heat energy available in a field and the rate at which it can be removed can be estimated using numerical modeling techniques. Since most hydrothermal systems are hot-water dominated [*White,* 1970], such a predictive tool could be very helpful in the economic evaluation and management of such systems.

The limitations of the present model preclude a full assessment of the Wairakei field, since it can no longer be considered a hot-water system after 1962. A more complete investigation of geothermal systems using a three-dimensional numerical model incorporating the behavior of steam-water interactions is now underway.

NOTATION

b, saturated thickness of the aquifer, L.
b', saturated thickness of the confining bed, L.
c_v, heat capacity at constant volume per unit mass, $L^2t^{-2}T^{-1}$.
g, gravitational constant, Lt^{-2}.
h_i, heat flux associated with diffusion and/or dispersion, Mt^{-3}.
K_{ij}, hydrodynamic thermal dispersion tensor (K_{zz}, vertical component), $MLt^{-3}T^{-1}$.
K_{ij}^m, mechanical thermal dispersion tensor, $MLt^{-3}T^{-1}$.
K^d, molecular thermal diffusion coefficient, $MLt^{-3}T^{-1}$.
K_{ij}^s, thermal diffusion tensor of the solid phase (K_{zz}^s, vertical component), $MLt^{-3}T^{-1}$.
K_t, K_l, transverse and longitudinal mechanical thermal dispersion coefficients, $MLt^{-3}T^{-1}$.
K', hydraulic conductivity of the confining bed, Lt^{-1}.
k_{ij}, local intrinsic permeability tensor (k_{zz}, vertical component), L^2.
k', permeability of the confining bed, L^2.
p, pressure, $ML^{-1}t^{-2}$.
p', pressure distribution above the confining bed, $ML^{-1}t^{-2}$.
Q, heat source term per unit mass, L^2t^{-3}.
Q', areally distributed heat source, Mt^{-3}.
q, strength of a point mass source function, Lt^{-1}.
q', vertical mass flow term, Lt^{-1}.
r, time rate of supply of mass per unit volume, $ML^{-3}t^{-1}$.
S_s, specific storage of confining bed, L^{-1}.
T, temperature, T.
T', temperature distribution at the top (or bottom) of the aquifer (in practice the temperature distribution above the confining bed is used), T.
t, time, t.
t', length of pumping period, t.
v_i, velocity (v_z, vertical component), Lt^{-1}.
α, vertical compressibility, Lt^2M^{-1}.
β, compressibility coefficient of the liquid phase, $LM^{-1}t^2$.
γ, mass density on a bulk volume basis where $\gamma = \rho\phi$, ML^{-3}.
λ, coefficient of thermal volume expansion for the liquid phase, T^{-1}.
μ, viscosity, $ML^{-1}t^{-1}$.
ρ, average density, ML^{-3}.
ϕ, porosity, dimensionless.
ψ_{ij}, porous medium tortuosity tensor, dimensionless.
ψ, tortuosity factor, dimensionless.
$(\ )^s$, refers to the solid phase.
$(\ )_z$, refers to the z direction (vertical).
$(\ )'$, indicates properties associated with confining beds.
$(\ )_0$, refers to a reference or initial quantity.

Acknowledgments. This study was a cooperative effort of the U.S. Geological Survey and the New Zealand government. The authors wish to thank all those who helped with various aspects of the study and in particular wish to thank Richard S. Bolton of the Ministry of Works for his helpful correspondence and organization of the data and Russell James of the Department of Scientific and Industrial Research for his assistance during the authors' visit to the field area. Finally, the authors wish to thank Dr. W. G. Gray for his critical review of the equation development.

REFERENCES

Aziz, K., P. H. Holst, and P. S. Karra, Natural convection in porous media, paper presented at 19th Annual Technical Meeting, Petrol. Soc. of Can. Inst. of Mining and Met., Calgary, Alta., May 7-10, 1968.
Banwell, C. J., Physical investigations, Geothermal Steam Power in New Zealand, *N.Z. Dep. Sci. Ind. Res. Bull., 117,* 45-74, 1955.
Benseman, R. F., Estimating the total heat output of natural thermal regions, *J. Geophys. Res., 64,* 1057-1062, 1959.
Bodvarsson, G., On thermal activity in Iceland, internal report, Geothermal Dep., State Elec. Auth., Reykjavik, Iceland, 1948.
Bodvarsson, G., Drilling for heat in Iceland, *Oil Gas J., 47,* 191, 1949.
Bodvarsson, G., Geophysical methods in prospecting for hot water in Iceland (in Danish), *Timarit Verkfraedingafelags Isl., 39,* 49, 1950.
Bodvarsson, G., Terrestrial heat balance in Iceland, *Timarit Verkfraedingafelags Isl., 39,* 69, 1954.
Bodvarsson, G., Physical characteristics of natural heat resources in Iceland, paper presented at U.N. Conference on New Sources of Energy, United Nations, Rome, Aug. 21-31, 1961.
Bolton, R. S., The behaviour of the Wairakei geothermal field during exploitation, paper presented at U.N. Symposium on Development and Utilization of Geothermal Resources, United Nations, Pisa, Sept. 22-Oct. 1, 1970.
Bolton, R. S., Management of a geothermal field, in *Geothermal Energy—Review of Research and Development,* edited by C. H. Armstead, *Unesco Earth Sci. Ser.,* vol. 12, pp. 175-184, Unesco, Paris, 1973.
Bredehoeft, J. D., and I. S. Papadopulos, Rates of vertical groundwater movement estimated from the earth's thermal profile, *Water Resour. Res., 1*(2), 325-328, 1965.
Bredehoeft, J. D., and G. F. Pinder, Digital analysis of areal flow in multiaquifer groundwater systems: A quasi three-dimensional model, *Water Resour. Res., 6*(3), 883-888, 1970.

Bredehoeft, J. D., and G. F. Pinder, Mass transport in flowing groundwater, *Water Resour. Res.*, *9*(1), 194–210, 1973.
Cady, G. V., Model studies of geothermal fluid production, Ph.D. dissertation, Stanford University, Stanford, Calif., 1969.
Chappelear, J. E., and C. W. Volek, The injection of a hot liquid into a porous media, paper presented at Symposium on Numerical Simulation of Reservoir Performance, Soc. of Petrol. Eng., Dallas, Texas, April 22–23, 1968.
DeVries, D. A., Simultaneous transfer of heat and moisture in porous media, *Eos Trans. AGU*, *39*(5), 909–916, 1958.
Domenico, P. A., and M. D. Mifflin, Water from low-permeability sediments and land subsidence, *Water Resour. Res.*, *1*(4), 563–576, 1965.
Donaldson, I. G., Temperature gradients in the upper layers of the earth's crust due to convective water flows, *J. Geophys. Res.*, *67*(9), 3449–3460, 1962.
Donaldson, I. G., The flow of steam water mixtures through permeable beds: A simple simulation of a natural undisturbed hydrothermal region, *N.Z. J. Sci.*, *11*(1), 3–23, 1968*a*.
Donaldson, I. G., A possible model for hydrothermal systems and methods of studying such a model, paper presented at Third Australasian Conference on Hydraulics and Fluid Mechanics, Sydney, Nov. 25–29, 1968*b*.
Donaldson, I. G., The simulation of geothermal systems with a simple convective model, *Geothermics*, *2*, part 1, 649–654, 1970.
Einarsson, T., The nature of the springs of Iceland (in German), *Rit. Visindafelag Isl.*, *26*, p. 1, 1942.
Elder, J. W., Some problems in fluid dynamics, Ph.D. thesis, Cambridge Univ., Cambridge, England, 1957.
Elder, J. W., Physical processes in geothermal areas, in *Terrestrial Heat Flow*, edited by W. H. K. Lee, *Geophys. Monogr. Ser.*, vol. 8, pp. 211–239, AGU, Washington, D. C., 1965.
Elder, J. W., Heat and mass transfer in the earth: Hydrothermal systems: *N.Z. Dep. Sci. Ind. Res. Bull.*, *169*, 155, 1966.
Ellis, A. J., and S. H. Wilson, The heat from the Wairakei-Taupo thermal region calculated from the chloride output, *N.Z. J. Sci. Technol.*, *36*(6), 622–631, 1955.
Fisher, R. G., Geothermal heat flow at Wairakei during 1958, *N.Z. J. Geol. Geophys.*, *7*, 172–184, 1964.
Gregg, D. R., Natural heat flow from the thermal areas of Taupo sheet district (N94), *N.Z. J. Geol. Geophys.*, *1*, 65–75, 1958.
Grindley, G. W., The geology, structure, exploitation of the Wairakei field, Taupo, N. Z., *N.Z. Geol. Surv. Bull.*, *75*, 131, 1965.
Harlow, F. H., and W. E. Pracht, A theoretical study of geothermal energy extraction, *J. Geophys. Res.*, *77*(35), 7033–7048, 1972.
Healy, J., Preliminary account of hydrothermal conditions of Wairakei, New Zealand, *Proc. Pacif. Sci. Congr. 8th*, *2*, 214–227, 1956.
Hulston, J. R., Isotope geology in the hydrothermal areas of New Zealand, paper presented at U.N. Conference on New Sources of Energy, United Nations, Rome, Aug. 21–31, 1961.
Hunt, T. M., Net mass loss from the Wairakei geothermal field, New Zealand, *Geothermics*, *2*, part 1, 487–491, 1970.
Jacob, C. E., Flow of groundwater, in *Engineering Hydraulics*, edited by H. Rouse, pp. 321–386, John Wiley, New York, 1950.
Lauwerier, H. A., The transport of heat in an oil layer caused by the injection of a hot fluid, *Appl. Sci. Res. A*, *5*(2–3), 145–150, 1955.
Marshall, D. C., Preliminary theory of the Wairakei geothermal field, *N.Z. J. Sci.*, *9*, 651, 1966.
Marshall, D. C., Development of a theory of the Wairakei geothermal field by the 'simplest cases first' technique, *Geothermics*, *2*, part 1, 669–675, 1970.
Marx, J. W., and R. N. Langenheim, Reservoir heating by hot fluid injection, *Trans. AIME*, *216*, 312, 1959.
McNabb, A., On convection in a porous medium, paper presented at Second Australasian Conference on Hydraulics and Fluid Mechanics, Univ. of Auckland, Auckland, Dec. 6–11, 1965.
Mercer, J. W., G. F. Pinder, and W. G. Gray, Galerkin-finite element analysis of heat transport in porous media, open file report, U.S. Geol. Surv., Reston, Va., in press, 1975.
Meyer, C. A., R. B. McClintock, G. J. Silvestri, and R. C. Spencer, *1967 ASME Steam Tables*, 2nd ed., American Society of Mechanical Engineers, New York, 1968.
Modriniak, N., and F. E. Studt, Geological structure and volcanism in the Taupo-Tarawera district, *N.Z. J. Geol. Geophys.*, *2*, 654–684, 1959.
Philip, J. R., and D. A. DeVries, Moisture movement in porous materials under temperature gradients, *Eos Trans. AGU*, *38*, 222–232, 1957.
Pinder, G. F., and J. D. Bredehoeft, Application of the digital computer for aquifer evaluation, *Water Resour. Res.*, *4*(5), 1069–1093, 1968.
Pinder, G. F., and E. O. Frind, Application of Galerkin's procedure to aquifer analysis, *Water Resour. Res.*, *8*(1), 108–120, 1972.
Reddell, D. L., and K. K. Sunada, Numerical simulation of dispersion in ground water aquifer, *Hydrol. Pap. 41*, p. 79, Colo. State Univ., Fort Collins, 1970.
Shutler, N. D., Numerical three-phase model of the two-dimensional steamfood process, paper presented at Second Symposium on Numerical Simulation of Reservoir Performance, Soc. of Petrol. Eng., Dallas, Texas, Feb. 5–6, 1970.
Stallman, R. W., Computation of ground-water velocity from temperature data, Methods of Collecting and Interpreting Ground-Water Data, *U.S. Geol. Surv. Water Supply Pap. 1544-H*, 36–46, 1963.
Studt, F. E., The Wairakei hydrothermal field under exploitation, *N.Z. J. Geophys.*, *1*, 703–723, 1958.
Thompson, G. E. K., C. J. Banwell, G. B. Dawson, and D. J. Dickinson, Prospecting of hydrothermal areas by surface thermal surveys, paper presented at U.N. Conference on New Sources of Energy, United Nations, Rome, Aug. 21–31, 1961.
Weber, R. L., N. W. White, and K. V. Manning, *Physics for Science and Engineering*, p. 640, McGraw-Hill, New York, 1959.
White, D. E., Thermal waters of volcanic origin, *Bull. Geol. Soc. Amer.*, *68*, 1637, 1957.
White, D. E., Preliminary evaluation of geothermal areas, paper presented at U.N. Conference on New Sources of Energy, United Nations, Rome, Aug. 21–31, 1961.
White, D. E., Geochemistry applied to the discovery, evaluation, and exploitation of geothermal energy resources, report presented at U.N. Symposium on the Development and Utilization of Geothermal Resources, United Nations, Pisa, Sept. 22–Oct. 1, 1970.
White, D. E., L. J. P. Muffler, and A. H. Truesdell, Vapor-dominated hydrothermal systems, *Econ. Geol.*, *66*, 75–97, 1971.
Whiting, R. L., and H. J. Ramey, Jr., Application of material and energy balances to geothermal steam production, *J. Petrol. Technol.*, 893–900, July 1969.
Wooding, R. A., Steady state free thermal convection of liquid in a saturated permeable medium, *J. Fluid Mech.*, *2*, 273, 1957.
Wooding, R. A., An experiment on free thermal convection of water in a saturated permeable medium, *J. Fluid Mech.*, *3*, 582, 1958.
Wooding, R. A., The stability of a viscous liquid in a vertical tube containing porous material, *Proc. Roy. Soc. Aust.*, *252*, 120, 1959.
Wooding, R. A., Instability of a viscous liquid of variable density in a vertical Hele-Shaw cell, *J. Fluid Mech.*, *7*, 501, 1960*a*.
Wooding, R. A., Rayleigh instability of a thermal boundary layer in flow through a porous medium, *J. Fluid Mech.*, *9*, 138, 1960*b*.
Wooding, R. A., Free convection of fluid in a vertical tube filled with porous material, *J. Fluid Mech.*, *13*, 129, 1962.
Wooding, R. A., Convection in a saturated porous medium at large Rayleigh number or Peclet number, *J. Fluid Mech.*, *15*, 527–544, 1963.
Zienkiewicz, O. C., and C. J. Parekh, Transient field problems: Two dimensional and three dimensional analysis by isoparametric finite elements, *Int. J. Numer. Meth. Eng.*, *2*, 61–71, 1970.

(Received November 7, 1973;
accepted February 10, 1975.)

NEW ZEALAND
JOURNAL OF GEOLOGY AND GEOPHYSICS

Department of Scientific and Industrial Research, Wellington

Editor: *I. W. Mackenzie*

VOLUME 15 SEPTEMBER 1972 NUMBER 3

RECENT GEOPHYSICAL EXPLORATION OF THE KAWERAU GEOTHERMAL FIELD, NORTH ISLAND, NEW ZEALAND

W. J. P. MACDONALD

Geophysics Division, Department of Scientific and Industrial Research, Wellington, New Zealand

and

L. J. P. MUFFLER

U.S. Geological Survey, Menlo Park, California, U.S.A.

(Received 20 August 1971)

ABSTRACT

Resistivity surveys carried out in 1970 have shown that the Kawerau Geothermal Field has a cross-sectional area of 6 to 10 km^2 at intermediate depths (approximately 1 km). In the light of these surveys, previously published geophysical data have been reinterpreted, and the geological setting and stratigraphy have been re-examined.

Assuming boiling point for depth temperatures to 250°C and a constant 250°C to a depth of 2 km, the field has a minimum stored heat of $3 \cdot 9 \times 10^{18}$ joules above a temperature of 100°C.

Temperature measurements made in wells during the injection of cold water indicate that the best production of hot water comes from andesite at a depth of 750 to 900 m. Because core samples of this andesite have low porosity, the major production is likely to be from fractures in the andesite. The fractures in the andesite are thought to have been caused by recent extrusion of dacite.

N.Z. Journal of Geology and Geophysics 15 (3): 303–17

INTRODUCTION

Kawerau Borough lies at an elevation of about 30 metres (m) on the flat land bordering the Tarawera River, approximately 19 kilometres (km) south of the Bay of Plenty and 29 km south-west of Whakatane (Fig. 1). Four km south-east of Kawerau is Mount Edgecumbe, a youthful (less than 10,000 years) volcanic cone that rises to an elevation of 822 m.

In the early 1950's Tasman Pulp and Paper Company started planning the construction of an integrated mill to produce annually some 75,000 tons of newsprint, 90,000 tons of Kraft paper, and 25 million board feet of sawn timber. The existence of thermal activity throughout the Kawerau area suggested that the mill might be located so as to make use of natural steam in the production of paper. Accordingly, geophysical and geological studies (Studt 1952, 1958; Beck 1952; Healy 1951, 1962) were made in the vicinity of the major hot-spring area of the region, Onepu Springs, approximately 2.5 km north of Kawerau. The results of these studies were sufficiently encouraging for the Ministry of Works to carry out an investigational drilling programme in order to evaluate the productivity of the field.

Between August 1952 and November 1955 the Ministry of Works drilled three holes to depth of about ½ km. Testing of these holes demonstrated that production of steam could be obtained from intermediate depths (Table 1). Production drilling was then commenced by a private contractor in April 1956 and by February 1957 an additional 7 holes had been drilled to depths of about 600 m. By the end of 1960 output had dwindled to the

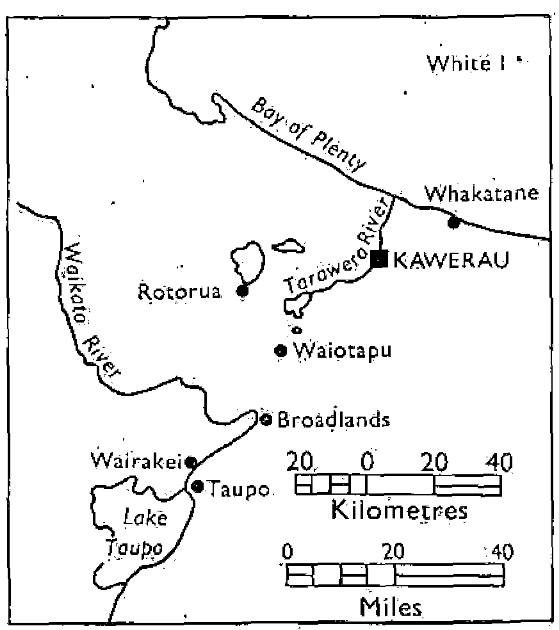

FIG. 1—Location of Kawerau Geothermal Field in Bay of Plenty area, North Island, New Zealand.

extent that holes 7A, 8, 12, and 14 had to be deepened to about 900 m by the Ministry of Works. The resulting increased output was sufficient to meet demands until 1967, when bores 3, 16, and 17 were drilled. The output of these three holes was approximately equivalent to the rest of the field combined (Table 1).

The techniques available in the early geophysical studies (Studt 1952, 1958) did not permit the Kawerau Geothermal Field to be accurately outlined at depth. During the 19 years since the early survey, however, extensive developments have been made in the use of electrical methods in geothermal areas, and far more sensitive equipment is available today than in 1951. Accordingly, electrical surveys of the Kawerau field were made during the 1969–70 field season, in order to determine the extent of the geothermal field at depth and to estimate the amount of stored heat. In this report the results of these electrical surveys are presented, together with a summary of the geology, and a reappraisal of the earlier geophysical work.

GEOLOGIC SETTING

Surface Geology

The Kawerau Geothermal Field lies near the axis of a north-east-trending complex graben that continues north-eastward out to sea to form the White Island Trench and extends south-westward as the Taupo Volcanic Depression (Healy *et al.* 1964). Interpretation of gravity data (Studt 1958, p. 240) indicates that the minimum depth to nonvolcanic basement (presumably greywacke) beneath Kawerau is about 1·5 km. Greywacke is exposed on the surface 12 km east of Kawerau in the Raungaehe Range and 22 km north-west of Kawerau near Otamarakau Valley.

In the vicinity of Kawerau this graben is filled with volcanic rocks and associated sedimentary rocks composed of volcanic detritus. The volcanic rocks are primarily of rhyolitic composition and include flows, tuff breccias, pumice breccias, and ignimbrites. There are a few andesitic rocks (Mt Edgecumbe, Manawahe, Whale Island, and at depth in the Kawerau borefield). Healy (1962, p. 7, section 3) expressed uncertainty concerning the nature

TABLE 1—Kawerau Borefield Data

Date	Production ($kg\ s^{-1}$) Steam	Water	Av. Pressure (Bars gauge)	Av. Maximum Temp. (°C)	Av. Depth (m)	Bores Used
1955	1·9	4·6	8·3	240	460	1, 4
1957	56·6	125·9	8·6	250	600	1, 3, 7A, 8, 10, 11, 12, 13, 14
1961	32·7	100·7	8·6	250	915	7A, 8, 14
1967	68·9	258·3	8·6	255	915	3, 7A, 8, 14, 16, 17

of the bedrock exposed in the young extrusions which form the Onepu Hills (*see* Fig. 5). Specimens from four localities were collected and studied by us. These specimens proved to be flow rocks of dacite composition and not rhyolite. No ignimbrite was identified.

All four specimens from the Onepu Hills are rich in large (1–10 mm) plagioclase phenocrysts, with subordinate quartz phenocrysts. Petrographic study of sample 70Mp13 (from hill 560') and 70Mp16 (from hill 600') showed both specimens to be fresh flow rocks containing 20–25% plagioclase phenocrysts (andesine to labradorite), 3–5% quartz phenocrysts, and minor amphibole, pyroxene, biotite, and magnetite. Groundmass material in both specimens is devitrified; 70Mp16 displays conspicuous irregular flow foliation, whereas in 70Mp13 the foliation has been obscured by spherulitic crystallisation of the groundmass. Partial chemical analysis of these specimens by the N.Z. Geological Survey (courtesy of Mr P. R. L. Browne) gave the following results:

Sample No.	Weight percent	
	K_2O	SiO_2
70Mp13	1·99	70·85
70Mp16	1·86	65·32

Comparison of these figures with the analyses given in Lewis (1968) and Ewart (1966) indicates that the two analysed samples are dacites.

All of the rocks in the Taupo Volcanic Depression except the oldest two ignimbrites are normally magnetised and are convincingly interpreted by Cox (1969) as younger than the 0·7 m.y. Matuyama–Brunhes boundary. Although the nearest outcrop of either of these two reversely magnetised ignimbrites is over 40 miles north of Kawerau, one cannot preclude the presence of reversely magnetised old ignimbrites at depth in the Kawerau area.

The surface geology at Kawerau has been summarised by Healy (1962, pp. 2–3) and depicted on figure 1 of his report. Although geologic relations are tenuous because of the thick, obscuring mantle of Holocene tephra, it appears that these dacite hills are extrusive domes that are younger than all rocks in the area excepting the Holocene tephra. The domes probably were extruded on the ground surface after pushing their way up through the sequence of volcanic and sedimentary rocks that underlie the geothermal area.

Most faults in the Kawerau region strike north-easterly, parallel to the regional structural grain (Healy *et al.* 1964). There is very little expression of faulting around Kawerau except at the borefield, where a linear north-west-facing scarp forming the steep north-west slope of the tephra-covered low ridge just north-west of bores 16 and 17 may represent a fault. In addition, the difference in elevation of the andesite between bore 17 and bore 3 (Fig. 2) may be due to faulting.

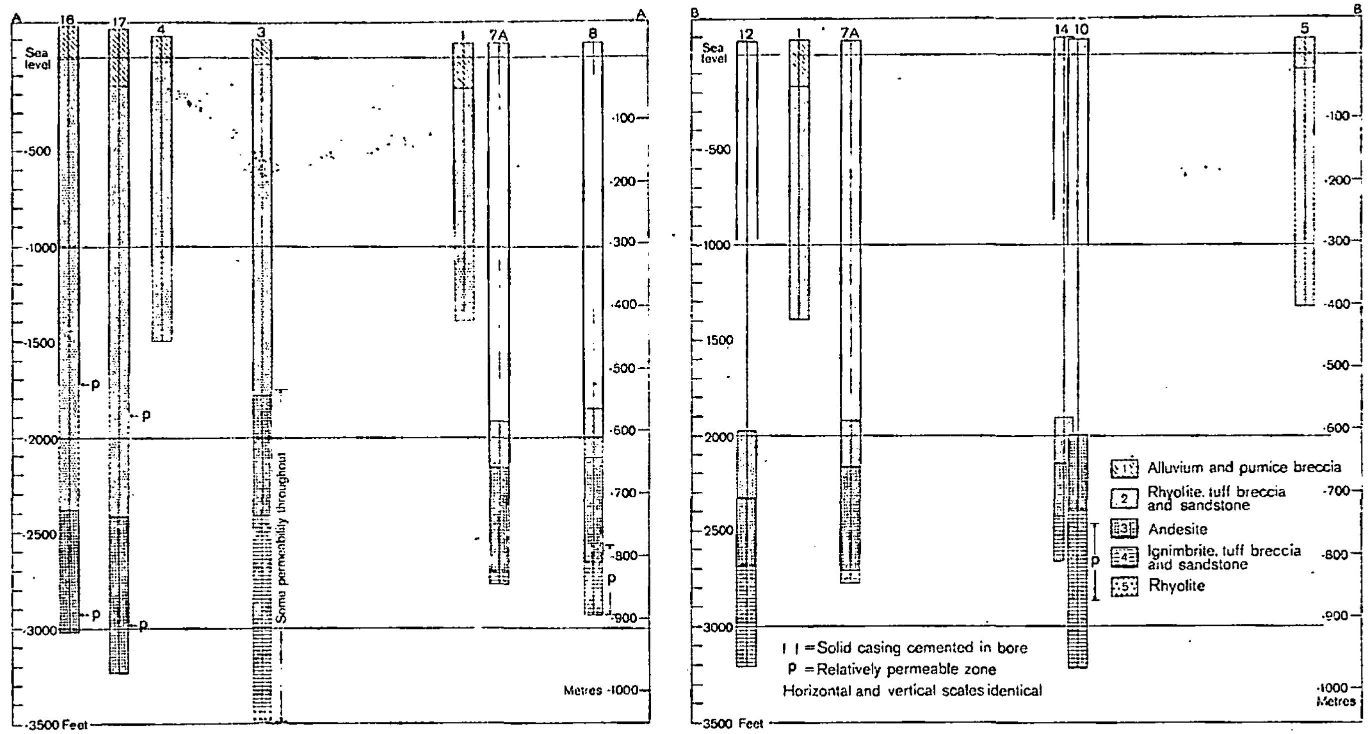

FIG. 2—Generalised geologic section of Kawerau geothermal area. Bores are projected on a vertical plane striking N 52° W through bores 16 and 8 (*see* A–A, Fig. 5) and N 28° E through bores 12 and 5 (*see* B–B, Fig. 5).

Stratigraphy in Bores

The stratigraphic information available in 1962 has been summarised by Healy (1962, pp. 8–9) and by Steiner (1962). Since then, bores 3, 16, and 17 have been drilled and carefully sampled throughout. Cuttings and cores from these bores were logged by J. Healy, and the available stratigraphic data for all the Kawerau bores were summarised by G. W. Grindley in a set of drill logs (written comm. 1970). The generalised geological sections shown in Fig. 2 were prepared by us from these logs, supplemented by additional study of samples and thin sections in the petrology collection of the N.Z. Geological Survey. Samples from bores 2, 9, 11, and 13 are not available (*see* Healy 1962, p. 3)

We have divided the stratigraphic section of the Kawerau borefield into five major units. From top to bottom, these are:

- Unit 1: Alluvium and pumice breccia (45 to 100 m thick).
- Unit 2: Rhyolite, with subordinate tuff breccia, ash, sandstone and siltstone (535 to 720 m thick).
- Unit 3: Andesite (85 to greater than 251 m thick).
- Unit 4: Ignimbrite, with intercalated tuff breccia and sandstone (315 m thick in bore 3).
- Unit 5: Rhyolite (greater than 15 m thick at the bottom of bore 3).

Only Unit 1 outcrops at the surface.

The various rock types in Unit 2 can readily be discriminated in any single bore, but it has not yet been possible to correlate sub-units among the various bores except between bores 16 and 17. This failure is due to (a) poor sampling in the pre-1961 bores, (b) pervasive hydrothermal alteration that has obscured much of the original textures and (c) lateral stratigraphic variation in Unit 2 throughout the borefield. Details of lateral stratigraphic variation are not clear in the older bores, but are evident in bores 16, 17, and 3. In bores 16 and 17 breccias and clastic rocks make up about 40 percent of Unit 2, whereas in bore 3 nearly the entire unit is rhyolite. Furthermore, Unit 2 is considerably thinner and the andesite (unit 3) higher in bore 3 than in bores 16 and 17, suggesting fault movement during the extrusion and deposition of the rocks in Unit 2.

The andesite (Unit 3) is a conspicuous stratigraphic marker readily identified in cuttings or core. It is greenish grey, with conspicuous plagioclase phenocrysts, and is intensely altered. Figures 3 and 4 show that, compared to other rocks of the borefield, the andesite is consistently more dense and less porous.

Unit 4 characterised by the presence of ignimbrite and the absence of rhyolite. Many specimens of ignimbrite and of pumice breccia display glass shards and aligned pumice fragments suggesting emplacement by ash flow; compaction foliation was seen in a few ignimbrite specimens. In bore 10, Unit 4 displays a regular increase in density and a nearly regular decrease in porosity with depth, suggesting increasing compaction and welding of a single ash-flow cooling unit (Ross and Smith 1961). The surface correlative of Unit 4 is not known. Petrographic criteria preclude correlation with the

Matahina Ignimbrite, the prominent ignimbrite exposed on the plateaus to the east and north-west of Kawerau (A. Steiner, quoted in Healy 1962).

Unit 5 was encountered only in bore 3, the deepest bore to date. This rhyolite is characterised by abundant quartz phenocrysts, and the available samples are not intensely altered.

Production Zones

The Kawerau bores have produced from two general levels. The earlier bores produced from breccias and sediments at depths of about 600 m (Healy 1962, p. 5), but falling discharges and temperatures occurred within three years and were attributed by Banwell (1962, p. 1) to invasion of the field by marginal cool water. The bores deepened in 1961 (7A, 8, 12, and 14) and the bores subsequently drilled (3, 16, and 17) produce from a deeper zone (760 m to 910 m).

Temperature runs made during injection of cold water into bores at varying injection rates allow permeable zones to be identified rather precisely. The permeable zones deduced from these temperature runs are indicated on Fig. 2, 3, and 4.

Comparison of temperature data taken at two injection rates in both bore 16 and 17 indicates that the major permeable zone in these bores is the deeper one, in the lower part of the andesite. The most permeable zone in bore 8 appears to be at the base of the andesite and in the immediately underlying ignimbrite. In bore 10, the permeable zone is entirely within the ignimbrite. For bore 3, the water injection temperature runs indicate that there are no well-defined major permeable zones, but that the permeability is rather uniformly distributed in the bore below the casing.

It is perhaps significant that production from the three best Kawerau bores (16, 8, and 17) comes from the andesite, consistently the densest and least porous rock encountered (*see* Fig. 4). This correlation, coupled with the very limited vertical extent of the permeable zones in bores 16 and 17, suggests that the production from these bores is from fissures in the andesite. Apparently for a bore at Kawerau to be a major producer, it must encounter fractures in the andesite or hard ignimbrite, rocks dense enough to support extensive fracture systems. The units which appear to be most porous in hand specimen apparently cannot supply sufficient fluid to the bore to become major production zones. Perhaps these stratigraphic units are not competent enough to allow major fractures to be developed and sustained.

PREVIOUS GEOPHYSICAL INVESTIGATION

Studt (1952, 1958) used a number of geophysical techniques to study the Kawerau area. Perhaps the most informative of these was the gravity survey, which gave a minimum depth of 1·5 km to basement greywacke. In addition the survey defined a local gravity high over an area that includes the present borefield. Studt interpreted this high as due either to a rhyolite intrusion or to densification caused by hydrothermal alteration of the rocks.

Studt's ground magnetic survey of the Kawerau area showed a negative anomaly just to the west of the present borefield. Studt (1958) interpreted the anomaly as caused by the hydrothermal alteration of magnetic minerals to nonmagnetic ones.

Seismic refraction studies at Kawerau (Studt 1958) identified a strongly refracting horizon at a depth of from 60 to 150 m, which apparently correlates with the top of Unit 2 (dominantly rhyolite) of this paper. No consistently deeper refracting horizon could be identified. Seismic refraction methods are of minimal use in this type of geothermal area because the high level of ground noise and high attenuation of the signal make recording difficult, and velocity reversals often prevent the detection of layers deeper than the shallowest high velocity layer.

Several resistivity profiles are given by Studt (1958). The electrode spacing used (30 m and 60 m) gave only a shallow penetration, and the work was hindered by instrumental inadequacies. The apparent resistivity values thus determined are considerably higher than those found in recent years in other New Zealand geothermal areas.

The geophysical investigations reported by Studt (1958) also include temperature data from 24 drillholes in the 30 to 60 m depth range. These data do little to outline the Kawerau field, but are of use when compared with the results of our electromagnetic survey.

Magnetic Survey

The vertical force ground magnetic survey of Studt (1958, fig. 10) is included here in Fig. 5. The two striking features of the magnetic map are the extensive magnetic high in the north-west and the elongated magnetic low trending north-east through the centre of the map. We assume that the magnetic high is caused by buried volcanic material, probably andesite, but any such rocks in the area of the high are obscured by the thick blanket of Rotoiti Breccia and by alluvium (Healy *et al.* 1964). The magnetic low, on the other hand, is probably best explained as partly a peripheral feature complementary to the magnetic high and partly a feature caused by hydrothermal alteration of magnetic materials to nonmagnetic ones.

To illustrate this point, the vertical magnetic field of a magnetic body, similar in area to the magnetic body in the north-west, has been calculated. This body consists of two vertical prisms, one from the surface to 150 m (outlined by the dashed line on Fig. 5) and the other from 150 to 600 m (outlined by the solid line on Fig. 5). The susceptibility used is $25{,}000 \times 10^{-6}$ SI units ($2{,}000 \times 10^{-6}$ cgs units), the average value for New Zealand andesite, and the direction of magnetisation is assumed to be that of the present-day field.

Although these calculations (*see* brown contours, Fig. 5) do not give a perfect fit with the observed magnetic field, they do demonstrate that the shape and magnitude of the measured negative anomaly could be caused by the magnetic high to the north-west. However, Fig. 4 shows that the susceptibilities of the core samples are much lower than expected of unaltered rock, and accordingly part of the magnetic low must be caused

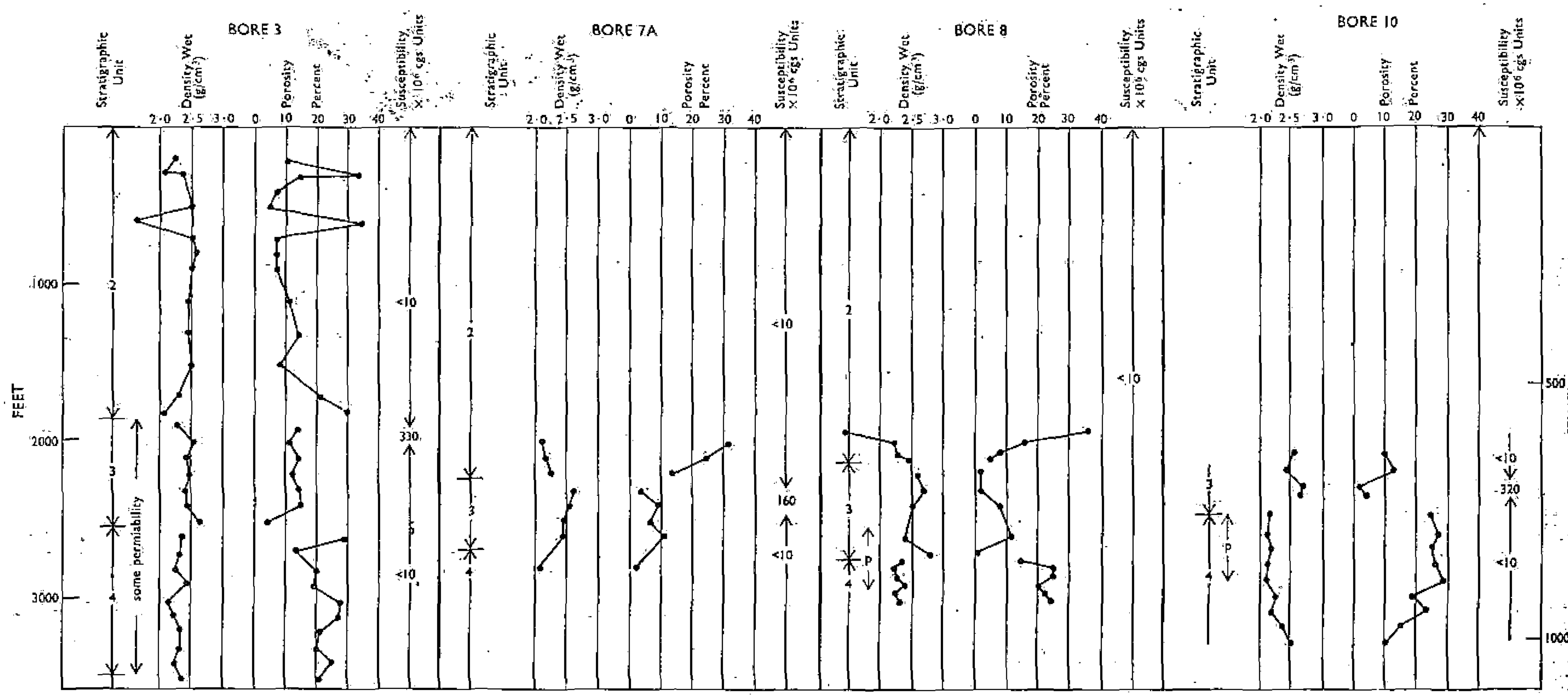

FIG. 3—Graphs showing wet density, porosity, and magnetic susceptibility of cores from Kawerau geothermal bores 3, 7A, 8, and 10.

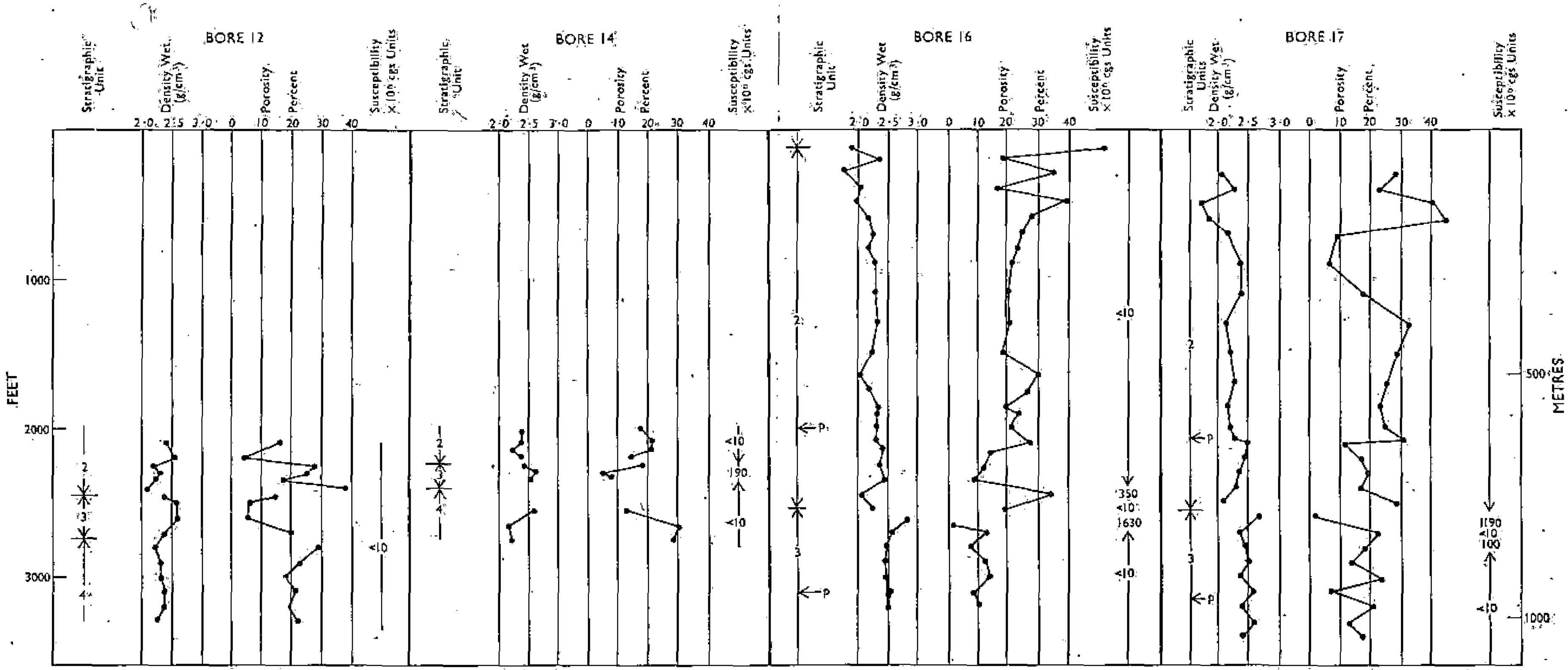

FIG. 4—Graphs showing wet density, porosity, and magnetic susceptibility of cores from Kawerau geothermal bores 12, 14, 16, and 17.

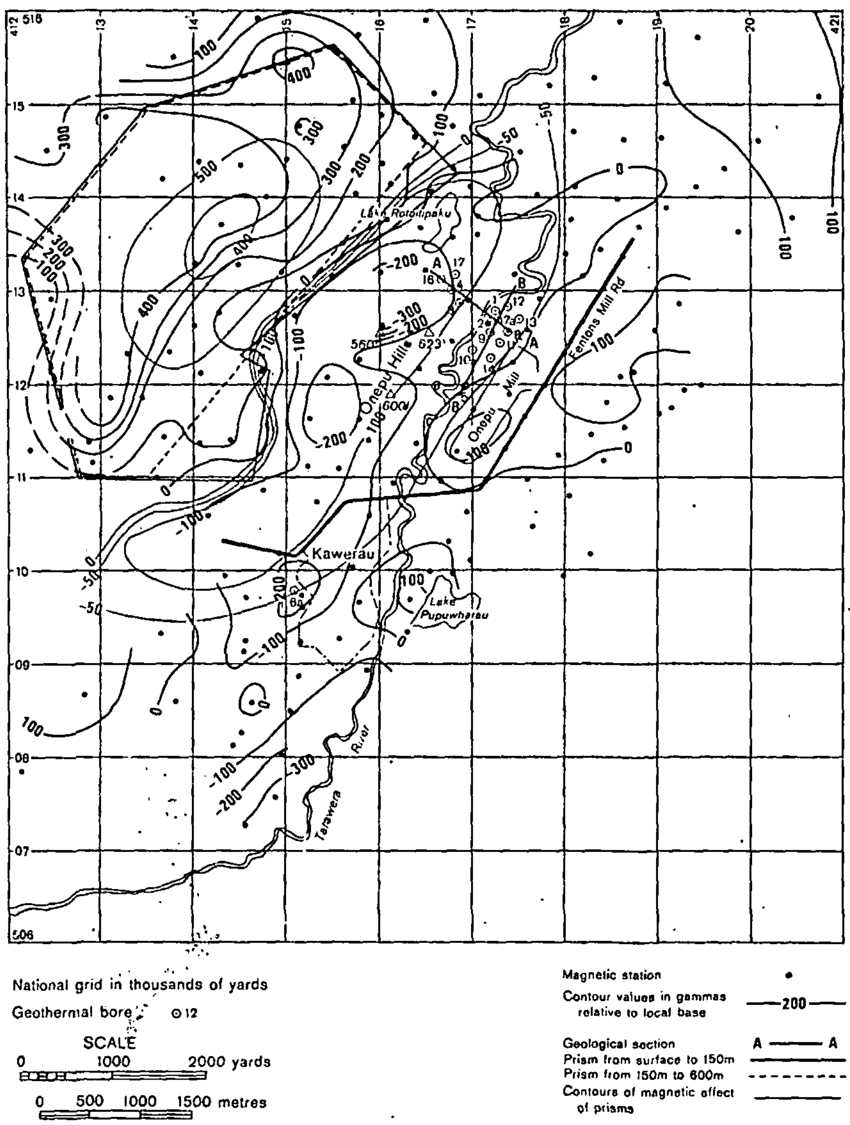

N.Z. Journal of Geology and Geophysics 15(3), 1972

FIG. 5—Vertical force ground magnetic survey of Kawerau geothermal area (after Studt 1958).

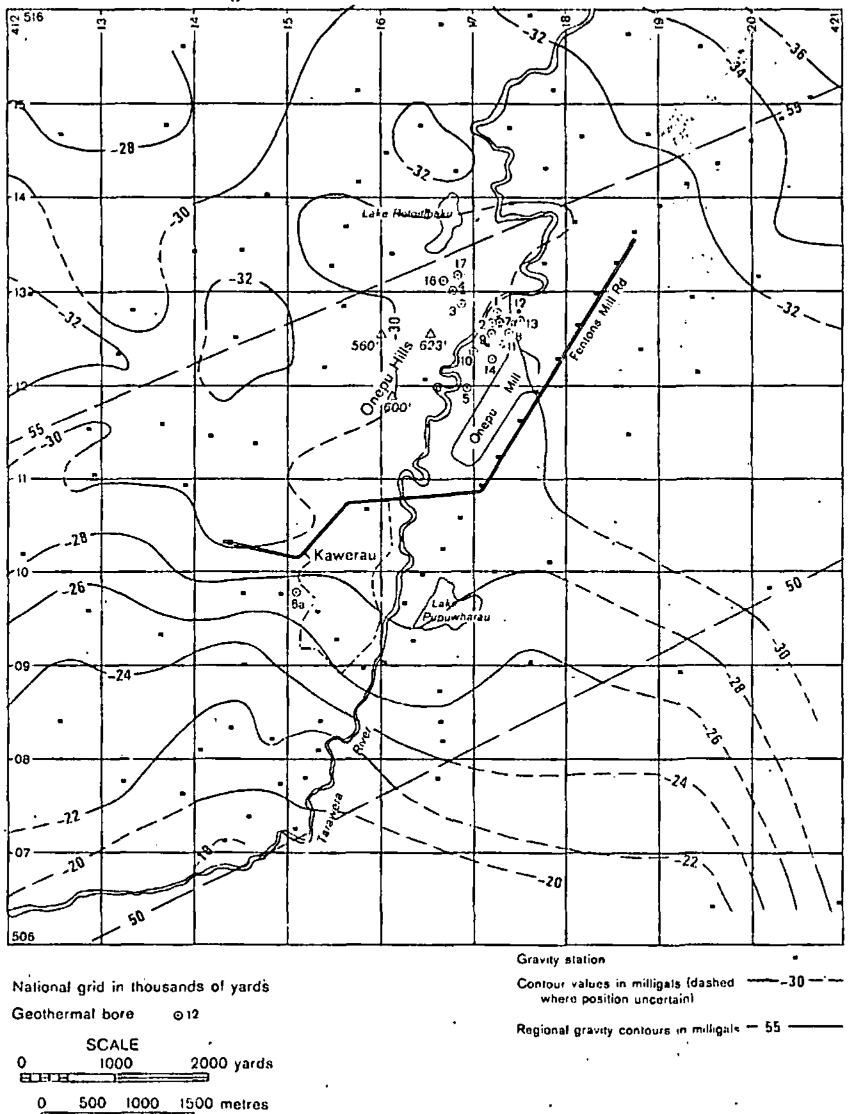

Fig. 6—Residual Bouguer gravity anomalies of Kawerau geothermal area.

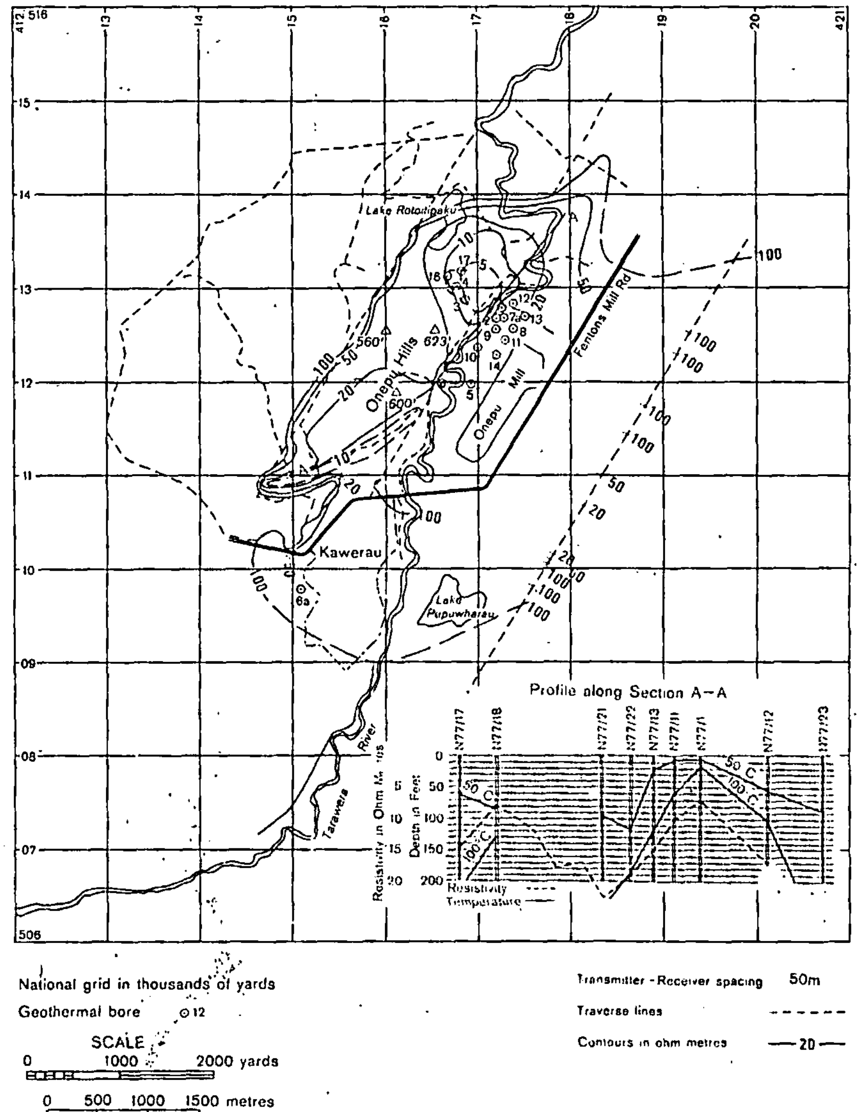

N.Z. Journal of Geology and Geophysics 15(3), 1972

FIG. 7—Electromagnetic gun survey of Kawerau geothermal area.

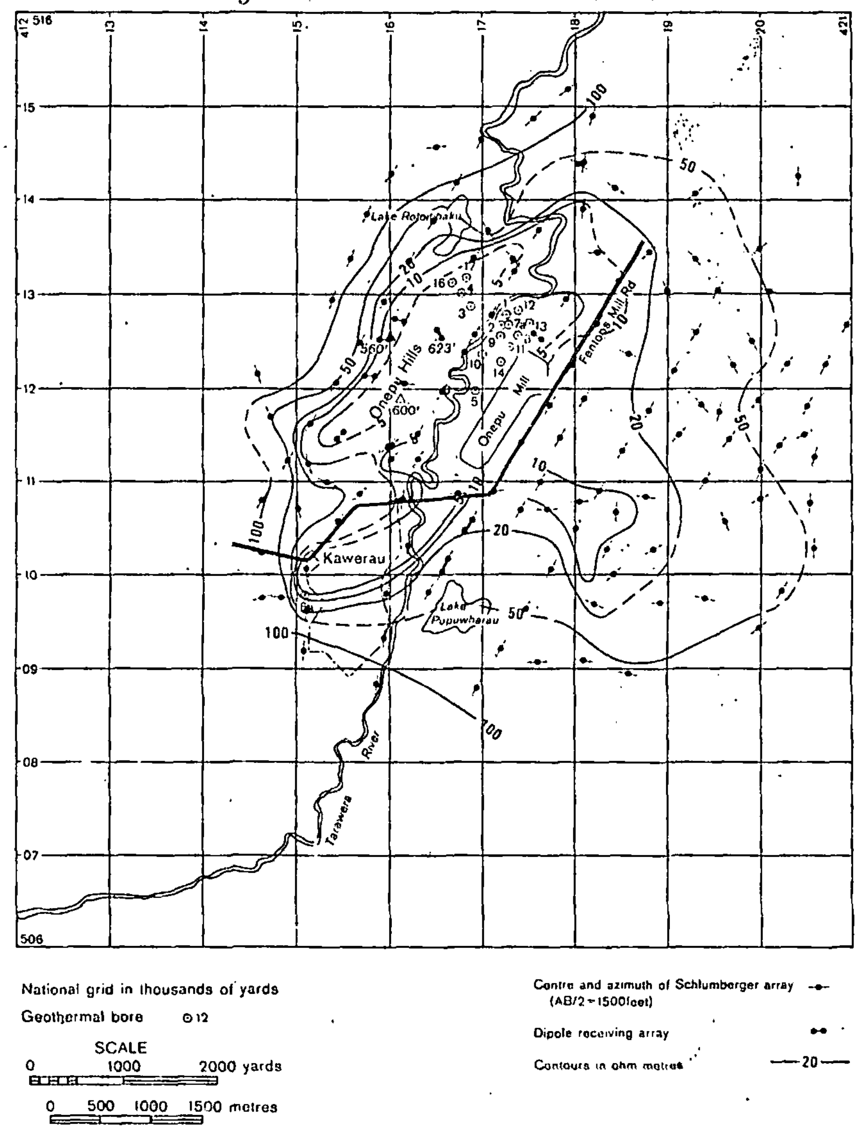

Fig. 8—Apparent resistivity contours of Schlumberger profiling survey (AB/2 = 1,500 ft), Kawerau geothermal area.

by hydrothermal alteration of the magnetic minerals to nonmagnetic ones. Hence interpretation of the Kawerau magnetic map is ambiguous, and the magnetic anomalies are of little use in delineating the boundaries of the Kawerau Geothermal Field or in the siting of drillholes.

Gravity Survey

The residual gravity map (Fig. 6) is based on the field data used by Studt (1958) and on 12 additional stations occupied by D. J. Woodward in 1970. The raw field data were reduced using a computer programme (GP–48) that corrects for latitude, elevation, terrain (to 167 km), and earth tides. A density of 2·67 Mg m^{-3} is used in the Bouguer and terrain corrections. The Bouguer anomalies thus calculated were further reduced by subtracting the regional Bouguer anomaly. The regional Bouguer anomaly used is the same as that depicted on fig. 8 of Studt (1958), except 5 mgal has been added to take into account the change of datum from the New Zealand Provisional System to the New Zealand Potsdam System (1959) (Robertson and Reilly 1960).

The residual gravity anomaly map thus produced (Fig. 6) is almost identical to fig. 8 of Studt (1958). A positive anomaly of about 2 mgal is located over the borefield and extends to the south toward Kawerau Borough. Studt (1958, fig. 9) analysed this high by matching the observed anomalies with computed profiles of two-dimensional models, and concluded that the anomaly over the borefield is due to an anomalous mass within the volcanic and sedimentary cover and probably not connected with changes in the basement greywacke surface. Without drillhole data from outside the anomaly we cannot discriminate between Studt's two alternative interpretations: rhyolite intrusion or hydrothermal alteration to denser rock. It should be noted, however, that at the Broadlands geothermal field a similar positive residual anomaly of up to 10 mgal could be resolved into an anomaly of 2 mgal due to the subsurface rhyolite domes and an anomaly of up to 8 mgal due to increased density brought about by hydrothermal alteration of the volcanic overburden (Hochstein and Hunt 1970).

GEOPHYSICAL INVESTIGATIONS IN 1970

The resistivity of ground is primarily dependent on four parameters:

(1) The temperature;
(2) The salinity of the pore water;
(3) The amount of interconnected pores (effective porosity); and,
(4) The amount of minerals of high ion-exchange capacity (mainly clays and zeolites).

Increasing any one of these factors decreases the resistivity. Above 170°C the rate of decrease of resistivity with increasing temperature becomes slight, and above 330°C may even reverse, with resistivity increasing at higher temperatures. Geothermal fields of the hot-water type like Kawerau are characterised by temperatures above 200°C, increased salinity relative to pore water outside the field, and local concentrations of clay and zeolites.

Therefore the resistivity inside such a geothermal field will be lower than the resistivity outside the field.

The spatial distribution of resistivity beneath a measuring point is usually complex and cannot be specified from a single measurement. Consequently, the quantity actually determined in an electrical survey is the "Apparent resistivity", which is the resistivity calculated from Ohm's Law assuming a homogeneous medium. In a layered earth, apparent resistivity can be thought of as a weighted average of the resistivity of the various layers beneath the measuring point.

Resistivities at shallow depths (15 to 45 m) are best investigated by a rapid electromagnetic technique, whereas resistivities at intermediate depths (150 to 1000 m) are most easily studied by direct current methods that use a linear array of four electrodes. Once the boundary of the field is roughly established, greater depths can be investigated by dipole-dipole methods.

Therefore, by using different techniques and geometric factors it is possible to calculate the apparent resistivity within and around a geothermal field at various depths, and thus to develop a three-dimensional picture of the geothermal system.

Electromagnetic Gun Survey

The electromagnetic gun survey (Lumb and Macdonald 1970) is a rapid, inexpensive means of measuring the apparent resistivity of ground at depths of approximately 15 to 45 m. The device consists of a vertical transmitting coil connected by a screen cable to a similar vertical receiving coil, in this survey, 50 m away. The apparent resistivity is calculated from the comparison of the magnetic field detected by the second coil and that of the reference signal fed along the cable.

Apparent resistivity contours of the electromagnetic survey are shown on Fig. 7. The intense electrical interference caused by power lines, fences, etc., east of the Tarawera River precluded use of the electromagnetic gun except along a line 915 m east of Fentons Mill Road.

These results are compared with measured ground temperatures in the insert to Fig. 7. These temperatures are taken from Studt (1958, p. 233) and Studt (1952). Holes with high temperatures along the section correspond to stations with low apparent resistivity. From this comparison one can predict that within the 50 ohm-meter contour, ground temperature will be above normal, and that within the 10 ohm-meter contour temperatures greater than 100°C will be encountered within 50 m of the surface.

DC Resistivity Survey

Measurement of apparent resistivity by DC methods has become a standard technique for outlining geothermal fields (Risk *et al.* 1970; Hatherton *et al.* 1966; Banwell and Macdonald 1965). In the Kawerau survey, spot measurements of apparent resistivity were made using a Schlumberger array, with the current electrodes 914 m apart ($AB/2 = 457$ m) and the potential electrodes 30 m apart ($MN/2 = 15$ m). At additional stations, current electrodes spacings ($AB/2$) up to 915 m were used. At stations with difficult access, such as in the Onepu Hills, Schlumberger arrays could not be used. Dipole-dipole arrays were substituted at 6 stations, using electrode spacings approximately equivalent to the Schlumberger AB/2 = 457 m.

The apparent resistivity values measured with a symmetric Schlumberger array at AB/2 = 457 m probably represent an average of the true resistivities for depths ranging from about 150 to 900 m.

The results of the Schlumberger DC resistivity survey are shown in Fig. 8 as contours of equal apparent resistivity interpolated from the values measured at the data points. The stations along Fentons Mill Road, near the Onepu Mill, and in the town of Kawerau are of low reliability owing to the presence of electrical noise, underground cables, railway tracks, and wire fences.

These resistivity measurements are bulk measurements that are influenced by a hemisphere of ground of radius approximately half the distance between the current electrodes (i.e., 450 m). Therefore, as the electrode system is moved over a vertical boundary between ground of differing resistivity, the measured values will be influenced by the resistivity on both sides of the boundary, and the measured apparent resistivity values will be different from the values on either side of the boundary. Although this boundary will be approximately parallel to the apparent resistivity contours, it need not coincide with any particular contour value.

Figure 9 (derived from Fig. 8), shows the area between the 10 and 20 ohm-metre contours as a shaded band, modified slightly by taking into account the reliability of individual measurements. Where the shaded band is narrow, the boundary of the field should be sharp and well defined; where the shaded zone is wide, the boundary is diffuse. The area of the Kawerau field lies between a minimum of 6 km^2 enclosed by the inner edge of the boundary zone and a maximum of 10 km^2 enclosed by the outer edge.

Ten measurements within the low resistivity area with current electrode half spacings (AB/2) of up to 915 m showed only slight increase in resistivity at the greater spacings. Drilling at Kawerau shows that high temperatures exist to depths of at least 1 km. Both drilling and resistivity measurements in the geothermal fields at Wairakei and Broadlands have shown that these fields have approximately vertical boundaries to depths of at least 2 km. The available evidence indicates that similar consideration apply also at Kawerau.

There are minor variations in the values of apparent resistivity within the resistivity low, with some values as low as 1 ohm-metre. Inasmuch as the salinity of the pore water at depth in the Kawerau field is essentially constant (W. A. J. Mahon, pers. comm. 1971) and the rate of change in resistivity is very small at temperatures greater than 170°c, this change in resistivity within the field is likely to represent either a change in effective porosity or variation in clay and zeolite content.

It is tempting to site drillholes on these areas of very low apparent resistivity with the field. But in the present Kawerau borefield production comes mostly from fissures within the andesite, the rock of lowest hand-specimen porosity. Also, the production level is well below the effective penetration

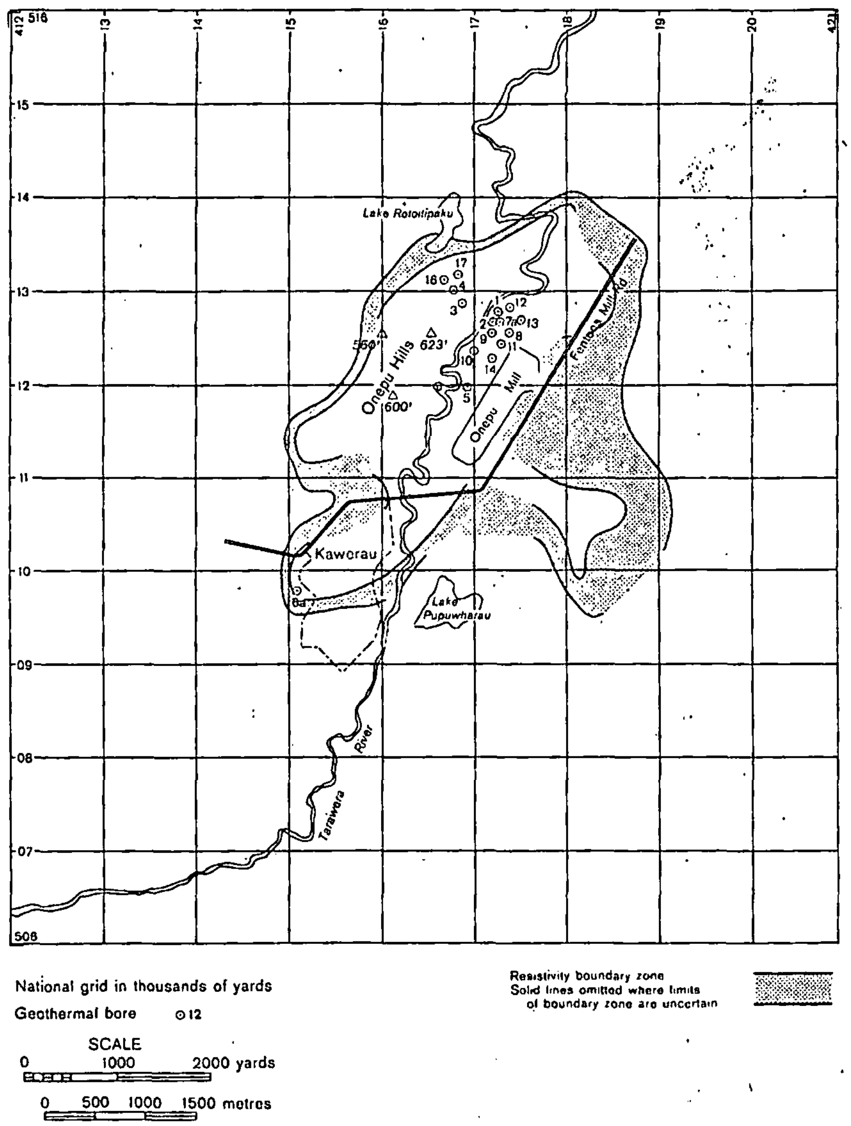

FIG. 9—Resistivity boundary zone derived from Schlumberger profiling survey (AB/2 = 457 m), Kawerau geothermal area.

depth of the AB/2 = 457 m Schlumberger array. Accordingly, the lows inside the resistivity boundary zone cannot be used to site drillholes. The boundary zone, however, does outline the area of probable production.

Ground Permeability

Within the boundary determined by the DC Schlumberger survey temperature at depth will almost certainly be sufficiently high for industrial use. But although high temperature is a necessary condition for geothermal power production, it is not a sufficient one. Productive bores must intersect zones that are sufficiently permeable for the heat available in the water and rock to be efficiently extracted.

Although there is some debate on the subject, it is becoming increasingly accepted that good geothermal bores are fed from fissures rather than from strata having high intergranular porosity. At Kawerau this certainly seems to be so, for best production is from the andesite, the least porous rock unit in the field (Fig. 4).

Unfortunately, there are as yet no good geophysical techniques for identifying fissured zones within the geothermal field as defined by the resistivity boundary, we therefore must fall back on geological interference. Fissures can be produced by faulting, and the fault pattern can be predicted sometimes, if sufficient surface and drillhole data are available. At Kawerau the evidence for faulting is tenuous (*see* p. 306), and predictions of faults, and hence of related fissures at depth, cannot be made with confidence.

Fissures and fractured ground can also be produced around a body of viscous magma as it forces its way to the surface. The dacite hills west of the Tarawera River are very young extrusions that appear to have been pushed up from depth through the older volcanic and sedimentary rocks of the area. The ground beneath and in the vicinity of the dacite hills is likely to have been extensively fractured during emplacement of the dacite, and consequently, bores drilled on the flanks of the hills within the resistivity boundary are likely to encounter fractured ground.

ENERGY STORED IN THE KAWERAU GEOTHERMAL SYSTEM

The minimum total heat stored in the Kawerau geothermal system above a temperature of 100°C can be calculated from the following assumptions:

(1) The system has a cross-sectional area of between 6 and 10 km^2, as suggested by the DC resistivity survey;
(2) the system has a depth of 2 km (the minimum depth proved by drilling at Wairakei and Broadlands);
(3) the average porosity to a depth of 2 km is 15% (the mean value suggested by the data of Fig. 4);
(4) the dry density of the rock is 2·4 Mg m^{-3};
(5) the specific heat of the rock is 0·83 kJ kg^{-1} °C^{-1};
(6) the specific heat of water is 4·18 kJ kg^{-1} °C^{-1};
(7) the temperatures are at boiling point for all depths until a temperature of 250°C is reached, and the temperatures remain at 250°C to a depth of 2 km.

Using these assumptions and appropriate steam tables (Keenan *et al.* 1969), we calculate that the minimum total heat stored in the Kawerau geothermal field above 100°C is $3{\cdot}9 \times 10^{18}$ to $6{\cdot}5 \times 10^{18}$ joules (J), depending on the cross sectional area chosen.

Only part of this heat can be economically extracted. If we assume that all the heat between 200°C and 250°C can be used, then between $1{\cdot}1 \times 10^{18}$ and $1{\cdot}9 \times 10^{18}$ J are available at depth. But the actual energy that can be brought to the surface will be less than these values, because of inefficiencies in extraction, impermeable zones, insufficient drillholes, etc. If we assume a 50% recovery, then only $0{\cdot}55 \times 10^{18}$ to $0{\cdot}95 \times 10^{18}$ J can be brought to the surface. This heat is about one-seventh of the minimum total heat above 100°C stored at depth in the Kawerau geothermal system.

Kawerau is a hot-water geothermal system; the reservoir fluid at depth is entirely liquid, and the wells produce a mixture of hot water and steam. Under present technology, only the steam can be used to generate electricity, and the hot water is rejected. If we assume a turbine inlet pressure of 50 psig (following James 1970), we can calculate that only 46% of the energy in the geothermal fluids delivered to the surface is in the steam phase and thus available for electrical generation. For Kawerau, this amounts to $0{\cdot}24 \times 10^{18}$ J to $0{\cdot}44 \times 10^{18}$ J, depending on the cross-sectional area chosen for the field.

Not all this energy can be converted to electricity. Using fig. 1 of James (1970), at 50 psig turbine inlet pressure, 1 kwh of electricity can be generated from 18 lb of steam. From Keenan *et al.* (1969) the enthalpy of saturated steam at 50 psig is $2743{\cdot}9\ \mathrm{J\,g^{-1}}$. We can thus calculate that it takes $22{\cdot}4 \times 10^{6}$ J of heat to generate 1 kWh of electricity. If the conversion was 100% efficient, it would take only $3{\cdot}6 \times 10^{6}$ J to generate 1 kWh, and thus the actual efficiency of electrical generation in this situation is only 16·1%. Accordingly, for Kawerau only $0{\cdot}04 \times 10^{18}$ to $0{\cdot}07 \times 10^{18}$ J of electrical energy can be produced from the $0{\cdot}25 \times 10^{18}$ to $0{\cdot}44 \times 10^{18}$ J of heat delivered in steam to the turbines. This electrical energy ($1{\cdot}1 \times 10^{10}$ to $1{\cdot}9 \times 10^{10}$ kWh) is equivalent to about 1% of the minimum total heat stored in the Kawerau geothermal field above 100°C.

ACKNOWLEDGMENTS

These surveys were conducted by staff of the Geophysical Survey, Wairakei. In particular, the authors would like to acknowledge the work of Messrs G. B. Dawson, H. H. Rayner, C. A. Y. Hewson, and B. R. F. McGregor. Mr A. E. Leopard made the measurements of rock properties.

REFERENCES

BANWELL, C. J. 1962: Development of the Kawerau geothermal field. Pp. 46–74. *In*: Report for Tasman Pulp and Paper Co. Ltd., on Geothermal Survey at Kawerau 1962. (Unpublished.) N.Z. Department of Scientific and Industrial Research, Wellington.

BANWELL, C. J.; MACDONALD, W. J. P. 1965: Resistivity surveying in New Zealand thermal areas. *Eighth Commonwealth Mining and Metallurgical Congress 1965, paper 213.*

BECK, A. C. 1952: Unpublished report No. 16. N.Z. Geological Survey, Regional Office, Rotorua.

COX, A. 1969: A paleomagnetic study of secular variation in New Zealand. *Earth and Planetary Science Letters 6 (4)*: 257–67.

EWART, A. 1966: Review of mineralogy and chemistry of the acidic volcanic rocks of Taupo Volcanic Zone, New Zealand. *Bulletin Volcanologique 29*: 147–69.

HATHERTON, T.; MACDONALD, W. J. P.; THOMPSON, G. E. K. 1966: Geophysical methods in geothermal prospecting in New Zealand. *Bulletin Volcanologique 29*: 485–97.

HEALY, J. 1951: Unpublished report No. 12. N.Z. Geological Survey, Regional Office, Rotorua.

——— 1962: Geology of the Kawerau geothermal field. Pp. 6–15. *In*: Report for Tasman Pulp and Paper Co. Ltd., on Geothermal Survey at Kawerau 1962. (Unpublished.) N.Z. Department of Scientific and Industrial Research, Wellington.

HEALY, J.; SCHOFIELD, J. C.; THOMPSON, B. N. 1964: Sheet 5 Rotorua (1st ed.). "Geological Map of New Zealand 1 : 250,000". N.Z. Department of Scientific and Industrial Research, Wellington.

HOCHSTEIN, M. P.; HUNT, T. M. 1970: Seismic, gravity and magnetic studies, Broadlands geothermal field, New Zealand. Geothermics (1970) Special issue 2. *United Nations Symposium on the Development and Utilisation of Geothermal Resources, Pisa, 1970.*

JAMES, R. 1970: Power station strategy. Geothermics (1970) Special issue 2. *United Nations Symposium on the Development and Utilisation of Geothermal Resources, Pisa, 1970.*

KEENAN, J. H.; KEYES, F. G.; HILL, P. G.; MOORE, J. G. 1969: "Steam tables: Thermodynamic properties of water including vapour, liquid, and solid phases" (International edition—metric units). John Wiley, New York.

LUMB, J. T.; MACDONALD, W. J. P. 1970: Near-surface resistivity of geothermal areas using the electromagnetic method. Geothermics (1970) Special issue 2. *United Nations Symposium on the Development and Utilisation of Geothermal Resources, Pisa, 1970.*

RISK, G. F.; MACDONALD, W. J. P.; DAWSON, G. B. 1970: DC resistivity surveys of the Broadlands geothermal region. Geothermics (1970) Special issue 2: 287–94. *United Nations Symposium on the Development and Utilisation of Geothermal Resources, Pisa, 1970.*

ROBERTSON, E. I.; REILLY, W. I. 1960: The New Zealand Primary Gravity Network. *N.Z. Journal of Geology and Geophysics 3 (1)*: 41–68.

ROSS, C. S.; SMITH, R. L. 1961: Ash-flow tuffs: their origin, geologic relations and identification. *U.S. Geological Survey Professional Paper 366*: 81.

STEINER, A. 1962: Subsurface geology and hydrothermal rock alteration at Kawerau. Pp. 16–26. *In*: Report for Tasman Pulp and Paper Co. Ltd. on Geothermal Survey at Kawerau 1962. (Unpublished.) N.Z. Department of Scientific and Industrial Research, Wellington.

STUDT, F. E. 1952: Unpublished Geophysics Division Report No. 4 (held in Geophysics Division Library, N.Z. Department of Scientific and Industrial Research, Wellington).

——— 1958: Geophysical reconnaissance at Kawerau, New Zealand. *N.Z. Journal of Geology and Geophysics 1 (2)*: 219–46.

From:
Bulletin Volcanologique
vol. 29, 1966

Geophysical Methods in Geothermal Prospecting in New Zealand *

T. HATHERTON, W. J. P. MACDONALD and G. E. K. THOMPSON

Geophysical Survey, Geophysics Division, Department of Scientific and Industrial Research, Wellington, New Zealand

Introduction

The development of exploration for naturally occurring steam and hot water in New Zealand provides an interesting case history in geophysical prospecting. In 1949 the New Zealand Government decided that the use of geothermal steam in the North Island volcanic region for power production must be investigated. An intensive geological and geophysical study of the region was started, adopting the thesis that the transmission of heat from the primary source to the Earth's surface is « structurally controlled ». Some years were spent in geophysical investigation from the structural point of view in the hope that it would assist the location of the primary sources of the heat. The methods used in these years were those developed principally for oil prospecting, *i.e.*, gravity, magnetic and seismic.

When the initial, structural approach proved to be relatively unrewarding in delineating the steam and hot water system a change was gradually made to the « geothermal » approach in which a study of the properties of the « mineral » itself, rather than the attitude and nature of the host rocks, is important. Thus temperature, and the physical property which changes most with temperature, *i.e.*, resistivity, have been the two parameters studied. Resistivity surveys appear to be particularly rewarding in delineating hot water systems.

There is now growing optimism that the results of the « geothermal » approach can be fed back into the « structural » picture to improve the interpretation of the latter.

---

* Paper read at the IAV International Symposium on Volcanology (New Zealand), scientific session of Nov. 29, 1965.

Structural (Gravity, Magnetic and Seismic) Studies

Conventional gravity, magnetic and seismic studies of the National Park-White Island depression were made during 1949-52. Plate 1 shows the residual Bouguer anomaly map of the area, compiled from stations at about 3 km intervals. Local surveys with stations about ½ km spacings have also been made. Geosynclinal greywackes of great thickness and uniform density occur on both sides of the volcanic area so a « basement-value » regional gravity gradient has been removed from the preferred density Bouguer anomaly values to give the residual anomaly map of Plate 1. This map has been interpreted by various authors (*e.g.*, BECK and ROBERTSON, 1955; MODRINIAK and STUDT, 1959) in terms of a depressed greywacke basement of density 2.62 gm/cm^3, covered by lighter volcanics of assumed density 2.12 gm/cm^3. One such interpretation is illustrated in Fig. 1. It is now considered that the density assumed for the volcanic fill may be too low, and that depths to greywacke basement will be greater than those indicated in Fig. 1. Further, much of the gravity relief within the depressed area may not be indicative of structure but rather due to varying densities of volcanic rocks.

The entire volcanic region was flown with an airborne total force magnetometer with flight lines at about 3 km spacing and a flight elevation of 5000 ft (∼ 1600 m). Little formal interpretation of the total-force anomaly map (Fig. 2) has been done, because of the profusion of volcanic rocks. Complexity of form and magnetisation makes simple models impossible to postulate. High permanent magnetisation produces differences in magnetic intensity between fragmental and massive rocks, even where rocks are of similar composition. The past hydrothermal history of the rocks may be reflected by replacement of magnetite by pyrite, with subsequent low magnetic intensities, but this concept has never been used to predict hot areas.

Seismic velocities have been measured at Wairakei and Waiotapu. Such studies in the thermal region are complicated by high absorption, high noise levels and strong surface waves. Nevertheless MODRINIAK and STUDT (1959) have published a velocity section (Fig. 3) which shows very low velocities (4,500 ft/sec) underlying normal velocities (12,000-13,000 ft/sec). Modriniak and Studt attribute the low velocities to high-temperature, porous rocks with high steam content.

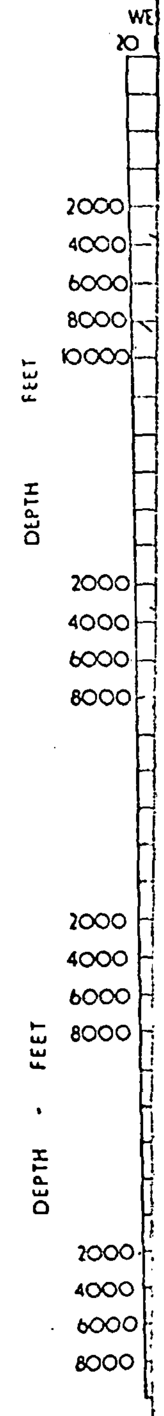

FIG. 1 - Two
Reg
dep
2.62

:and Seismic) Studies

:seismic studies of the National
le during 1949-52. Plate 1 shows
he area, compiled from stations
ys with stations about ½ km
synclinal greywackes of great
on both sides of the volcanic
al gravity gradient has been
Bouguer anomaly values to give
This map has been interpreted
OBERTSON, 1955; MODRINIAK and
greywacke basement of density
anics of assumed density 2.12
illustrated in Fig. 1. It is now
for the volcanic fill may be too
ement will be greater than those
f the gravity relief within the
of structure but rather due to

wn with an airborne total force
out 3 km spacing and a flight
le formal interpretation of the
been done, because of the pro-
f form and magnetisation makes
. High permanent magnetisation
ensity between fragmental and
of similar composition. The past
ay be reflected by replacement.
nt low magnetic intensities, but
predict hot areas.
ured at Wairakei and Waiotapu.
complicated by high absorption,
waves. Nevertheless MODRINIAK
velocity section (Fig. 3) which
c) underlying normal velocities
studt attribute the low velocities
th high steam content.

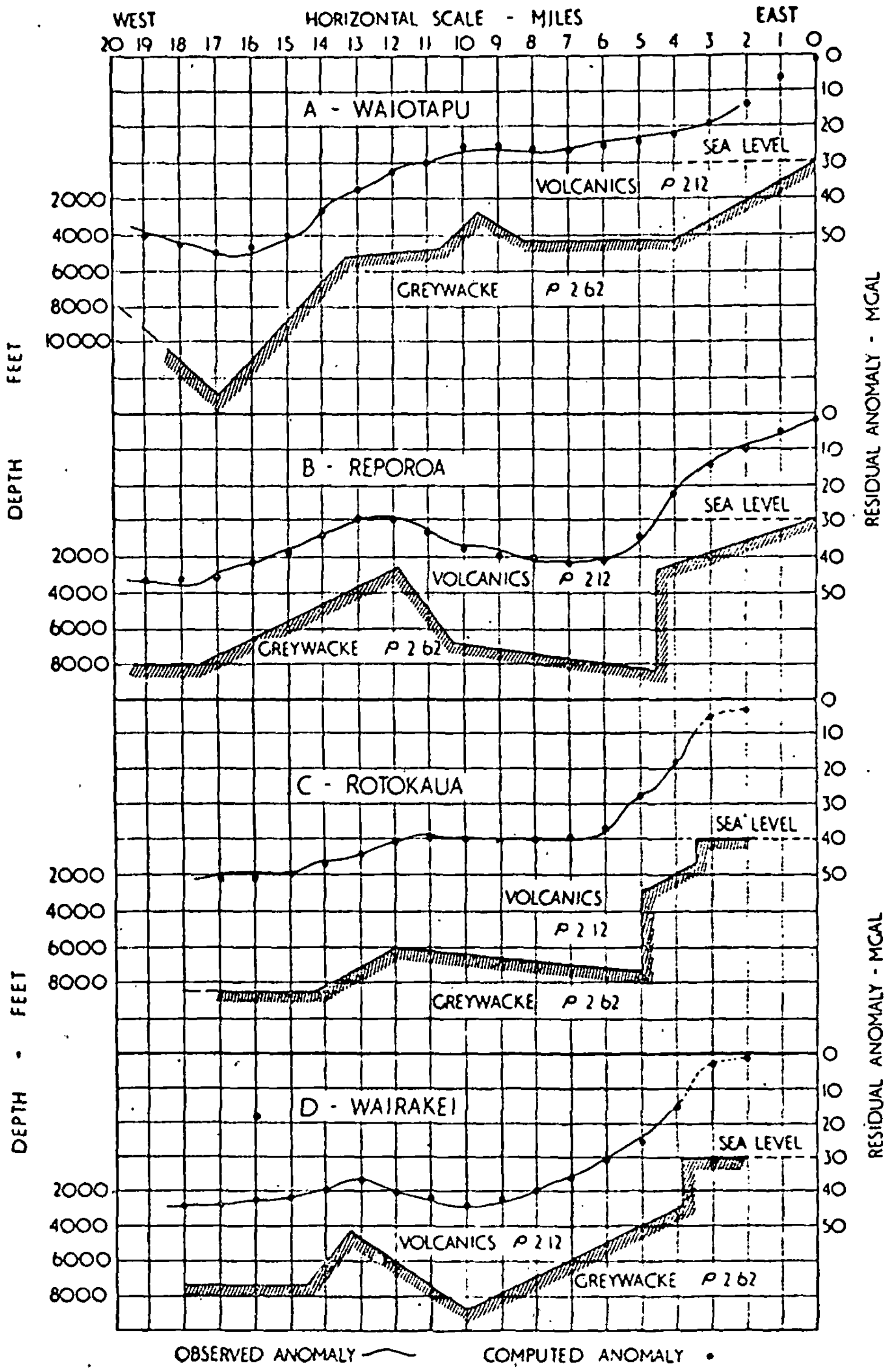

FIG. 1 - Two-layer interpretations of gravity-sections across New Zealand Geothermal Region. (From MODRINIAK and STUDT, 1959). Cross-sections showing minimum depths to basement: computed from residual anomalies, assumed densities 2.62 and 2.12 g/cm³ in basement rocks and covering strata respectively.

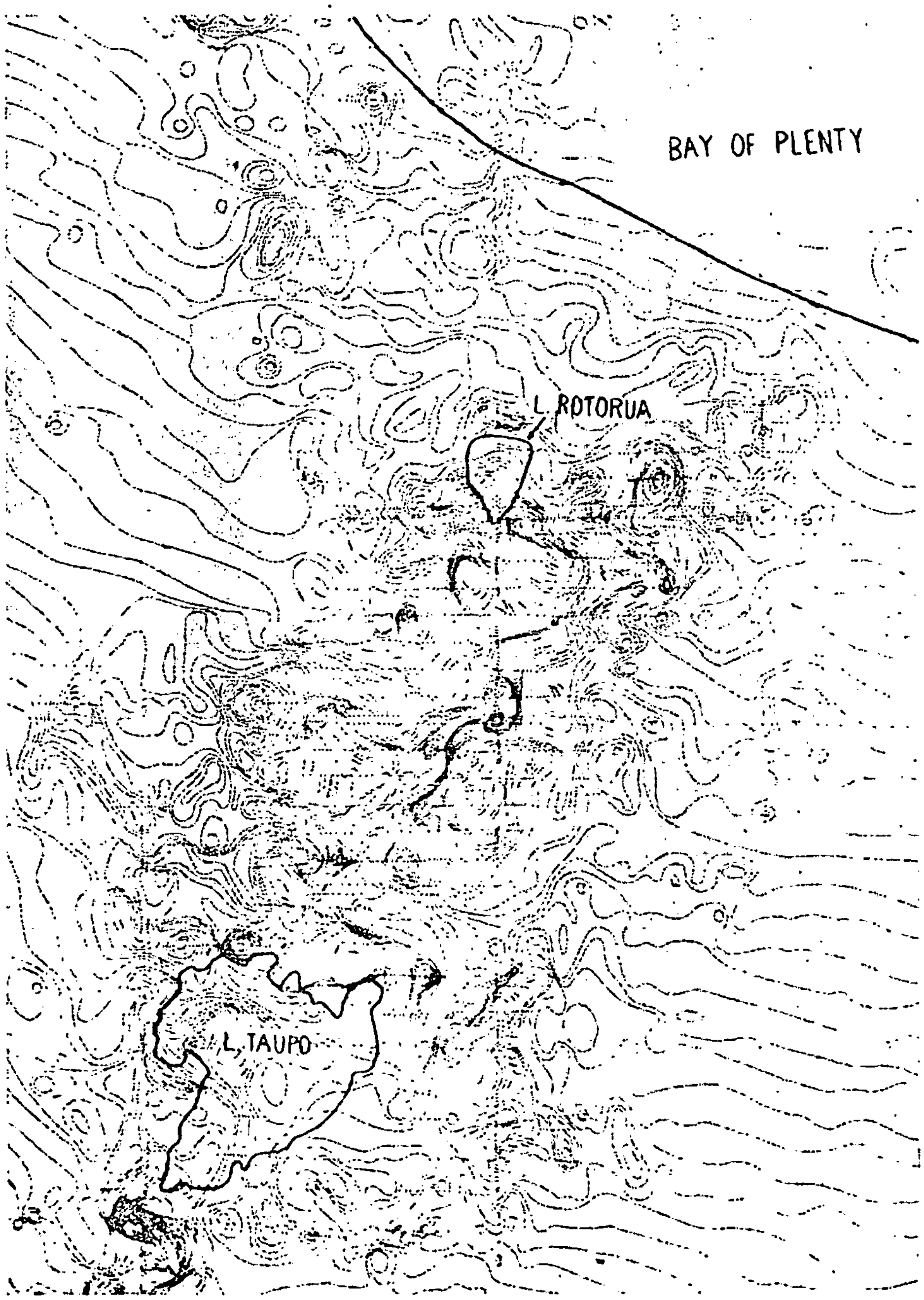

FIG. 2 - Total Magnetic Force Map, New Zealand Geothermal Region. Contour Interval, 25 gammas (After GERARD and LAWRIE, 1955).

Geothermal Region. Contour Interval,
55).

Mineral (Temperature and Electrical Resistivity) Studies

Temperature and heat discharge have not been entirely satisfactory parameters for prospecting methods. In a purely conductive system measurements of geothermal gradients and heat flux could

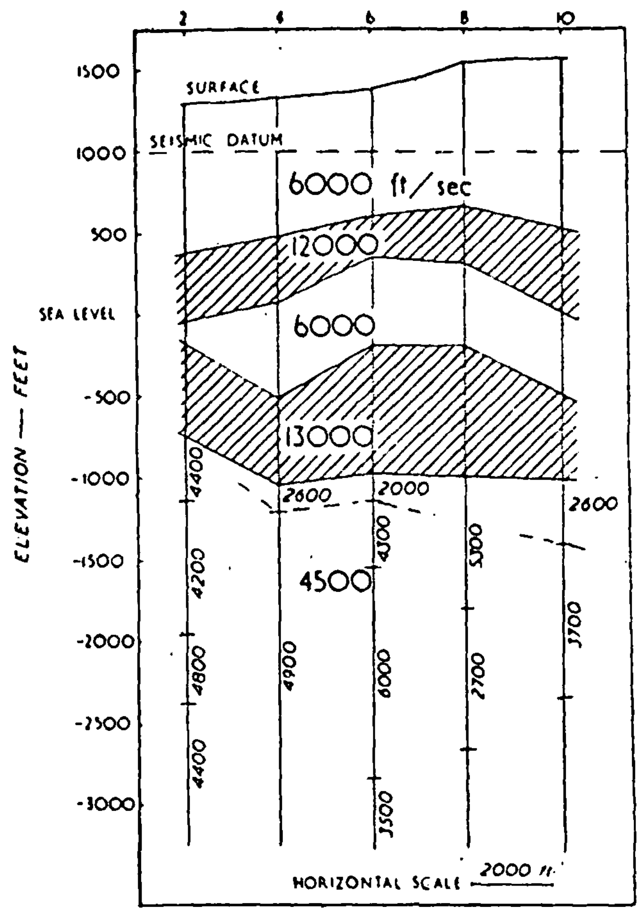

Fig. 3 - Seismic velocity section, line N, Wairakei. (From Modriniak and Studt, 1959).

be treated in a manner analogous to the other « potential » methods (gravity and magnetic). But the effects of mobile waters in the fragmented and permeable covering rocks of the geothermal belt have rendered temperature-based methods relatively ineffective in prospecting for steam and hot water.

An early requirement in geothermal power utilisation was the assessment of total natural heat discharged from an area. Geysers, fumaroles and hot springs were quickly located, and their individual heat discharges totalled, but it was apparent that a considerable amount of heat loss was occurring by means of conduction from surrounding areas of lesser intensity, and indeed from some areas where there was no sign of natural surface heat. A technique was evolved (THOMPSON, 1960) which measured the temperature at a depth of 1 metre. The « metre-probe » survey has proved useful in several ways. It allowed the conduction contribution to heat loss to be accounted for, improving the calculation of minimum power potential; it provided a suitable method of monitoring changes in the geothermal fields as exploitation proceeded, and boundaries obtained from the initial surveys are now relocated annually; and it has been applied to a wide range of unrelated problems where more specific details of ground temperatures are required. Fig. 4 shows the 1 metre depth temperatures of the Wairakei hydrothermal field in 1958. Fig. 5 compares temperatures from the 1 metre isotherm map, across part of the Wairakei field with a section compiled from drilled holes. While the metre-probe is capable of defining the boundaries of hot areas and (as Fig. 5 shows) displaying their near-surface morphology it will not give indications of the prospects of steam production at depth.

During the late 1950's Geophysical Survey, DSIR, was preoccupied by IGY investigations. It was not until 1961 that a serious start was made on electrical resistivity surveys of the thermal regions, although their importance had been recognised for some years previously. The very high contact resistances in the dry pumice, resulting in low current input, together with the very low resistivity of hot chloride waters, resulting in low potentials to be measured in a high resistance circuit, were the technical difficulties which had to be resolved. The use of a switched D.C. system with a vacuum tube voltmeter enabled electrical soundings to be made to a Wenner system electrode separation of 5000 ft ($\sim$ 1600 m) even under the worst conditions, that is surface resistivities $\sim$ 10,000 Ωm and resistivities at depth of $<$ 5 Ωm.

It was decided to produce, in the first instance, a constant spacing contour map of the thermal region. The thermal region divides physiographically into two parts, the southern one from Lake Taupo to Waiotapu and the northern part from Waiotapu to the Bay of Plenty

mal power utilisation was the
harged from an area. Geysers,
ly located, and their individual
apparent that a considerable
by means of conduction from
and indeed from some areas
surface heat. A technique was
asured the temperature at a
» survey has proved useful in
n contribution to heat loss to
lation of minimum power po-
of monitoring changes in the
eded, and boundaries obtained
ated annually; and it has been
problems where more specific
ired. Fig. 4 shows the 1 metre
drothermal field in 1958. Fig. 5
tre isotherm map, across part
compiled from drilled holes.
efining the boundaries of hot
their near-surface morphology
ospects of steam production

urvey, DSIR, was preoccupied
1961 that a serious start was
the thermal regions, although
or some years previously. The
lry pumice, resulting in low
ow resistivity of hot chloride
measured in a high resistance
hich had to be resolved. The
cuum tube voltmeter enabled
Venner system electrode sep-
er the worst conditions, that
nd resistivities at depth of

t instance, a constant spacing
thermal region divides phys-
rn one from Lake Taupo to
aiotapu to the Bay of Plenty

coast. A resistivity contour map of the southern part is almost complete and is reproduced in Fig. 6. The fixed electrode spacing, 1800 ft (∼ 600 m) was chosen to compromise a number of factors, chiefly the logistic problems of handling cables which required as short a

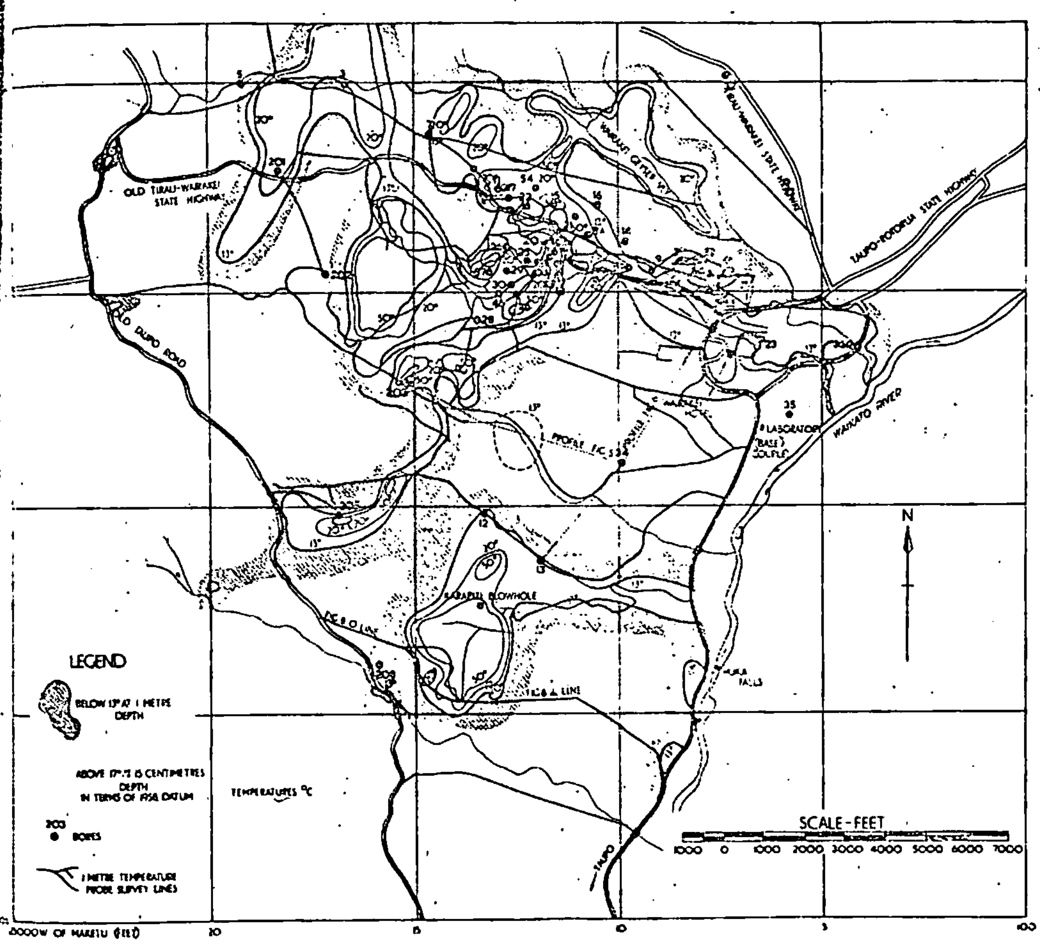

FIG. 4 - Shallow (1-metre) temperature survey of Wairakei hydrothermal field. (From THOMPSON, 1960).

spread as possible, and the knowledge that the production of steam at Wairakei power station was from depths of less than 2000 ft (600 m).

The resistivity of a rock is a function of the porosity and the resistivity of the porewater. The resistivity of the porewater is mainly dependent upon its chloride content and temperature. From measurements made on the waters of the New Zealand thermal regions

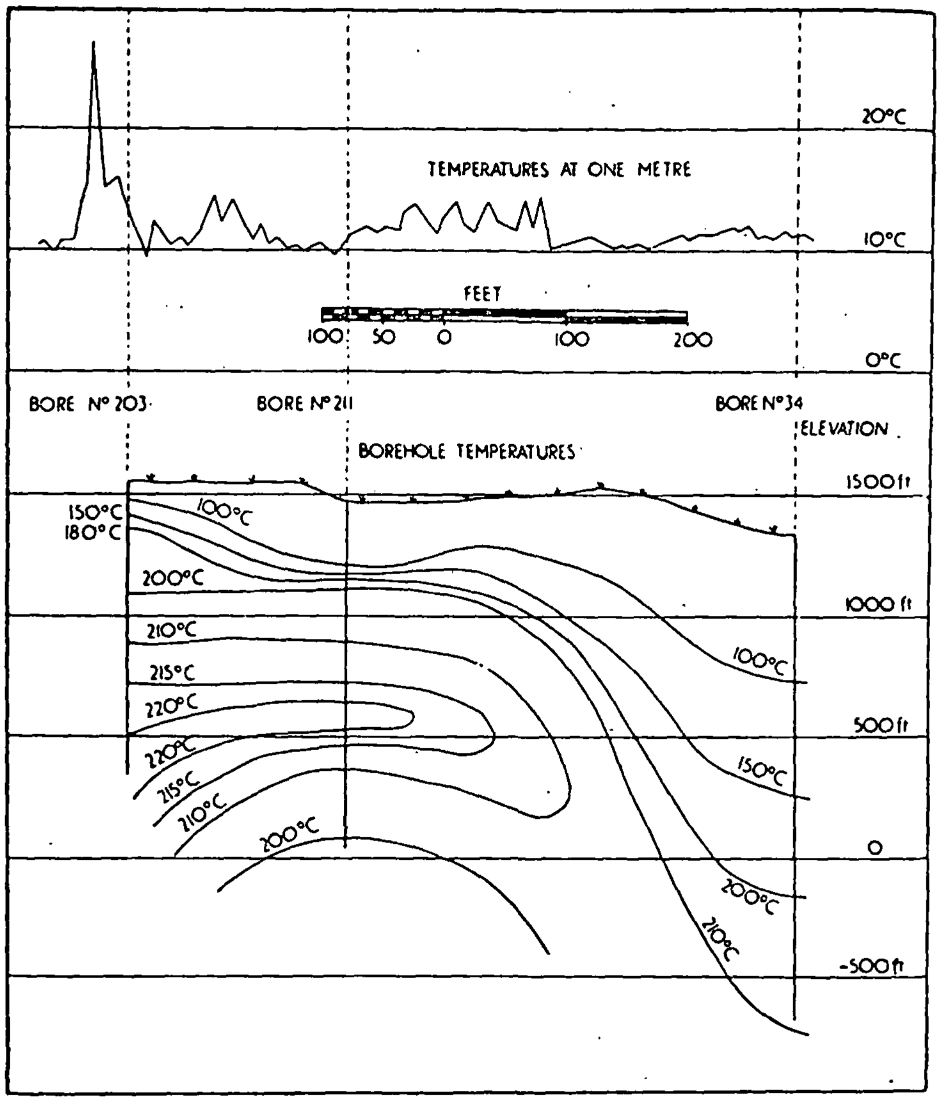

FIG. 5 - Comparison of shallow and deep temperature measurements, Wairakei. (From THOMPSON, 1960).

it has been found that the chloride content of the hot waters east of the Paeroa block ranges from 1200 to 1500 parts per million. A

ınd temperature. From meas-
New Zealand thermal regions

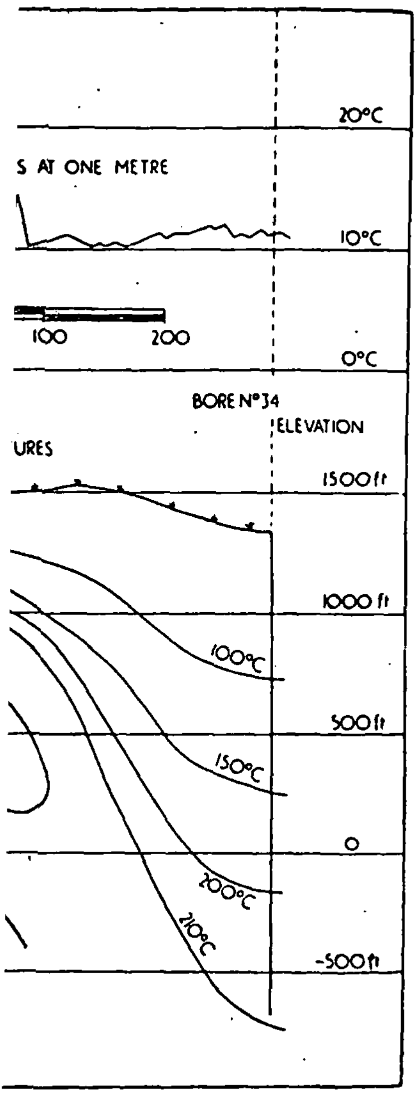

rature measurements, Wairakei. (From

content of the hot waters east
0 to 1500 parts per million. A

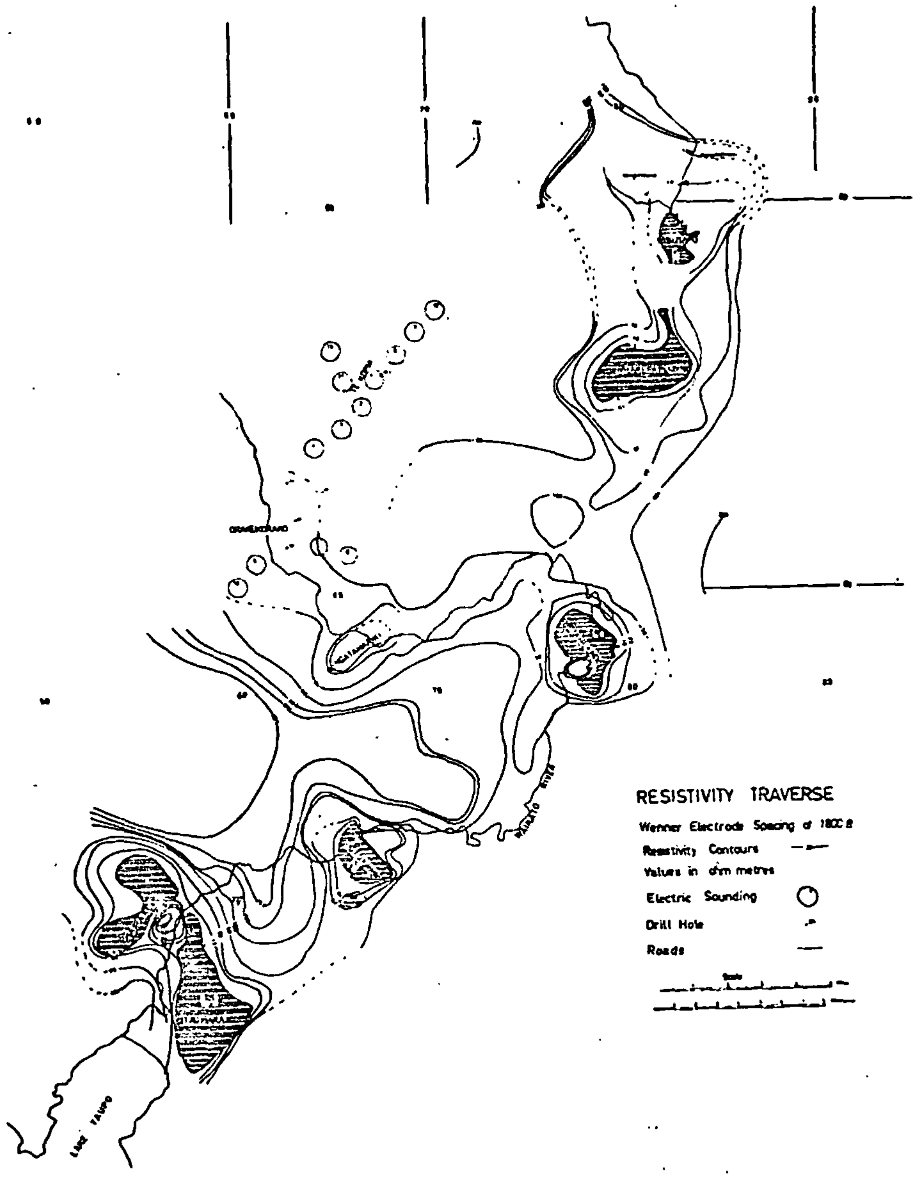

FIG. 6 - Apparent resistivity map (a = 1800 ft) of Taupo-Waiotapu area, New Zealand Thermal Region. Areas of resistivity less than 5 ohm-metres are shaded.

series of curves of porosity, temperature and resistivity has been drawn (Fig. 7) using the well-logging relationship

$$F = 1/\Phi^{m}$$

$$\text{where } F = \text{formation factor } \left(= \frac{\text{resistivity of saturated rock}}{\text{resistivity of saturating fluid}}\right)$$

$$\Phi = \text{porosity}$$

$$m = \text{cementation factor.}$$

The higher boundary of the chloride values (1500 ppm) has been taken to make temperature estimates conservative. m has been taken as 2.2. From. Fig. 7 it can be seen that in rock of porosity 25-33 % temperatures of porewater within the 5 Ωm contour can be expected to be greater than 200°C.

The resistivity data from the Wairakei field has been compared with the temperatures at different levels in the bores. From this comparison it appears that the 1800 ft electrode spacing resistivities are reflecting conditions between 1000 ft (∼ 300 m) and 1500 ft (∼ 450 m) in depth. Thus Fig. 6 may be expected to be a map of temperature conditions between 1000 and 1500 ft at depth. All holes so far drilled within the 5 Ωm areas have been hot at these depths, though some have not been good producers of steam. Satisfactory holes have been drilled within the 10 Ωm boundary, and this is not inconsistent with Fig. 4. It seems justifiable to expect that all holes drilled within the 5 Ωm contour should be hot and that most should be satisfactory producers.

Fig. 6 indicates that in addition to the Wairakei field there are five areas of low resistivity and, therefore, high temperatures. These are, from south to north

(i) The area south-east of Wairakei, the *Tauhara* field.
(ii) The area north of Rotokawa, the *Rotokawa* field.
(iii) The area south-east of Ohaki Springs, the *Broadlands* field.
(iv) The area south of Waiotapu, the *Wharepaina* field.
(v) The *Waiotapu* field.

In the southern part of the geothermal region which is covered by this map the total area bounded by a 5 Ωm contour is about 42.5 km².

ıture and resistivity has been
elationship

istivity of saturated rock
istivity of saturating fluid

le values (1500 ppm) has been onservative. *m* has been taken ıt in rock of porosity 25-33 % 5 Ωm contour can be expected

akei field has been compared s in the bores. From this com- :trode spacing resistivities are 300 m) and 1500 ft (∼ 450 m) to be a map of temperature depth. All holes so far drilled at these depths, though some . Satisfactory holes have been l this is not inconsistent with at all holes drilled within the most should be satisfactory

the Wairakei field there are re, high temperatures. These

i, the *Tauhara* field.
the *Rotokawa* field.
Springs, the *Broadlands* field.
ie *Wharepaina* field.

region which is covered by m contour is about 42.5 km².

The area of the Wairakei low is 7.8 km² and a station of about 150 megawatts capacity is run from this field. Simple extrapolation suggests that 800 megawatts of power is available from the area east of the Paeroa Block, obtainable by drilling to 2000 ft (600 m), though exploitation of this in all cases may not be possible for engineering reasons.

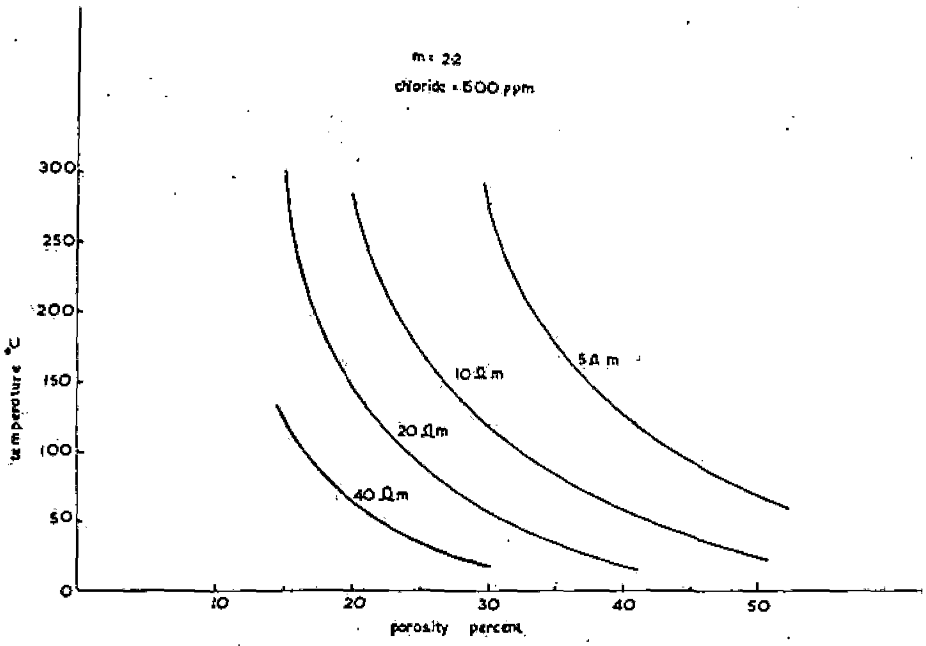

FIG. 7 - Ground resistivity variation with temperature and porosity. Chloride content is assumed constant and *m* (cementation factor) is taken as 2.2.

The disposition of the resistivity lows along the eastern margin of the volcanics-filled trough, the regularity in size, and, to some degree, in spacing, must be indicative of the disposition of the heat source and of the mechanism by which this heat reaches the surface. If there is a continuous strip heat source at depth there should be a higher than normal temperature gradient at depth. Hole 227, drilled on the flank of a resistivity high, has an increase in temperature at the bottom. A nearby electrical sounding also shows decreasing resistivities at depths ∼ 10,000 ft (∼ 3000 m). Plans for future investigations include an attempt at deep soundings by means of fixed cables, up to 25 miles (40 km) long, suspended from lines of poles, as well as the extension of the fixed spread profiling northwards of Waiotapu.

Conclusions

The electrical resistivity method appears to be the most appropriate method of delineating geothermal waters in the New Zealand Volcanic Region. The early concept of structural control of heat loss (within reasonable drilling distance from the surface) appears invalid except in isolated instances. The prospecting methods used to delineate structure have failed to prove profitable in discovering heat sources.

References

BECK, A. C., and ROBERTSON, E. I., 1955 - *Geothermal Steam for Power in New Zealand* (compiled by L. I. GRANGE). Chapter II: *Geology and Geophysics.* Bulletin 117. Department of Scientific and Industrial Research, New Zealand.

GERARD, V. B., and LAWRIE, J. A., 1955 - *Aeromagnetic Surveys in New Zealand, 1949-52.* Geophysical Memoir 3 , Department of Scientific and Industrial Research, New Zealand.

MODRINIAK, N., and STUDT, F. E., 1959 - *Geological Structure and Volcanism of the Taupo-Tarawera District.* N.Z.J. Geol. Geophys., 2: 654-84.

THOMPSON, G.E.K., 1960 - *Shallow Temperature Surveying in the Wairakei-Taupo Area.* N.Z.J. Geol. Geophys., 3: 553-62.

Discussion

C. J. BANWELL: Does not the measurement of ground noise level in thermal areas represent a possibly very useful survey method for detecting active hydrothermal system?

T. E. HATHERTON: The seismic noise in the New Zealand Thermal Region ranges from that of surficial origin to that of the Earthquake Swarm Type. Whilst it might be, and indeed would be, desirable to know the noise distribution in the thermal area, such a project would practically be very difficult to carry out.

R. CATALDI: Temperature surveys for geothermal prospecting purposes were systematically carried out in the Monte Amiata region (Italy) all over impermeable formations where no hydrothermal surface manifestations occur. In this region, the seasonal thermal excursions get out at a depth of about 10 m. Accordingly temperature measurements have been carried out within 15-30 m of depth. I would ask at what depth do you measure temperatures when the prospecting wells are sited in localized impermeable formations where there are no surface evidences of hot manifestations?

T. HATHERTON and C. J. BANWELL: No bores have been located in New Zealand on the results of temperature measurements alone. Our temperature work has been concerned with: 1) 1 metre temperature probe measurements which quickly define thermal boundaries (see reprint « *Shallow Temperature Surveying in Wairakei-Taupo Area* » — THOMPSON, N. Z. Jour. Geol. & Geophys.). 2) Measurement of temperature at depth intervals of 10 feet (≃ 3 m) in holes drilled to a depth of 100 feet (≃ 33 m) (see, D.S.I.R. Bulletin No. 155 « *Waiotapu Geothermal Field* »).

The bores at Broadlands and Rotokawa to which I referred were located on electrical resistivity work. Both are in areas of less than 10 Ohm-metres as mapped by our survey using the Wenner configuration with electrode separation of 1800 feet (≃ 600 m) which gives a penetration of 1000-1500 feet (≃ 330-500 m). However at Ngawha some temperature holes have been drilled and measured and it was found that pure conductive gradients were not encountered until depths of greater than 100 feet (33 m).

G. W. GRINDLEY: Dr Hatherton has illustrated an extremely effective method of detecting shallow reservoirs of heat by electrical resistivity surveys. I would like to mention that geothermal prospecting in this region (Wairakei) is far removed from throwing arrows at a dartboard. We have always been well aware of the importance of thermal detection methods such as shallow drilling and metre probe surveys as a guide to the location of shallow hot aquifers. The other principle method of investigation has been by locating the faults and fissure zones that transect and feed these aquifers. Our wells have normally been located along such faults (as found by geological and photogeological studies) to give optimum production. I would like to know whether there is any electrical method of detecting these faults, particularly those feeding the shallow aquifers from greater depth. This could be of particular interest in connection with the deep drilling programme soon to be conducted in this region.

T. HATHERTON: I was referring to geophysical darts. Geologists have euphemisms for this word.

Whilst in some conditions electrical methods can be used to detect faults, the dominance of water temperature and chloride content in the New Zealand geothermal areas precludes the inference of faults from electrical measurements. In Fig. 6 it can be seen that the individual low resistivity areas are more circular in nature than would be expected from a fault controlled source. However these circular « lows » lie on a line which may be a structural feature at depth.

T. HATHERTON, W. J. P. MACDONALD and G. E. K. THOMPSON — *Geophysical Methods in Geothermal Prospecting in New Zealand.*

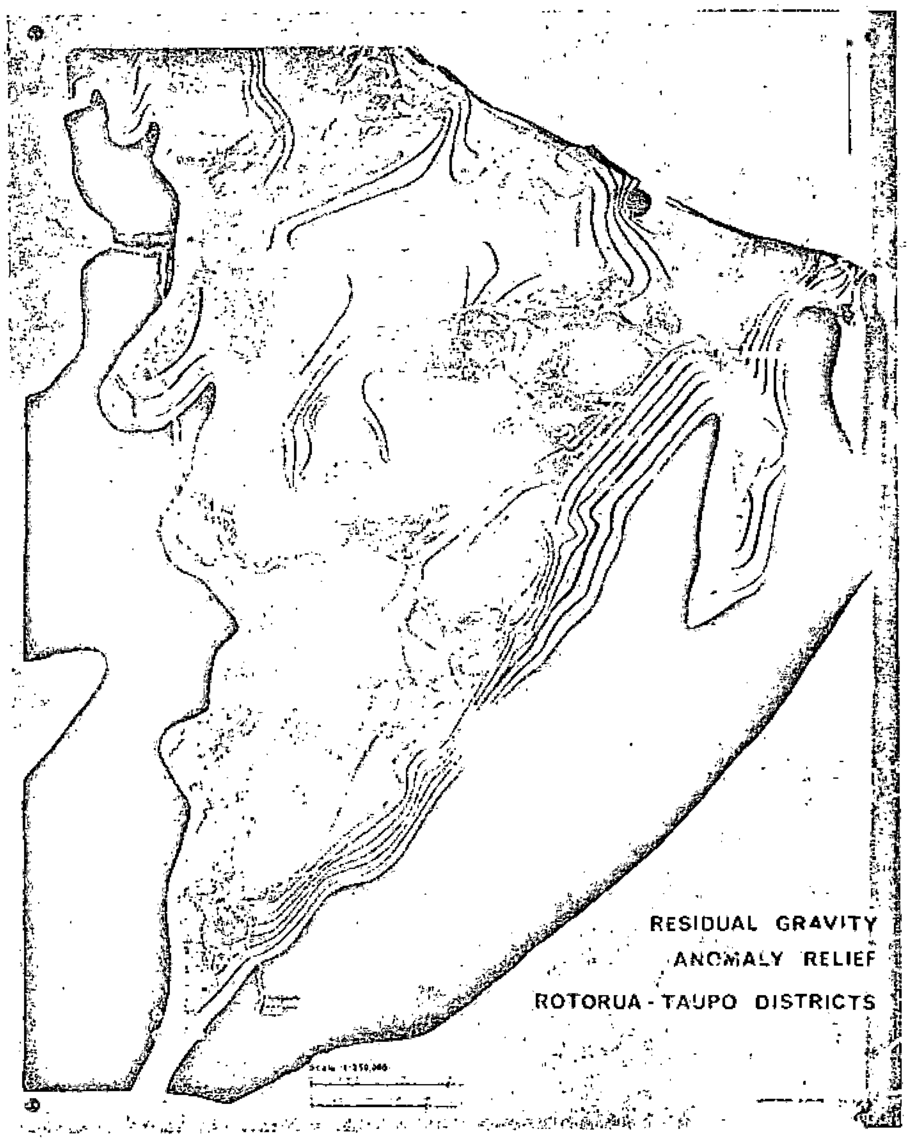

Residual Bouguer anomaly model of New Zealand Geothermal Region. Contour Interval. - 5 mgal, all anomalies negative.

Geophysical

In Japan, th
islands. This co
fumaroles and h
heat of fumarole
In 1947, a g
M.I.T.I. (Ministry
a plan to obtain
geothermal energ
tion was begun
and they succeed
It was only a t
pilot plant.
Since that ti
geothermal area
in Japan. Howe
recently.
In the mon
borehole was sta
of the mainland
to a subsidy fro
of our Geologic
selected by dis
seismic, electric
geochemical an
This boreh
January of 196

* Paper read a
scientific session of

N.Z. Journal of Geology and Geophysics Vol. 21, No. 4 (1978): 443–8

Fission-track age and trace element geochemistry of some Minden Rhyolite obsidians

NEIL F. RUTHERFORD

*Department of Geology, University of Auckland, New Zealand**

ABSTRACT

Fission-track age determinations on obsidians from Mt. Young on Great Barrier Island, Hahei near Whitianga, Bowentown, and Mt. Maunganui give ages of 8·32, 7·80, 2·29, and 4·34 million years respectively. An approximate age of 7–8 million years has been estimated for Paku Island at Tairua.

X-ray fluorescence analyses of trace elements of obsidian from the above localities and from the Alderman Islands show some distinct differences from rhyolites of the Taupo Volcanic Zone, namely a relative enrichment in the light rare earths, especially La, Ce, and Nd. Ce is strongly enriched; Rb is more, and Sr less abundant. The differences may be indicative of a different genesis.

INTRODUCTION

The Minden Rhyolites (Thompson 1966) are a group of upper Miocene–Pliocene dome and flow rhyolites and welded pumice breccias which outcrop on Great Barrier Island, on the eastern side of Coromandel Peninsula, and on a few islands offshore from Coromandel (Fig. 1).

Petrological and geochemical work published on the group is limited. Sollas & McKay (1906) give a number of thin section descriptions of rocks from Paku Island, and Fraser & Adams (1907), Bell & Fraser (1912), and Henderson & Bartrum (1913) describe some regional aspects of the rhyolites. Harvey (1967) describes the geology and petrology of the rhyolites from the Whitianga area, Johnston (1970) the rhyolites from the Maunganui area, and Rutherford (1970) rhyolites from Paku Island, Whiritoa, Minden, and Bowentown.

The Minden Rhyolites overlie extensive andesitic eruptives (Beesons Island Volcanics) which have K-Ar ages ranging from about 16 m.y. to 7 m.y. In some areas the rhyolites are locally intruded and overlain by small andesite (Omahia andesite) and dacite (Waitawheta dacite) domes and flows with K-Ar ages ranging from about 4·0–3·75 m.y. (Stipp 1968; Richards *et al.* 1966; Adams 1975).

Hayward (1974; pers. comm.) indicates that, on limited palynological evidence from Great Barrier Island, Whitianga, and Table Mountain areas, the early Minden Rhyolite eruptives are probably of Tongaporutuan–Waipipian age (Upper Miocene–Lower Pliocene).

The age determinations on the andesites from Coromandel suggest that volcanism began about 16 m.y. ago throughout the region, then ceased in the north, but continued in the south up to about 7 m.y. ago.

Renewed andesitic and dacitic volcanism began about 4 m.y. ago in the Paeroa–Thames area and continued until about 2·54 m.y. ago (K-Ar age, Stipp 1968) in the Te Puke area. Fission-track age determinations on an ignimbrite "owharoite" and "tridymite rhyolite" from Waikino give ages of 2·89 ± 0·38 and 1·5 ± 0·23 m.y. respectively (Kohn 1973). The ignimbrite and rhyolite are considered by Rabone (1975) on stratigraphic grounds to be younger than the Minden Rhyolites of that area.

On geomorphic and stratigraphic evidence, the Minden Rhyolites appear to show younging southward which parallels the younging to the south noted for the andesitic volcanism.

The age relations outlined suggest that the age of the rhyolites should lie between about 7–10 m.y. and 3–4 m.y. with the youngest ages to the south.

FISSION-TRACK AGE DETERMINATIONS

Obsidian samples from rhyolite domes and flows on Great Barrier Island (Mt. Young), Hahei near Whitianga, Paku Island at Tairua, Bowentown, and Mt. Maunganui were selected for dating by the fission-track method.

The procedures essentially follow the standard methods used by other workers, e.g., Fleischer *et al.* (1964; 1965), Naeser (1967; 1969), and Seward (1974) and the reader is referred to these and Rutherford (1976) for details of the method.

The age equation used in the calculations was:

$$A = 6 \cdot 168 \frac{\rho_s}{\rho_i} \cdot \phi \times 10^{-8}$$

which is a reduction of the general equation below by substitution of the constant values, but disregarding the total decay constant for ^{238}U, (λ_D), which for relatively young rocks is not a significant factor.

$$A = \frac{1}{\lambda_D} \ln \left[1 + \frac{\rho_s \lambda_D \sigma \psi \phi}{\rho_i \lambda_F} \right]$$

where

λ_D = total decay constant for ^{238}U (= $1 \cdot 54 \times 10^{-10}$ yr^{-1})
σ = thermal neutron X-section for ^{235}U fission (= $5 \cdot 82 \times 10^{-24}$ cm^2)

Received 18 April 1977, revised 1 November 1977
*Present address: Union Corporation (Australia) Pty Ltd, 55 Macquarie Street, Sydney, Australia.

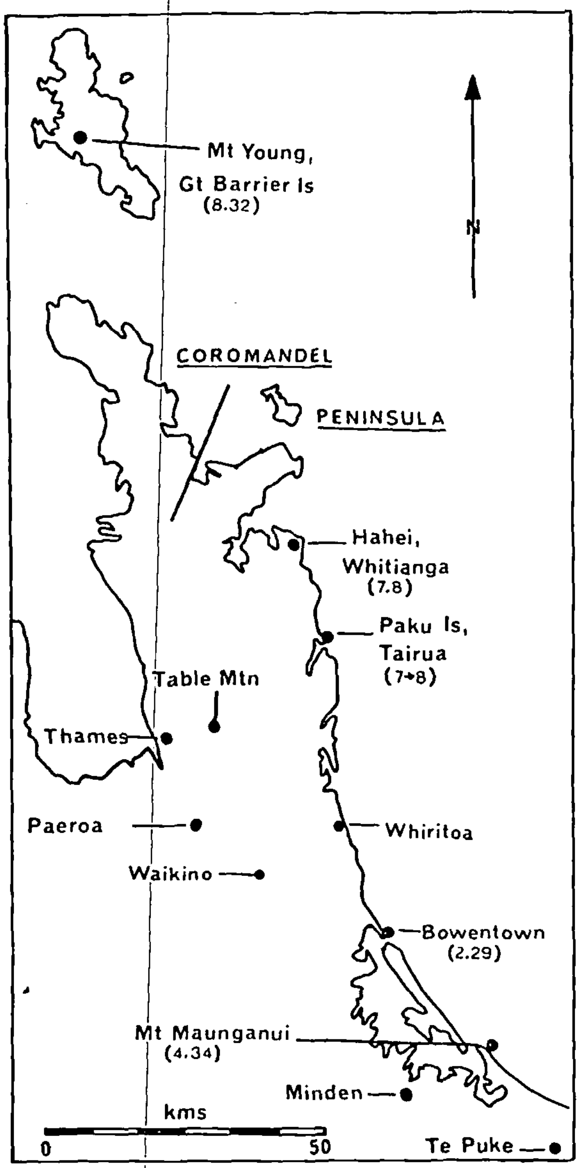

FIG. 1—Locality map, with ages of the dated samples (in million years) in parentheses.

ϕ = thermal neutron dose (n cm^{-2})
ψ = isotopic ratio $^{235}U/^{238}U$ (= $7 \cdot 26 \times 10^{-3}$)
λ_F = fission decay constant for ^{238}U (= $6 \cdot 85 \times 10^{-17}$ yr^{-1})
ρ_s = spontaneous or natural ^{238}U fission-track density
ρ_i = induced ^{235}U fission-track density (per unit area).

Pieces of obsidian from each locality were examined and those which showed least evidence of devitrification were selected; those pieces with a cloudy appearance, abundant microlites, perlitic cracks, etc. were rejected.

This was not possible for Paku Island obsidian, where all material examined was cloudy and showed strong development of a perlitic fracture. After etching it was not found possible to use the obsidian for accurate dating and an age was estimated by counting a few small areas of a number of obsidian pieces which were most free of perlitic cracks and devitrification to determine the approximate ratio of spontaneous to induced fission tracks from which an age could be calculated. However, as the obsidian was not of an acceptable standard—there was evidence of track facing or annealing (spontaneous track size smaller than induced track size), and the area counted not large—the age is considered unreliable. The age is consistent with that determined for the Whitianga sample and the inferred age based on stratigraphy.

The samples were irradiated by the Isotope Division of the Australian Atomic Energy Commission in their thermal neutron facility at Lucas Heights, New South Wales. The total thermal neutron dose received by the samples was estimated using National Bureau of Standards (N.B.S.), Washington, fission-track glass (1 p.p.m. uranium) standards. In order to check the N.B.S. glass standards dose estimate, a sample of Borchers Ash was included with the obsidians sent for irradiation. The age calculated for the Borchers Ash sample using the dose determined from the glass standards was $1 \cdot 94 \pm 0 \cdot 23$ m.y. which is consistent with that found by other workers (e.g., Boellstorff & Te Punga 1977, p. 48).

The glass standards were placed at the top and bottom of the irradiation can containing the samples to check for possible flux gradient. None was noted and the dose estimate was calculated from the mean of the counts determined from the glasses at the top and bottom of the can. The dose was calibrated against pre-irradiated glasses supplied by the N.B.S. using their Au-foil determined dosage. Tracks were counted directly from the glass standards after etching for 12 seconds in 48% hydrofluoric acid.

After etching, all samples were cleaned in nitric acid (this enhances track rendition by "cleaning out" etch pits), washed in dilute ammonia, and finally washed in distilled water. Counting of tracks was done under reflected light at 450 × magnification using a grid eyepiece (for area determination) in conjunction with a point count stage (to move sample).

Track densities were not recalculated to a basis of tracks per cm^2 but tracks per equal area which is equivalent. The ratio of spontaneous to induced tracks is used in the age equation and, thus, it is necessary only to determine track density for spontaneous and induced tracks over some arbitrary but known area, for example, in this case track density per number of grid squares.

Sample localities, track densities, and ages determined are given in Table 1.

DISCUSSION OF AGES

As with most volcanic glasses, in particular older glasses, there is the possibility of track loss through annealing. There is a noticeable reduction in spontaneous track size compared with the induced track size, especially in the older samples dated here. Thus, there

TABLE 1—Fission-track age data for Minden Rhyolite obsidians. $\lambda_F = 6{\cdot}85 \times 10^{-17}\,yr^{-1}$; $\phi = 15{\cdot}755 \times 10^{14}\,n\,cm^{-2}$. Induced track density is total measured density minus spontaneous track density.

Sample number	Locality (Grid reference)	Spontaneous tracks		Induced tracks		Age (m.y. B.P.)
		Counted	Per unit area	Counted	Per unit area	
A.U. 17466	Bowentown (N53/473859)	133	52	2244	2192	2.29 ± 0.21
A.U. 17472	Mount Maunganui (N58/647658)	164	46	1064	1018	4.34 ± 0.38
A.U. 10261	Hahei, Whitianga (N44/283632)	227	71	955	884	7.80 ± 0.60
A.U. 475	Mount Young, Great Barrier Island	217	217	2753	2536	8.32 ± 0.62
A.U. 17413) A.U. 17401)	Paku Island, Tairua (N44/355425)	See text		Estimate 7 to 8 m.y.		

TABLE 2—Trace element contents and some potassium to trace element ratios for Minden Rhyolite obsidians.

	Great Barrier Island	Hahei, Whitianga	Paku Island	Alderman Islands	Bowentown	Mount Maunganui	Average, Taupo Volcanic Zone*
Ba	842	955	895	1345	1012	1055	870
Rb	220	172	195	259	167	187	150
Sr	19	79	57	106	96	66	125
Y	70	60	30	57	49	32	25
Zr	215	185	144	139	161	136	180
Nb	19	18	16	11	24	10	10
La	45	40	35	32	36	29	30
Ce	117	103	59	65	71	59	40
Nd	45	38	17	17	22	11	15
Pb	32	29	19	20	32	21	20
Zn	70	55	34	39	47	28	45
Ga	21	39	20	20	30	24	20
Cl	1168	1550	1025	520	1015	1505	-
S	186	221	252	1616	445	202	-
K/Rb	-	154.4	148.9	-	144.1	168.6	-
K/Ba	-	27.8	32.45	-	23.78	29.89	-
Rb/Sr	11.05	2.18	3.42	2.44	1.74	2.83	--

*from Ewart *et al.* (1968) and Rutherford (1976).

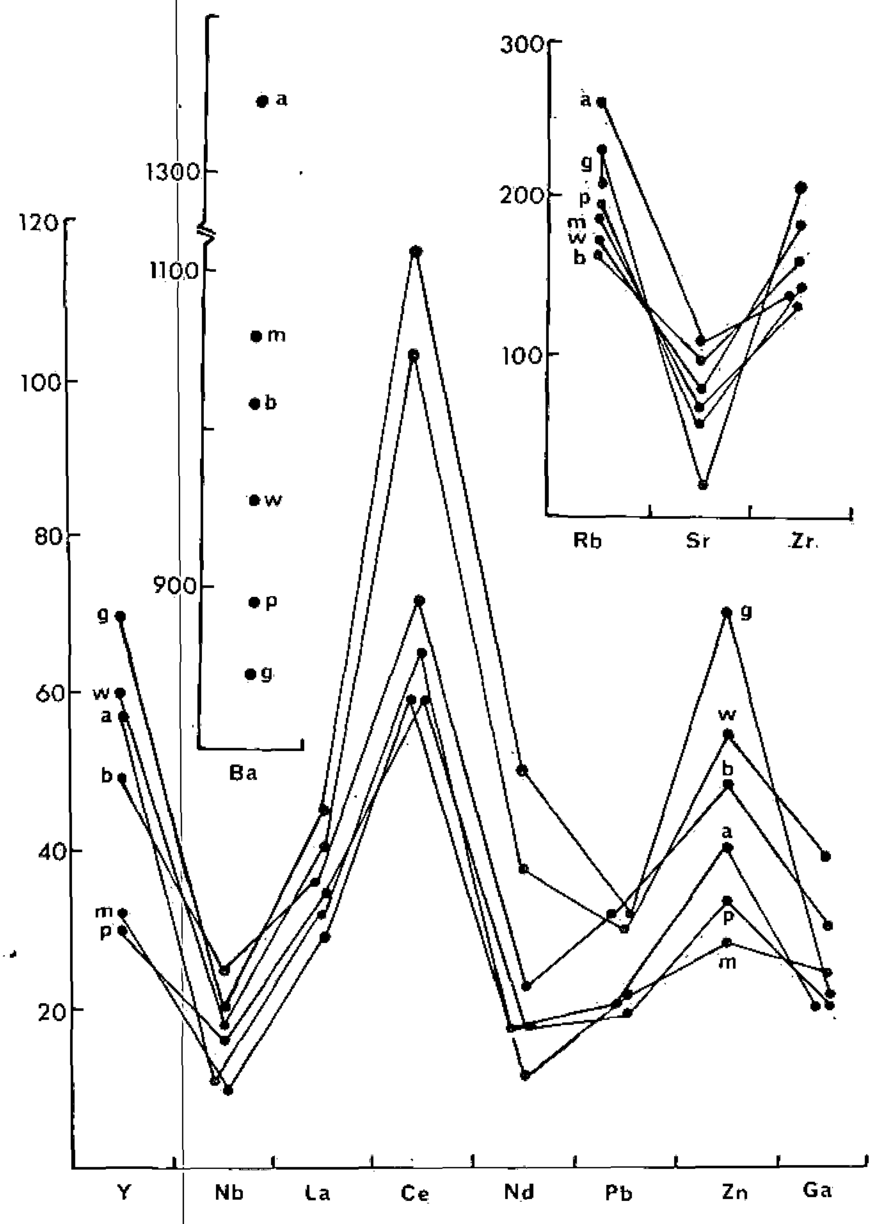

FIG. 2—Summary of trace element data from Table 2. Values in parts per million.

g—Great Barrier Island; w—Hahei, Whitianga; p—Paku Island; a—Alderman Islands; b—Bowentown; m—Mount Maunganui.

could have been some spontaneous track loss. This, in effect, means that the ages given in Table 1 should be regarded as minimum ages.

The Hahei and Great Barrier Island ages and the inferred age for Paku Island are consistent with the age brackets imposed by the K-Ar ages on the andesites and dacites and also with the inferred palynological ages.

The Bowentown age is similar to that determined by Kohn (1973) for the ignimbrite and "rhyolite" at Waikino (2·89 ± 0·38 and 1·5 ± 0·23 m.y.) and to the K-Ar ages on andesites from the Te Puke area (2·95 and 2·54 m.y.; Stipp 1968). Geomorphically the domes at Bowentown are the most youthful of the Minden Rhyolites. The young age for these domes suggests that they should be separated from the considerably older rhyolites to the north and placed in a new group along with the ignimbrites and rhyolites of the Waikino area.

The Mount Maunganui age is similar to that of the younger andesite and dacite eruptives of the Thames–Paeroa area and to the inferred main period of alteration in the Tui Mine area, Te Aroha (Adams 1975). The dome at Mount Maunganui is much eroded and on geomorphic grounds would be considered somewhat older than those at Bowentown. Fission-track ages support this.

TRACE ELEMENT ANALYSES

Trace element analyses were performed by X-ray fluorescence on pressed powder plates of obsidians from the domes fission-track dated and from the Alderman Islands. The results are given in Table 2 and summarised in Fig. 2. Details of the analytical methods can be found in Rutherford (1976).

DISCUSSION OF RESULTS

Several authors, for example, Ewart & Stipp (1968), Ewart *et al.* (1968), and Rutherford (1976), have proposed from trace element characteristics of the rhyolitic and dacitic volcanics of the Taupo Volcanic Zone and the Mesozoic greywackes of the North Island of New Zealand, that the acid volcanics of that area have been derived by various degrees of fusion from the greywackes. The notion of the acid volcanics being derived from more basic andesitic or basaltic parent magmas has not been favoured on geochemical and geophysical grounds. For example, there is no geophysical evidence for large quantities of basic magma within the Taupo Volcanic Zone from which the acid magmas could have fractionated or for chemical continuity between the acid and more basic rocks of the volcanic zone. Similarly, in ancient, much eroded, acid volcanic terrains elsewhere in the world, there is no evidence of extensive basic affiliates from which the acid volcanics could have been derived, which suggests that basic melts were not necessary for the production of acid magma.

In the Coromandel area there is a relatively extensive development of andesitic volcanics with lesser quantities of rhyolitic volcanics. As in the Taupo Volcanic Zone, the basement rocks are Mesozoic greywackes.

Unfortunately, there are no trace element data available for the andesitic volcanics to allow comparison between a fractionation model (from more basic volcanics) and a crustal fusion model for the origin of the rhyolites. There are plutonic intrusions in the north of Coromandel, e.g., granodiorite plutonics at Paritu and Cuvier Island.

Comparison of the trace element data presented in this study with average values of the acid volcanics from the Taupo Volcanic Zone show that the Coromandel rhyolites are more enriched in the light rare earth elements La, Ce, and Nd; Ce in particular is strongly enriched (1·5–3×). The elements Ba, Rb, and Y are also relatively enriched and Sr is depleted, when compared with average Taupo Volcanic rocks.

If the Minden Rhyolites have been derived from crustal fusion of basement greywackes as has been proposed for the acid rocks of the Taupo Volcanic Zone, then they must represent early formed fractions to account for the enrichment of Ba, Rb, Y, and the light rare earths relative to their Taupo Zone equivalents. The relative depletion of Sr would also tend to support this proposal. In general, under conditions of partial melting, Sr tends to become more abundant as melting proceeds, and Ba, Rb, Y, and the light rare earths become more dilute because they tend to associate with the early melt fractions, i.e., compatible and incompatible elements.

Because little is known of the trace element characteristics of the andesites and dacites which are associated with the Minden Rhyolites in Coromandel, it is not possible to assess, on the basis of trace elements, the possibility that the rhyolites represent part of a typical calc-alkalic suite and are not products of crustal fusion.

The andesites and dacites in Coromandel are proportionately far more abundant than in the Taupo Zone and the presence of plutonics in Coromandel suggests that the rhyolites and the more basic rocks may be associated with plutonism in the area.

ACKNOWLEDGMENTS

The fission-track irradiations were funded by a grant from the University of Auckland Research Committee. I wish to record my thanks to those staff and students in the Geology Department at the University of Auckland who assisted me in this work, in particular, Terry Barter for his help and co-operation with irradiation dose determination and discussions on procedures.

REFERENCES

ADAMS, C. J. D. 1975: New Zealand potassium-argon age list—2. *N.Z. Journal of Geology and Geophysics 18 (3)*: 433–67.

BELL, J. M.; FRASER, C. 1912: Geology of the Waihi–Tairua Subdivision, Hauraki. *N.Z. Geological Survey Bulletin 15.* 192 p.

BOELLSTORFF, J. D.; TE PUNGA, M. T. 1977: Fission-track ages and correlation of middle and lower Pleistocene sequences from Nebraska and New Zealand. *N.Z. Journal of Geology and Geophysics 19 (1)*: 47–58.

EWART, A.; STIPP, J. J. 1968: Petrogenesis of the volcanic rocks of the Central North Island, New Zealand, as indicated by a study of Sr^{87}/Sr^{86} ratios, and Sr, Rb, K, U and Th abundances. *Geochemica et Cosmochimica Acta 32*: 699–736.

EWART, A.; TAYLOR, S. R.; CAPP, A. C. 1968: Trace and minor element geochemistry of the rhyolitic volcanic rocks, central North Island, New Zealand. Total rock and residual liquid data. *Contributions to Mineralogy and Petrology 18*: 76–104.

FLEISCHER, B. L.; PRICE, P. B.; WALKER, R. M. 1964: Techniques for geological dating of minerals by chemical etching of fission fragment tracks. *Geochemica et Cosmochimica Acta 28*: 1705–14.

——— 1965: Neutron flux measurement by fission tracks in solids. *Nuclear Science and Engineering 22*: 153–56.

FRASER, C.; ADAMS, J. H. 1907: Geology of the Coromandel Subdivision, Hauraki. *N.Z. Geological Survey Bulletin 4.* 154 p.

HARVEY, C. C. 1967: Rock alteration in the southeast Whitianga. (Unpublished M.Sc. Thesis, lodged in the Library, University of Auckland, Auckland.)

HAYWARD, B. W. 1974: Geology and eruptive history of Table Mountain area, Coromandel Peninsula. *N.Z. Journal of Geology and Geophysics 17* (2): 403–22.

HENDERSON, J.; BARTRUM, J. A. 1913: The Geology of the Aroha Subdivision, Hauraki, Auckland. *N.Z. Geological Survey Bulletin 16*. 127 p.

JOHNSTON, C. 1970: The geology of the Mount Maunganui Area (Unpublished B.Sc.(Hons.) Thesis, lodged in the Library, University of Auckland, Auckland.)

KOHN, B. P. 1973: Some studies of New Zealand Quaternary pyroclastic rocks. (Unpublished Ph.D. Thesis, lodged in the Library, Victoria University of Wellington, Wellington.)

NAESER, C. W. 1967: The use of apatite and sphene for fission-track age determinations. *Geological Society of America Bulletin 78*: 1523–6.

——— 1969: Fission track ages of accessory minerals from granitic rocks of the Central Sierra Nevada batholith, California. *Geological Society of America Bulletin 80*: 2201–12.

RABONE, S. D. C. 1975: Petrography and hydrothermal alteration of Tertiary andesite–rhyolite volcanics in the Waitekauri Valley, Ohinemuri, New Zealand. *N.Z. Journal of Geology and Geophysics 18* (2): 239–58.

RICHARDS, J. R.; COOPER, R. A.; BLACK, P. M. 1966: Potassium-argon age of plutonic intrusives on Cape Colville and Cuvier Island. *Nature 211*: 725–6.

RUTHERFORD, N. F. 1970: The geology of Paku Island with comments on the geology at Whiritoa, Bowentown, and Minden and the Minden Rhyolite Group of volcanics (Unpublished B.Sc. (Hons.) Thesis, lodged in the Library, University of Auckland, Auckland.)

——— 1976: Petrochemistry of ignimbrites from the Central North Island and Coromandel, N.Z. (Unpublished Ph.D. Thesis, lodged in the Library, University of Auckland, Auckland.)

SEWARD, D. 1974: Age of New Zealand Pleistocene substages by fission track dating of glass shards from tephra horizons. *Earth and Planetary Science Letters 24*: 242–48.

STIPP, J. J. 1968: The geochronology and petrogenesis of the Cenozoic volcanics of the North Island, New Zealand. (Unpublished Ph.D. Thesis, lodged in the Library, Australian National University, Canberra.)

SOLLAS, W. J.; MCKAY, A. 1906: "The rocks of Cape Colville Peninsula, Auckland, New Zealand". Vols. 1 and 2. Government Printer, Wellington.

THOMPSON, B. N. 1966: The Geology of the Coromandel Region. *N.Z. Geological Survey Report 14*.

N.Z. Journal of Geology and Geophysics Vol. 21, No. 3 (1978): 287–91

Hydrothermal metamorphism of the Whangakea Basalt, New Zealand

EVAN C. LEITCH

Department of Geology & Geophysics, University of Sydney, Sydney, Australia

ABSTRACT

The Cretaceous Whangakea Basalt has undergone two episodes of alteration. The earlier one pervasively affected part of the formation and produced greenschist mineral facies assemblages of the type quartz–albite–chlorite–epidote–actinolite–sphene. The later episode gave rise to zeolites, including stilbite, analcime, thomsonite, epistilbite, heulandite–clinoptilolite, and laumontite, none of which co-exist stably wth quartz. Products of the zeolitic alteration are widespread, but occur predominantly in and adjacent to veins. Calcite crystallised at a late stage in this episode. Greenschist alteration probably occurred at temperatures in excess of 320°C, whereas zeolite alteration is believed to have taken place below 165–180°C.

The Whangakea Basalt, together with an associated gabbro–peridotite body, constitute an ophiolite complex. The localised development of the greenschist alteration, the presence of relic magmatic phases, the lack of preferred orientation of the secondary minerals, and their common pseudomorphous habit suggest that this alteration resulted from hydrothermal metamorphism. Zeolitic alteration may have occurred late in this metamorphism, or may have occurred while the basaltic rocks were buried beneath some 3000 m of Tertiary strata.

INTRODUCTION

The Te Rake and Waipahirere masses comprise the more easterly of the several inliers of Cretaceous Whangakea Basalt that form the rugged headlands of northernmost New Zealand (Fig. 1). They are surrounded mainly by Tertiary and Quaternary sedimentary material and are locally intruded by middle Tertiary microdiorite bodies. I have previously described the geology of the masses and the adjacent strata (Leitch 1970). Both the Te Rake and Waipahirere masses are formed of pillowed and unpillowed basaltic flows intruded by sills and dykes of dolerite. Minor intercalations of autoclastic breccia and rare radiolarian chert occur within the dominantly extrusive piles.

This paper is concerned with the nature, origin, and significance of the alteration of the Whangakea Basalt in the two masses. Phases have been identified optically and by X-ray diffraction. Plagioclase compositions were determined with the universal stage using the curves of Slemmons (1962), and by refractive index measurements. Except where otherwise noted, zeolite identifications have been confirmed by X-ray diffraction. Refractive indices are believed accurate to ± 0·003 (± 0·002 for zeolites), and optic axial angles to ± 2°. Specimen numbers are those of the petrology collection, Department of Geology, University of Auckland.

IGNEOUS PETROGRAPHY

All of the rocks are altered, those of the Waipahirere mass almost pervasively, and those of the Te Rake mass mainly in and adjacent to veins that seam all outcrops. The following descriptions are based largely on material from the latter mass; texturally comparable rocks, believed to have had initially similar compositions, form the Waipahirere mass.

Received 17 February 1977, revised 31 October 1977

BASALT: Textures vary from perhyaline with only scattered phenocrysts of plagioclase and augite set in a dark glassy groundmass, to intersertal where glass, now usually replaced by secondary phases, occurs in interstices between subophitically intergrown augite and plagioclase. Some pillows have a variolitic texture resulting from a radial arrangement of slender labradorite laths scattered between which are small augite granules set in glass. Comb-like and aborescent clinopyroxene intergrowths with interstitial glass occur in pillow selvedges.

In most rocks plagioclase averaging about An_{60} is the most abundant magmatic phase. Phenocrysts show normal zoning from cores as calcic as An_{75} to rims of An_{50}. The phenocrysts of one specimen (9087) are spongy cores of oligoclase (An_{25}), with clear rims of labradorite, set in a hyaline groundmass containing euhedral augite phenocrysts and small clear labradorite laths. Another (9088) consists of calcic oligoclase and augite phenocrysts surrounded by an intergranular groundmass of plagioclase laths, augite granules, and opaque oxide.

Colourless clinopyroxene occurs in all little-altered basalts, typically in subhedral grains smaller than the associated plagioclase. Optical data ($2V_z$ 50–53°, β 1·684–1·696) indicate it is a normal augite. Specimen 9092 contains scattered microphenocrysts of bronzite ($2V_x$ 98°, $\beta < 1·70$).

Small needles and equant grains of opaque oxide occur in most basalts and rare brown amphibole is found in the core of a variolitic pillow (9091).

DOLERITE: The dolerites, holocrystalline rocks with a hypidiomorphic-granular texture, contain the same simple primary mineral assemblage as the basalts: plagioclase, augite, and opaque oxide. Plagioclase is the most abundant phase, constituting about 60% of the rocks. The bulk of this feldspar is labradorite, with

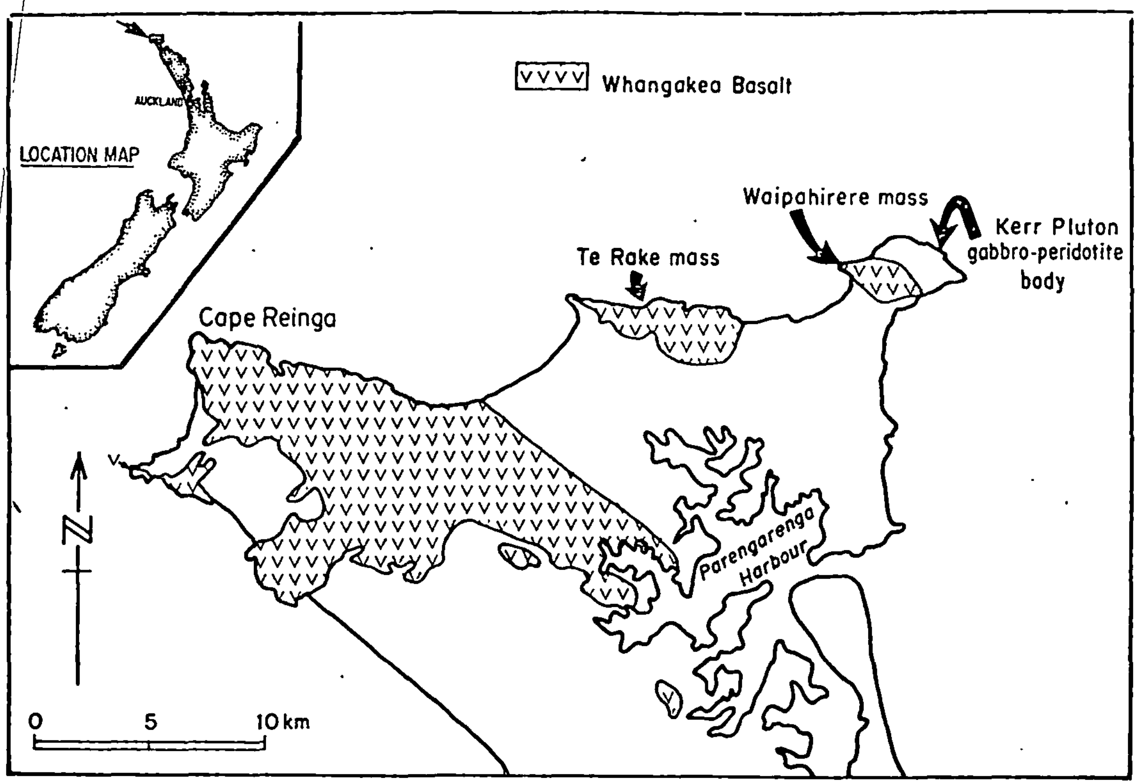

FIG. 1—Northernmost New Zealand showing location of Te Rake and Waipahirere masses.

most crystals normally zoned from cores occasionally as calcic as An_{76} to margins as sodic as An_{20}. Subhedral augite ($2V_z$ 48–52°, β 1·691–1·697) is colourless or sometimes very pale pink. Opaque oxide occurs in amounts of up to 5%, in some rocks as well-formed crystals and in others in large skeletal units. Apatite is a minor but widespread phase. Bronzite ($2V_z$ 115°, β <1·72), forms slender pale-orange to colourless pleochroic rods and constitutes 2% of specimen 9100.

Neither magmatic quartz nor olivine were found in the dolerites or basalts.

ALTERATION

Two distinct episodes of alteration of the Whangakea Basalt are recognised. The earlier episode affected only rocks of the Waipahirere mass, especially those along the northern coast of North Cape headland. It resulted in the crystallisation of typical greenschist mineral facies assemblages, and most rocks affected show few relic magmatic phases. Augite persists occasionally, and calcic plagioclase rarely. The textures of the rocks have, however, been little modified, except in zones of tectonic brecciation and shearing, or along major vein systems where epidosites have formed. The rocks lack schistosity or cleavage, and no preferred orientation of secondary phases has been discerned.

The second episode affected rocks of both masses. Alteration was confined largely to ramifying vein systems that criss-cross the rocks, although there was also some replacement of earlier phases found in the body of the rocks. The main products of this alteration are zeolites and calcite.

Overprinting of the zeolitic alteration on the greenschist event is clearly demonstrated by the replacement of greenschist phases, especially quartz and albite, by zeolites, and by zeolite veins cutting earlier greenschist facies veins.

Greenschist facies alteration

Typically, the products of this alteration are green rocks, composed mainly of chlorite, epidote, and actinolite. Pillow lavas frequently show a zonal arrangement of these phases, with chlorite concentrated in the cores of the pillows and epidote in the selvedges and inter-pillow interstices. In other pillows actinolite is concentrated in the outer zones.

The greenschist facies mineralogy is described below:

QUARTZ, typically in clear unstrained grains, occurs in nearly all rocks, although it has been replaced to varying degrees by zeolites during later alteration. It occupies amygdules and veins as well as being disseminated through the fabric of the rocks.

ALBITE has widely, though not completely, replaced calcium-bearing plagioclase. It has not been identified in veins or amygdules.

CHLORITE is present in most specimens, occupying amygdules and veins as well as replacing much of the bulk of the original rocks. This phase is optically negative and shows anomalous interference colours. n_{max} ranges from 1·605 to 1·612, suggesting a variation in Fe (Fe+Mg) of between about 0·28 and 0·35.

EPIDOTE occurs in all rocks. It is most common in veins, but also occupies amygdules and interpillow interstices, and occurs scattered throughout the rocks. Optical and X-ray measurements indicate it is iron-rich (Ps_{22}–Ps_{30}).

ACTINOLITE is found only in the main fabric of the rocks, where it has replaced ferromagnesium phases and glass. It is commonly intergrown with chlorite. Refractive indices (α 1·619–1·626, γ 1·646–1·650) indicate a magnesium-rich actinolite.

SPHENE is found in all rocks, generally in dark irregular aggregates.

PYRITE is a widespread, although minor, phase in veins and amygdules. It is occasionally accompanied by small amounts of chalcopyrite, the latter showing marginal replacement by digenite and chalcocite.

HEMATITE occurs mainly in narrow veins, frequently associated with pyrite.

The most common mineral assemblages, quartz–albite–chlorite–actinolite–epidote–sphene and quartz–albite–chlorite–epidote–sphene, are typical products of the greenschist facies alteration of basic igneous rocks. Alteration has mainly involved hydration of the parent rocks. The development of widespread mono-, bi-, and polymineralic veins and segregations was also undoubtedly aided by abundant hydrous fluids. Although calcite is present in some rocks, it occurs only in veins formed during or after zeolitic alteration, and the greenschist episode fluids probably contained little CO_2.

All of the greenschist phases are stable over a wide pressure interval. Only the temperature of alteration can be estimated. Replacement of calcium-bearing plagioclase by albite rather than analcime suggests temperatures exceeded 200°C (Liou 1971a). Epidote normally occurs in geothermal systems at temperatures in excess of 230°C (Muffler & White 1969; Browne & Ellis 1970; Tomasson & Kristmannsdottir 1972), although epidote in basaltic rocks from the hydrothermal system at Reykajavik is believed to have formed at temperatures as low as 135°C (Sigvaldason 1963). Keith *et al* (1968) recorded the assemblage quartz–tremolite–epidote at about 320°C in the Salton Sea geothermal system, and Browne (1969) found an amphibole he tentatively suggested was tremolite in the Broadlands field at about 275°C. The absence of prehnite and pumpellyite may be indicative of temperatures in excess of 350°C, according to the analysis of Nitsch (1971). A tentative minimum temperature of 320–350°C is thus suggested for the greenschist facies alteration.

Zeolitic alteration

The formation of zeolites and calcite are grouped together as products of zeolitic alteration, although the status of the latter phase is unclear. Calcite veins frequently cut zeolite-bearing ones, and textural relationships in calcite–zeolite veins and segregations often suggest that calcite is replacing zeolite. Thus, the crystallisation of calcite may have resulted from a third separate alteration episode, or may have occurred at a late stage during zeolitic alteration, attendant upon an increase in the mole proportions of CO_2 in the vein fluid.

Phases formed during this alteration episode are described below:

STILBITE is the most abundant zeolite and occurs both in veins and amygdules and in the fabric of the rocks. Refractive indices vary, suggesting some compositional variation (α 1·479–1·486, γ 1·487–1·497). Associated minerals are analcime, epistilbite, thomsonite, natrolite, and calcite.

ANALCIME is a common phase in amygdules and veins, and replaces earlier minerals, especially calcic plagioclase. It frequently shows low birefringence and repeated lamellar twinning. Refractive index is relatively constant (n 1·486–1·488). Associated minerals are stilbite, thomsonite, gonnardite, and calcite.

THOMSONITE is a minor, but widespread, phase. It has been found together with stilbite, analcime, gonnardite, and calcite.

GONNARDITE has been tentatively identified in specimen 9098 as a low-birefringent fibrous zeolite (α 1·499, γ 1·503) associated with analcime and thomsonite. Insufficient material was available for X-ray diffraction study.

?EPISTILBITE has been identified only from the Waipahirere mass, where an inclusion-charged zeolite replacing quartz in amygdules yields X-ray diffraction patterns appropriate to this phase. Optical properties generally support the identification, although the bifringence (α 1·492, γ 1·495) is lower than typical of epistilbite (Deer *et al* 1963, p. 377). Epistilbite is associated with heulandite–clinoptilolite and stilbite.

HEULANDITE–CLINOPTILOLITE. A zeolite yielding a diffraction pattern similar to that tabulated by Mumpton (1960) for clinoptilolite occurs occasionally in both the Te Rake and Waipahirere masses. Refractive indices (α 1·490, β 1·491, γ 1·495) are higher than those for typical clinoptilolite, and the mineral is probably an intermediate member of the heulandite–clinoptilolite series (Boles 1972). It is found associated with analcime, epistilbite, and calcite.

NATROLITE, found at only one locality, is intergrown with stilbite.

LAUMONTITE cements brecciated igneous material in both masses; it is not associated with other zeolites. Refractive indices show a small range (α 1·506–1·510, β 1·517–1·518, γ 1·519–1·521).

GREEN PHYLLOSILICATES. Moderately birefringent green and green-brown phyllosilicates are associated with other zeolitic phases, and have partially replaced ferromagnesium silicates. They have not been conclusively identified, but probably include oxidised chlorite and celadonite.

CALCITE is probably the most widespread and common secondary mineral in the Whangakea Basalt. It is found in amygdules and veins and in the fabric of the rocks replacing almost all other phases. Refractive indices indicate a composition close to pure $CaCO_3$.

Physical conditions of the zeolitic alteration are difficult to establish. Experimental data for the reaction analcime+quartz=albite are not applicable, for quartz is not a stable phase in analcime-bearing assemblages, and in silica-deficient environments analcime may exist stably to 600°C (Liou 1971a). Widespread stilbite indicates that temperatures of 165–180°C were generally not attained, for in this range stilbite dehydrates to laumontite plus quartz and water (Liou 1971b). Laumontite in the Whangakea Basalt is not associated with quartz, and the crystallisation of this phase or stilbite was probably conditioned by the activity of silica in the fluid phase present during alteration. Although these fluids appear to have been undersaturated in silica, as indicated by the instability of quartz, the presence of thomsonite, formation of which is favoured by a silica-deficient environment, and stilbite, epistilbite, and heulandite–clinoptilolite, which commonly occur associated with quartz (Coombs *et al* 1959), suggests variations in silica activity. Neither epistilbite nor heulandite–clinoptilolite have been found associated with thomsonite in the Whangakea Basalt.

Few data are available to set a minimum temperature for zeolitic alteration. The zeolite distributions found by Walker (1960a; b), in which intensity of zeolitisation decreases towards the top of thick lava piles, indicate that some elevation of temperature is necessary for the widespread development of these minerals in basaltic rocks. The distribution of laumontite in thick stratified sequences and geothermal drill holes suggests this phase forms only at temperatures above those at the Earth's surface or corresponding to shallow burial (Hay 1966).

Evidence outlined in the next section suggests that zeolitic alteration may have occurred subsequent to the Early Miocene. The lithostatic load on now-exposed Whangakea Basalt at this time is unlikely to have exceeded 0·8 kb, assuming an average density of 2·7 g/cm³ for the overlying strata.

DISCUSSION

The restricted extent of the greenschist metamorphism, the absence of a tectonic fabric, and the commonly pseudomorphous habit of secondary minerals, suggest the greenschist facies assemblages were produced by hydrothermal metamorphism in a region of highly variable heat flux. Secondary mineral assemblages very similar to those in the Whangakea Basalt have been reported from geothermal fields in California (Keith *et al* 1968) and Iceland (Sigvaldason 1963). Identical assemblages to those produced by the greenschist alteration have been recorded in rocks from the Mid-Atlantic Ridge and spreading ridges in the Indian Ocean (Bonatti *et al.* 1971; Aumento *et al.* 1971; Cann 1969; Melson & van Andel 1966). The latter are considered the result of hydrothermal alteration under a high geothermal gradient (Spooner & Fyfe 1973; Cann 1974).

Immediately east of the Waipahirere mass a gabbro–peridotite body shows a sequence from serpentinised peridotite, through layered gabbro and peridotite, to gabbro and, in its uppermost levels, sheeted dykes (Leitch 1970). This body closely resembles the well-documented Tethyan ophiolites and, although it is now in fault with Whangakea Basalt, these latter rocks would complete an ophiolite sequence (Bennett 1976). Bennett suggested that alteration of the ultramafic–mafic complex might have resulted from ocean-floor metamorphism, and drew attention to the possibility that this alteration continued up into the Whangakea Basalt. This interpretation accords with the prevalent opinion on the origin of ophiolites and is supported by the similarity of the greenschist facies assemblages to those in ocean-floor basalts and in the Lower Pillow Lavas of the Troodos Massif (Gass & Smewing 1973). However, interpretation of the Whangakea Basalt and associated mafic and ultramafic rocks as the products of early island arc magmatic activity is not precluded by the presence of hydrothermal metamorphism. Indeed, such alteration would proceed in any pervious igneous pile erupted in a marine environment, provided a heat flux sufficient to initiate and maintain convective circulation existed.

Zeolite assemblages similar to those in the Whangakea Basalt occur in basic rocks dredged from the ocean floor (Miyashiro *et al.* 1971; Aumento *et al.* 1971). It is tempting to seek the origin of the zeolitic alteration in the same hydrothermal system, with these phases forming first in the upper levels of the accreting igneous pile, and migrating deeper as the heat flux decreased. However, both analcime and laumontite occur in Miocene rocks close to the Te Rake mass, laumontite in laumontite–calcite–pyrite veins in a small microdiorite body, and analcime replacing clastic plagioclase in Lower Miocene rocks close to the edge of a similar microdiorite dyke. The zeolites may thus be the products of local phenomena arising from the cooling of the microdiorite intrusions, or alternatively may be the result of burial of the Whangakea Basalt beneath some 3000 m of sedimentary rocks in the Miocene (Leitch 1970).

CONCLUSIONS

1. The Whangakea Basalt has been affected by two episodes of alteration, the earlier producing mineral assemblages of the greenschist facies and the latter mainly zeolites and calcite.

2. Greenschist alteration occurred in a water-saturated environment at a minimum temperature of 320–350°C.

3. Zeolitic alteration took place at a temperature below 165–180°C. The accompanying fluid was undersaturated with silica, although variations occurred in the chemical potential of silica in the fluid. The mole proportion of CO_2 in the fluid remained low until towards the end of alteration.

ACKNOWLEDGMENTS

This study commenced in the Department of Geology, University of Auckland under the guidance and encouragement of Professor R. N. Brothers, to whom I am much indebted. The study continued in the Department of Geology and Geophysics, University of Sydney, and was written up during a stay in the Department of Geology, University of Cambridge. I acknowledge the use of facilities at all these institutions.

I thank Dr P. M. Black, who provided much help with X-ray diffraction; Dr D. O. Zimmerman, who aided in the identification of opaque minerals; and Dr J. R. Cann for constructive criticism of a draft of the paper.

My investigation of low-grade metamorphic rocks is supported by funds provided by the Australian Research Grants Committee.

REFERENCES

AUMENTO, F.; LONGAREVIC, B. D.; ROSS, D. I. 1971: Hudson geotraverse: geology of the Mid-Atlantic Ridge at 45°N. *Philosophical Transactions of the Royal Society, London, Series A 268*: 623–50.

BENNETT, M. C. 1976: The ultramafic-mafic complex at North Cape, northernmost New Zealand. *Geological Magazine 113*: 61–7.

BOLES, J. R. 1972: Composition, optical properties, cell dimensions and thermal stability of some heulandite group zeolites. *American Mineralogist 57*: 1463–93.

BONATTI, E.; HONNOREZ, J.; FERRARA, G. 1971: Peridotite–gabbro–basalt complex from the equatorial Mid-Atlantic Ridge. *Philosophical Transactions of the Royal Society, London. Series A, 268*: 385–402.

BROWNE, P. R. L. 1969: Sulfide mineralisation in a Broadlands geothermal drillhole, Taupo Volcanic Zone, New Zealand. *Economic Geology 64*: 156–9.

BROWNE, P. R. L.; ELLIS, A. J. 1970: The Ohaki–Broadlands hydrothermal area, New Zealand: mineralogy and related geochemistry. *American Journal of Science 269*: 97–131.

CANN, J. R. 1969: Spilites from the Carlsberg Ridge, Indian Ocean. *Journal of Petrology 10*: 1–19.

——— 1974: A model for oceanic crustal structure developed. *Geophysical Journal of the Royal Astronomical Society 39*: 169–87.

COOMBS, D. S.; ELLIS, A. J.; FYFE, W. S.; TAYLOR, A. M. 1959: The zeolite facies with comments on hydrothermal synthesis. *Geochimica et Cosmochimica 19*: 53–107.

DEER, W. A.; HOWIE, R. A.; ZUSSMAN, J. 1963: "Rock-forming minerals". Vol. 3. John Wiley & Sons, New York.

GASS, I. G.; SMEWING, J. D. 1973: Intrusion, extrusion and metamorphism at constructive margins: evidence from the Troodos Massif, Cyprus. *Nature 242*: 26–9.

HAY, R. L. 1966: Zeolites and zeolitic reactions in sedimentary rocks. *Geological Society of America, Special Paper 85*: 1–130.

KEITH, T. E. C.; MUFFLER, L. J. P.; CREMER, M. 1968: Hydrothermal epidote formed in the Salton Sea geothermal system, California. *American Mineralogist 53*: 1635–44.

LEITCH, E. C. 1970: Contributions to the geology of northernmost New Zealand: II—The stratigraphy of the North Cape district. *Transactions of the Royal Society of N.Z., Earth Sciences 8*: 45–68.

LIOU, J. G. 1971a: Stilbite-laumontite equilibrium. *Contributions to Mineralogy and Petrology 31*: 171–7.

——— 1971b: Analcime equilibria. *Lithos 4*: 389–402.

MELSON, W. G.; VAN ANDEL, TJ. H. 1966: Metamorphism in the Mid-Atlantic Ridge, 22°N latitude. *Marine Geology 4*: 165–86.

MIYASHIRO, A.; SHIDO, F.; EWING, M. 1971: Metamorphism in the Mid-Atlantic Ridge near 24° and 30° N. *Philosophical Transactions of the Royal Society, London, Series A, 268*: 589–603.

MUFFLER, L. J. P.; WHITE, D. E. 1969: Active metamorphism of Upper Cenozoic sediments in the Salton Sea geothermal field and the Salton Trough, Southeastern California. *Geological Society of America Bulletin 80*: 157–82.

MUMPTON, F. A. 1960: Clinoptilolite redefined. *American Mineralogist 45*: 351–69.

NITSCH, K. H. 1971: Stabilitätsbeziehungen von Prehnit und Pumpellyite—haltigen Paragenesen. *Contributions to Mineralogy and Petrology 30*: 240–60.

SIGVALDASON, G. E. 1963: Epidote and related minerals in two deep geothermal drillholes, Reykajavik and Hveragerdi, Iceland. *U.S. Geological Survey Professional Paper 450-E*: E77–9.

SLEMMONS, D. B. 1962: Determination of volcanic and plutonic plagioclases using a three-or-four-axis universal stage. *Geological Society of America, Special Paper 69*: 1–64.

SPOONER, E. T. C.; FYFE, W. S. 1973: Sub-sea-floor metamorphism, heat and mass transfer. *Contributions to Mineralogy and Petrology 42*: 287–304.

TOMASSON, J.; KRISTMANNSDOTTIR, H. 1972: High temperature alteration minerals and thermal brines, Reykjanes, Iceland. *Contributions to Mineralogy and Petrology 36*: 123–34.

WALKER, G. P. L. 1960a: Zeolite zones and dike distribution in relation to the structure of the basalts of eastern Iceland. *Journal of Geology 68*: 515–28.

——— 1960b: The amygdale minerals in the Tertiary lavas of Ireland. III. Regional distribution. *Mineralogical Magazine 32*: 503–27.

Geochimica et Cosmochimica Acta, 1977, Vol. 41, pp. 143 to 150. Pergamon Press. Printed in Great Britain

Experimental hot water–rock interactions and their significance to natural hydrothermal systems in New Zealand

G. R. EWERS*

Department of Geology, University of Melbourne, Parkville, Australia

(*Received* 14 *April* 1976; *accepted in revised form* 15 *July* 1976)

Abstract—A study has been made of the interaction of a New Zealand greywacke and hot water at temperatures up to 500°C. Comparisons are drawn between the trace element content of the reaction solutions and the composition of New Zealand thermal waters with particular reference to the Broadlands geothermal field.

The experiments have demonstrated that hot water can extract significant quantities of As, Sb, Se and S at temperatures below the maximum temperatures recorded for the major geothermal fields in New Zealand.

The amount of Tl and Co leached up to 500°C was below the limits of detection and data could not be obtained for Au, Ag, Te and Bi.

INTRODUCTION

ELLIS and MAHON (1964, 1967), ELLIS (1968) and MAHON (1967) investigated the compositions of solutions obtained from hot water–rock interactions. They described experiments in which volcanic and sedimentary rocks common to the Taupo Volcanic Zone in the North Island of New Zealand, were reacted with water at temperatures varying from 100 to 600°C and pressures ranging from 500 to 1500 bars. They demonstrated that appreciable quantities of constituents such as K, Na, Li, Rb, Ca, Mg, SiO_2, Cl, F, B and NH_3 were readily taken into solution along with trace amounts of Fe, Mn, Cu and Pb. Their studies indicated that the compositions of waters in natural hydrothermal systems could be approached by the interaction of hot water and rock, without requiring a contribution from a magmatic fluid rich in these elements. CRAIG (1965) concluded from isotopic investigations that geothermal waters are generally meteoric and in this regard New Zealand geothermal waters appear to be no exception (GIGGENBACH, 1971; GRINDLEY, 1965).

In the present study, a series of hot water–rock leaching, experiments were undertaken to ascertain whether trace elements not previously investigated were readily available for solution at temperatures and pressures likely to be encountered in natural hydrothermal systems.

EXPERIMENTAL TECHNIQUES

(a) *Procedure*

All reactions were conducted in sealed, high purity silica ampoules at temperatures up to 500°C. The rock fragments (0.4–0.7 mm, about 210 mg) were contained in a perforated gold capsule crimped almost closed at each end. The charge was loaded into a silica tube (10 mm o.d., 7 mm i.d.) sealed at one end and a slight constriction was made about 4 cm from that end. After streaming high purity dry N_2 through the tube for 15 min to expel as much air as possible, 1.4 ml of distilled water (previously boiled to remove dissolved CO_2) were pipetted into the tube and the streaming of N_2 was continued. After the contents of the tube had been frozen in a dry ice–alcohol bath, the tube was then sealed about 4 cm above the constriction to give an 8 cm long ampoule.

The ampoule was loaded into a stainless steel pressure vessel which was suspended vertically inside a tube furnace. Water was added to the pressure vessel to balance the pressures generated within the ampoule. Pressure vessel temperatures were measured twice daily using chromel–alumel thermocouples connected to a potentiometer. Variations were controlled within ± 3°C.

The volume of liquid contained in each ampoule was sufficient to maintain a two-phase system up to the critical point of water (374°C). Hence pressures could be accurately determined from tables of the vapour pressure of water. Above the critical point (to 500°C) pressures were calculated less accurately using the Law of Corresponding States (KAUZMANN, 1966).

On the completion of an experiment, the furnace was tilted and the pressure vessel and its contents withdrawn in an inverted position. In the process the solution ran through the constriction, thus becoming isolated from the rock fragments, preventing any back reaction during cooling. The ampoule was removed and its contents frozen with a dry ice–alcohol bath prior to being broken open. The gold capsule and its contents were recovered and the solution retained for analysis if required. The gold capsule was forced open at each end and the rock fragments were flushed on to a watch glass with distilled water. After several washings, the fragments were air dried and retained for analysis.

(b) *Analytical methods*

Analyses were carried out using neutron activation analysis. A flow chart outlining the procedure used to determine As, Sb, Tl, Bi, Se, Te and Co is given in Fig. 1. The Bi and Tl methods were developed by HUGHES (1976), while the Se and Te methods were adapted from

* Present address: Bureau of Mineral Resources, P.O. Box 378, Canberra City, A.C.T. 2601, Australia.

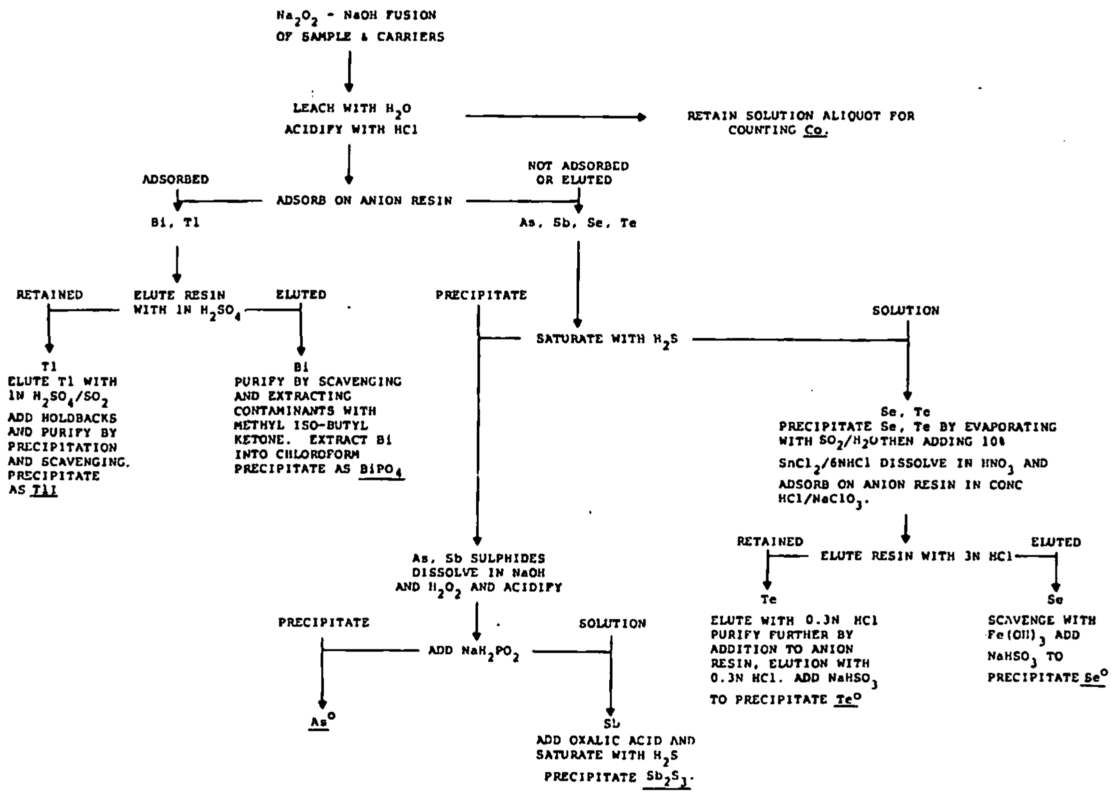

Fig. 1. Flow chart of analytical scheme used for As, Sb, Se, Te, Bi, Tl and Co.

those of MORRIS and KILLICK (1963). The methods used for As and Sb draw substantially from the work of FOUCHÉ and SMALES (1967) and HAMAGUCHI *et al.* (1969). Au and Ag were determined by a procedure modified after that of Keays *et al.* (1974). Samples and standards were irradiated for 6 days in a thermal neutron flux of 6×10^{12} neutrons/cm^2/sec and cooled for 3 days before processing. Bi and Tl were counted on a Beckman Widebeta detector and the remaining elements were γ-counted on a 45 cm^3 Canberra Industries Ge(Li) detector. Sulphur determinations were made with a Leco automatic sulphur titrator (model 532).

Table 1. Analyses for U.S.G.S. standards, DTS-1 and BCR-1

ELEMENT	DTS-1	BCR-1
Ag (ppm)	0.043, 0.059	0.031, 0.032
As (ppm)	0.036, 0.026	0.55, 0.53
Au (ppb)	0.75, 0.73	0.66
Bi (ppm)	< 0.010, < 0.010	0.050, 0.048
Co (ppm)	159, 153 154, 147	41.8, 41.1 40.5, 38.9
Sb (ppm)	0.64, 0.53	0.76, 0.76
Se (ppm)	< 0.005, < 0.005	0.082, 0.084
Te (ppm)	< 0.05, < 0.05	< 0.05, < 0.05
Tl (ppm)	0.003, 0.002	0.285, 0.280

The analytical methods have been assessed by analysing the U.S.G.S. standards BCR-1 and DTS-1. The values obtained are quoted in Table 1 and are consistent with the published data in FLANAGAN (1969) and LAUL *et al.* (1970a, b, c).

Analyses were made on the rock fragments before and after leaching rather than the leaching solutions for several reasons. It was considered that with the anticipated low trace element concentrations in the solutions, the presence of some fine suspended material might have contributed significantly to these values giving erroneous results. It was also not possible to irradiate liquids in the reactor HIFAR and the risks of losses through volatilization and contamination when evaporating the liquid on to powdered silica for irradiation were considered to be too great. The rock fragments recovered from each experiment were divided into two approximately equal portions for duplicate analyses.

SELECTION OF ROCK TYPE

For the following reasons, a greywacke was chosen as the most suitable starting material. First, Mesozoic greywackes and argillites are likely source rocks for metals found in New Zealand geothermal waters since they flank both sides of the Taupo Volcanic Zone and are thought to underlie it extensively. Second, analyses for a selection of greywackes, argillites and acid volcanics (seemingly unaffected by hydrothermal fluids and collected from various localities in the North Island of New Zealand) indicated that those elements being considered were more abundant in the sediments (EWERS, 1975). Although the greywackes

Table 2. Analyses for unaltered greywacke, P 23556

	As (ppm)	Sb (ppb)	Tl (ppb)	Bi (ppb)	Se (ppb)	Te (ppb)	Au (ppb)	Ag (ppb)	Co (ppm)	S (ppm)
	8.02	320	395	170	66	n.f.	1.97	< 20	5.99	490
	10.54	300	420	190	66	n.f.	2.46	22	7.26	510
	9.95	280	380	220	74	n.f.	-	-	7.17	480
	9.85	330	420	130	72	n.f.	1.63	< 20	6.10	500
AVERAGE	9.59	310	405	177	70	-	2.02	< 20	6.63	495
STANDARD DEVIATION	1.09	22	20	66	4	-	0.42	-	0.68	13
% STANDARD DEVIATION	11.4%	7.1%	4.9%	37.3%	5.7%	-	20.8%	-	10.3%	2.6%

n.f. = not found.

and argillites in the North Island have been divided into three distinct lithological groups, depending upon their provenance (EWART and STIPP, 1968), the trace element concentrations were similar in the two types most intimately associated with the geothermal areas (i.e. greywackes of andesitic and granitic derivation).

The greywacke selected (P 23556) came from an outcrop about 70 km south of Lake Taupo and according to EWART and STIPP (1968) was derived from a granitic plutonic terraine. It was a coherent, fine-grained rock with a uniform texture and was composed of angular to sub-rounded quartz fragments, acidic plagioclase, alkali feldspar, muscovite, iron oxides, minor biotite and some secondary chlorite. Calcite veining was also quite common. In polished thin section, a number of small rounded pyrite grains were found to be randomly distributed throughout the rock.

RESULTS

To establish the elemental concentrations in P 23556 with more precision, the rock fragments used in the leaching experiments were analysed in quadruplicate and the results are presented in Table 2. Included in the table are average concentrations, standard deviations and percentage standard deviations for each element. While the As, Sb, Tl, Se, S and Co analyses for each sample deviate little from the mean, the Bi and Au analyses have a wider spread and consequently much larger standard deviations. The Ag and Te contents are generally below the limits of detection. Since leaching was anticipated to be minor for low temperature experiments, the standard deviations for Bi and Au were considered to be too large and might have obscured whether leaching had in fact occurred. For these reasons only the elements As, Sb, Tl, Se, Co and S are dealt with further.

Table 3. Experimental and analytical data for hydrothermally leached greywacke, P 23556

RUN NUMBER	TIME (hours)	TEMPERATURE (°C)	PRESSURE (bars)	H_2S ODOUR	As (ppm)	Sb (ppb)	Tl (ppb)	Se (ppb)	Co (ppm)
					3.49	120	430	53	6.17
1	53	487	770 $\pm$ 100	STRONG	3.27	115	460	56	6.86
					9.35	170	450	66	
2	23	152	6.5 $\pm$ 0.5	-	8.12	185	390	62	n.d.
					9.35	190	420	71	
3	48	153	6.5 $\pm$ 0.5	-	9.68	200	440	73	n.d.
					8.38	160	410	74	
4	95	151	6.5 $\pm$ 0.5	-	7.40	180	415	61	n.d.
					7.92	180	470	60	
5	449	151	6.5 $\pm$ 0.5	-	9.99	205	460	69	n.d.
					7.00	115	400	51	7.28
6	24	343	154 $\pm$ 2	SLIGHT	7.12	115	440	61	6.97
					7.05	110	395	58	6.59
7	42	342	152 $\pm$ 2	SLIGHT	7.16	140	450	71	6.80
					6.02	90	395	69	7.68
8	114	347	162 $\pm$ 2	SLIGHT	8.70	95	405	63	9.13
					6.61	90	410	64	7.63
9	278	346	160 $\pm$ 2	SLIGHT	6.63	105	400	59	7.61
					10.31	230	435	61	7.08
10	72	106	2.5 $\pm$ 0.5	-	9.00	260	390	68	6.31
					8.32	185	350	71	6.28
11	72	196	16 $\pm$ 0.5	-	9.99	190	395	59	6.88
					7.12	140	390	60	6.63
12	72	288	74 $\pm$ 1	SLIGHT	6.78	130	395	58	6.34
					4.38	115	400	56	6.20
13	72	387	440 $\pm$ 80	STRONG	6.21	85	345	52	6.99
					3.15	100	360	30	6.83
14	72	484	780 $\pm$ 100	STRONG	2.41	120	390	40	5.98
AVERAGE CONCENTRATION IN UNREACTED GREYWACKE					9.59	310	405	70	6.63

n.d. = not determined.

Table 4. Experimental data and sulphur analyses for hydrothermally leached, greywacke, P 23556

RUN NUMBER	TIME (hours)	TEMPERATURE (°C)	PRESSURE (bars)	H_2S ODOUR	S (ppm)
15	48	142	5.5 ± 0.5	-	370 460
16	48	295	82 ± 1	SLIGHT	230 340
17	48	510	830 ± 100	STRONG	110 210

Table 3 summarizes the run data and analytical results for As, Sb, Tl, Se and Co after leaching for periods of up to 449 hr and temperatures in the range 100–484°C. Since only small quantities of the rock fragments could be leached at one time, there was insufficient sample to analyse for these elements and S simultaneously. Consequently, a number of experiments were repeated for the S determinations, the results of which are given in Table 4.

Having ascertained in the first run that hot water at a temperature of 467°C was capable of leaching at least some of the elements (i.e. As, Sb and Se) within 53 hr, a series of runs was conducted at constant temperatures to establish the minimum time for optimum leaching. The first series of runs (nos. 2–5) was carried out at about 150°C with times varying from 23 to 449 hr and indicated that Sb was the only element to be significantly leached. For each run, the concentration of Sb in the rock fragments was consistently depleted by about 130 ppb (approximately 40%). The results of a second series of experiments at about 350°C (run nos. 6–9), where the duration of each run varied from 24 to 278 hr, have been presented diagrammatically in Fig. 2. Although As, Sb and possibly Se (percentage leaching generally $<10\%$) were the only elements leached at this temperature, it would appear that they were substantially taken into solution in less than 24 hr.

In the remaining experiments (run nos. 10–14) the duration of each run was kept constant at 72 hr while the temperatures were increased from 100 to 500°C in 100°C intervals. The results of these experiments have been summarized in Fig. 3. Also included in this diagram are the results for S determinations on the leached rock fragments from a series of 48 hr experiments (run nos. 15–17). The data indicates that while As, Sb, Se and S are appreciably leached at temperatures up to 500°C, there is no perceptible depletion in the Tl or Co contents of the rock fragments.

Examination of polished thin sections of rock fragments that had been leached showed there were no signs of alteration at temperatures up to 200°C. However, above 200°C, it was evident that the fragments were more heavily stained with iron oxides, due probably to slight oxidation of the matrix and the breakdown of pyrite. On breaking open the ampoules used in experiments above 200°C, the smell of H_2S was noticeable.

It was noted that the solutions recovered after leaching in the higher temperature experiments (>200°C) developed a gelatinous white precipitate on standing. This was later identified as amorphous silica. Since the silica ampoules showed signs of having been etched (especially at high temperatures), it was concluded that this was the main source of silica with some also being derived from the quartz in the greywacke. From data on the solubility of amorphous silica and quartz in water (KENNEDY, 1950), concentrations of up to 2000 ppm could be anticipated in the reaction solutions at 300°C.

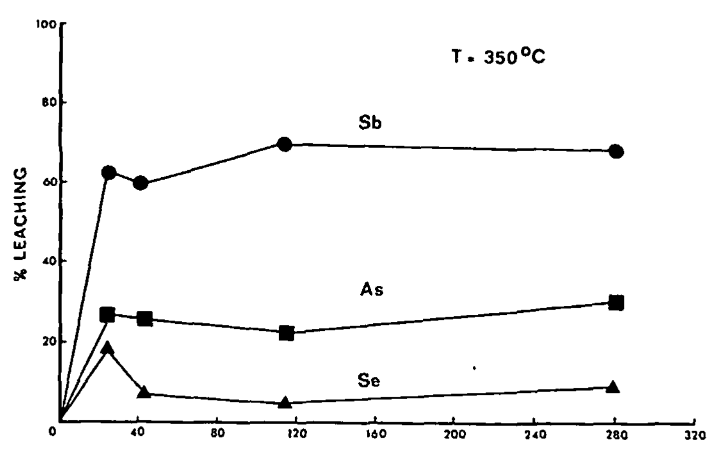

Fig. 2. Variation with time in the percentage of constituents leached from greywacke, P 23556.

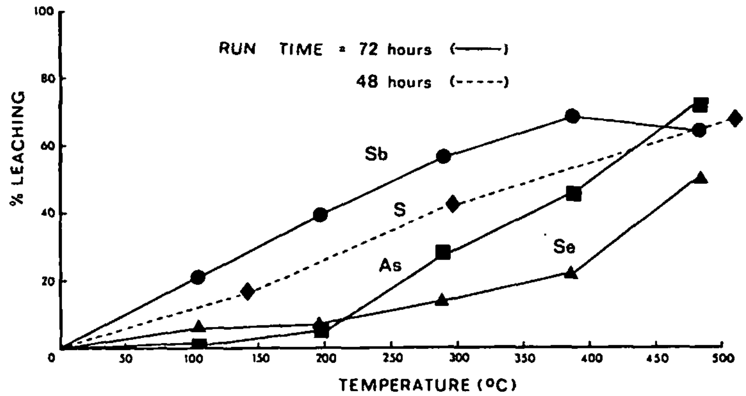

Fig. 3. Variation with temperature in the percentage of constituents leached from greywacke, P 23556.

Although no pH measurements were made on the reaction solutions, measurements by MAHON (1967) for solutions recovered after leaching greywackes with hot water indicate that they should be near neutral to slightly acid.

DISCUSSION

(a) *General considerations*

While the experimental data demonstrate that appreciable quantities of some elements were readily leached from the greywacke, the exact amounts are not of great significance. The ratios of rock to water in natural hydrothermal systems would be much higher than the 0.14 ratio used in the present experiments. ELLIS and MAHON (1964) have concluded from porosity measurements that ratios of ten to twelve appear reasonable for recent volcanic areas and these may be higher in sedimentary or metamorphic rocks. It follows that elemental concentrations in geothermal waters could be at least a factor of 70 higher than in the experimental solutions providing concentrations are not held at lower levels by solubility product relationships involving any of the elements. There is also the possibility that since the trace elements considered are not all extracted with the same ease (e.g. As and Sb in Fig. 3), then the trace element content of geothermal waters would probably show variations over the lifetime of the hydrothermal system. Although estimates have been made of the duration of hydrothermal activity in some New Zealand geothermal fields (GRINDLEY, 1965), there are no reliable estimates for the total volume of water which has passed through a given system or its rate of turnover. It could be expected that as the water in the system is recharged and recirculated, those rocks already leached would tend to release progressively lower amounts of the trace elements for solution. On the other hand, trace element concentrations could be maintained if fracturing (through fault movement) exposed fresh rocks for leaching, while pre-existing channelways were closed by mineral deposition.

It should also be emphasized that the reaction times for the experiments were very short in comparison to those available in natural systems. While significant concentrations of As, Sb, Se and S were released to the solutions in 72 hr at 300°C (Fig. 3), it is doubtful whether chemical equilibrium was established. With much longer reaction times and the opportunity for greater hydrothermal alteration an increased portion of those elements bound up in silicate and sulphide structures would probably be liberated.

(b) *Individual constituents*

Arsenic. It is evident from Fig. 3 that appreciable quantities of As were leached from the greywacke at temperatures greater than 250°C and that at about 480°C more than 70% or 7 ppm of the As was liberated to the solution. It is also apparent that the As was taken into solution rapidly (Fig. 2). These results supplement the data obtained by ELLIS and MAHON (1964), who observed that hot water contained trace amounts of As (< 1 ppm) after leaching acid volcanics for up to 480 hr at 300–350°C.

The results indicate that the source of As found in geothermal waters need not be magmatic as ONISHI and SANDELL (1955) have proposed. If the assumptions are made that (1) the As contents of natural waters are not depressed by either solubility product relationships or adsorption on to the surface of minerals (such as clays) and (2) the rock to water ratio is ten, then concentrations of 25–30 ppm As in the fluid phase could be anticipated for solutions at 300°C in contact with a greywacke (such as P 23556) containing 10 ppm As. Applying the same boundary conditions, ELLIS and MAHON (1964) have concluded that concentrations of at least 6–8 ppm As could be expected in thermal waters percolating through andesites or rhyolitic pumice. Since the drillhole waters in many New Zealand geothermal fields attain maximum temperatures approaching 300°C at depth and generally contain less than 6 ppm As (ELLIS and MAHON, 1964), the volcanics and sediments of the

Taupo Volcanic Zone may act as source materials.

The fact that appreciable quantities of As were not readily available for solution at <200°C may indicate that it is mainly contained within mineral lattices rather than being held adsorbed on to mineral surfaces within the greywacke. The leaching profiles for As and S (Fig. 3) indicate that the As is possibly being liberated from pyrite as it breaks down to release S.

Antimony. The form of the Sb leaching profile differs significantly from that of As (Fig. 3). At 100°C, about 20% of the Sb was in solution and at 200°C, 40% had been leached. In contrast, the As content of the greywacke had been depleted by less than 10% at 200°C. In addition to this, the percentage of Sb leached between 350 and 500°C remained reasonably constant, while the depletion of As over the same temperature interval almost doubled.

The explanation of these differences may lie in the availability of each element for extraction by water. Although it is likely that pyrite in the greywacke would contain Sb, it is also possible that some Sb may be present either in other submicroscopic sulphide phases (e.g. stibnite, tetrahedrite) or adsorbed on to crystal surfaces and the walls of microfissures. Low temperature leaching experiments of short duration would probably produce negligible hydrothermal alteration and liberate very little Sb from the pyrite. However, these reaction times and temperatures may be sufficient to readily dissolve more soluble Sb-bearing sulphides and/or any adsorbed Sb. Ellis and Mahon have concluded from their experimental studies that a proportion of constituents such as chloride, boric acid and ammonia is held adsorbed on surfaces in rocks and is readily available for solution by water. The importance of adsorption phenomena has also been verified by GONI and GUILLEMIN (1968) for a wide range of trace elements.

Calculations of the likely Sb contents of thermal waters, using the experimental leaching data and applying the same assumptions made for As, suggest that at 300°C the solutions in contact with the greywacke P 23556 would contain up to 2 ppm Sb. Higher Sb concentrations in solution could be anticipated, as some greywackes and acid volcanics analysed contained greater Sb concentrations than P 23556. However, since the rate at which Sb would be liberated from a rock depends on the way in which the Sb is held and the rate of reaction between the rock and the solution, no quantitative estimates can be made. It would appear though from the above calculation that with the Sb concentrations of the Broadlands waters no more than 2 ppm (WEISSBERG, 1969; BROWNE, 1971) and the Sb contents of New Zealand thermal waters generally less than 0.3 ppm (RITCHIE, 1961), the elements may originate from the sediments and acid volcanics of the Taupo Volcanic Zone through leaching.

Selenium. Only traces of Se were leached from the rock fragments up to 300°C. In view of the ability Se has to substitute for S in sulphides, there is a strong possibility that it is mainly contained in pyrite and that as the pyrite dissociates, Se is liberated to the solution.

Extrapolating the experimental data as before, it can be calculated that in a natural hydrothermal system at least 100 ppb Se could be released to a solution at 300°C in contact with this greywacke. Unfortunately, there are no data for the Se concentrations in thermal waters from which comparisons can be made. However, if Se is to be derived by leaching, the argillites and greywackes are more likely source rocks than the acid volcanics which generally contain less than 10 ppb Se (EWERS, 1975).

Sulphur. Insufficient S determinations were made on the leached samples to enable many conclusions to be drawn. Analyses for the New Zealand greywackes and argillites indicate that S concentrations are typically in the range 500–2500 ppm. GIGGENBACH (in preparation) has shown that this sulphur is a mixture of sulphide and sulphate, though it is present mainly as pyrite. The efficient extraction of S from P 23556 by hot water as leaching temperatures were increased (see Fig. 3), illustrates the potential for these sediments to act as source material.

ELLIS and MAHON (1964) have stated that sulphides in contact with hot water containing oxygen would hydrolyse to H_2S and then the latter would partly oxidize to sulphate. Although the present experiments were carried out in a nitrogen atmosphere and the distilled water was boiled, it is probable that some air trapped between rock fragments and along microfractures produced appreciable quantities of sulphate. This may explain why H_2S was not detected at 150°C even though almost 20% of the S in the greywacke had been leached.

Of further significance is the fact that the greywacke is a suitable source rock for As and Sb as well as S. Since it is known that As and Sb form very stable thio complexes (WEISSBERG *et al.*, 1966; BROOKINS, 1972; NORTON, 1964), the availability of S in a reduced form could play an important role in their transport.

Thallium. The fact that large amounts of Tl were not readily liberated on leaching suggests that Tl is incorporated into silicate lattices (substituting for K in K-feldspars and K-micas). With prolonged leaching (such as in natural hydrothermal systems) these silicates would alter and small quantities of Tl would be released for solution. However, under the experimental conditions, reaction times were too short for silicate alteration to take place. If Tl were in the pyrite or adsorbed on to crystal surfaces, some leaching should have occurred below 500°C as was the case for As, Sb, Se and S.

Although the data suggest that Tl was not leached to a significant extent from the greywacke up to 500°C, it would be inappropriate to assume that some other source must therefore be invoked. Analyses for Broadlands drillhole waters indicate that Tl concentrations are less than 10 ppb (WEISSBERG, 1969; BROWNE, 1971). For these concentrations to be obtained by the interaction of greywacke P 23556 with hot water (assuming a rock to water ratio of ten) less than 1% leaching would be required. Obviously, at such low levels of leaching, the precision of the analytical technique and variations in the Tl content of the starting materials would make it difficult to establish whether leaching had occurred.

Cobalt. The absence of significant Co leaching was perhaps surprising in view of the probable high Co content of the pyrite in the greywacke. It might be expected that as the pyrite breaks down, Co would be released to the solution. The fact that this was not the case suggests that most of the Co is either incorporated in the lattices of the new hydrothermal minerals (e.g. iron oxides) or retained in the unaltered Fe-bearing silicates (such as biotite) and is not readily available for solution.

Gold, silver, bismuth and tellurium. For reasons already stated, leaching data was not obtained for these elements. However, for a rock to water ratio of ten, only minor leaching would be necessary to produce the low concentrations of these elements found in the Broadlands waters [Au 0.1–1 ppb, Ag 2 ppb and Bi 0.3 ppb, according to BROWNE (1969)]. WEISSBERG (1969) has shown that waters from the Broadlands drillhole, BR 2 contain only 0.04 ppb Au and 0.6 ppb Ag, even though discharge precipitates with 55 ppm Au and 200 ppm Ag are forming from them. Data collected by GOTTFRIED *et al.* (1972) have indicated that the thermal waters of Yellowstone National Park generally contain 0.004–0.04 ppb Au, though the sinters deposited from them contain up to 5 ppm Au. They have concluded that above average Au concentrations in the country rocks are not required for them to serve as a possible source for the Au.

Acknowledgements—The author wishes to acknowledge the many helpful discussions with Dr. R. R. KEAYS, Dr. W. NESBITT and Mr. S. E. SMITH; also the assistance of Dr. P. R. L. BROWNE and the New Zealand Geological Survey in supplying suitable source rock material, and the comments of Dr. A. J. ELLIS and Dr. A. EWART in reviewing the manuscript. Thanks are due to Professor J. F. LOVERING of the Department of Geology at the University of Melbourne for permission to use departmental facilities. Financial assistance throughout this work in the form of a University of Melbourne Research Grant followed by a Commonwealth Postgraduate Research Award was greatly appreciated. The research was also funded, in part, by grants to R.R.K. from the Australian Institute of Nuclear Science and Engineering and the Australian Research Grants Committee.

REFERENCES

BROOKINS D. G. (1972) Stability of stibnite, metastibnite, and some probable dissolved antimony species at 298.15°K and 1 atmosphere. *Econ. Geol.* **67**, 369–372.

BROWNE P. R. L. (1969) Sulphide mineralization in a Broadlands geothermal drillhole, Taupo Volcanic Zone, New Zealand. *Econ. Geol.* **64**, 156–159.

BROWNE, P. R. L. (1971) Mineralization in the Broadlands geothermal field, Taupo Volcanic Zone, New Zealand. *Soc. Mining Geol. Japan, Spec. Issue* **2**, 64–75.

CRAIG H. (1965) The isotopic geochemistry of water and carbon in geothermal areas. In *Nuclear Geology on Geothermal Areas*, (editor E. Tongiorgi), pp. 17–53.

ELLIS, A. J. and MAHON W. A. J. (1964) Natural hydrothermal systems and experimental hot water/rock interactions. *Geochim. Cosmochim. Acta* **28**, 1323–1357.

ELLIS A. J. and MAHON W. A. J. (1967) Natural hydrothermal systems and experimental hot water/rock interactions (Part II). *Geochim. Cosmochim. Acta* **31**, 519–538.

ELLIS A. J. (1968) Natural hydrothermal systems and experimental hot water/rock interaction: reactions with NaCl solutions and trace metal extraction. *Geochim. Cosmochim. Acta* **32**, 1356–1363.

EWART A. and STIPP J. J. (1968) Petrogenesis of the volcanic rocks of the Central North Island, New Zealand, as indicated by a study of Sr^{87}/Sr^{86} ratios and Sr, Rb, K, U and Th abundances. *Geochim. Cosmochim. Acta* **32**, 699–735.

EWERS G. R. (1975) Volatile and precious metal zoning in the Broadlands geothermal field, New Zealand. Ph.D. thesis, University of Melbourne.

FLANAGAN F. J. (1969) U.S. Geological Survey standards—II. First compilation of data for the new U.S.G.S. rocks. *Geochim. Cosmochim. Acta* **33**, 81–120.

FOUCHÉ K. J. and SMALES A. A. (1967) The distribution of trace elements in chondritic meteorites. 2. Antimony, arsenic, gold, palladium and rhenium. *Chem. Geol.* **2**, 105–134.

GONI J. and GUILLEMIN C. (1968) L'importance géochimique des éléments fissuraux dans l'étude du bilan et de la mobilité des éléments en traces. In *Origin and Distribution of the Elements*, (editor L. H. Ahrens), pp. 1093–1112. Pergamon Press.

GIGGENBACH W. (1971) Isotopic composition of waters of the Broadlands geothermal field. *N.Z. J. Sci.* **14**, 959–970.

GIGGENBACH W. (in preparation) The isotopic composition of sulphur in sedimentary rocks bordering the Taupo Volcanic Zone.

GOTTFRIED D., ROWE J. J. and TILLING R. I. (1972) Distribution of gold in igneous rocks. *U.S. Geol. Surv. Prof. Paper*, **727**.

GRINDLEY G. W. (1965) The geology, structure and exploitation of the Wairakei geothermal field, Taupo New Zealand. *N.Z. Geol. Surv. Bull.* **75**.

HAMAGUCHI H., ONUMA N., HIRAO Y., YOKOYAMA H., BANDO S. and FURUKAWA M. (1969) The abundances of arsenic, tin and antimony in chondritic meteorites. *Geochim. Cosmochim. Acta* **33**, 507–518.

HUGHES T. C. (1976) The geochemistry of S, Se, Te, Hg, Tl and Bi—their determination by thermal neutron activation analysis and their geochemical significance. Ph.D. thesis, University of Melbourne.

KAUZMANN W. (1966) *Kinetic Theory of Gases*. Benjamin.

KEAYS R. R., GANAPATHY R., LAUL J. C., KRÄHENBÜHL U. and MORGAN J. W. (1974) The simultaneous determination of 20 trace elements in terrestrial, lunar and meteoric material by radiochemical neutron activation analysis. *Anal. Chim. Acta* **72**, 1–29.

KENNEDY G. C. (1950) A portion of the system silica–water. *Econ. Geol.* **45**, 629–653.

LAUL J. C., CASE D. R., WECHTER M., SCHMIDT-BLEEK F. and LIPSCHUTZ M. E. (1970a) An activation analysis technique for determining groups of trace elements in rocks and chondrites. *J. Radioanal. Chem.* **4**, 241–264.

LAUL J. C., CASE D. R., SCHMIDT-BLEEK F. and LIPSCHUTZ M. E. (1970b) Bismuth contents of chondrites. *Geochim. Cosmochim. Acta* **34**, 89–103.

LAUL J. C., PELLY I. and LIPSCHUTZ M. E. (1970c) Thallium contents of chondrites. *Geochim. Cosmochim. Acta* **34**, 909–920.

MAHON W. A. J. (1967) Natural hydrothermal systems and the reaction of hot water with sedimentary rocks. *N.Z. J. Sci.* **10**, 206–221.

MORRIS D. F. C. and KILLICK R. A. (1963) The determination of traces of selenium and tellurium in samples of platinum by neutron activation analysis. *Talanta* **10**, 279–285.

NORTON D. L. (1964) Geological and geochemical investigations of stibnite deposits. Ph.D. thesis, University of California.

ONISHI H. and SANDELL E. B. (1955) Geochemistry of arsenic. *Geochim. Cosmochim. Acta* **7**, 1–33.

RITCHIE J. A. (1961) Arsenic and antimony in some New Zealand thermal waters. *N.Z. J. Sci.* **4**, 218–229.

WEISSBERG B. G. (1969) Gold–silver ore-grade precipitates from New Zealand thermal waters. *Econ. Geol.* **64**, 95–108.

WEISSBERG B. G., DICKSON F. W. and TUNELL G. (1966) Solubility of orpiment (As_2S_3) in Na_2S–H_2O at 50–200°C and 100–1500 bars, with geological applications. *Geochim. Cosmochim. Acta* **30**, 815–827.